

REMOTE CONTROL OF THE DIASTEREOSELECTIVITY
IN THE PAUSON–KHAND REACTIONS OF
CHIRAL ENYNES

A THESIS SUBMITTED TO
THE GRADUATE SCHOOL OF NATURAL AND APPLIED SCIENCES
OF
MIDDLE EAST TECHNICAL UNIVERSITY

BY

SERDAR SEZER

IN PARTIAL FULFILLMENT OF THE REQUIREMENTS
FOR
THE DEGREE OF DOCTOR OF PHILOSOPHY
IN
CHEMISTRY

DECEMBER 2011

Approval of the thesis:

**REMOTE CONTROL OF THE DIASTEREOSELECTIVITY
IN THE PAUSON–KHAND REACTIONS OF
CHIRAL ENYNES**

submitted by **SERDAR SEZER** in partial fulfillment of the requirements for the degree of **Doctor of Philosophy in Chemistry Department, Middle East Technical University** by,

Prof. Dr. Canan Özgen _____
Dean, Graduate School of **Natural and Applied Sciences**

Prof. Dr. Çiğdem ÖZKAN _____
Head of Department, **Chemistry**

Prof. Dr. Cihangir Tanyeli _____
Supervisor, **Chemistry Dept., METU**

Examining Committee Members:

Prof. Dr. Metin Balcı _____
Chemistry Dept., METU

Prof. Dr. Cihangir Tanyeli _____
Chemistry Dept., METU

Prof. Dr. Metin Zora _____
Chemistry Dept., METU

Prof. Dr. Özdemir Doğan _____
Chemistry Dept., METU

Assoc. Prof. Dr. Adnan Bulut _____
Chemistry Dept., Kırıkkale University

Date: 02.12.11

I hereby declare that all information in this document has been obtained and presented in accordance with academic rules and ethical conduct. I also declare that, as required by these rules and conduct, I have fully cited and referenced all material and results that are not original to this work.

Name, Last name : Serdar Sezer

Signature :

ABSTRACT

REMOTE CONTROL OF THE DIASTEREOSELECTIVITY IN THE PAUSON–KHAND REACTIONS OF CHIRAL ENYNES

Sezer, Serdar
Ph. D., Department of Chemistry
Supervisor: Prof. Dr. Cihangir Tanyeli

December 2011, 193 pages

In this thesis, an intramolecular Pauson-Khand reaction of chiral enynes derived from homoallyl, allyl and homopropargyl alcohols is described. For this purpose, 2-heteroaryl substituted homoallyl, allyl and homopropargyl alcohols are easily and efficiently resolved through enzymatic resolution in a high ee (91-99%) with a known stereochemistry. Each enantiomerically enriched enyne derived from homoallyl and homopropargyl alcohols affords the conformationally most stable diastereomeric cyclopenta[c]pyran ring system as a sole product, whereas enantiomerically enriched enynes derived from allyl alcohols give the diastereomeric *cis:trans* mixture of cyclopenta[c]furan ring system. In addition these, an intramolecular Pauson–Khand reaction of camphor tethered enynes derived from homoallyl, homomethallyl, and homopropargyl alcohols is also described. Accordingly, homoallyl, homomethallyl, and homopropargyl moieties are easily constructed on the camphor carbonyl group with excellent diastereoselectivity due to endo-face selectivity, and with known stereochemistry. Each enantiomerically pure enyne affords the conformationally most stable diastereomeric spirocyclic cyclopenta[c]pyran ring system.

Key words: Pauson-Khand reaction, Lipase, Enzymatic resolution.

ÖZ

KİRAL ENİNLERİN PAUSON-KHAND REAKSİYONLARINDA DİYASTERYOSEÇİCİLİĞİN UZAKTAN KONTROLÜ

Sezer, Serdar
Doktora, Kimya Bölümü
Tez Yöneticisi: Prof. Dr. Cihangir Tanyeli

Aralık 2011, 193 sayfa

Bu tezde, homoalil, alil ve homopropargil alkollerden elde edilen kiral eninlerin Pauson-Khand reaksiyonu incelenmiştir. Bu amaçla, 2-Heteroaril süstitüe homoalil, alil ve homopropargil alkoller, bilinen stereokimya ve yüksek ee ile (%91-99) enzimatik rezolüsyon edilmişlerdir. Homoalil ve homopropargil alkollerden elde edilen her bir enantiomerce zengin enin, konformasyona göre en kararlı diastereomerik siklopenta[c]piran halka sistemini tek bir ürün olarak oluştururken, alil alkollerden elde edilen eninler siklopenta[c]furan halka sisteminin diastereomerce *cis:trans* karışımını oluşturmuştur. Bunlara ilaveten, homoalil, homometalil ve homopropargil alkollerden türeyen kamfora bağlanmış eninlerin Pauson Khand reaksiyonu ayrıca incelenmiştir. Bu doğrultuda, homoalil, homometalil ve homopropargil grupları kamfor üzerindeki karbonil grubuna *endo*-yüz seçiciliğinden dolayı mükemmel diastereoseçicilikle, kolayca ve bilinen stereokimya ile takılmışlardır. Herbir enantiyomerce saf enin, konformasyonca en kararlı diastereomerik spirociklik siklopenta[c]piran sistemini oluşturmuştur.

Anahtar kelimeler: Pauson-Khand tepkimesi, Lipaz, Enzimatik rezolüsyon.

To my dear wife and parents ...

ACKNOWLEDGEMENTS

I would like to express my sincere thanks to my supervisor Prof. Dr. Cihangir Tanyeli for his guidance, encouragement and support throughout the my research.

I thank to Assoc. Prof. Dr. Cavit Kazaz for NOE experiments and Assoc. Prof. Dr. Ertan Şahin for X-ray analysis.

I would also thank to Prof. Dr. İdris Mecidođlu and Assoc. Prof. Dr. Devrim Özdemirhan for their help and suggestions.

And also I would like to thank to Emre Y. Yazıcıođlu and Murat Işık for their valuable friendship and support.

I would like to give special thanks to Assist. Prof. Dr Hüseyin Karaca for his friendship, support and encouragement.

I would like to give special thanks to Murat Kaya, Mustafa Emrullahođlu, Taner Atalar and Tuna Subaşı for their friendship and support.

In addition, I want to thank to my lab mates from D-251, D-254 and D-255 and students, Nurlan, Yasemin Gümrükçü, Esra Aşan, Salih Ertan, Merve Çayır, Sema Demirci, Melis Şardan, Şeyma Ekiz, Melda İşler, Yağız Ünver, İrem Bakirci, Nurdan Sargın working with me, for their help and friendship.

Finally, I owe great thanks to my wife Ümran Aydemir Sezer and parents Nezihä and Arif Hikmet Sezer and my brother Ufuk Sezer for their endless love, unlimited patient and support; I devote this thesis to them.

TABLE OF CONTENTS

ABSTRACT.....	iv
ÖZ.....	v
ACKNOWLEDGEMENTS.....	vii
LIST OF TABLES.....	xiii
LIST OF FIGURES.....	xiv
LIST OF SCHEMES.....	xix
LIST OF ABBREVIATIONS.....	xxi

CHAPTERS

1 INTRODUCTION.....	1
1.1 Chirality.....	1
1.1.1 Chiral Recognition and Discrimination.....	2
1.1.2 Chirality in Drug Action.....	5
1.2 Source of enantiomerically pure compounds.....	9
1.2.1 Chiral Pool.....	10
1.2.2 Kinetic Resolution.....	11
1.2.3 Asymmetric Synthesis.....	14
1.3 Biotransformation and Green Chemistry.....	19
1.3.1 Enzymes.....	20
1.4 Pauson Khand Reaction.....	33
1.4.1 Mechanism.....	34
1.4.2 Promotion.....	36
1.4.3 Asymmetric Pauson Khand Reaction.....	37
1.4.4 Applications in Natural Product Synthesis.....	40

1.5	Aim of the Work.....	42
2	RESULTS AND DISCUSSION.....	44
2.1	Racemic Synthesis of Heteroaryl Substituted Allylic, Homoallylic and Homopropargylic Alcohols	44
2.2	Enzymatic Resolution Studies of Racemic Homoallylic, Allylic and Homopropargylic Alcohols.	49
2.2.1	Homoallylic Alcohols	50
2.2.2	Allylic Alcohols	54
2.2.3	Homopropargylic Alcohols.....	56
2.3	Synthesis of Enyne Systems.....	58
2.3.1	Synthesis of Enynes Derived from Homoallylic Alcohols.	59
2.3.2	Synthesis of Enynes Derived from Allylic Alcohols.	61
2.3.3	Synthesis of Enynes Derived from Homopropargylic Alcohols.....	62
2.4	Pauson Khand Cyclization of Enyne System	64
2.4.1	Synthesis of Cyclopenta[<i>c</i>]pyran Bicyclic Compounds Derived from Homoallyl Alcohol Backbone.....	65
2.4.2	Synthesis of Cyclopenta[<i>c</i>]pyran Bicyclic Compounds Derived from Homopropargyl Alcohol Backbone	68
2.4.3	Synthesis of Cyclopenta[<i>c</i>]furan Bicyclic Compounds Derived from Allylic Alcohol Backbone.....	70
2.5	Chiral Spirocyclic Compounds via Pauson Khand Reaction	73
2.5.1	Synthesis of Tertiary Alcohols.....	74
2.5.2	Construction of Enyne Systems	75
2.5.3	Synthesis PK Products	77
3	CONCLUSION.....	81
4	EXPERIMENTAL.....	83
4.1	General Procedure for Synthesis of Racemic Homoallylic Alcohols, <i>rac</i> -95-97.....	84
4.1.1	1-(Furan-2-yl)but-3-en-1-ol, (\pm)- <i>rac</i> -95	84
4.1.2	1-(Thiophen-2-yl)but-3-en-1-ol, (\pm)- <i>rac</i> -96	85
4.1.3	1-(Pyridin-2-yl)but-3-en-1-ol, (\pm)- <i>rac</i> -97	85
4.2	General Procedure for Synthesis of Racemic Allylic Alcohols, <i>rac</i> -99-101	86

4.2.1	1-(Furan-2-yl)prop-2-en-1-ol, (\pm)- <i>rac</i> -99	86
4.2.2	1-(Thiophen-2-yl)prop-2-en-1-ol, (\pm)- <i>rac</i> -100	87
4.2.3	1-(pyridin-2-yl)prop-2-en-1-ol, (\pm)- <i>rac</i> -101	87
4.3	General Procedure for Synthesis of Racemic 2-Furyl and 2-thienyl substituted Homopropragylic Alcohols, <i>rac</i> -103-105	87
4.3.1	1-(Furan-2-yl)but-3-yn-1-ol, (\pm)- <i>rac</i> -103	88
4.3.2	1-(Thiophen-2-yl)but-3-yn-1-ol, (\pm)- <i>rac</i> -104	88
4.3.3	Procedure for Synthesis of 1-(pyridin-2-yl)but-3-yn-1-ol, (\pm)- <i>rac</i> -105	89
4.4	General Procedure for Enzymatic Resolution of Homoallylic, Allylic and Homopropragylic Alcohols	90
4.4.1	(<i>S</i>)-(-)-1-(2-Furyl)but-3-en-1-ol, (<i>S</i>)-(-)-95	90
4.4.2	(<i>S</i>)-(-)-1-(Thiophen-2-yl)but-3-en-1-ol, (<i>S</i>)-(-)-96.....	90
4.4.3	(<i>S</i>)-(-)-1-(Pyridin-2-yl)but-3-en-1-ol, (<i>S</i>)-(-)-97	91
4.4.4	(<i>S</i>)-(+)-1-(Furan-2-yl)prop-2-en-1-ol, (<i>S</i>)-(+)-99.....	91
4.4.5	(<i>S</i>)-(-)-1-(Thiophen-2-yl)prop-2-en-1-ol, (<i>S</i>)-(-)-100	91
4.4.6	(<i>S</i>)-(+)-1-(Pyridin-2-yl)prop-2-en-1-ol, (<i>S</i>)-(+)-101	92
4.4.7	(<i>S</i>)-(+)-1-(Furan-2-yl)but-3-yn-1-ol, (<i>S</i>)-(+)-103	92
4.4.8	(<i>S</i>)-(+)-1-(Thiophen-2-yl)but-3-yn-1-ol, (<i>S</i>)-(+)-104.....	92
4.4.9	(<i>S</i>)-(-)-1-(Pyridin-2-yl)but-3-yn-1-ol, (<i>S</i>)-(-)-105	93
4.5	General Procedure for <i>O</i> -allylation and <i>O</i> -propargylation.....	93
4.5.1	(<i>S</i>)-(-)-2-(1-(Prop-2-ynyloxy)but-3-enyl)furan, (-)-116.....	94
4.5.2	(<i>S</i>)-(-)-2-(1-(Prop-2-ynyloxy)but-3-enyl)thiophene, (<i>S</i>)-(-)-117	94
4.5.3	(<i>S</i>)-(-)-2-(1-(Prop-2-ynyloxy)but-3-enyl)pyridine, (<i>S</i>)-(-)-118.....	95
4.5.4	(<i>S</i>)-(-)-2-(1-(Prop-2-ynyloxy)allyl)furan, (<i>S</i>)-(-)-119	95
4.5.5	(<i>S</i>)-(-)-2-(1-(Prop-2-ynyloxy)allyl)thiophene, (<i>S</i>)-(-)-120.....	96
4.5.6	(<i>S</i>)-(-)-2-(1-(Prop-2-ynyloxy)allyl)pyridine, (<i>S</i>)-(-)-121	96
4.5.7	(<i>S</i>)-2-(1-(Allyloxy)but-3-ynyl)furan, (<i>S</i>)-(-)-122	97
4.5.8	(<i>S</i>)-(-)-2-(1-(Allyloxy)but-3-ynyl)thiophene, (<i>S</i>)-(-)-123	97
4.5.9	(<i>S</i>)-(-)-2-(1-(Allyloxy)but-3-ynyl)pyridine, (<i>S</i>)-(-)-124.....	98
4.6	General Procedure for Pauson-Khand Reaction.....	99
4.6.1	(3 <i>S</i> ,4 <i>aR</i>)-(+)-3-(Furan-2-yl)-3,4,4 <i>a</i> ,5-tetrahydrocyclopenta[<i>c</i>]pyran- 6(1 <i>H</i>)-one, (+)-125	99

4.6.2	(3 <i>S</i> ,4 <i>aR</i>)-(+)-3-(Thiophen-2-yl)-3,4,4 <i>a</i> ,5-tetrahydrocyclopenta[<i>c</i>]pyran-6(1 <i>H</i>)-one, (3 <i>S</i> ,4 <i>aR</i>)-(+)-126	100
4.6.3	(3 <i>S</i> ,4 <i>aR</i>)-(+)-3-(Pyridin-2-yl)-3,4,4 <i>a</i> ,5-tetrahydrocyclopenta[<i>c</i>]pyran-6(1 <i>H</i>)-one, (3 <i>S</i> ,4 <i>aR</i>)-(+)-127	100
4.6.4	(3 <i>S</i> ,7 <i>aR</i>)-(+)-3-(Furan-2-yl)-3,4,7,7 <i>a</i> -tetrahydrocyclopenta[<i>c</i>]pyran-6(1 <i>H</i>)-one, (+)-128	101
4.6.5	(3 <i>S</i> ,7 <i>aR</i>)-(+)-3-(Thiophen-2-yl)-3,4,7,7 <i>a</i> -tetrahydrocyclopenta[<i>c</i>]pyran-6(1 <i>H</i>)-one, (3 <i>S</i> ,7 <i>aR</i>)-(+)-129	101
4.6.6	(3 <i>S</i> ,7 <i>aR</i>)-(+)-3-(Pyridin-2-yl)-3,4,7,7 <i>a</i> -tetrahydrocyclopenta[<i>c</i>]pyran-6(1 <i>H</i>)-one, (3 <i>S</i> ,7 <i>aR</i>)-(+)-130	102
4.6.7	(3 <i>S</i> ,3 <i>aR</i>)-(+)-3-(Furan-2-yl)-3 <i>a</i> ,4-dihydro-1 <i>H</i> -cyclopenta[<i>c</i>]furan-5(3 <i>H</i>)-one, (3 <i>S</i> ,3 <i>aR</i>)-(-)-131	102
4.6.8	(3 <i>S</i> ,3 <i>aS</i>)-(-)-3-(Furan-2-yl)-3 <i>a</i> ,4-dihydro-1 <i>H</i> -cyclopenta[<i>c</i>]furan-5(3 <i>H</i>)-one, (3 <i>S</i> ,3 <i>aS</i>)-(+)-131	103
4.6.9	(3 <i>S</i> ,3 <i>aR</i>)-(+)-3-(Thiophen-2-yl)-3 <i>a</i> ,4-dihydro-1 <i>H</i> -cyclopenta[<i>c</i>]furan-5(3 <i>H</i>)-one, (3 <i>S</i> ,3 <i>aR</i>)-(-)-132	104
4.6.10	(3 <i>S</i> ,3 <i>aS</i>)-(-)-3-(Thiophen-2-yl)-3 <i>a</i> ,4-dihydro-1 <i>H</i> -cyclopenta[<i>c</i>]furan-5(3 <i>H</i>)-one, (3 <i>S</i> ,3 <i>aS</i>)-(+)-132	104
4.6.11	(3 <i>S</i> ,3 <i>aS</i>)-(+)-3-(Pyridin-2-yl)-3 <i>a</i> ,4-dihydro-1 <i>H</i> -cyclopenta[<i>c</i>]furan-5(3 <i>H</i>)-one, (3 <i>S</i> ,3 <i>aS</i>)-(+)-133	105
4.6.12	(3 <i>S</i> ,3 <i>aR</i>)-(-)-3-(Pyridin-2-yl)-3 <i>a</i> ,4-dihydro-1 <i>H</i> -cyclopenta[<i>c</i>]furan-5(3 <i>H</i>)-one, (3 <i>S</i> ,3 <i>aR</i>)-(-)-133	105
4.7	X-Ray Structure Determination of Compound (+)-125 and (+)-128	106
4.7.1	Crystal Data for Compound (+)-125:cis	106
4.7.2	Crystal Data for Compound (+)-128:trans	107
4.8	X-Ray Structure Determination of Compound (+)-129 and (+)-130	107
4.8.1	Crystal Data for Compound (3 <i>S</i> ,7 <i>aR</i>)- (+)-129	108
4.8.2	Crystal Data for Compound (3 <i>S</i> ,7 <i>aR</i>)- (+)-130	108
4.9	Synthesis of Spiro Compounds	109
4.9.1	Synthesis of Homoallyl and Homomethallyl Alcohols.....	109
4.9.2	Synthesis of Homopropargyl Alcohols	109
4.9.3	General Procedure for <i>O</i> -allylation, <i>O</i> -methallylation and <i>O</i> -propargylation.....	110

4.9.4	General Procedure for The Pauson-Khand Reaction	113
4.9.5	X-ray Structure Analysis.....	115
	REFERENCES	118
	APPENDIX A. SUPPORTING INFORMATION	130
	CURRICULUM VITAE.....	192

LIST OF TABLES

TABLES

Table 1. Comparison of asymmetric methods.....	18
Table 2. Advantages and drawbacks of enzymes as catalysts.....	20
Table 3. Selected commercially available popular lipases.....	22
Table 4. Results of allylic, homoallylic and propargylic alcohols.....	48
Table 5. PLE and CCL catalyzed resolutions of <i>rac-96</i> and <i>rac-107-8</i>	51
Table 6. PS-C Amona II catalyzed resolutions of <i>rac-95-97</i>	52
Table 7. Other immobilized lipases catalyzed resolutions of <i>rac-95-97</i>	53
Table 8. Enzymatic kinetic resolution of allylic alcohols <i>rac-99-101</i>	56
Table 9. Enzymatic kinetic resolution of allylic alcohols <i>rac-103-105</i>	58
Table 10. Enynes derived from homoallylic alcohols.....	60
Table 11. Enynes derived from allylic alcohols.....	61
Table 12. Reaction results of enynes from homopropargylic alcohols.....	63

LIST OF FIGURES

FIGURES

Figure 1. Example of a “lock and key” interaction	2
Figure 2. Molecular structures of <i>R</i> - and <i>S</i> -carvone.....	3
Figure 3. Molecular structures of <i>R</i> - and <i>S</i> -limonene	4
Figure 4. Molecular structures of (+)-and (-)-nootkatone	4
Figure 5. Examples of the different behaviors of the enantiomers	5
Figure 6. The Hypothetical Interaction Between the 2 Enantiomers of a Chiral Drug and Its Binding Site.....	6
Figure 7. Molecular structures of adrenaline and thalidomide enantiomers	7
Figure 8. Different behaviors of the drug enantiomers.	8
Figure 9. Popular drugs in today	9
Figure 10. Synthetic route to enantiomerically pure compounds.....	10
Figure 11. Schematic Representation of DKR.....	13
Figure 12. Selected chiral auxiliaries in asymmetric synthesis.....	15
Figure 13. Selected typical chiral organocatalysts	17
Figure 14. Schematic representation of Kazlauskas rule in the Enzymatic KR of an secondary alcohol.....	26
Figure 15. Schematic representation of faster enantiomer in the PCL catalyzed acylation of primary alcohol	26
Figure 16. Examples of activated acyl donors for acylation of alcohols	29
Figure 17. The CAL-B catalyzed resolution of 2-alkanols and cyclic secondary alcohols.	30
Figure 18. Kilogram-scale routes to pharmaceutical precursors involving lipases	32
Figure 19. Retrosynthetic analysis towards cyclopenta[<i>c</i>]pyran and cyclopenta[<i>c</i>]furan bicyclic systems.....	43
Figure 20. Retrosynthetic analysis towards spiro cyclopentapyran systems.....	43
Figure 21. NOE correlations observed between H _a and H _b protons of (+)- 126 (<i>cis</i> -1,3) and (+)- 127 (<i>cis</i> -1,3).....	67

Figure 22. X-ray structure of compounds (3 <i>S</i> ,4 <i>aR</i>)-(+)- 125 (<i>cis</i> -1,3).....	67
Figure 23. X-ray structure of compounds (+)- 128 (<i>trans</i> -1,4), (+)- 129 (<i>trans</i> -1,4) and (+)- 130 (<i>trans</i> -1,4)	70
Figure 24. Proposed intermediate conformers in PKR	73
Figure 25. Molecular structures of the compounds (+/-)- 141-144 with atom numbering scheme. The thermal ellipsoids are drawn at the 50% probability level	79
Figure A1. ¹ H-NMR spectrum of <i>rac</i> -95.....	130
Figure A2. ¹³ C-NMR spectrum of <i>rac</i> -95	131
Figure A3. ¹ H-NMR spectrum of <i>rac</i> -96	131
Figure A4. ¹³ C-NMR spectrum of <i>rac</i> -96	132
Figure A5. ¹ H-NMR spectrum of <i>rac</i> -97	132
Figure A6. ¹³ C-NMR spectrum of <i>rac</i> -97	133
Figure A7. ¹ H-NMR spectrum of <i>rac</i> -99	133
Figure A8. ¹³ C-NMR spectrum of <i>rac</i> -99	134
Figure A9. ¹ H-NMR spectrum of <i>rac</i> -100	134
Figure A10. ¹³ C-NMR spectrum of <i>rac</i> -100	135
Figure A11. ¹ H-NMR spectrum of <i>rac</i> -101	135
Figure A12. ¹³ C-NMR spectrum of <i>rac</i> -101	136
Figure A13. ¹ H-NMR spectrum of <i>rac</i> -103	136
Figure A14. ¹³ C-NMR spectrum of <i>rac</i> -103	137
Figure A15. ¹ H-NMR spectrum of <i>rac</i> -104	137
Figure A16. ¹³ C-NMR spectrum of <i>rac</i> -104	138
Figure A17. ¹ H-NMR spectrum of <i>rac</i> -105	138
Figure A18. ¹³ C-NMR spectrum of <i>rac</i> -105	139
Figure A19. HPLC chromatogram of <i>rac</i> -95	140
Figure A20. HPLC chromatogram of (<i>S</i>)-(-)-95	140
Figure A21. HPLC chromatogram of <i>rac</i> -96	141
Figure A22. HPLC chromatogram of (<i>S</i>)-(-)-96.....	141
Figure A23. HPLC chromatogram of <i>rac</i> -97	142
Figure A24. HPLC chromatogram of (<i>S</i>)-(-)-97	142
Figure A25. HPLC chromatogram of <i>rac</i> -99	143
Figure A26. HPLC chromatogram of (<i>S</i>)-(+)-99	143

Figure A27. HPLC chromatogram of <i>rac</i> -100	144
Figure A28. HPLC chromatogram of (<i>S</i>)-(-)-100	144
Figure A29. HPLC chromatogram of <i>rac</i> -112	145
Figure A30. HPLC chromatogram of (<i>S</i>)-(-)-112	145
Figure A31. HPLC chromatogram of <i>rac</i> -103	146
Figure A32. HPLC chromatogram of (<i>S</i>)-(+)-103	146
Figure A33. HPLC chromatogram of <i>rac</i> -104	147
Figure A34. HPLC chromatogram of (<i>S</i>)-(+)-104	147
Figure A35. HPLC chromatogram of <i>rac</i> -105	148
Figure A36. HPLC chromatogram of (<i>S</i>)-(-)-105	148
Figure A37. ¹ H-NMR spectrum of (<i>S</i>)-(-)-116.....	149
Figure A38. ¹³ C-NMR spectrum of (<i>S</i>)-(-)-116.....	149
Figure A39. ¹ H-NMR spectrum of (<i>S</i>)-(-)-117.....	150
Figure A40. ¹³ C-NMR spectrum of (<i>S</i>)-(-)-117	150
Figure A41. ¹ H-NMR spectrum of (<i>S</i>)-(-)-118.....	151
Figure A42. ¹³ C-NMR spectrum of (<i>S</i>)-(-)-118	151
Figure A43. ¹ H-NMR spectrum of (<i>S</i>)-(-)-119.....	152
Figure A44. ¹³ C-NMR spectrum of (<i>S</i>)-(-)-119	152
Figure A45. ¹ H-NMR spectrum of (<i>S</i>)-(-)-120.....	153
Figure A46. ¹³ C-NMR spectrum of (<i>S</i>)-(-)-120	153
Figure A47. ¹ H-NMR spectrum of (<i>S</i>)-(-)-121.....	154
Figure A48. ¹³ C-NMR spectrum of (<i>S</i>)-(-)-121	154
Figure A49. ¹ H-NMR spectrum of (<i>S</i>)-(-)-122.....	155
Figure A50. ¹³ C-NMR spectrum of (<i>S</i>)-(-)-122	155
Figure A51. ¹ H-NMR spectrum of (<i>S</i>)-(-)-123.....	156
Figure A52. ¹³ C-NMR spectrum of (<i>S</i>)-(-)-123	156
Figure A53. ¹ H-NMR spectrum of (<i>S</i>)-(-)-124.....	157
Figure A54. ¹³ C-NMR spectrum of (<i>S</i>)-(-)-124	157
Figure A55. ¹ H-NMR spectrum of (+)-125.....	158
Figure A56. ¹³ C-NMR spectrum of (+)-125	158
Figure A57. DEPT-90 spectrum of (+)-125	159
Figure A58. COSY spectrum of (+)-125.....	160
Figure A59. HSQC spectrum of (+)-125.....	161

Figure A60. HMBC spectrum of (+)-125.....	162
Figure A61. ¹ H-NMR spectrum of (+)-126.....	163
Figure A62. ¹³ C-NMR spectrum of (+)-126	163
Figure A63. ¹ H-NMR spectrum of (+)-127.....	164
Figure A64. ¹³ C-NMR spectrum of (+)-127	164
Figure A65. ¹ H-NMR spectrum of (+)-128.....	165
Figure A66. ¹³ C-NMR spectrum of (+)-128	165
Figure A67. ¹ H-NMR spectrum of (+)-129.....	166
Figure A68. ¹³ C-NMR spectrum of (+)-129	166
Figure A69. ¹ H-NMR spectrum of (+)-130.....	167
Figure A70. ¹³ C-NMR spectrum of (+)-130	167
Figure A71. ¹ H-NMR spectrum of (-)-131.....	168
Figure A72. ¹³ C-NMR spectrum of (-)-131	168
Figure A73. ¹ H-NMR spectrum of (+)-131	169
Figure A74. ¹³ C-NMR spectrum of (+)-131	169
Figure A75. ¹ H-NMR spectrum of (-)-132.....	170
Figure A76. ¹³ C-NMR spectrum of (-)-132	170
Figure A77. ¹ H-NMR spectrum of (+)-132.....	171
Figure A78. ¹³ C-NMR spectrum of (+)-132	171
Figure A79. ¹ H-NMR spectrum of (+)-133.....	172
Figure A80. ¹³ C-NMR spectrum of (+)-133	172
Figure A81. ¹ H-NMR spectrum of (-)-133.....	173
Figure A82. ¹³ C-NMR spectrum of (-)-133.....	173
Figure A83. ¹ H-NMR spectrum of (-)-136.....	174
Figure A84. ¹³ C-NMR spectrum of (-)-136	174
Figure A85. ¹ H-NMR spectrum of (+)-137.....	175
Figure A86. ¹³ C-NMR spectrum of (+)-137.....	175
Figure A87. ¹ H-NMR spectrum of (+)-138.....	176
Figure A88. ¹ H-NMR spectrum of (-)-139.....	176
Figure A89. ¹³ C-NMR spectrum of (-)-139	177
Figure A90. ¹ H-NMR spectrum of (-)-140.....	177
Figure A91. ¹³ C-NMR spectrum of (-)-140.....	178
Figure A92. ¹ H-NMR spectrum of (+)-141.....	178

Figure A93. ^{13}C -NMR spectrum of (+)-141	179
Figure A94. ^1H -NMR spectrum of (-)-142.....	179
Figure A95. ^{13}C -NMR Spectrum of (-)-142.....	180
Figure A96. ^1H -NMR spectrum of (+)-143.....	180
Figure A97. ^{13}C -NMR spectrum of (+)-143	181
Figure A98. ^1H -NMR spectrum of (+)-144.....	181
Figure A99. ^{13}C -NMR spectrum of (+)-144	182
Figure A100. NOE spectrum of (+)-126	182
Figure A101. NOE spectrum of (+)-126	183
Figure A102. NOE spectrum of (+)-127	183
Figure A103. NOE spectrum of (+)-127	184
Figure A104. GC-MS spectrum of (<i>S</i>)-(-)-117.....	184
Figure A105. GC-MS spectrum of (<i>S</i>)-(-)-118.....	185
Figure A106. GC-MS spectrum of (<i>S</i>)-(-)-119.....	185
Figure A107. GC-MS spectrum of (<i>S</i>)-(-)-120.....	186
Figure A108. GC-MS spectrum of (<i>S</i>)-(-)-121.....	186
Figure A109. GC-MS spectrum of (<i>S</i>)-(+)-127.....	187
Figure A110. GC-MS spectrum of (<i>S</i>)-(+)-129.....	187
Figure A111. GC-MS spectrum of (-)-131.....	188
Figure A112. HRMS spectrum of (+)-126.....	188
Figure A113. HRMS spectrum of (+)-127	189
Figure A114. HRMS spectrum of (+)-129.....	189
Figure A115. HRMS spectrum of (+)-130	190
Figure A116. HRMS spectrum of (-)-131	190
Figure A117. HRMS spectrum of (-)-132.....	191

LIST OF SCHEMES

SCHEMES

Scheme 1. Retro synthesis of (+)- <i>exo</i> -brevicommin	11
Scheme 2. Schematic representation of kinetic resolution.	11
Scheme 3. Kinetic resolution of <i>trans</i> -sobrerol	12
Scheme 4. Fu's kinetic resolution of secondary alcohol	12
Scheme 5. DKR of indanol.....	14
Scheme 6. Parallel kinetic resolution of β -Keto ester	14
Scheme 7. Corey's auxiliary in the asymmetric synthesis of frontalin	16
Scheme 8. List's organocatalyst catalyzed Mukaiyama aldol reaction.....	18
Scheme 9. Lipase catalyze hydrolysis of triolein to diolein	23
Scheme 10. Mechanism of Lipase catalyze hydrolysis of ester	24
Scheme 11. Lipase catalyzed enantioselective acylation of an alcohol.....	25
Scheme 12. The lipase catalyzed irreversible transesterifications.....	29
Scheme 13. Enzymatic resolution of a building block for antibiotic synthesis.....	32
Scheme 14. Intramolecular Mitsunobu Reaction	33
Scheme 15. Intramolecular Pauson-Khand reaction.....	34
Scheme 16. Proposed mechanism of Pauson-Khand reaction.....	35
Scheme 17. Mechanism of Intramolecular Pauson Khand cyclization	36
Scheme 18. Optically active products derived from diethyl <i>L</i> -tartrate.....	37
Scheme 19. Selected chiral auxiliaries and methylthioisoborneol mediated intramolecular PK reaction.....	38
Scheme 20. Intramolecular asymmetric PK reaction	39
Scheme 21. The brucine mediated cyclization of norbornene in the presence of propargyl alcohol.....	40
Scheme 22. Schreiber's retrosynthetic strategy towards (+)-epoxydicymene ...	41
Scheme 23. Synthesis of homoallylic alcohols.....	45

Scheme 24. Synthesis of allylic alcohols.....	46
Scheme 25. Synthesis of homopropargylic alcohols	47
Scheme 26. Ezymatic resolution of homoallylic alcohols.....	51
Scheme 27. Ezymatic resolution of allylic alcohols.....	54
Scheme 28. Enzymatic resolution of homopropargylic alcohols	57
Scheme 29. Synthesis of cyclopenta[<i>c</i>]pyran and cyclopenta[<i>c</i>]furan systems	65
Scheme 30. Synthesis of PK products from chiral enynes derived from homoallyl alcohols.....	66
Scheme 31. Synthesis of PK products from chiral enynes derived from homopropargylic alcohols.....	68
Scheme 32. Synthesis of PK products from chiral enynes derived from allylic alcohols	71
Scheme 33. Synthesis of tertiary alcohols	75
Scheme 34. Synthesis of enyne systems derived from tertiary alcohols	76
Scheme 35. Synthesis of spirobicyclic PK products	78
Scheme 36. Plausible conformations of the intermediates in the Pauson Khand reaction.....	80

LIST OF ABBREVIATIONS

KR: Kinetic Resolution

DKR: Dynamic Kinetic Resolution

DMAP: Dimethylaminopyridine

PKR: Pauson-Khand Reaction

TMS: Trimethylsilyl

CBS: Corey-Bakshi-Shibata Reagent

DME: Dimethoxyethane

NMO: *N*-methylmorpholine *N*-oxide

TMANO: Trimethylamine *N*-oxide

THF: Tetrahydrofuran

DIPE: Diisopropyl ether

DCM: Dichloromethane

CHAPTER 1

INTRODUCTION

1.1 Chirality

“...The universe is dissymmetrical; for if the whole of the bodies which compose the solar system were placed before a glass moving with their individual movements, the image in the glass could not be superimposed on reality... Life is dominated by dissymmetrical actions. I can foresee that all living species are primordially, in their structure, in their external forms, functions of cosmic dissymmetry...”

—Louis Pasteur

The development of stereochemistry has been profoundly influenced by these visionary words of Pasteur [1], written in the middle of the nineteenth century. It has increasingly become clear that dissymmetry plays a key role in many fundamental phenomena and laws of nature. Molecular chirality (handedness) is an important term to describe dissymmetry in modern chemistry. The word *chirality* is derived from Greek word χείρ (cheir) which means *hand*. It was firstly used by Lord Kelvin (Sir William Thomson) in 1884 [2]. Very simply, If a system is chiral, the mirror image of the system is not superimposable on the original system. The human hand is the best example of this explanation. These mirror images are called enantiomers and are not identical. “A wide range of biological and physical functions are generated through precise molecular recognition that requires matching of chirality. Life itself depends on chiral recognition, because living systems interact with enantiomers in decisively different manners. A variety of functions responsible for metabolism and

numerous biological responses occur because enzymes, receptors, and other natural binding sites recognize substrates with specific chirality” [3].

1.1.1 Chiral Recognition and Discrimination

Chirality is important for living systems occurring in nature in one enantiomeric form only. Because, a biologically active chiral substances react with its receptor site in a chiral manner, and enantiomers may be discriminated by the receptor in very different ways and so the two enantiomers of a drug may interact differently with the receptor which leads to different effects. “Indeed, it is very important to keep the idea of chiral discrimination or stereoisomeric discrimination in mind when designing biologically active molecules” [4]. Emil Fischer, who used the term “lock and key”, first proposed that biochemical processes follow specific chemical recognition/response events. The implication here is that a specific chemical compound “fits” into a specific location in a biochemical and that this then initiates a certain biochemical response. This phenomenon can be explained via basic model by referring to Figure 1.

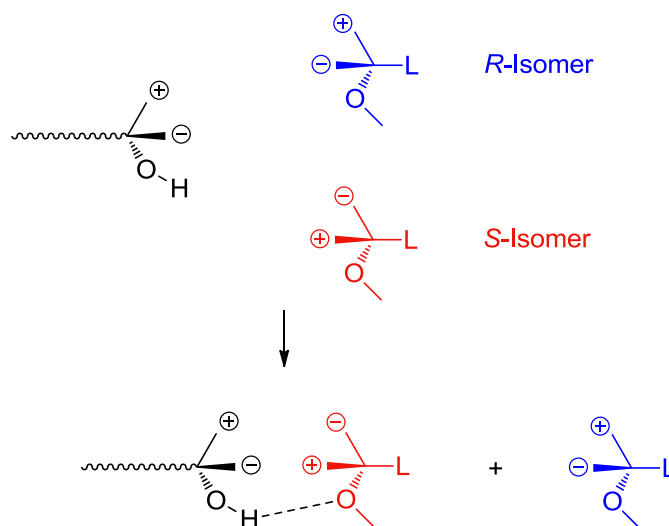


Figure 1. Example of a “lock and key” interaction.

The drawing on the left is intended to represent a tetrahedral carbon attached to a larger molecular fragment, for example, a protein, and the two molecules are mirror-image enantiomers as potent ligands. The type of interactions that could be important in this situations are electrostatic and weak attractive forces like the “hydrogen” bonding that we have seen in the structures of proteins and DNA, or the formation of strong or weak “covalent” bonding or they might be simple structural considerations due to the size and shape of the approaching species. It can be seen that the preferred (most stable, lowest energy, etc.) arrangement is the *S*-isomer in the orientation as shown in the bottom of Figure 1. These types of chemical recognition/responses are central to the biochemistry of life in which chiral substances may react differently when exposed by other chiral substances.

In the case of human sense of smell, our body use the odorant binding proteins (OBPs) and odorant receptors [5-6]. These proteins and receptors themselves are composed of L -amino acids. Because of chirality, it should be said that nose can be quite sensitive to the chirality of the odorant molecules in addition to many other aspects of size, shape and chemical structure. Louis Pasteur was actually the first person to mention that the olfactory senses might be dependent on the dissymmetry of the molecule involved [7].

In the middle of the twentieth century, scientists were able to prepare “pure” compounds of enantiomers and then verify the different smells. One of the first examples of such compounds are enantiomers of carvone. While *R*-(-)-carvone smells like spearmint, *S*-(+)-carvone smells caraway.

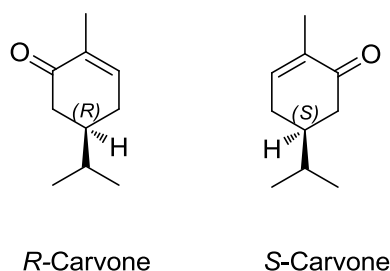


Figure 2. Molecular structures of *R*- and *S*-carvone.

There are now many other examples of this difference in the smell of enantiomers [8]. Another popular example is limonene. *R*-(+)-limonene has an orange aroma, whereas *S*-(-)-limonene smells like lemon.

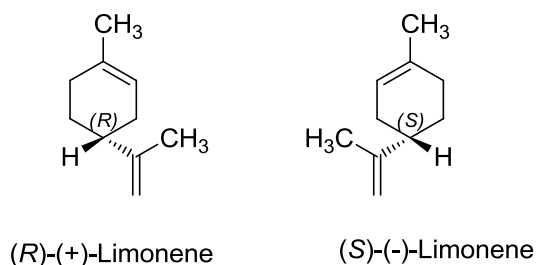


Figure 3. Molecular structures of *R*- and *S*-limonene.

It is not the certain issue that this type of enantiomers behave different odors. Sometimes, the difference between enantiomers is more in the sensitivity than the smell. For example, the compound (+)-nootkatone, drawn in Figure 4, smells like odor of grapefruit. However, its sensitivity threshold of smelling is approximately 2000 times lower than its enantiomer.

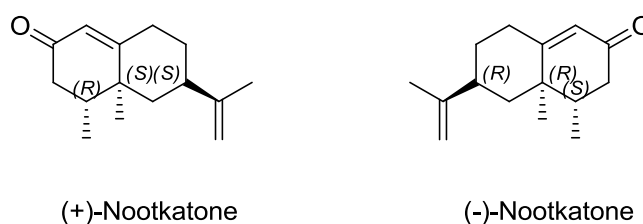


Figure 4. Molecular structures of (+)-and (-)-nootkatone.

Same discrimination also has been seen in the case of human sense of taste or pheromones chemistry. A lot of works depended on discrimination of molecular chirality can be found in the literature [9]. Selected examples are shown in Figure 5.

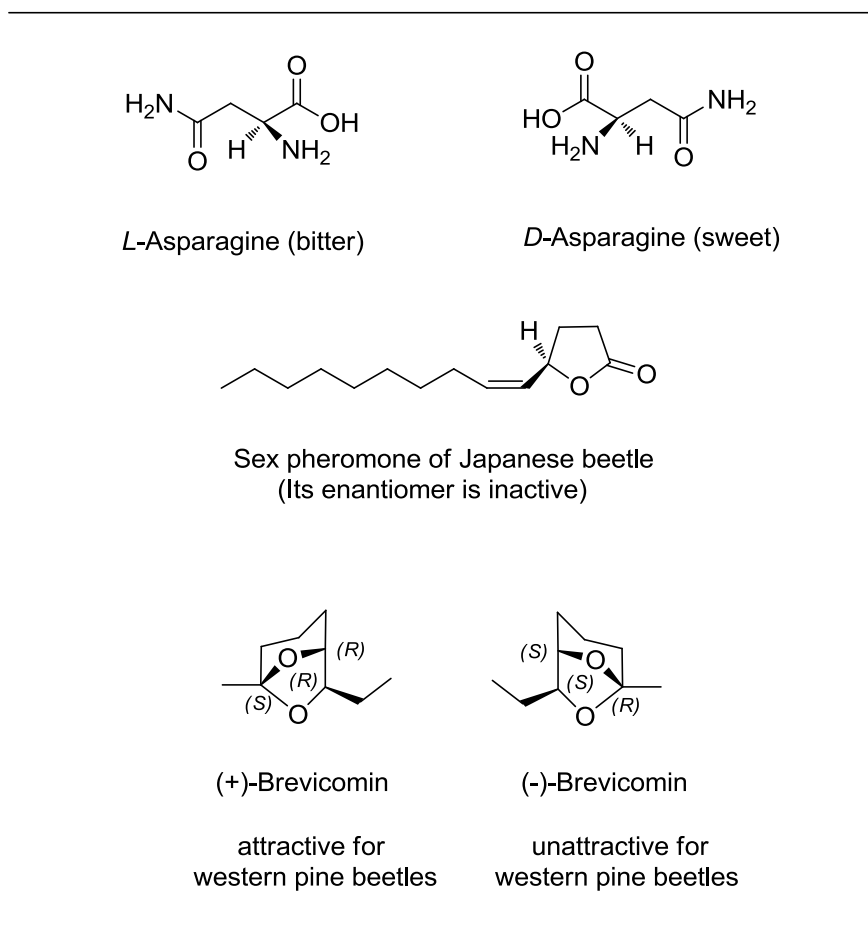


Figure 5. Examples of the different behaviors of the enantiomers.

1.1.2 Chirality in Drug Action

The importance of chirality in the development of drugs for the treatment of disease is gaining attention in medical practice. Most of the pharmaceuticals in drug industry have chiral structures and they are available as either racemic mixtures or pure enantiomers. For some therapeutic cases, single enantiomer formulations can provide greater selectivities for their biological targets, improved therapeutic indices, and better pharmacokinetics than a mixture of enantiomers.

M. J. Owens and J. McConathy explained the difference between 2 enantiomers of a drug illustrated in Figure 6 using a hypothetical interaction between a chiral drug and its chiral binding site. “In this case, one enantiomer is biologically active while the other enantiomer is not. The portions of the drug labeled A, B, and C must interact

with the corresponding regions of the binding site labeled a, b, and c for the drug to have its pharmacologic effect. The active enantiomer of the drug has a 3-dimensional structure that can be aligned with the binding site to allow A to interact with a, B to interact with b, and C to interact with c. In contrast, the inactive enantiomer cannot bind in the same way no matter how it is rotated in space. Although the inactive enantiomer possesses all of the same groups A, B, C, and D as the active enantiomer, they cannot all be simultaneously aligned with the corresponding regions of the binding site. This difference in 3 dimensional structure prevents the inactive enantiomer from having a biological effect at this binding site. In some cases, the portion of a molecule containing the chiral center(s) may be in a region that does not play a role in the molecule's ability to interact with its target. In these instances, the individual enantiomers may display very similar or even equivalent pharmacology at their target site. Even in these cases, the enantiomers may differ in their metabolic profiles as well as their affinities for other receptors, transporters, or enzymes" [10].

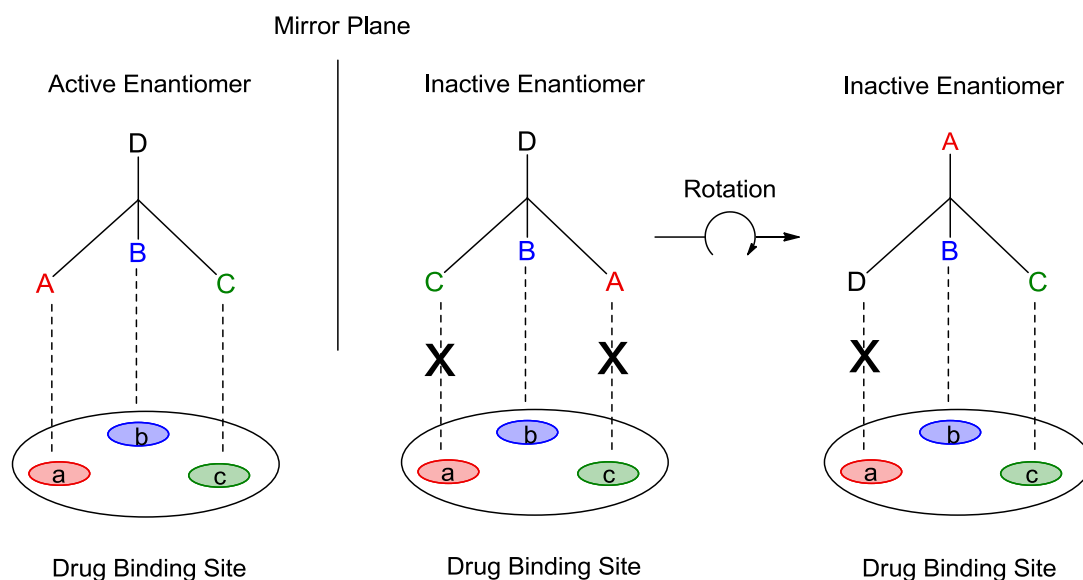


Figure 6. The hypothetical interaction between the 2 enantiomers of a chiral drug and its binding site.

1.1.2.1 Historical View on Drug Development

After the mid-1990s, there has been a sharp increase in the approval of chiral drugs towards racemic mixtures [11]. For example, Food and Drug Administration (FDA) approved more than 85% chiral drugs in 2006 [12]. Moreover, more than 75% of these were being produced and marketed as a single enantiomer. In the beginning of the twentieth century, there were a number of studies related to comparison of pure naturally occurring compound compared in effectiveness to racemic mixture. For example, activity of (-)-adrenaline on blood pressure was found 50% more active than its racemic mixture and thus concluded that (-)-adrenaline was 30 times more active than (+)-adrenaline [13] (Figure 7).

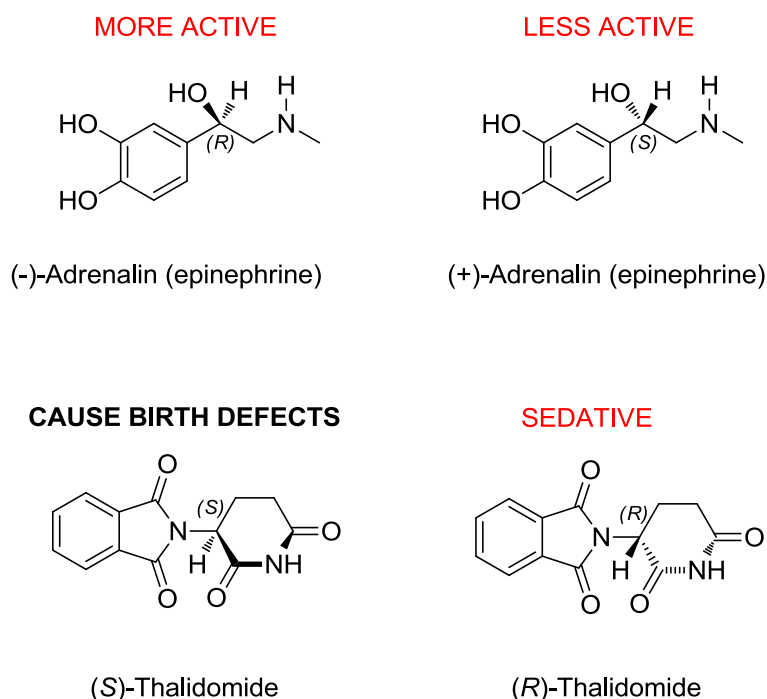
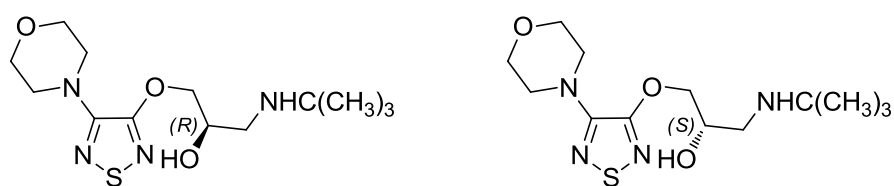


Figure 7. Molecular structures of adrenaline and thalidomide enantiomers.

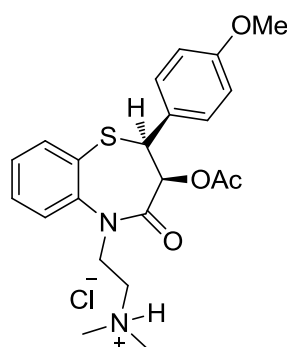
By the midtwentieth century, beside the new progresses in natural and unnatural drug production, there were a few tragedies. One of the worst was the marketing of the drug thalidomide. It has now been well known that the (*R*)-(+)-

thalidomide enantiomer is responsible for the sedative effects of this drug, and that the (*S*)-(-)-enantiomer is responsible for causing the birth defects [14]. It might seem that (*R*)-thalidomide could be used as a sedative drug. However, when the pure form of thalidomide is taken in the body, rapid racemization is occurred. As a result, our body is always exposed to the harmful enantiomer. Similar examples are shown in Figure 8.



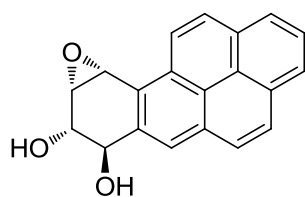
(*R*)-Timolol (adrenergic blocker)

(*S*)-Timolol (ineffective)

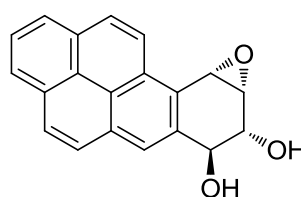


Diltiazem

(the (*S,S*)-form is effective in relieving myocardial infarction)



(-)-Benzopyryldiol
(strong carcinogenicity)



(+)-Benzopyryldiol
(no carcinogenicity)

Figure 8. Different behaviors of the drug enantiomers.

This story affected the regulation of new drug approval in the world and highlights the importance of chirality in drug development. In today, some of the popular drugs are drawn in Figure 9.

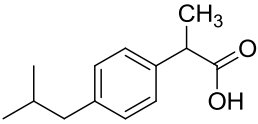

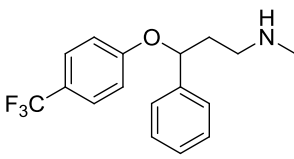

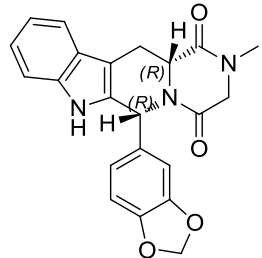

Structure	Sold as	Commercial name(s)
 <p>Ibuprofen</p>	<i>Racemic mixture</i>	
 <p>Fluoxetine</p>	<i>Racemic mixture</i>	
 <p>Tadalafil</p>	<i>(R,R)-Enantiomer</i>	

Figure 9. Popular drugs in today.

1.2 Source of Enantiomerically Pure Compounds

Economic, environmental and pharmacodynamic considerations all explain to develop methods for enantiomerically pure drugs and agrochemicals [15-18]. Basically, there are three main sources of homochiral compounds. These sources are:

- i. Chiral Pool
- ii. Resolution Methods
- iii. Enantioselective synthesis

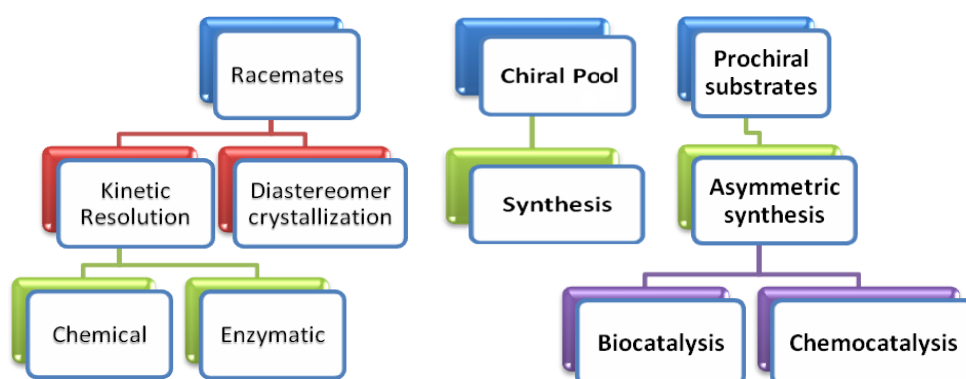
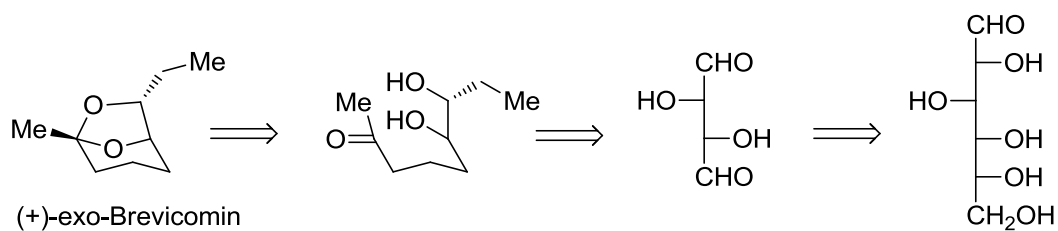


Figure 10. Synthetic route to enantiomerically pure compounds [19].

All of them are included in the concept of asymmetric synthesis. Beside the first explanation of asymmetric synthesis, current time, it is referred as a all methods to obtain enantiopure compounds.

1.2.1 Chiral Pool

The term chiral pool usually refers to the vast array of enantiomerically pure products, e.g. carbohydrates, terpenes, and alkaloids, that are readily available from nature. A lot of chiral molecules can be synthesized from natural carbohydrates or amino acids. The syntheses of (+)-*exo*-brevicomine shows the application of such naturally occurring material. 6,8-Dioxalicyclo[3.2.1]octane, or (+)-*exo*-brevicomine is the aggregating pheromone of the western pine beetle. It has been started from glucose using a procedure based on the retro synthesis design shown in scheme 1 [20].

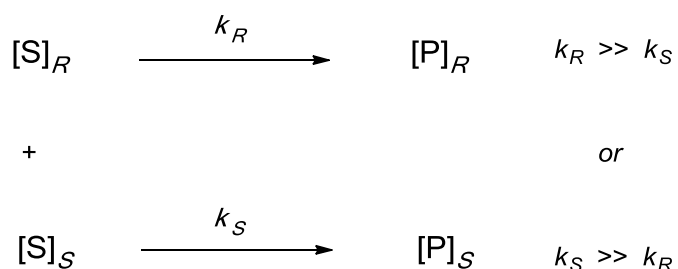


Scheme 1. Retro synthesis of (+)-*exo*-brevicomin.

However, there are limited number of compounds found in nature regarding complex structure and stereochemistry. Because of that, asymmetric synthesis and resolution will always be important strategies for gaining enantiopure compounds.

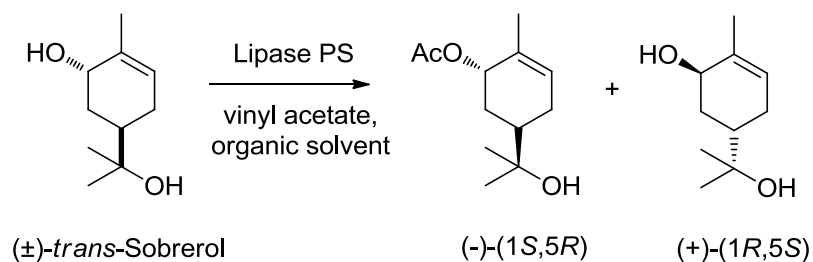
1.2.2 Kinetic Resolution

Beside the crystallization techniques, preferential[21] and diastereomer crystallization[22], especially on amine chemistry, one of the major strategies for enantiomerically pure compound preparation is the kinetic resolution (KR) of racemic mixtures, by chemical[23] or enzymatic[24] methods. In this case, one substrate enantiomer reacts much faster than the other one. Substrate or product (or both) can be obtained in high enantiomeric excess (*ee*) at a certain conversion value (Scheme 2).



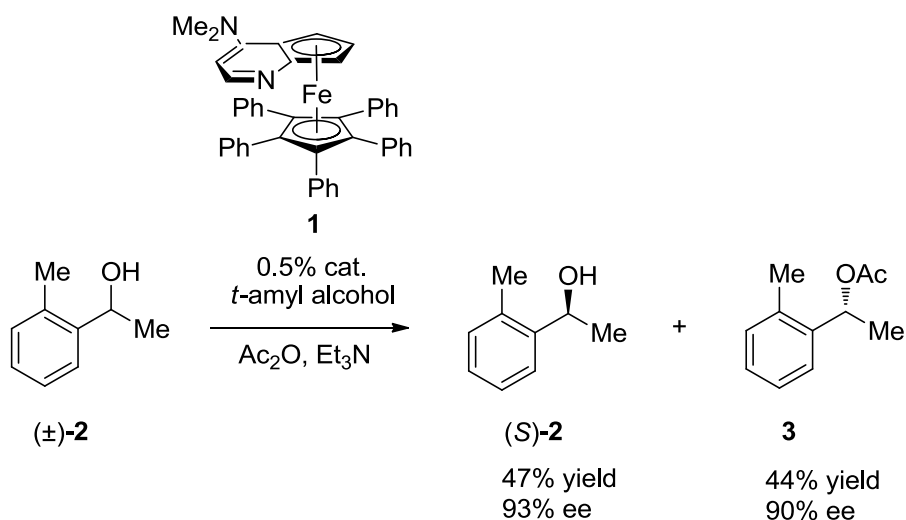
Scheme 2. Schematic representation of kinetic resolution.

One of important example of the classical kinetic resolution is acyl transfer reactions. A wide range of effective biocatalysts and chiral synthetic catalysts has been identified for acyl transfer reactions [25]. As an example for enzymatic method, the resolution of the mucolytic drug (\pm)-*trans*-sobrerol by enzyme is shown in scheme 3 [26].



Scheme 3. Kinetic resolution of (\pm)-*trans*-sobrerol.

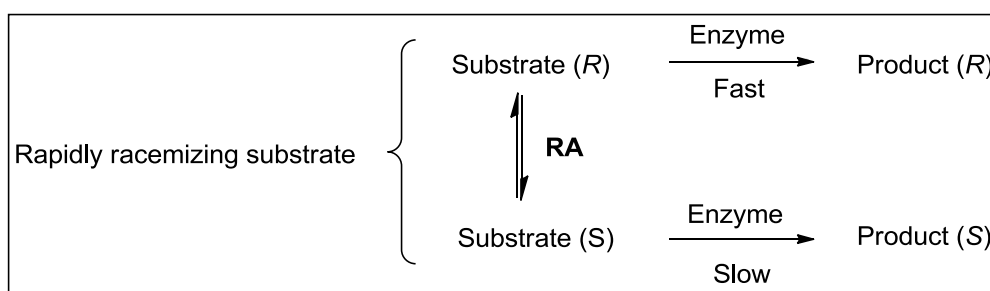
For chemical method, Fu et al. published in 1996, a new class of nucleophilic catalysts with a ferrocene substructure and planar chirality elements [27]. A carefully-designed dimethylaminopyridine (DMAP) analogue **1** proved to be most effective for the catalytic acylation of certain racemic secondary aryl alcohols **2** with good enantiodiscrimination, shown in scheme 4, [28,29].



Scheme 4. Fu's kinetic resolution of secondary alcohol.

Classical kinetic resolutions (KR) has the limitation of having a maximum theoretical yield of 50%. Although efficient in terms of producing highly enantiomerically pure compounds, it can be seen as displaying inherently poor atom economy [30]. However, the result of the resolution is a great chance to synthesize both form of enantiomers in one step regarding pharmacokinetic and pharmacodynamic differences between the enantiomers of drug.

There is a great effort the develop new strategies for kinetic resolution because of poor atom economy. The important one is called dynamic kinetic resolution (DKR). In this way, all of the reagent can be transformed to a single enantiomeric product via *in situ* racemization of slowly reactant substrate (Figure 11).

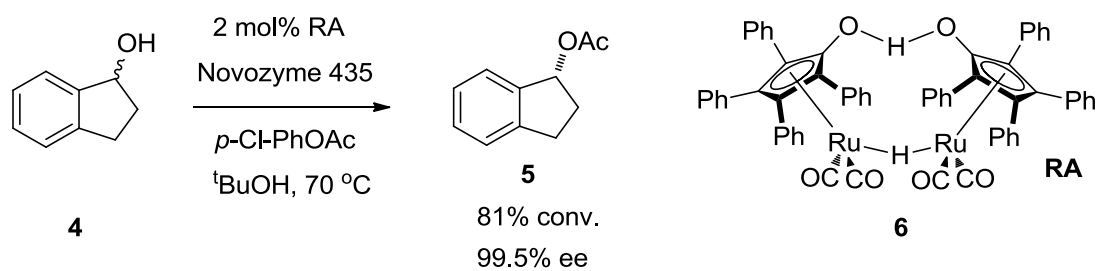


***RA**: Racemization Agent

*The production of enantiomerically pure products in theoretical 100% ee and with 100% conversion.

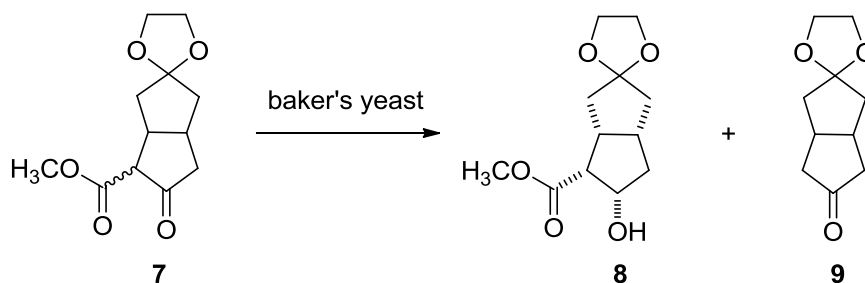
Figure 11. Schematic representation of DKR.

The important challenge in efficient DKR is obtaining suitable racemizing conditions that do not affect the resolution step and do not cause racemization of the final product. Scheme 5 shows the DKR of indenol (**4**) in the presence of RA **6** and enzyme [31].



Scheme 5. DKR of indanol.

Alternatively, it can be said that parallel kinetic resolution is another type of kinetic resolution. However, the major drawback of this technique is max 50% theoretical yield. In this methodology, the slower reacting enantiomer can be removed by a parallel reaction to different product. Scheme 6 shows an example of parallel kinetic resolution of an ester **7** [32].



Scheme 6. Parallel kinetic resolution of β -keto ester.

1.2.3 Asymmetric Synthesis

Asymmetric synthesis is described as stereoselective conversion of a prochiral substrate to an chiral product using chiral reagent or catalyst. There are a lot of ways to produce chiral compounds from achiral substrates. Apart from resolution, asymmetric synthesis can provide a more general approach to the

preparation of enantioenriched compounds. It is limited by the range and scope of available methodology [33].

Alternative to methodologies described in above chapter that is source of enantiomerically pure compounds, usage of chiral catalyst, chiral reagents and chiral auxiliaries are another methods for enantioselective synthesis.

In the chiral auxiliary strategy; an enantiopure compound usually derived from a natural product like an simple amino acid, called a chiral auxiliary, is attached to the starting material [34]. After reaction, chiral auxiliary is removed and single enantiomeric product of reaction is obtained. Scientists have developed numerous chiral auxiliaries **10-18** shown in Figure 12 over the past years. Most of them are derived from cheap natural compounds.

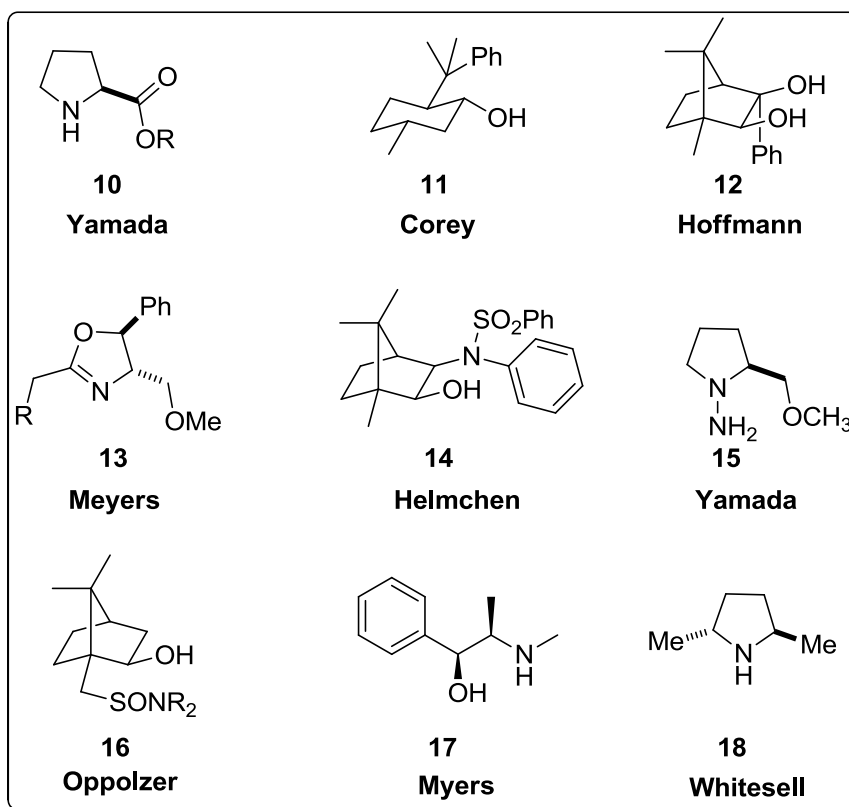
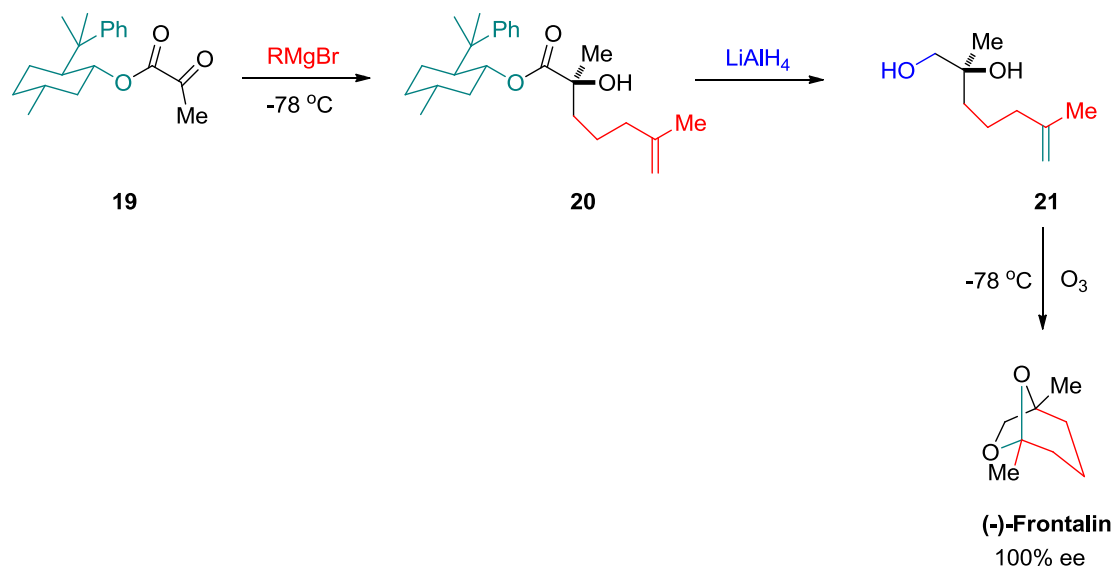


Figure 12. Selected chiral auxiliaries in asymmetric synthesis.

Asymmetric Diels-Alder and alkylation reactions are the main applications of chiral auxiliaries. Scheme 7 shows the Corey's auxiliary **12** in the asymmetric synthesis of (-)-frontalin aggregation pheromone of the *Southern Pine Beetle*. It is the the most destructive beetle to pine forests in southeastern united states.



Scheme 7. Corey's auxiliary in the asymmetric synthesis of frontalin.

Chiral catalysis is an important method for synthesizing optically active compounds. In this way, small amount of man-made chiral catalyst produces chiral materials from achiral substrates. It is now the most significant subject in asymmetric synthesis. There have been many reports in the literature to develop new catalysts, since the obvious benefit of catalytic asymmetric synthesis is that only small amounts of chiral catalysts are needed to generate large quantities of chiral products just as enzymes do in biological systems. Chiral transition metal complexes, enzyme and the new concept , organocatalysis after 2000 [35], are the main categories of this title. During the past decade, there has been a remarkable increase in interested works in the area of organocatalysis [36]. Figure 13 shows the some selected typical chiral organocatalysts.

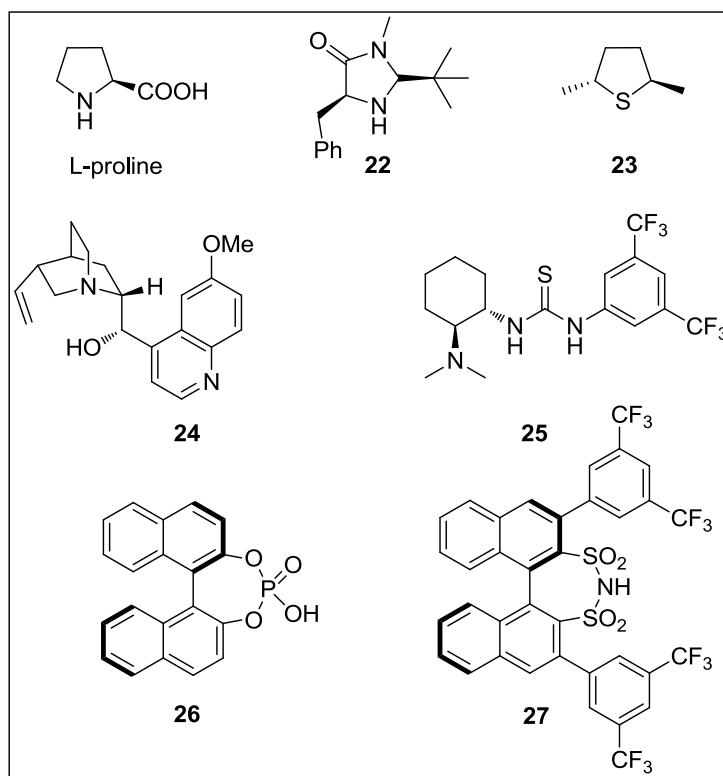
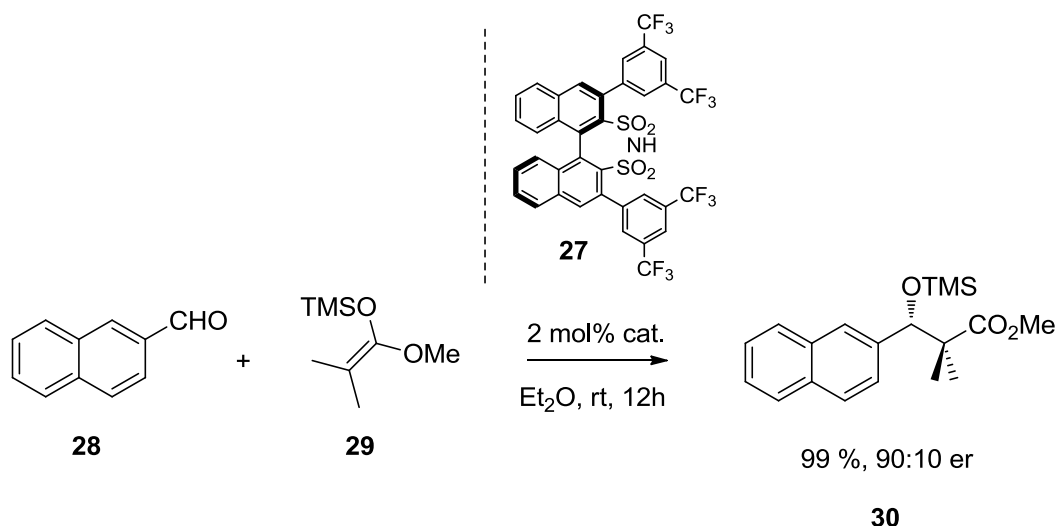


Figure 13. Selected typical chiral organocatalysts.

As an example, recently, Benjamin List et al. published a new type of highly efficient organocatalyst **27** for the Mukaiyama aldol reaction. The desired product **30** was obtained in high yield and enantioselectivity in the presence of 2 mol% catalyst **27** after the reaction between naphthaldehyde **28** and ketene acetal **29** [37], (Scheme 8).



Scheme 8. List's organocatalyst catalyzed Mukaiyama aldol reaction.

All of the methods for asymmetric synthesis have disadvantages and advantages. Table 1 shows these comparisons.

Table 1. Comparison of asymmetric methods

Method	Advantages	Disadvantages	Examples
Resolution	Both enantiomers available	Max 50% yield	Synthesis of BINAP
Chiral pool	100% ee guaranteed	Often only one enantiomer available	Amino acid and sugar derived synthesis
Chiral auxiliary	Often excellent ees; can recrystallize to purify to high ee	Extra step to introduce and remove the auxiliary	oxazolidinones
Chiral reagent	Often excellent ees; can recrystallize to purify to high ee	Only a few reagents are successful and often for few substrates	Enzymes, CBC reducing agent
Chiral catalyst	Economical; only small amounts of recyclable material used	Only a few reactions are really successful; recrystallization only improve already high ee	Asymmetric hydrogenation, epoxidation, dihydroxylation

1.3 Biotransformation and Green Chemistry

The use of biological systems to perform chemical modifications on compounds are referred as biotransformations [38]. Biotransformations have many advantages when compared to related chemical methods. Most of them are not only stereo and regiospecific but also enantiospecific producing chiral compounds from racemic mixture. Major advantages of biotransformations are that the reaction conditions are mild and it doesn't require to protect other functional group on the molecule. The other parameter is Green Chemistry. Cheaper, atom economical and environmentally reaction conditions are simply included in this approach. The term "Green Chemistry" was firstly used by Anastas in 1993 [39]. Green Chemistry can be further explained by Sheldon as follows; "*Green chemistry efficiently utilized (preferably renewable) raw materials, eliminates waste and avoids the use of toxic and/or hazardous reagents and solvents in the manufacture and application of chemical products*" [40].

Anastas has pointed out the 12 main principles[41-43] which can be paraphrased as:

1. Waste prevention instead of remediation
2. Atom efficiency
3. Less hazardous/toxic chemicals
4. Safer products by design
5. Innocuous solvents and auxiliaries
6. Energy efficient by design
7. Preferably renewable raw materials
8. Shorter synthesis (avoid derivatization)
9. Catalytic rather than stoichiometric reagents
10. Design products for degradation
11. Analytical methodologies for pollution prevention
12. Inherently safer processes

There are many advantages e.g. mild reaction conditions and often reduced steps than classical chemical procedures because of that it is not necessary to protect and deprotect the functional groups. Nowadays, there has been increasing interest in the use of biocatalytic alternative methods instead of conventional chemical procedures in the fine chemicals industry [44].

1.3.1 Enzymes

Metabolism of all living cells need to be catalyzed by biocatalyst referring to use of enzymes, protein molecules that have evolved to perform efficiently under the mild conditions. Enzymes have distinct properties when compared with chemical catalyst because of their complex molecular structure [45]. Advantages and drawbacks of enzymes as catalysts are summarized in Table 2.

Table 2. Advantages and drawbacks of enzymes as catalysts

Advantages	Drawbacks
<i>High specificity</i>	<i>High molecular complexity</i>
<i>High activity under moderate conditions</i>	<i>High production costs</i>
<i>High turnover number</i>	<i>Intrinsic fragility</i>
<i>Highly biodegradable</i>	
<i>Generally considered as natural products</i>	

Enzymes are used in a wide variety of industrial sectors. In recent years, enzymes have been adopted by the pure chemical industries especially in the context of stereomerically pure products [46]. There are also some disadvantages e.g. instability, deactivation by high pH, temperature, and solvents for enzymes. However, new developments on enzyme engineering have done important

advancements and discovered very mild and efficient conditions for fine chemical production.

1.3.1.1 Enzymes Classes

Enzymes are classified into 6 main classes according to type of reactions by International Union of Biochemistry (IUB). The main classes are further subdivided into subclasses and subgroups.

➤ Oxidoreductases

These type of enzymes catalyze the oxidation-reduction reactions in which hydrogen, oxygen and electrons are transferred between molecules. Subclasses are;

Dehydrogenases: hydride transfer

Oxidases: electron transfer to molecular oxygen

Oxygenases: oxygen transfer from molecular oxygen

Peroxidases: electron transfer to peroxide

➤ Hydrolases

These type of enzymes catalyze the hydrolytic cleavage of bonds. Many commercially important enzymes belong to this class, proteases, amylases, acylases, lipases and esterases.

➤ Lyases

These type of enzymes catalyze the non hydrolytic cleavage of bonds. Addition-elimination reactions on C=C, C=N, C=O bonds are evolved in this class. Subclasses are fumarase, aspartase, decarboxylases, dehydratases and aldolases.

➤ Isomerases

These type of enzymes catalyze isomerization and transfer reaction within one molecule. D-xylose ketol isomerase is the most important member of this class also known as glucose isomerase.

➤ Ligases

These type of enzymes catalyze the covalently bonded of two molecules coupled with the hydrolysis of an energy rich bond in ATP or similar triphosphates. Important example is γ -L-glutamyl-L-cysteine: glycine ligase (ADP-forming) known as glutathion synthetase.

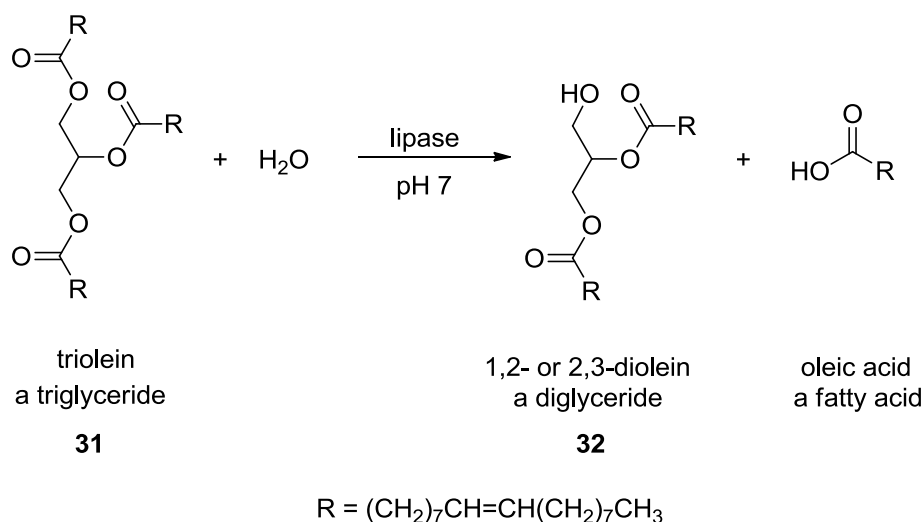
1.3.1.2 Lipases

Lipases are found in animals, plants and microorganism. Their role in these is probably digestive. Most biotransformations use commercial lipases. There are 70% of lipase now available. Table 3 shows the popular ones. Lipases are named regarding to organisms producing lipases.

Table 3. Selected commercially available popular lipases

Abbreviation	Origin of lipase (Other Name)	Commercial source and name
Mammalian Lipase		
PPL	Porcine pancreas	Amano, Fluka, sigma
Fungal Lipase		
CRL	<i>Candida Rugosa (Candida cylindracea)</i>	Amano (lipase AY)
RJL	<i>Rhizomucor javanicus (Mucor javanicus)</i>	Amano (lipase M)
CAL-A	<i>Candida antartica A</i>	Novozyme (SP 526)
CAL-B	<i>Candida antartica B</i>	Novozyme (Novozym 435), Sigma
CLL	<i>Candida Lipolytica</i>	Amano (lipase L)
PFL	<i>Pseudomonas fluorescens</i>	Amano (lipase AK), Biocatalyst Ltd

Lipases and esterases are important parts of hydrolyases. Both of them catalyze the hydrolysis of ester but lipases specially catalyze the hydrolysis of triglycerides which are water insoluble. As an example, scheme 9 shows the lipase catalyze hydrolysis of triglyceride triolein **31** to diolein **32**.



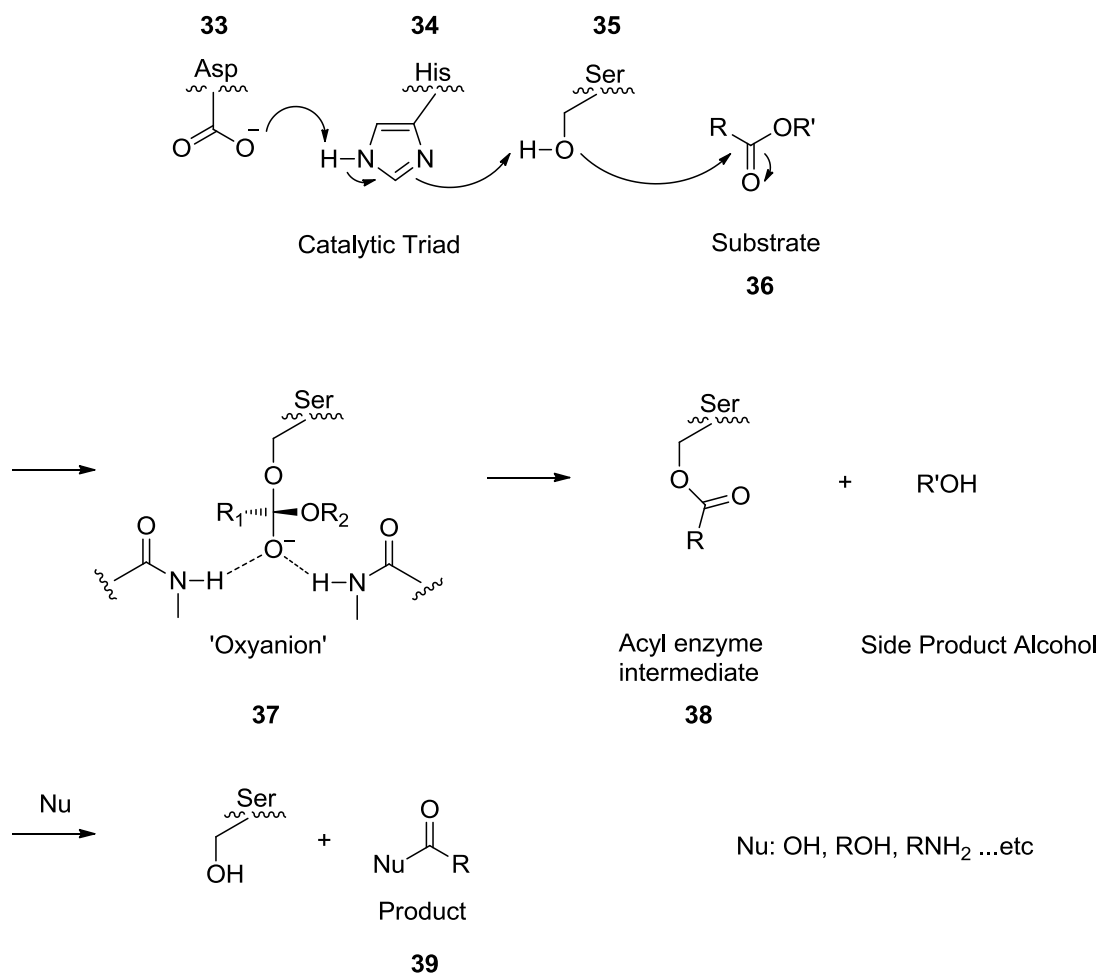
Scheme 9. Lipase catalyze hydrolysis of triolein to diolein.

Moreover, lipases also catalyze the hydrolysis of other majority of natural and unnatural ester while retaining high regio or enantioselectivity. These high selectivity and broad substrate range make lipases a preferred biocatalysts for organic synthesis. In chemical industry, lipase are widely used biocatalyst in hydrolytic kinetic resolution reactions of alcohols and amines to obtain enantiomerically pure pharmaceuticals and synthetic intermediates, because of their high catalytic activity and stability in organic solvents [47].

1.3.1.2.1 Selectivity of Lipases

Lipases come from serin hydrolyse family and have same active site of the serine proteases. The active side of lipases consist of catalytic triad composed of

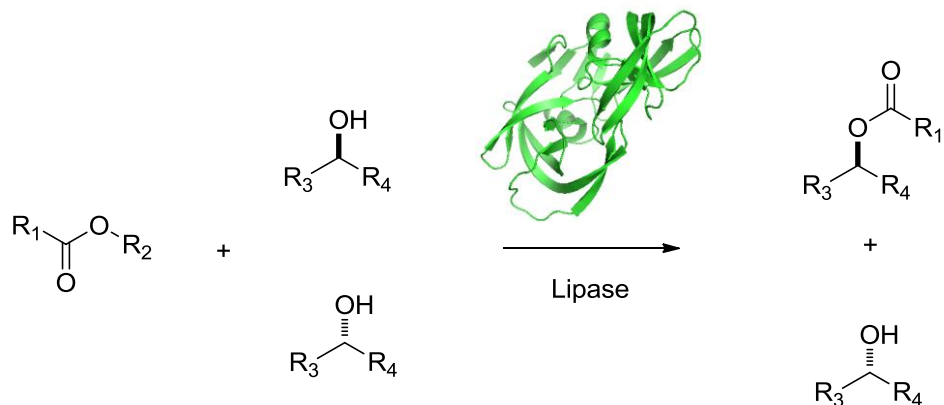
serine **35**, histidine **34**, aspartate **33** and oxyanion hole **37** [48-51]. The reaction mechanism called as bi-bi ping-pong is illustrated in scheme 10.



Scheme 10. Mechanism of Lipase catalyze hydrolysis of ester.

The catalytic triad of lipase starts with serine residue **35** activated by histidine **34** and aspartate residues **33**. In the first step, oxygen atom belonging serine residue reacts with carbonyl group of ester **36** to form tetrahedral acyl enzyme intermediate. At this point, forming negatively charged oxygen is stabilized by the oxyanion hole **37**. In the second step, alcohol attached to acyl enzyme intermediate is removed and serinate ester **38** is formed. After that nucleophile attacks the serinate ester and the

product **39** and free enzyme are formed. The kinetic resolution of an alcohol via lipase catalyzed acylation is shown in scheme 11.



Scheme 11. Lipase catalyzed enantioselective acylation of an alcohol.

Since lipase catalysis is enantiospecific, there are such rules to explain these enantioselectivity comparing with lipase family. The important and widely used one is Kazlauskas rule [52-55]. According to this rule, many lipase preferentially catalyse the one of the enantiomer of alcohol or amine faster than other enantiomer in the resolution process (Figure 14). Depend on the stereochemical outcome, if the medium-sized group has lower priority than larger group (L), the (*R*) acetate is obtained. Generally, major size difference between large and medium-sized groups give the better enantioselectivities.

X-ray studies have explained this stereoselectivity based spatial arrangement of the catalytic residue of enzyme. All of the lipase work with a catalytic triad based on this studies [56-57].

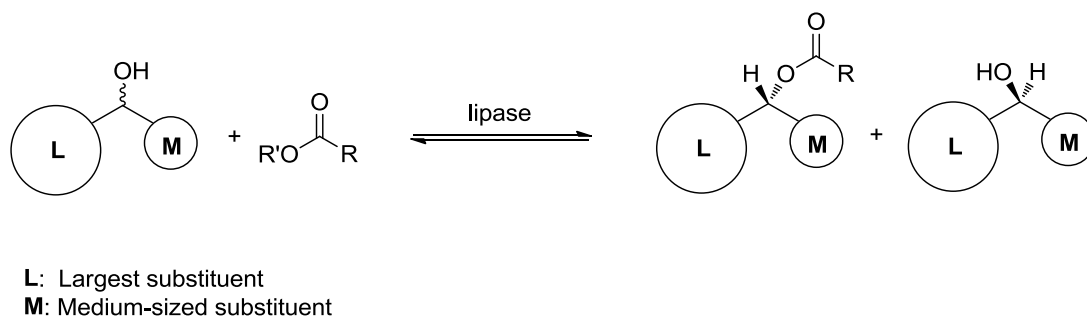
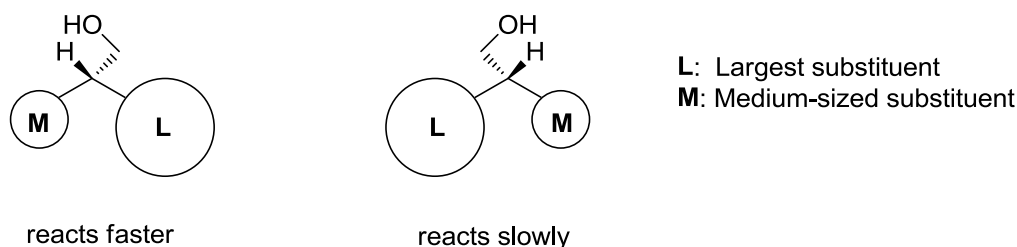


Figure 14. Schematic representation of Kazlauskas rule in the Enzymatic KR of an secondary alcohol.

Most of the lipase obey this rule, however there are such limitations [58]. For example, in the PCL (*Pseudomonas cepacia lipase*) catalyzed conversions of primary alcohols having chiral carbon in the β -position, the rule is only reliable, if there are no oxygen placed on next to the chiral carbon (Figure 15).



! The selectivity is low if oxygen is bound to the chiral carbon

Figure 15. Schematic representation of faster enantiomer in the PCL catalyzed acylation of primary alcohol.

For comparison of enzyme catalyzed reactions, two important term, the enantiomeric excess (ee) and enantiomeric ratio (E), are defined.

The ee value expresses the enantiomeric purity of any compound. It is defined as follow:

$$\%ee_R = \frac{R - S}{R + S} \times 100 \quad \text{For } R > S$$

Where R and S are enantiomeric substrates. In theory, the ee value of racemic compound is zero, whereas the enantiopure compound's ee is 1 or 100% ee. The enantiomeric ratio is a parameter to describe enantioselectivity of lipase catalyze reactions. There are such expressions for determination of E value. In this thesis, E value was determined by equation shown below. Chen et al. [59-60] developed this equation based on ee of the product (ee_p), conversion (c) and ee of the unreacted substrate (ee_s).

$$E = \frac{\ln[(1-c)(1-ee_s)]}{\ln[(1-c)(1+ee_p)]}$$

Where conversion (c) is calculated by:

$$c = \frac{ee_s}{ee_s + ee_p}$$

1.3.1.2.2 Enantioselective Lipase Catalyzed Reactions in Organic Chemistry

Enzyme catalyzed reactions carried out in organic solvents have some advantages over aqueous based biocatalysis [61]. The reason is that water is not suitable catalysis for most organic compounds which are unstable and poorly soluble in water. Moreover, water can't be remove easily from reaction medium because of its high boiling point. “ These advantages are indicated in review by Ghanem et al [62];

- The use of organic solvents having low boiling point facilitate the recovery of product with better overall yield
- Non-polar substrates are converted at a faster rate due to their increased solubility in the organic solvent [63].
- Deactivation and/or substrate or product inhibition is minimized,
- Side reactions are largely suppressed,
- Immobilization of enzymes is not required,
- Denaturation of enzymes (loss of the native structure and thus catalytic activity) is minimized,
- Shifting thermodynamic equilibria to favor synthesis over hydrolysis.”

Lipase have been widely used as a valuable catalyst in organic synthesis especially in three main categories which are kinetic resolution of alcohols, amines or carboxylic acid, enantioselective differentiations of meso diols or carboxylic acid and enantiotopic group differentiation of prochiral diol and carboxylic acid derivatives [64].

These transesterification reactions generally are applied with enol ester such as vinyl acetate . The choice of acetyl donor source is important because it effects the reaction rate (Figure 16). For example, kinetic resolution of alcohol in the presence of vinyl acetate or isopropenyl acetate much faster than reactions using esters such as ethyl acetate and the back reaction is suppressed due to the tautomerization of the forming enol alcohol **42**. In addition to enol esters **41**, oxime esters **40** have been applied as acyl transfer agents as well. However this approach has some disadvantages in the case of reversibility and limited-rate of the reaction like trichloroethyl or trifluoroethyl esters used in resolution [65]. Scheme 12 shows the lipase catalyzed irreversible transesterifications.

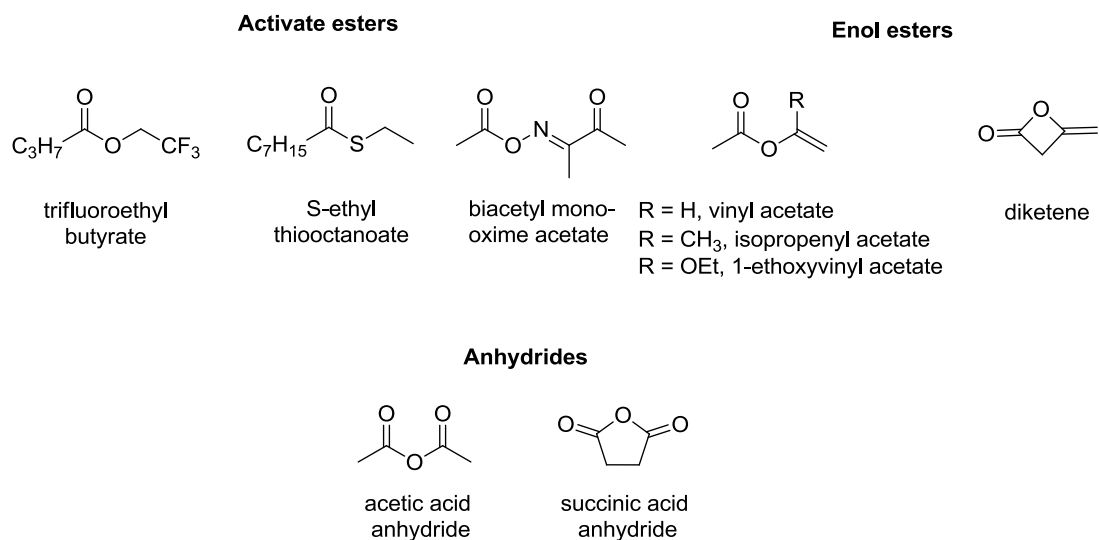
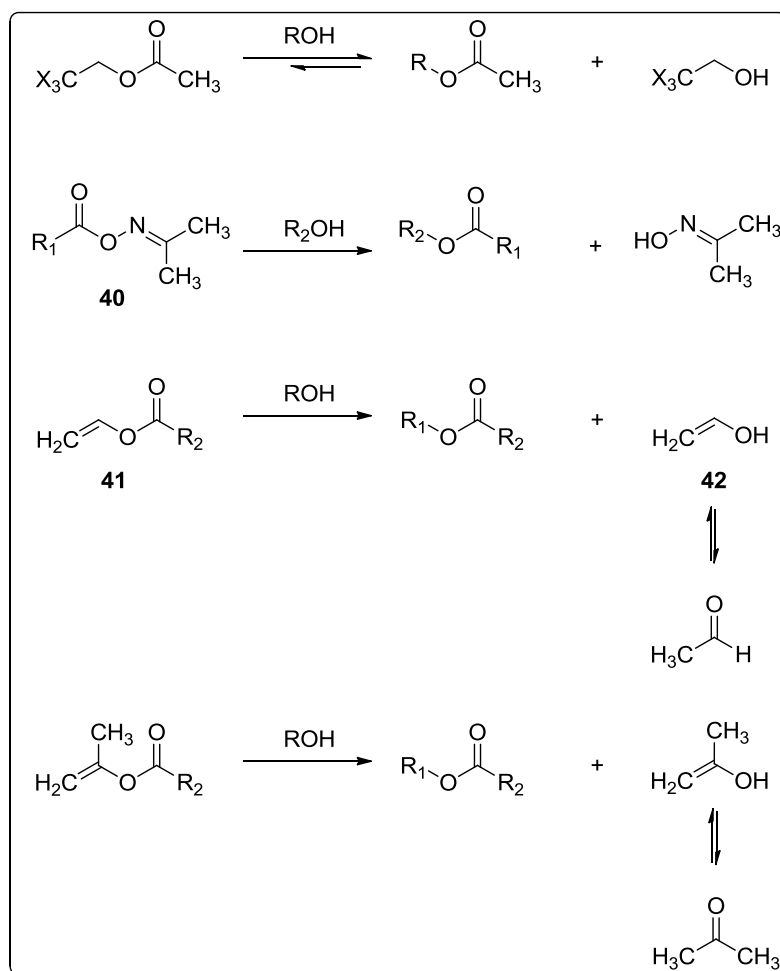


Figure 16. Examples of activated acyl donors for acylation of alcohols.



Scheme 12. The lipase catalyzed irreversible transesterifications.

1.3.1.2.2.1 Lipase Catalyzed Resolutions of Secondary Alcohols

Lipases are highly efficient biocatalyst for wide range of racemic substrates. Secondary alcohols are the most common substrates and there are many works to find out efficiency of lipases on these type of substrates [66]. As mentioned earlier, most lipases follow the Kazlauskas rule, based on the size of substituents. A number of studies have been published to increase the enantioselectivity of lipase catalyzed reactions by changing the size of substituents. Selected examples of the 2-alkanols **43-59** and cyclic secondary **60-65** alcohols are shown in Figure 17 regarding this phenomenon.

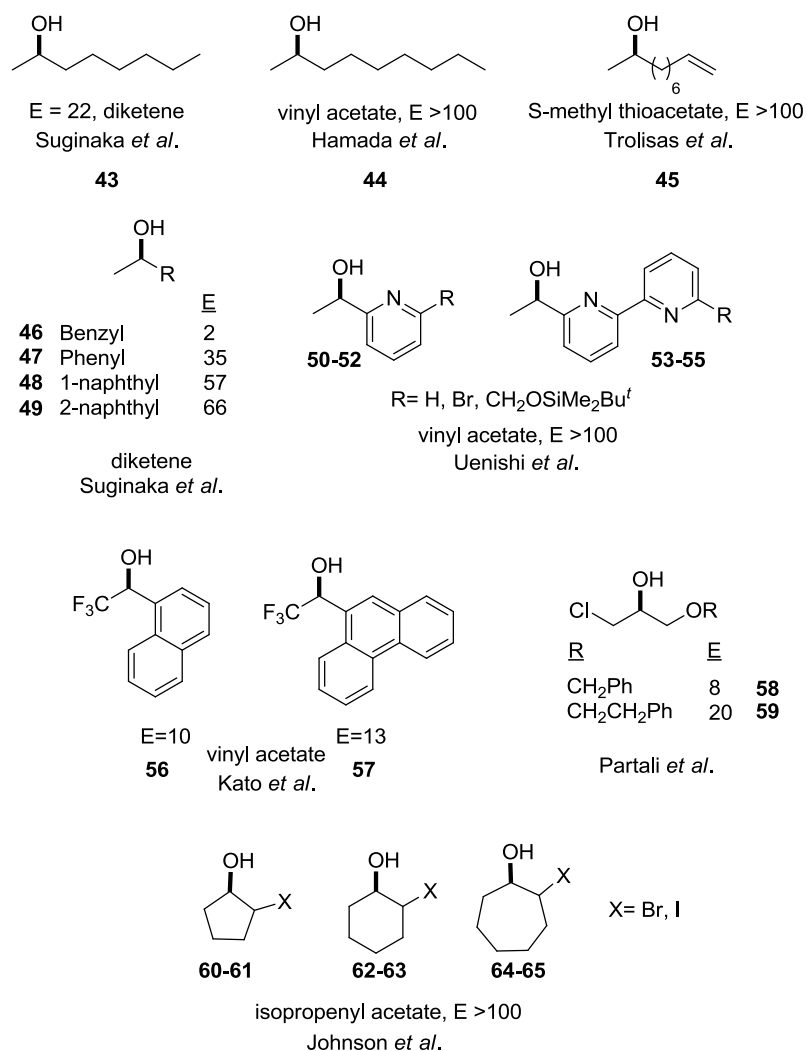
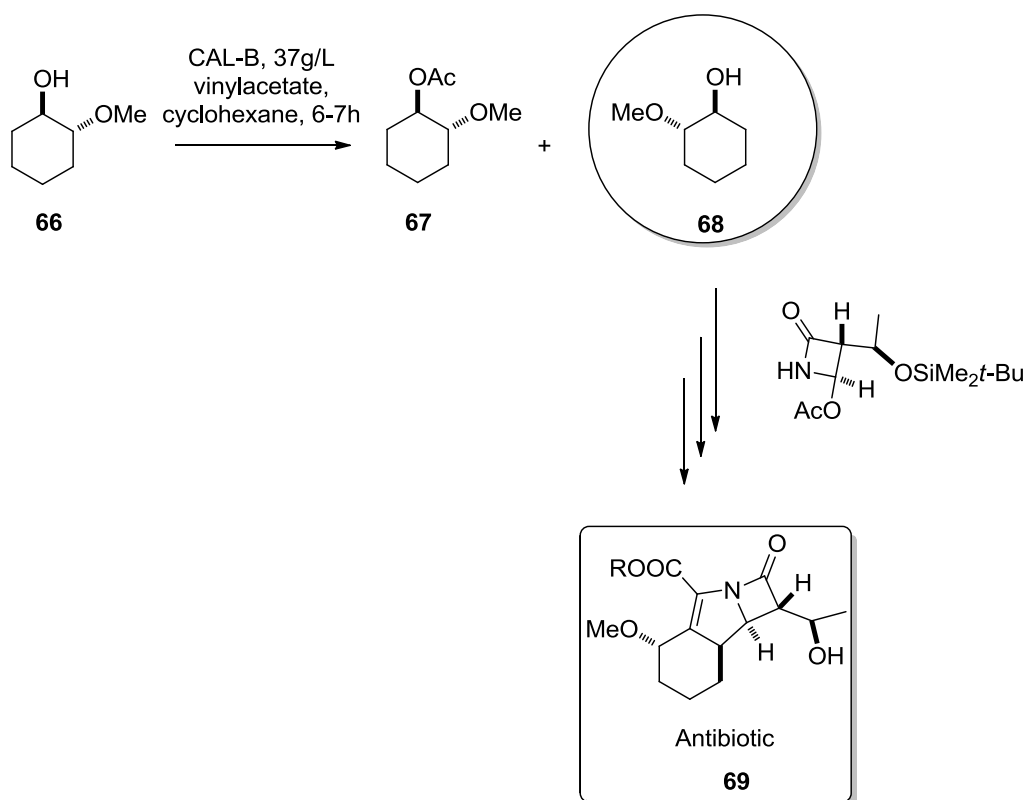


Figure 17. The CAL-B catalyzed resolution of 2-alkanols and cyclic secondary alcohols [67-75].

1.3.1.2.2 Lipases in Preparation of Pharmaceuticals

Enzymatic resolution for drug intermediates with especially chiral amine or alcohol is a well developed approach in pharmaceutical industry. Lipase catalyzed resolution of chiral amines or alcohols is rapidly being increased [76-82] related to such reports indicating that companies applies these resolutions at a scale of 1000 t/a [83].

One of the example is that enzymatic resolution of (1*S*,2*S*)-*trans*-2-methoxycyclohexanol (**66**), a key intermediate for the synthesis of β -lactam antibiotic **69** [84]. GlaxoSmithKline (gsk, UK) resolves this secondary alcohol over a ton scale for the production. The reaction is carried out at RT in the presence of CAL-B and vinyl acetate and slow reacting enantiomer **68** is obtained in 99% ee. PFL is also used and show high enantioselectivity, however, immobilized CAL-B is more stable over reuses. Although there is another way that is hydrolysis of its ester to obtain (1*S*,2*S*)-*trans*-2-methoxycyclohexanol (**66**), GlaxoSmithKline prefer to use resolution via acylation of the alcohol because it gives directly the required alcohol (Scheme 13).



Scheme 13. Enzymatic resolution of a building block for antibiotic synthesis.

There are many reports found in the literature that involve production of building blocks for important drugs. Some of them **70-72** are summarized in Figure 19.

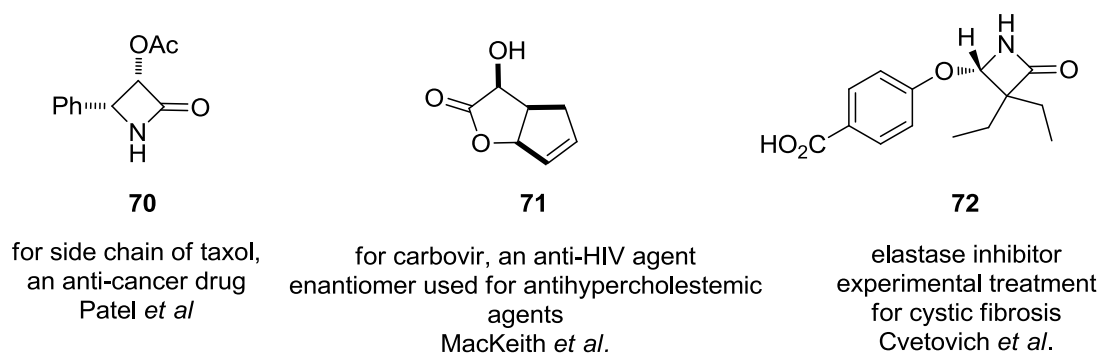
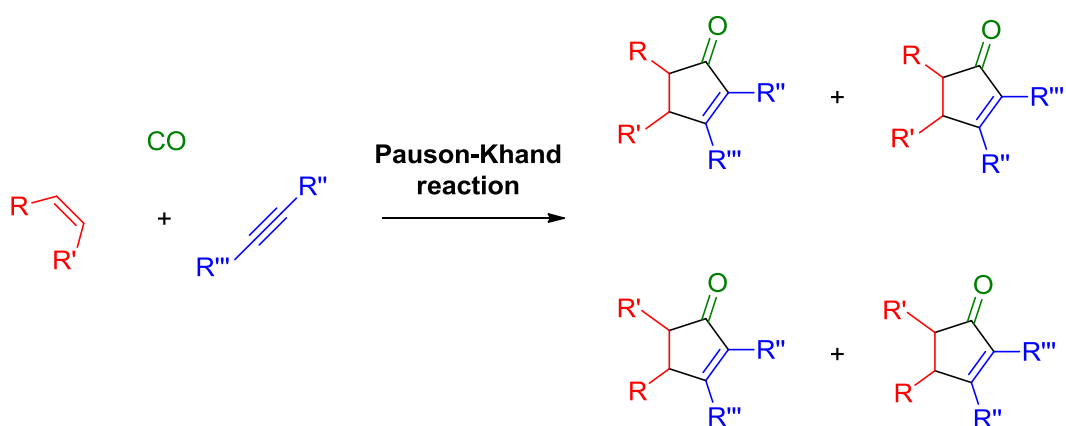


Figure 18. Kilogram-scale routes to pharmaceutical precursors involving lipases [85-88].

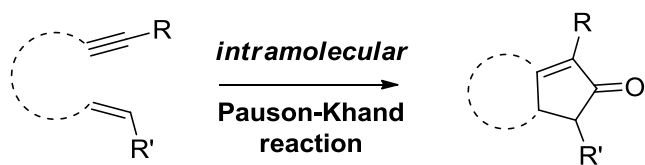
1.4. Pauson Khand Reaction

Transition metal catalyzed reactions play an important role in especially C-C bond forming reactions allowing construction of complex molecules [89]. For the synthesis of five-membered rings, Pauson Khand reaction (PKR) is one of the earliest and most useful reaction. This reaction was first discovered in 1971 by Pauson and Khand [90-91]. PKR is described as the transition metal (cobalt) mediated formal [2+2+1] cycloaddition of alkenes, alkynes and CO to form substituted cyclopentenones (Scheme 14).



Scheme 14. Intermolecular Pauson-Khand reaction.

In the beginning of the early studies, only symmetrical alkenes or alkynes such as norbornene or ethylene were used because it was envisaged that if other unsymmetrical alkynes or alkenes were used, the unwanted regioisomers could be formed and this could cause poor atom economy and difficulties in purification and separation. However, continued studies have shown that after reaction, the regiochemistry regarding alkyne part is predictable and reaction give only one isomer. At this point, intramolecular version of the PKR could be expected that it prevent formation of mixtures of regioisomers and give one type of expected cyclopentenone. (Scheme 15). The first example of the intramolecular PKR was introduced in 1981 by Schore et al [92].



Scheme 15. Intramolecular Pauson-Khand reaction.

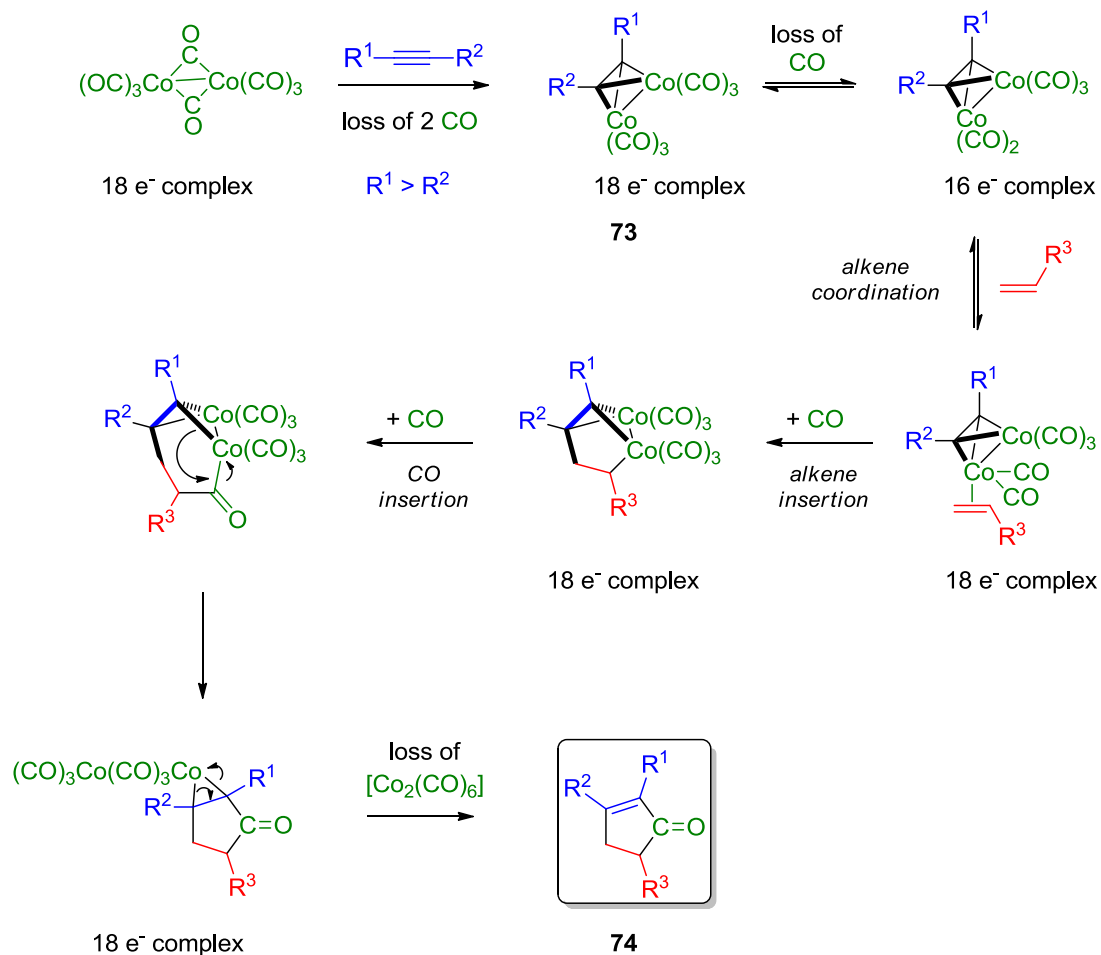
Although PKR had wide range of applications on such as esters, thioethers, amines, sulfonamides, and alcohols, it also had many limitations. One of them was indicated in original paper where stoichiometric amount of $\text{Co}_2(\text{CO})_8$ was used. Moreover, the reaction needed high temperature for transformation, and this could cause decomposition of substrates and/or products. Also, terminal alkynes were more reactive than internal alkynes and strained olefins were necessary for efficient intermolecular cyclization.

1.4.1 Mechanism

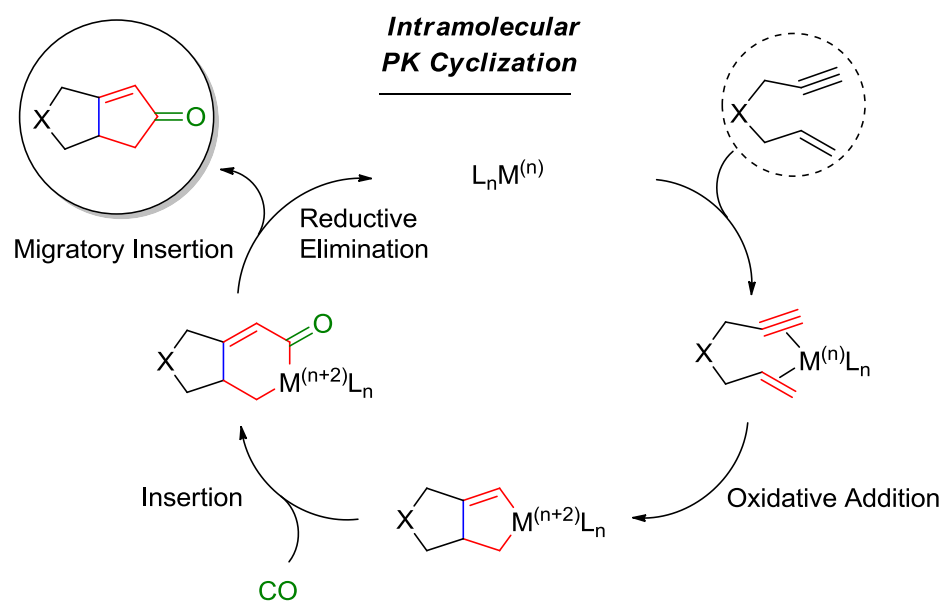
Although there is no exact mechanistic explanation for PKR, many examples have been proposed the mechanism based on regio- and stereochemical observations [93]. This proposed mechanism is shown in scheme 16. The initial step is formation of stable alkyne- $\text{Co}_2(\text{CO})_6$ **73**. After, it is assumed that this complex coordinates to the alkene and so CO ligand dissociation is happened. Then, the next step involves irreversibly insertion of alkene into one of the cobalt-carbon bonds. Also, this step is referred as rate determining step as well as product determining. After this step, the reaction follows the formation of carbonyl moiety via migratory insertion of a CO ligand bound to cobalt, and reductive elimination of the $\text{Co}(\text{CO})_3$. Finally, the cyclopentenone product **74** is formed after loss of the $\text{Co}_2(\text{CO})_6$ fragment.

The alkene insertion step is thought to determine the regioselectivity. In this case, alkene insertion takes place on exclusively at the carbon having less steric hindrance, if unsymmetrical alkyne is involved in cobalt-alkyne complex.

Therefore, it can be said that regioselectivity of the product is predictable respecting to alkyne.



Scheme 16. Proposed mechanism of Pauson-Khand reaction.



Scheme 17. Mechanism of Intramolecular Pauson Khand cyclization.

1.4.2 Promotion

The main disadvantages of the PKR are the high temperatures and long reaction times. To overcome to these problems, many methods have been developed for the promotion of the reaction. Schreiber [94] and Jeong [95] first reported a real improvement in the utility of the PKR. They independently explored that tertiary amine *N*-oxides were useful promoters for the reaction. In the first step of mechanism, reaction is needed harsh reaction conditions for CO loss leading to alkene insertion in the thermally promoted PKR. Schreiber found that NMO (*N*-methylmorpholine *N*-oxide) was effective in promoting the PKR at room temperature. Jeong et al. extended the promoter option by using trimethylamine *N*-oxide (TMANO). They assumed that the *N*-oxide responsible for removing a CO ligand from the metal oxidatively as carbon dioxide. There are other promoters been reported so far such as molecular sieves [96-97], amines [98-99], silica [100] and sulfides [101] but tertiary amine *N*-oxides are still widely used.

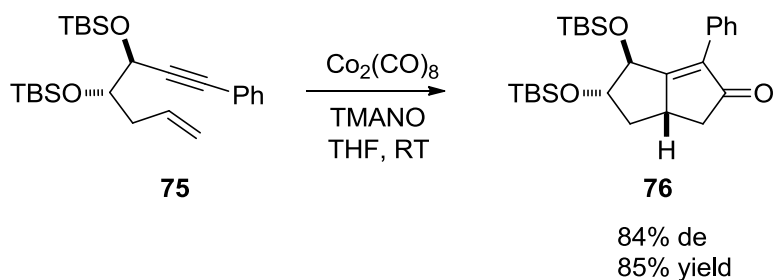
1.4.3 Asymmetric Pauson Khand Reaction

There are many advances been made in the development of asymmetric PKR. They are devided four main catagories. These approaches are;

- Chiral pools (precursor)
- Chiral auxiliaries
- Chiral metal complexes
- Chiral promoters

1.4.3.1 Chiral Pools

Many researcher have used chiral pool approache to transfer chirality in PK cycloaddition. One of the examples utilizes the diethyl *L*-tartrate as the starting material of precursor **75** for the asymmetric cycloaddition. Depending on the reaction conditions, acceptable diastereoselectivity and good yields were obtained [102-103] (Scheme 18).

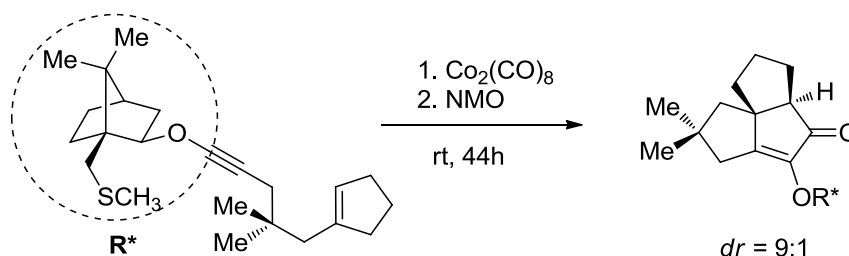
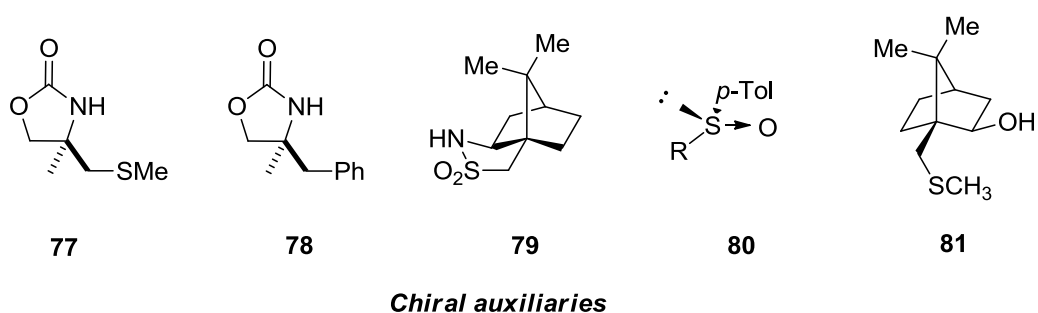


Scheme 18. Optically active products derived from diethyl *L*-tartrate.

1.4.3.2 Chiral Auxiliaries

The other technique for introducing chirality on aimed product is chiral auxiliaries approache. It has attracted the researchers because the diastereomers

formed after reaction are separable by chromatography and chiral auxiliary can be removed from product. Another advantage that chiral auxiliary could be used several times without any decrease on diastereomeric excess. Many different and useful auxiliaries have been involved in PKR (Scheme 19), including chiral oxazolidinones **77-78** [104], Oppozzer's sultam **79** [105] and *tert*-butylsulfinyl group (**80**) [106]. Moreover, Pericas and co-workers have explored new set of chiral auxiliaries derived from 10-methylthioisoborneol (**81**) and they assumed that cobalt-sulfur chelation improve diastereoselectivity [107-108].

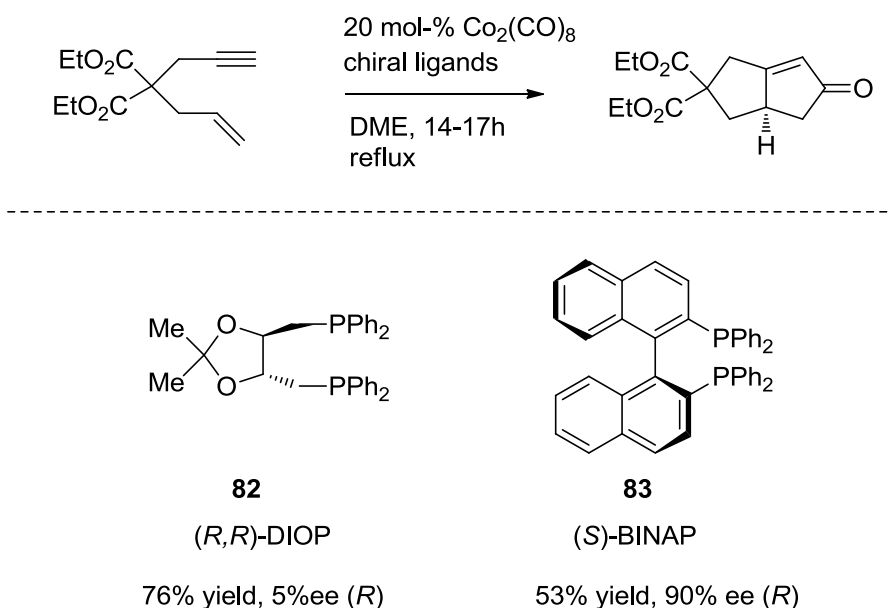


Scheme 19. Selected chiral auxiliaries and methylthioisoborneol mediated intramolecular PK reaction.

1.4.3.3 Chiral Metal Complexes

To effect the enantioselectivity in Pauson-Khand reaction, chiral metal (generally cobalt) complexes has been employed in cyclization. Popular chiral

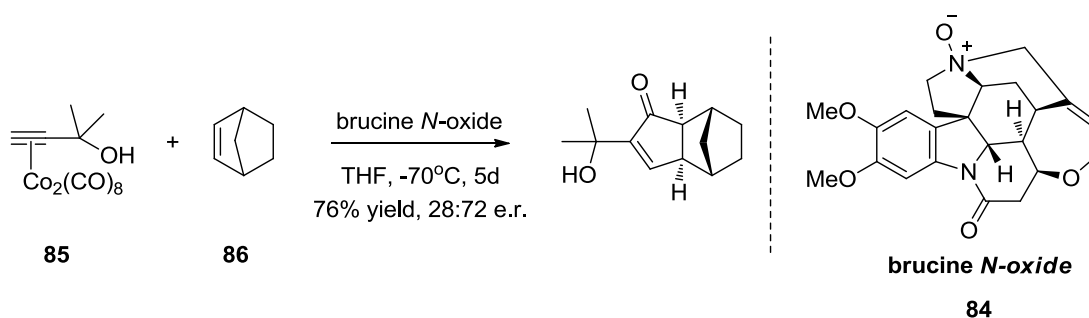
phosphine ligands, such as (*R,R*)-DIOP (**82**) or (*S*)-BINAP (**83**) are the most feasible examples for the formation of pure metal complexes (Scheme 20). Excellent or acceptable enantiomeric or diastereomeric excesses were obtained with these complexes in mild reaction conditions [109-111]. Chiral heterobimetallic complexes also were used as an alternative approach where the reaction could take place at only one metal center preferentially. These complexes give diastereomerically or enantiomerically enriched products as well [112-113].



Scheme 20. Intramolecular asymmetric PK reaction.

1.4.3.4 Chiral Promoters

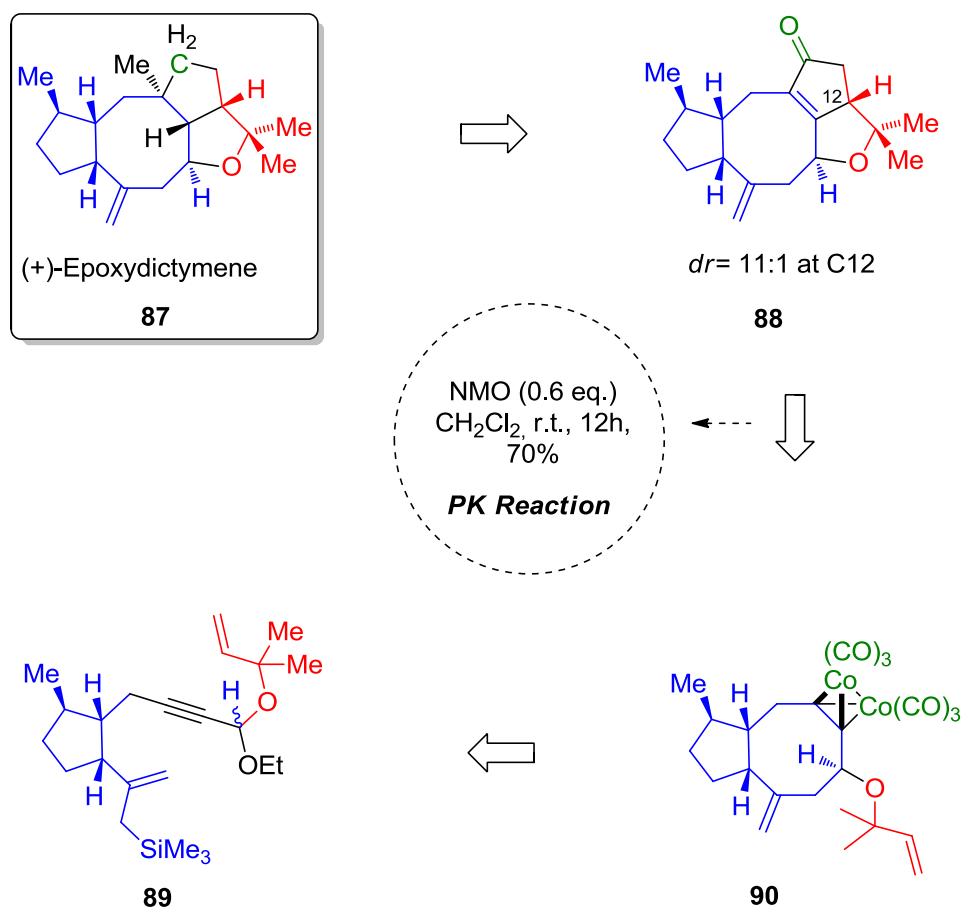
To use chiral promoter is an alternative and interesting approach in PKR. This method uses the chiral amine *N*-oxides such as Brucine *N*-oxide (**84**) [114] or (-)-sparteine *N*-oxides [115] be able to differentiate between two enantiotopic CO ligands. However, so far, max 44% ee has been obtained. Scheme 21 shows the brucine mediated cyclization of norbornene (**86**) in the presence of propargyl alcohol-cobalt complex **85**.



Scheme 21. The brucine mediated cyclization of norbornene in the presence of propargyl alcohol.

1.4.4 Applications in Natural Product Synthesis

Pauson Khand reaction in the synthesis of natural products have been frequently demonstrated [125]. Especially, the intramolecular version of the reaction has gained much popularity since it can afford cyclopentenone-fused ring systems, which are difficult to construct. It has also been used as a key step in the synthesis of a number of natural products including hirsutene [126], kainic acid [127], pentalenene [128-129], epoxydicytymene [130], incarvilline [131], paecilomycine A [132], magellanine, magellaninone, and paniculatine [133]. One of the important examples is the natural product epoxydicytymene **87** synthesized by Schreiber *et al* (Scheme 22). The Pauson Khand substrate **90**, which was converted into precursor of epoxydicytymene **88**, was prepared via Lewis acid mediated conversion of **89** called as Nicholas reaction [134].



Scheme 22. Schreiber's retrosynthetic strategy towards (+)-epoxydictymene.

As a conclusion, Pauson Khand reaction has attracted many researcher and it has been seen increasing effort to develop new improvements for this unique cyclization since its discovery in 1973 [116-124]. Especially, catalytic asymmetric versions have been discovered with different metal complexes and this promising works has many advantages over classical conditions. This continues efforts indicate that the PKR will continue to be a powerful synthetic tool for constructing of cyclopentenones.

1.5 Aim of the Work

The aim of the work of mainly involves 4 main categories. First one is to develop efficient chemoenzymatic procedures for 2-heteroaryl substituted allylic, homoallylic and homopropargylic alcohols in the concept of green chemistry. For this purpose, several commercial enzymes were planned to apply resolution process. Beside the enzymes, the other reaction parameters were planned to investigate such as solvents and temperature. Here in this point, we aimed to present the utility of biocatalysts in the resolution of racemic α -heterocyclic carbinols as a potentially useful scaffold for carrying out intramolecular PKRs. The important characteristics of this scaffolds are the availability of the starting material, easy enzymatic resolution of the products, and the easy construction of enyne systems on it. Before this, classical Grignard reaction was planned to use for synthesizing racemic alcohol backbones. The second one is to convert these alcohols to enyne systems which are useful precursors for Pauson-Khand reaction. In the third part of the thesis, another alcohol family, tertiary alcohols were planned to study with the same approach regarding secondary alcohols. The synthesis of enyne systems on tertiary alcohols is going to be studied. The last part is thought to be as the main part. Firstly, we set our sign on synthesizing diastereomerically enriched heteroaryl substituted cyclopenta[*c*]pyran and furan units (Figure 20). The second, we aim to built diastereomerically enriched spiro cyclopenta[*c*]pyran units on enantiomerically pure camphor (Figure 21).

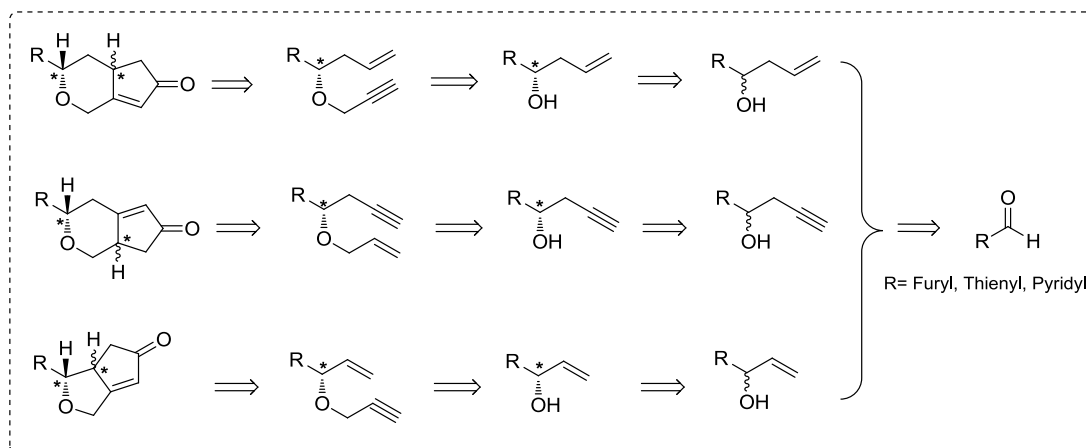


Figure 19. Retrosynthetic analysis towards cyclopenta[*c*]pyran and cyclopenta[*c*]furan bicyclic systems.

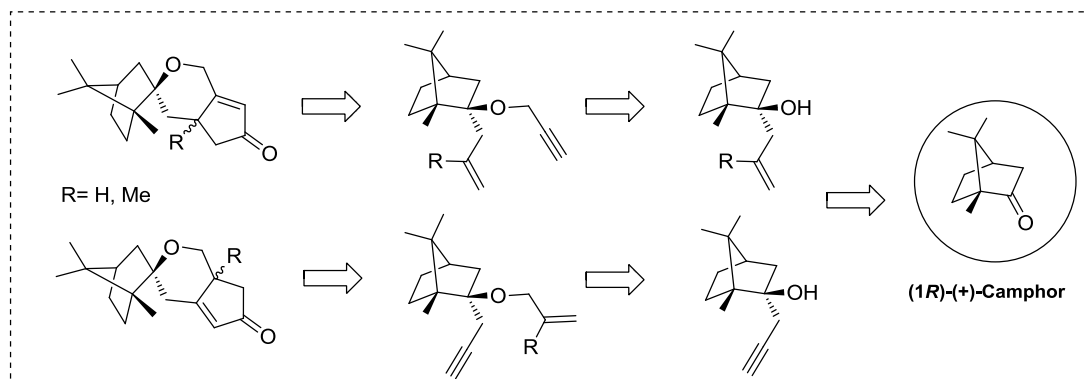


Figure 20. Retrosynthetic analysis towards spiro cyclopenta[*c*]pyran systems.

CHAPTER 2

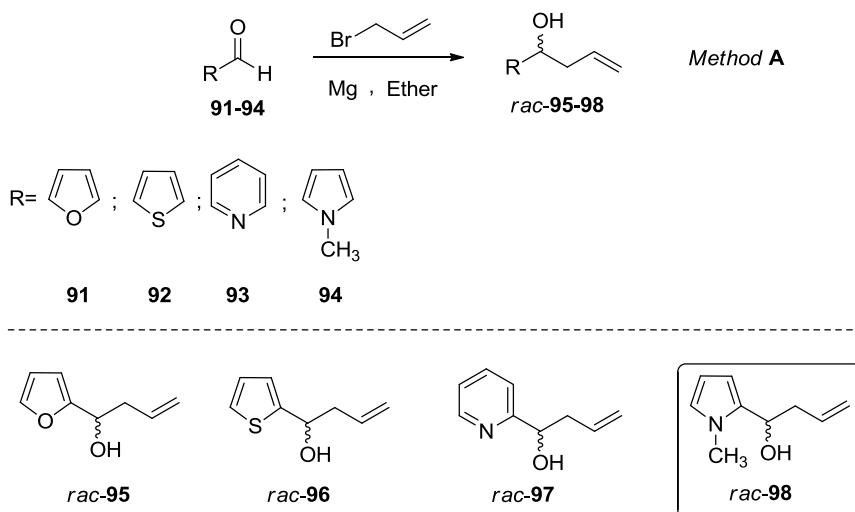
RESULTS AND DISCUSSION

2.1 Racemic Synthesis of Heteroaryl Substituted Allylic, Homoallylic and Homopropargylic Alcohols

Heterocyclic natural products having a α -heterocyclic carbinol moieties, are exceptionally valuable compounds for biomedical and pharmaceutical research, owing to their structural features and diverse medicinal values [135-142]. A number of heterocyclic natural products exhibiting useful biological activities have been isolated from natural sources. There are several methods in the literature to synthesize secondary alcohols from aldehydes. Most of them involve the organometallic addition using different metals. The addition of vinylic, allylic, and propargylic nucleophiles to carbonyl groups is one of the most effective methods for the construction of allylic, homoallylic, and homopropargylic alcohols, respectively.

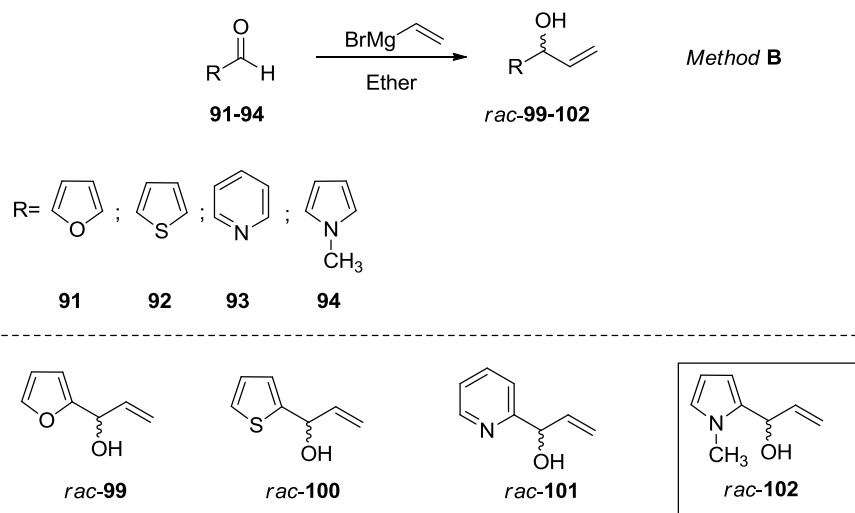
Initial efforts have been done for racemic synthesis of heteroaryl substituted allylic, homoallylic and homopropargylic alcohols which are valuable candidates for preparing chiral scaffolds for target heterocycles *via* Grignard and Reformatsky type reaction. Homoallylic alcohols *rac-95-97* were synthesized *via* Grignard reaction (*Method A*) involved *in situ* preparation of allylmagnesium bromide subjected to aldehyde in the presence of dry ether (Scheme 23). *In situ* preparation of allylmagnesium bromide was achieved by the help of catalytic amount of iodine. Compounds *rac-95-97* were obtained in high yields (Table 4). For large scale synthesis, fractional distillation was preferred for purification because of difficulty in

separation of starting aldehyde and target alcohol via column chromatography. Homoallylic alcohol *rac-98* couldn't be synthesized and non-isolable and insoluble viscous mixture was obtained after reaction. Because, it was envisaged that pyrrole has a tendency to polymerization.



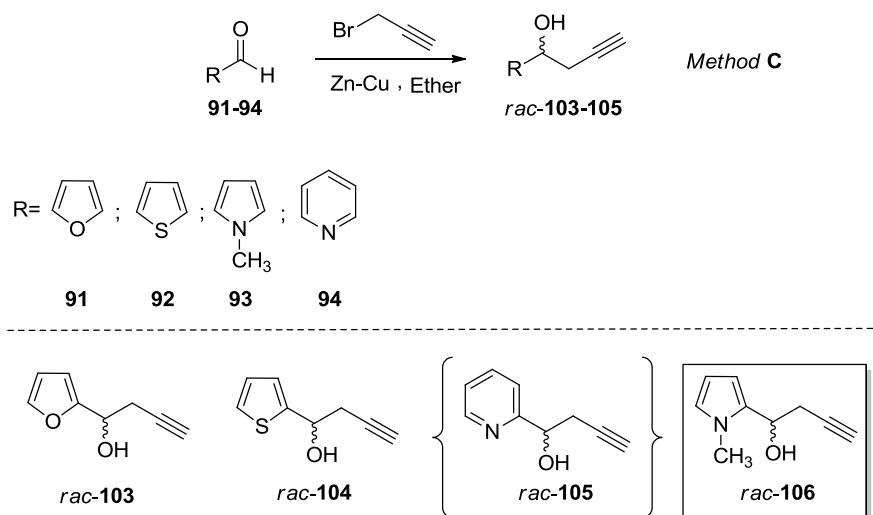
Scheme 23. Synthesis of homoallylic alcohols.

In the case of allylic alcohols *rac-99-102* (Scheme 24), commercially available Grignard reagent vinylmagnesium bromide was used since the laboratory preparation of this reagent by reaction between gaseous vinylbromide and magnesium in dry ether is difficult and resulted decrease in yields. Allylic alcohols were synthesized via Grignard reaction (*Method B*) involved readily available vinylmagnesium bromide subjected to aldehyde in the presence of dry ether. Similar to homoallylic alcohol *rac-98*, corresponding allylic alcohol *rac-102* couldn't be synthesized because of tendency of pyrrole to polymerization.



Scheme 24. Synthesis of allylic alcohols.

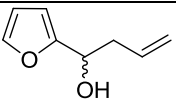
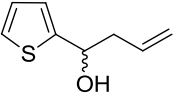
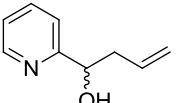
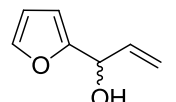
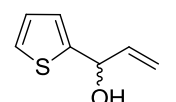
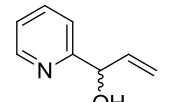
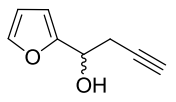
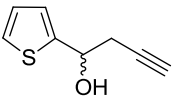
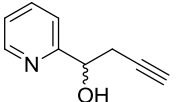
Homopropargylic alcohols *rac-103-106* could not be obtained with the Grignard procedure. It was envisaged that acidic proton of terminal alkyne effects the formation of Grignard reagent. Moreover, there is no commercially available propargylic Grignard reagents in chemical industry. Because of that we used Reformatsky type reaction in which the addition of propargyl bromide to a carbonyl group proceeds readily by using a Zn–Cu couple [143-144]. Although the synthesis of homopropargyl alcohols *rac-103-104* were achieved in high yield with this strategy, pyridyl-substituted homopropargylic alcohol *rac-105* could not be synthesized (Scheme 25). This was presumably due to the complexation of nitrogen with the Zn–Cu couple. In order to overcome this problem, we applied another procedure (*Method D*) in which catalytic amount of HgCl_2 is added to the mixture of propargyl bromide and Mg in dry ether. *rac-105* was obtained in 81% yield via this strategy. Similarly, homopropargylic alcohol *rac-106* could not be synthesized and removed from our synthetic plan.



Scheme 25. Synthesis of homopropargylic alcohols.

All results are summarized in Table 4 indicating substrate, method, reaction time and yield. The structure elucidation of all allylic, homoallylic and homopropargylic alcohols were analyzed with ^1H and ^{13}C NMR spectroscopy. These spectra are shown in appendix part (Figure A1-A18) and in accordance with literature [143-144, 155-159].

Table 4. Results of allylic, homoallylic and propargylic alcohols

<i>Substrate</i>	<i>Product</i>	<i>Method</i>	<i>Time</i>	<i>Yield</i>
91	 <i>rac-95</i>	A	12	75
92	 <i>rac-96</i>	A	7	80
93	 <i>rac-97</i>	A	8	78
91	 <i>rac-99</i>	B	5	85
92	 <i>rac-100</i>	B	3	80
93	 <i>rac-101</i>	B	8	84
91	 <i>rac-103</i>	C	18	70
92	 <i>rac-104</i>	C	12	72
93	 <i>rac-105</i>	D	15	81

2.2 Enzymatic Resolution Studies of Racemic Homoallylic, Allylic and Homopropargylic Alcohols.

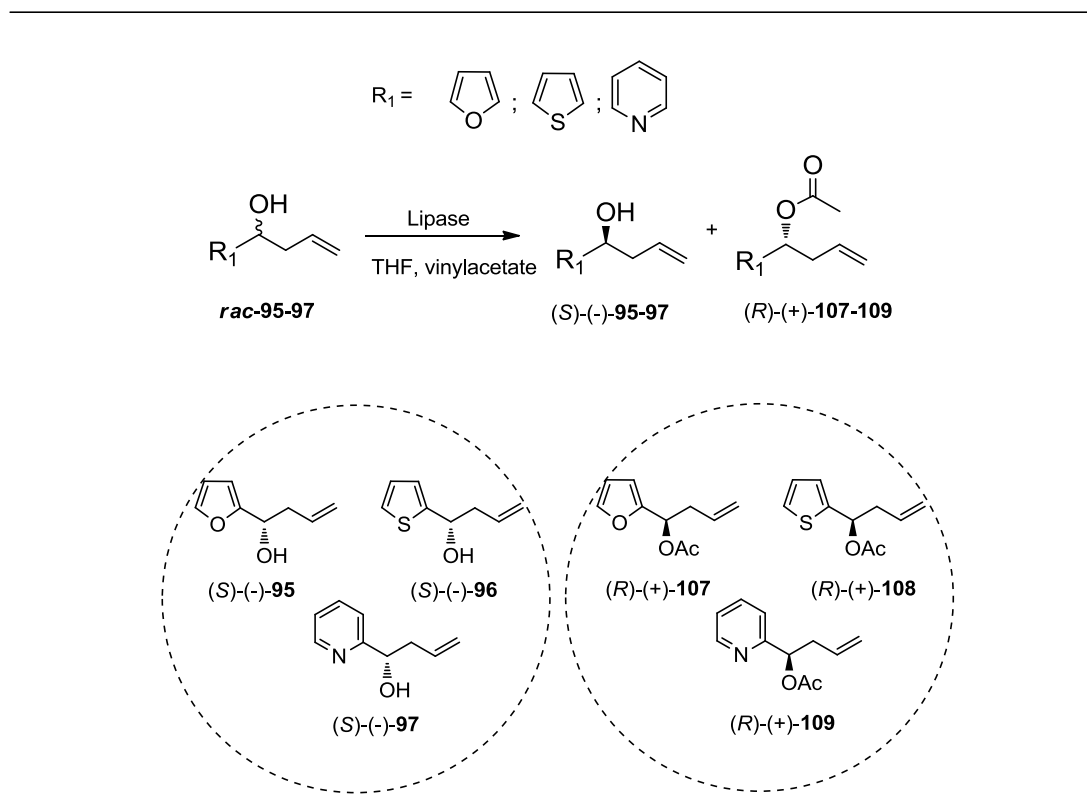
Chiral homoallylic, allylic and homopropargylic alcohols are all good candidates for preparing chiral enyne systems because of their oxygen-anchoring site [145-148]. The development of convenient synthetic routes to prepare enantiomerically enriched heteroaryl substituted homoallyl, allyl and homopropargyl alcohols has attracted considerable attention because these compounds constitute advanced intermediates for many natural compounds [149-152]. Although a wide range of synthetic procedures including the asymmetric allyl boration of heterocyclic aldehydes with diterpenylallylboranes [153-155], and catalytic enantioselective allylation and propargylation methods [156] has been reported, the most convenient synthesis of enantiomerically enriched alcohols is carried out with biocatalysts as explained in section 1.3. Biocatalytic approaches have emerged over the last few decades as a powerful and alternative tool for the development of enantioselective processes because of the fact that mild and environmentally friendly conditions are applied to the production of chiral compounds. In many cases, enzymatic resolution can be very useful if it works well for individual alcohols. Our group reported the first enzyme-catalyzed resolution of racemic furyl [157] and thienylcarbinols [143] with high enantiomeric purity and chemical yields.

In the enzymatic resolution studies, (Scheme 26-28), various lipases, *Candida Rugosa* lipase (CRL), *Pseudomonas cepacia* lipase (PS-C II), *Thermomyces lanuginosus* lipase (Lipozyme TL IM) and *Candida antarctica* lipase B (CAL-B, Novozym 435) were tested to obtain enantiopure secondary alcohols. Especially, immobilized lipase PS-C II and CAL-B gave the better results. All the reactions with these immobilized lipases were carried out by using a substrate/enzyme ratio 1:1 (w/w) and afforded excellent enantioselectivities which varied between 92% and 99% ee. Enantiomeric excess values were determined by HPLC analysis. For this purpose, we tried firstly to find HPLC conditions of racemic secondary alcohols. In some cases, conditions for racemic alcohols could not be found. Because of that we converted these alcohols into its *O*-acetyl derivatives and HPLC conditions of acetate esters were found. Different type of chiral columns which are Diacel,

chiralcel OJ-H, OD-H, OD, AS, and AD-H were used for separations. The absolute configurations were found to be (*S*) for alcohols according to specific rotations reported in literature and they all strongly confirm the Kazlauskas rule explained in section 1.3.1.2.1. Detailed explanations of all resolution results are found in related section.

2.2.1 Homoallylic Alcohols

Among racemic homoallylic alcohols and its corresponding *O*-acetylated derivatives, initially, the enantiomeric resolutions of homoallylic *rac*-**95**, *rac*-**107**, and *rac*-**108** were performed with various lipases and the results are summarized in Table 5 (Scheme 26). During the course of these biotransformation reactions, racemate *rac*-**95** was examined with CRL, whereas racemates *rac*-**107**, and *rac*-**108** were tested with PLE. Because Tanyeli et al. reported the first enzymatic resolution studies of these substrates, we followed the same procedure indicated in related papers [143,157] and obtained both enantiomers of *rac*-**96** and (*R*)-(-)-**95** in high ee value. Especially, PLE catalyzed reactions give us flexibility to obtained both enantiomers of alcohols.



Scheme 26. Enzymatic resolution of homoallylic alcohols.

Table 5. PLE and CRL catalyzed resolutions of *rac-96* and *rac-107-8*

<i>Substrate</i>	<i>Enzyme</i>	<i>Time(h)</i>	<i>Conv.(%)</i>	<i>ee(%)</i>	<i>Configuration</i>
<i>rac-96</i>	CRL	32	46	92	<i>S</i>
<i>rac-107</i>	PLE	4.5	47	93	<i>R</i>
<i>rac-108</i>	PLE	4	48	97	<i>R</i>

Although highly enantiopure products were obtained in all cases, we changed our attention to use immobilized type enzymes. Because, in PLE catalyzed reactions, we need to keep pH at constant values and the shelf life of PLE is so short. Moreover, CRL catalyzed reactions are sluggish and in some cases enzyme:substrate ratio reaches up to 1: 1.5 or 1:2 resulting poor atom economy.

Related to this facts mentioned already, enzymatic resolution of alcohols *rac-95-97* was performed by using *Pseudomonas cepacia lipase* (PS-C II) and vinyl acetate as an acyl donor and THF as a solvent at 24 °C according to the procedure given in the literature [159]. The reactions were monitored by TLC controlling and ended up when alcohol to ester ratio was close to 50%. All the reactions were carried out by using a substrate:enzyme ratio 1:1 (w/w) and afforded excellent enantioselectivities which varied between 98% and 99% ee (Table 6). Comparing results of first and second resolution methods show that PS-C Amona II catalyzed resolutions of *rac-95-97* give high ee than CRL catalyzed reaction and reaction time is short. In addition, while PLE catalyzed reactions need conversion of alcohol to acetate for enzymatic hydrolysis, PS-C Amona II catalyzed reaction resolve corresponding alcohol directly and give better ee values.

Table 6. PS-C Amona II catalyzed resolutions of *rac-95-97*

Entry	Substrate	Lipase	Time (h)	Esters (^d)	Alcohols (^d)	<i>c</i> (%) ^b	<i>E</i> ^c
				ee _p (%) ^a	ee _s (%) ^a		
1	<i>rac-95</i>	PS-C Amona II ^e	4 h	96 (<i>R</i>)	99 (<i>S</i>)	51	211
2	<i>rac-96</i>	PS-C Amona II ^e	20 h	91 (<i>R</i>)	99 (<i>S</i>)	71	137
3	<i>rac-97</i>	PS-C Amona II ^e	30 h	95 (<i>R</i>)	98 (<i>S</i>)	51	154

^a Determined by HPLC analysis employing Diacel Chiralcel OD-H and OJ-H columns.

^b $c = ee_s / (ee_s + ee_p)$.

^c $E = \ln[(1-c)(1-ee_s)] / \ln[(1-c)(1+ee_s)]$.

^d The absolute configurations were found to be (*S*) for alcohols and (*R*) for esters according to the specific rotations reported in literature.

^e The reactions were carried out at 24°C.

We also planned to study the enzyme-mediated resolution of the same substrates with other immobilized lipases from *Thermomyces lanuginosus lipase* (Lipozyme TL IM) and *Candida antarctica lipase B* (CAL-B, Novozym 435). Biotransformation of *rac-95* was chosen as a test reaction. Firstly, Both enzymes were tested under different temperatures and solvents. After several trials, optimum conditions were found and applied on the other substrates *rac-96-97*. Resolution

details are summarized in Table 7. Accordingly, lipozyme TL IM also gave excellent enantioselectivities which varied between 85% and 99% ee by using vinyl acetate as an acyl donor and DIPE as solvent at 30 °C (entries 1,5 and 6). THF was not an proper solvent for lipozyme catalyzed reaction and resulted decrease in enantiomeric excess (entry 2). Although the enantioselectivities were very similar, the resolutions with Lipozyme TL IM required longer reaction times compared with PS-C II resolutions. To check the efficiency of other immobilized lipase CAL-B, first, different temperatures were tested and 24 °C was found as a adequate temperature. After that DIPE and THF were tested as a reaction solvent, however low ee values were obtained in both cases (entries 3 and 4). For this reason, it was concluded that CAL-B, as a biocatalyst, was not an adequate lipase for substrates *rac*-**95-97** and the some of the results are not given in Table 7, since all the resolutions did not reach 50% conversion value. Considering all the results obtained so far, PS-C II was chosen as the best biocatalyst for enzymatic resolution of *rac*-**95-97** and its reaction condition would be used to obtain chiral corresponding scaffolds.

Table 7. Other immobilized lipases catalyzed resolutions of *rac*-**95-97**

Entry	Substrate	Lipase	Time (h)	Esters (^d)	Alcohols (^d)	<i>c</i> (%) ^b	<i>E</i> ^c
				ee _p (%) ^a	ee _s (%) ^a		
1	<i>rac</i> - 95	Lipozyme IM ^{1, g}	16 h	n.d.	99 (<i>S</i>)	55	n.d.
2	<i>rac</i> - 95	Lipozyme IM ^{f, h}	48	n.d.	79 (<i>S</i>)	52	n.d.
3	<i>rac</i> - 95	CAL-B ^{e, h}	26	n.d.	65 (<i>S</i>)	52	n.d.
4	<i>rac</i> - 95	CAL-B ^{e, g}	48	n.d.	75 (<i>S</i>)	53	n.d.
5	<i>rac</i> - 96	Lipozyme IM ^f	23 h	91 (<i>R</i>)	85 (<i>S</i>)	48	67
6	<i>rac</i> - 97	Lipozyme IM ^f	49 h	98 (<i>R</i>)	94 (<i>S</i>)	49	327

^a Determined by HPLC analysis employing Diacel Chiralcel OD-H and OJ-H columns.

^b $c = ee_s / (ee_s + ee_p)$.

^c $E = \ln[(1-c)(1-ee_s)] / \ln[(1-c)(1+ee_s)]$.

^d The absolute configurations were found to be (*S*) for alcohols and (*R*) for esters according to the specific rotations reported in literature.

^e The reactions were carried out at 24°C.

^f The reactions were carried out at 30°C.

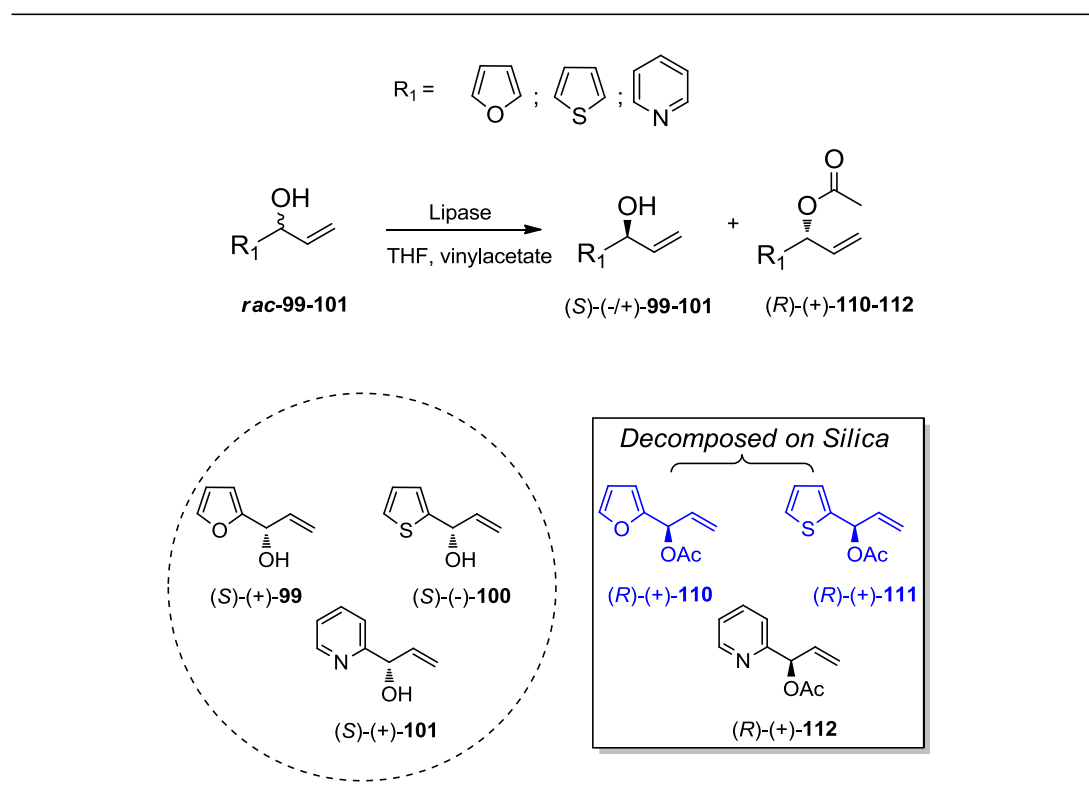
^g Co-solvent is DIPE

^h Co-solvent is THF.

After resolution process, purification of chiral alcohols and acetates were done by column chromatography. Conversion values of reactions were also determined by comparison of amount after isolation of the products and in accordance with our calculation seen in Table 7. Enantiomeric excess values of *rac*-**95-97** were determined by using HPLC with OJ-H and OD-H chiral columns (Figure A19-A24).

2.2.2 Allylic Alcohols

For enzymatic resolution of allylic alcohols, we applied the same reaction condition indicated in resolution of homoallylic alcohols because of affirmative results (Scheme 27).



Scheme 27. Enzymatic resolution of allylic alcohols.

The enzymatic kinetic resolution of allylic alcohols *rac*-**99-101** was performed by PS-C II and CAL-B using the similar procedure given in section 2.1.1. The results are summarized in Table 8. Initially, *rac*-**99** was first tested with PS-C II in vinyl acetate used both as an acyl donor and as the solvent at 27°C and afforded (*S*)-**99** in 51% ee (entry 1). When the resolution was carried out in THF under the same condition, we observed the substantial increment in the ee and conversion values as 77% and 48%, respectively (entry 2). Based on this result, the conversions were exceeded to 54% and 60% and the alcohol (*S*)-**99** was isolated with excellent ee values as 92% and 99%, respectively (entries 3 and 4). These results showed that the increment in the conversion had an effect on the ee value of the alcohol. When substrate *rac*-**99** was subjected to CAL-B mediated acetylation under the same reaction condition, similar excellent result was obtained in terms of enantioselectivity as 99% ee (entry 5). In the case of *rac*-**100**, PS-C II mediated acetylation afforded (*S*)-**100** with 83% ee (entry 6), whereas CAL-B showed the highest 97% ee value (entry 7). Because of decomposition during the chromatographic separation of acetylated products (*R*)-**110** and (*R*)-**111**, we could not determine the ee values of them. In the PS-C II mediated resolution of *rac*-**101**, the conversion did not exceed 10% (entry 8), on the other hand, CAL-B mediated acetylation afforded the alcohol (*S*)-**101** with 48% conversion and 90% ee after 13 h under the same condition applied for the other substrates (entry 9).

Table 8. Enzymatic kinetic resolution of allylic alcohols *rac-99-101*

Entry	Substrate	Enzyme	Time	Temp.	Conv.(%) ^a	Alcohols (^d)	Solvent
						ee _s (%) ^b	
1	<i>rac-99</i>	PS-C II	55 min.	27	40	51 (<i>S</i>)	-
2	<i>rac-99</i>	PS-C II	55 min	27	48	77 (<i>S</i>)	THF
3	<i>rac-99</i>	PS-C II	65 min.	27	54	92 (<i>S</i>)	THF
4	<i>rac-99</i>	PS-C II	70 min.	26	60	99 (<i>S</i>)	THF
5	<i>rac-99</i>	CAL-B	75 min.	26	56	99 (<i>S</i>)	THF
6	<i>rac-100</i>	PS-C II	75 min.	26	47	83 (<i>S</i>)	THF
7	<i>rac-100</i>	CAL-B	65 min.	26	56	97 (<i>S</i>)	THF
8	<i>rac-101</i>	PS-C II	24 h	27	<10	n.d.	THF
9	<i>rac-101</i>	CAL-B	13 h	30	48	91 ^c (<i>S</i>)	THF

^a Determined by HPLC and NMR.

^b Determined by HPLC analysis employing a Diacel Chiralcel OD-H and OJ-H columns.

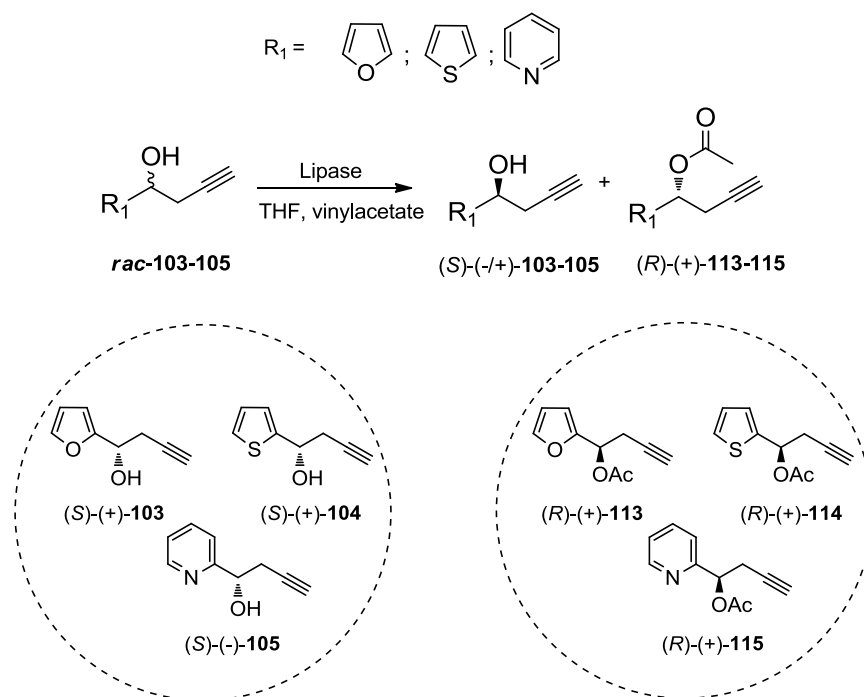
^c Ee was calculated after transforming to corresponding acetate.

^d The absolute configurations were found to be (*S*) for alcohols according to the specific rotations reported in literature.

Enantiomeric excess values of *rac-99-101* were determined by using HPLC with OJ-H and OD-H chiral columns (Figure A25-A30).

2.2.3 Homopropargylic Alcohols

As the last class of carbon scaffolds, enzymatic resolution of homopropargylic alcohols were studied (Scheme 28). We followed the similar procedures mentioned in previous sections to find adequate conditions.



Scheme 28. Enzymatic resolution of homopropargylic alcohols.

The enzymatic kinetic resolution of homopropargylic alcohols *rac*-**103-105** was performed by PS-C II and CAL-B using the same procedure given in sections 2.1.1 and 2.1.2. The results are summarized in Table 9. All the reactions afforded excellent enantioselectivities which varied between 85% and 98% ee. During the resolution of *rac*-**103-105**, PS-C II catalyzed reactions gave higher ee value and short reaction times than Lipozyme TL IM catalyzed reactions. Enantiomeric excess values of (*S*)-(-)-**103-105** were determined by using HPLC with OJ-H and OD-H chiral columns and spectra are shown in appendix part (Figure A31-A36).

Table 9. Enzymatic kinetic resolution of homopropargylic alcohols *rac*-**103-105**

Entry	Substrate	Lipase	Time (h)	Esters (^d)	Alcohols (^d)	<i>c</i> (%) ^b	<i>E</i> ^c
				ee _p (%) ^a	ee _s (%) ^a		
1	<i>rac</i> - 103	PS-C Amona II ^e	1.5 h	n.d.	93 (<i>S</i>)	52	n.d.
2	<i>rac</i> - 103	Lipozyme IM ^e	16 h	n.d.	85 (<i>S</i>)	55	n.d.
3	<i>rac</i> - 104	PS-C Amona II ^e	2.5 h	92 (<i>R</i>)	99 (<i>S</i>)	52	116
4	<i>rac</i> - 104	Lipozyme IM ^f	24 h	80 (<i>R</i>)	99 (<i>S</i>)	56	41
5	<i>rac</i> - 105	PS-C Amona II ^e	25 h	92 (<i>R</i>)	95 (<i>S</i>)	51	82
6	<i>rac</i> - 105	Lipozyme IM ^f	43 h	75 (<i>R</i>)	98 (<i>S</i>)	57	30

^a Determined by HPLC analysis employing Diacel Chiralcel OD-H and OJ-H columns.

^b $c = ee_s / (ee_s + ee_p)$.

^c $E = \ln[(1-c)(1-ee_s)] / \ln[(1-c)(1+ee_s)]$.

^d The absolute configurations were found to be (*S*) for alcohols and (*R*) for esters according to the specific rotations reported in literature.

^e The reactions were carried out at 24°C.

^f The reactions were carried out at 30°C.

As a summary, we found that PS-C II, Lipozyme and CAL-B type immobilized enzymes were proper biocatalyst to find optimized conditions for resolution of heteroaryl substituted homoallylic, allylic and homopropargylic alcohols. In all cases, the best reaction conditions would be used before transformation of corresponding chiral scaffolds to target structures.

2.3. Synthesis of Enyne Systems

Enyne systems are valuable precursors for intramolecular PK cyclization. The purpose of this part indicated in the “Aim of the Work” section is to synthesize chiral enyne systems for PK cyclization. For this goal, we first introduced chirality on our carbinol scaffolds via enzymatic resolution. Enzymatic resolution of racemic secondary allylic, homoallylic and homopropargylic alcohols afforded highly enantiopure secondary alcohols. After resolution process, chiral alcohols underwent allylation or propargylation process to get chiral enyne backbones. In synthetic pathway, the enyne systems were first built on enantiomerically enriched homoallylic

(*S*)-(-)-**95-97**, allylic (*S*)-(+)-**99**, (*S*)-(-)-**100**, (*S*)-(+)-**101** and homopropargylic alcohol (*S*)-(+)-**103-104**, (*S*)-(-)-**105** backbones by *O*-propargylation and *O*-allylation, respectively using propargyl bromide and allylbromide with NaH and tetrabutylammonium iodide (TBAI) in THF. During to course of the reactions, racemization was not observed and so the chirality introduced on enynes from alcohols were kept constant.

Initially, we tried to find optimum conditions for *O*-allylation and *O*-propargylation. For this purpose, several bases such as K₂CO₃ and NaH and solvents like DMF and THF were tested. Firstly, *O*-allylation reactions were studied and as the optimum condition, NaH, dry THF system was found. This reaction afforded acceptable yields in very short times although there is an acidic hydrogen on terminal alkyne. We did not observe any side product. Same method was applied on *O*-propargylation of homoallylic and allylic alcohols and succesful results were gained. However, in the case of compound (*S*)-(-)-**101**, the yield was obtained in 41%.

Characterization of all enyne compounds was done by ¹H, ¹³C NMR and GC-MS spectroscopy which are shown in appendix part (Figure A37-A54 for NMR, Figure A104-A108 for GC-MS).

2.3.1 Synthesis of Enynes Derived from Homoallylic Alcohols.

In this part, chiral enyne systems were derived from homoallylic alcohols by propargylation process as explained before. The results are summarized in Table 10.

Table 10. Enynes derived from homoallylic alcohols

$$\text{(S)-(-)-95-97} \xrightarrow[\text{THF, NaH, TBAI}]{\text{Propargyl Br}} \text{(S)-(-)-116-118}$$

<i>Substrate</i>	<i>Product</i>	<i>Configuration</i>	<i>Time (h)</i>	<i>Yield</i>
 (S)-(-)-95	 (S)-(-)-116	<i>(S)</i>	3	83
 (S)-(-)-96	 (S)-(-)-117	<i>(S)</i>	2.5	80
 (S)-(-)-97	 (S)-(-)-118	<i>(S)</i>	2	89

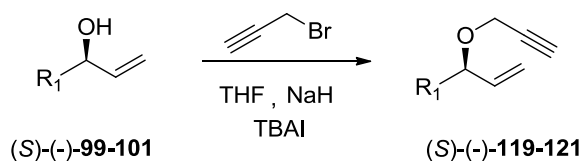
As indicated in section 2.3, the structure elucidation of enyne systems was done with ^1H and ^{13}C NMR spectroscopy. The introducing of propargyl unit on homoallylic alcohols affording compounds (S)-(-)-116-118 was strongly confirmed by ^1H NMR. In ^1H NMR of compound (S)-(-)-116, propargylic methylene protons having AB systems, appear as doublet of doublets at 4.07 and 3.86 ppm with the coupling constants values $J = 15.9$ and 2.4 Hz due to the geminal coupling and the coupling with terminal acetylenic proton. In addition, other characteristic NMR signal of terminal acetylenic proton resonates at 2.31 ppm as triplet with the coupling constant value of $J = 2.4$ Hz. Compounds (S)-(-)-117 and (S)-(-)-118 have similar signals regarding propargyl unit. In ^1H NMR of compound (S)-(-)-117, propargylic methylene protons appear as doublet of doublets at 4.08 and 3.85 ppm with the coupling constants values $J = 15.8, 2.4$ Hz and terminal acetylenic proton resonates at 2.32 ppm a triplet with the coupling constant value of $J = 2.4$ Hz. Parallel to these

observations, in ^1H NMR of compound (*S*)-(-)-**118**, propargylic methylene protons appear as doublet at 4.12 and 3.94 ppm with the coupling constants values $J = 15.8$ and terminal acetylenic proton resonates at 2.33 ppm as broad singlet. Another important clue for structural similarities are shown in GC-MS spectra (Figure A104-5). According to relative intensities towards mass in GC-MS spectra, (*S*)-(-)-**117** and (*S*)-(-)-**118** show the similar signals in which the removal of allylic group from molecule ($151 (\text{M}^+ - 41(^+\text{CH}_2\text{CH}=\text{CH}_2))$ for (*S*)-(-)-**117** and $146 (\text{M}^+ - 41(^+\text{CH}_2\text{CH}=\text{CH}_2))$ for (*S*)-(-)-**118**) was detected.

2.3.2 Synthesis of Enynes Derived from Allylic Alcohols

Chiral enynes derived from allylic alcohols were obtained by using same procedure indicated in previous section. The results are summarized in Table 11.

Table 11. Enynes derived from allylic alcohols



<i>Substrate</i>	<i>Product</i>	<i>Configuration</i>	<i>Time (h)</i>	<i>Yield</i>
		(<i>S</i>)	1.5	78
(S)-(-)-99	(S)-(-)-119			
		(<i>S</i>)	2	80
(S)-(-)-100	(S)-(-)-120			
		(<i>S</i>)	2	41
(S)-(-)-101	(S)-(-)-121			

Similar to homoallylic alcohol backbone, the introducing propargyl unit to on allylic alcohol backbone affording compounds (*S*)-(-)-**119-121** was strongly confirmed by ^1H and ^{13}C NMR spectroscopy. In ^1H NMR of compound (*S*)-(-)-**119**, AB system propargylic protons appear as doublet of doublets at 4.09 and 4.01 ppm with the coupling constants values $J = 15.8$ and 2.4 Hz due to the geminal coupling and the coupling with terminal acetylenic proton. In addition, other characteristic NMR signal of terminal acetylenic proton resonates at 2.34 ppm a triplet with the coupling constant value of $J = 2.4$ Hz. Compounds (*S*)-(-)-**120** and (*S*)-(-)-**121** have similar signal sets regarding propargyl unit. In ^1H NMR of compound (*S*)-(-)-**120**, methylene protons appear as doublet of doublets at 4.10 and 4.02 ppm with the coupling constants values $J = 15.9$ and 2.4 Hz and terminal acetylenic proton resonates at 2.30 ppm as a triplet with the coupling constant value of $J = 2.3$ Hz. In ^1H NMR spectrum of compound (*S*)-(-)-**121**, the characteristic AB system methylene protons resonate at 4.17 as doublet with the coupling constant value $J = 2.4$ and terminal acetylenic proton appears as a triplet at 2.37 ppm ($J = 2.4$ Hz). GC-MS spectroscopy also confirms the structural assignments. For compound (*S*)-(-)-**119**, molecular ion peak ((162 (M^+ , 4) was observed beside other fragments. For compound (*S*)-(-)-**120**, removal of vinylic groups was observed as a base peak (151 ($\text{M}^+ - 27$ ($^+\text{CH}=\text{CH}_2$, base) beside other fragment as well. Compound (*S*)-(-)-**121** show also the similar fragments in GC-MS spectrum (Figure A106-108).

2.3.3 Synthesis of Enynes Derived from Homopropargylic Alcohols.

As the last class of enyne backbones, compounds (*S*)-(-)-**122-124** derived from homopropargylic alcohol scaffold were synthesized and the results are shown in Table 12.

Table 12. Reaction results of enynes from homopropargylic alcohols

$$\text{R}_1\text{-CH(OH)-CH}_2\text{-C}\equiv\text{CH} \xrightarrow[\text{THF, NaH, TBAI}]{\text{CH}_2=\text{CH-CH}_2\text{Br}} \text{R}_1\text{-CH(O-CH}_2\text{-CH=CH}_2\text{)-CH}_2\text{-C}\equiv\text{CH}$$

(S)-(-)-**103-105** (S)-(-)-**122-124**

<i>Substrate</i>	<i>Product</i>	<i>Configuration</i>	<i>Time (h)</i>	<i>Yield</i>
<p>(S)-(-)-103</p>	<p>(S)-(-)-122</p>	(S)	3	79
<p>(S)-(-)-104</p>	<p>(S)-(-)-123</p>	(S)	2.5	82
<p>(S)-(-)-105</p>	<p>(S)-(-)-124</p>	(S)	2	90

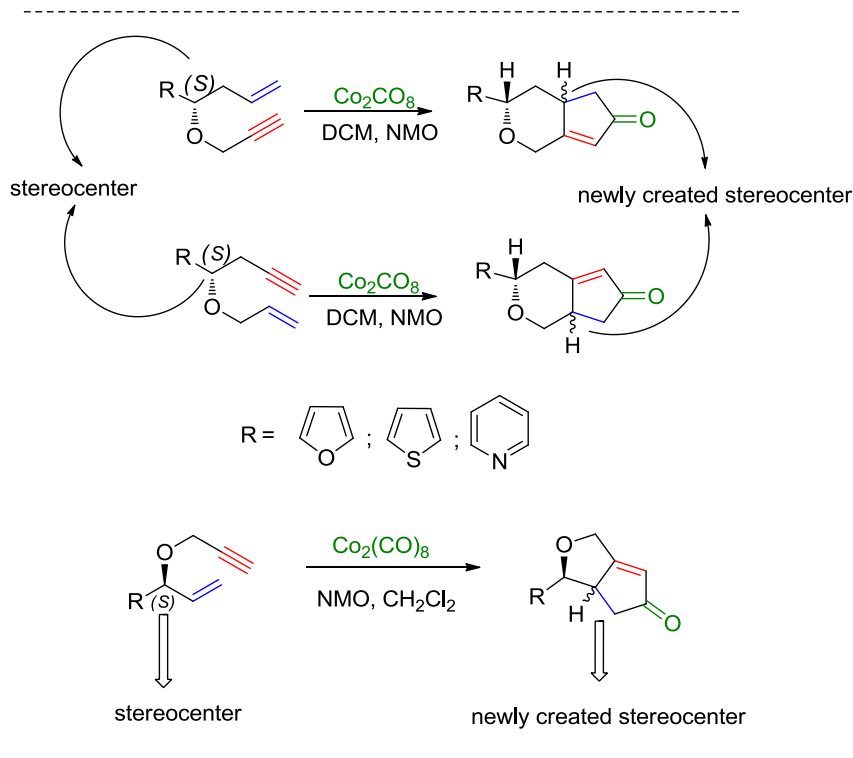
Anchoring allyl unit on propargyl alcohol backbones yielding compounds (S)-(-)-**122-124** was confirmed by ^1H and ^{13}C NMR spectroscopy. As an representative example, in ^1H NMR spectrum of (S)-(-)-**123**, allylic methylene protons having AB system resonate at 3.97 and 3.83 ppm as doublet of doublets with the coupling constant values $J = 12.8, 5.0$ Hz and $J = 12.8, 6.3$ Hz, respectively, due to the geminal coupling and the coupling with internal olefinic proton. The other characteristic signal belonging to methine proton of olefinic unit was observed at 5.77-5.87 as multiplet. Terminal olefinic protons resonate at 5.10-5.12 and 5.18-5.22 as doublet of multiplets, with the coupling constant values $J = 10.3$ Hz and $J = 15.7$ Hz, respectively. It can be decided that the latter one is the *trans* proton with respect to olefinic methine proton because of larger J value (15.7 Hz).

2.4. Pauson Khand Cyclization of Enyne Systems

The Pauson-Khand reaction (PKR) has been established as a powerful method for the synthesis of the cyclopentenone framework by a cobalt-mediated reaction performed by joining an alkyne, an olefin, and carbon monoxide as explained in section 1.4. The intramolecular version of the reaction has gained much popularity because it can afford cyclopentenone-fused ring systems, which are difficult to construct. Although the application of this useful method in the construction of chiral cyclopentenone-pyran ring skeletons using carbohydrate templates has been documented, little attention has been focused on the PKR of chiral enyne systems. Initial results of this thesis have demonstrated the utility of biocatalysts in the resolution of racemic α -heterocyclic carbinols as a potentially useful scaffold for carrying out intramolecular PKRs. The important characteristics of this scaffold are the availability of the starting material, easy enzymatic resolution of the substrates, and the easy construction of enyne systems on it.

We planned firstly to synthesize chiral bicyclic cyclopentenone systems. For this purpose, enyne systems were subjected to the most common conditions for PKR resulting cyclopenta[*c*]pyran and cyclopenta[*c*]furan systems. In this protocol, cobalt alkyne complexes were prepared using enyne-dicobalt octacarbonyl in a molar ratio of 1.0:1.7 in DCM, and then *N*-methyilmorpholine *N*-oxide monohydrate was added as a promoter. It was envisaged that PKR of enynes was carried out in a stereoselective manner since our chiral enyne systems would control the stereochemistry of the newly created stereogenic center. Especially in pyran fused systems, we could expect the remote control of stereoselectivity.

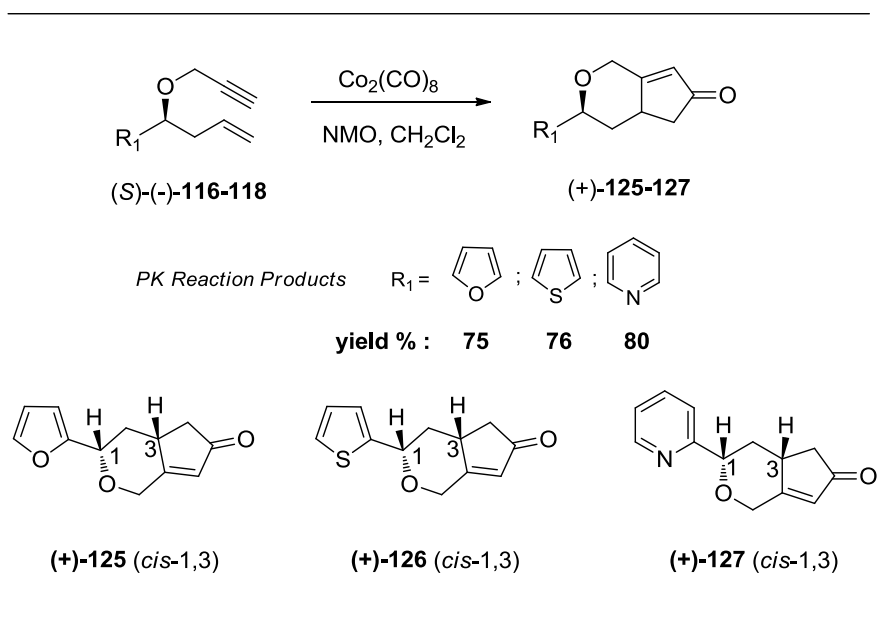
Initial studies were started with the synthesis of chiral cyclopentenone fused pyran systems. Reaction details are given in related section. On the basis of our expectations given above, we thought that it would be interesting to explore the diastereoselectivity in the construction of cyclopentenone-furan ring systems too (Scheme 29).



Scheme 29. Synthesis of cyclopenta[*c*]pyran and cyclopenta[*c*]furan systems.

2.4.1 Synthesis of Cyclopenta[*c*]pyran Bicyclic Compounds Derived from Homoallyl Alcohol Backbone

To evaluate precisely the applicability of the intramolecular PKR of enynes anchored to chiral 2-heteroarylcarbinols on the remote control of stereochemistry in the synthesis of cyclopentenone-pyran ring systems, the compounds (*S*)-(-)-**116-118** were subjected to the most common conditions for PKR (Scheme 30). In all cases, single diastereomer of cyclopenta[*c*]pyran products (+)-**125-127** was obtained. ¹H and ¹³C NMR spectra strongly confirmed the formation of single diastereomeric product for each. The absolute configuration of each bicyclic product has been determined by X-ray analysis and by differential NOE experiments by taking the known configuration of homoallylic alcohol backbone as a reference.



Scheme 30. Synthesis of PK products from chiral enynes derived from homoallyl alcohols.

The structure elucidations of (+)-**125-127** were done by ^1H , ^{13}C NMR and also with full NMR analysis including DEPT, COSY, HSQC and HMBC (Figure A55-A64). As a representative example, the olefinic proton of the (+)-**126** resonates at 5.94 ppm as a singlet. The characteristic ketone carbonyl signal appears at 206.3 ppm in ^{13}C NMR. The absolute configuration of (+)-**126** was determined by differential NOE experiments (Figure A100-A101). Since the absolute configuration of stereocenter already present on the enyne backbone known and preserved during to course of the reaction, it was taken as reference for differential NOE experiment. The methine proton attached to the stereogenic carbon of the pyran ring resonated at 4.82 ppm and the methine proton of cyclopenta[*c*]pyran fused position carbon resonated at 3.00-3.03 ppm show significant NOE enhancements, which indicate the *cis*-relationship between the stereogenic center protons (Figure 22). Consequently, the absolute configuration of (+)-**126** was found as (3*S*,4*aR*). The absolute configuration of (+)-**127** was also determined by differential NOE experiments (Figure A102-A103). Significant NOE enhancement was observed between the methine proton attached to the stereogenic carbon of the pyran ring at 4.68 ppm and the methine proton of newly created stereogenic carbon center at 3.03-3.09 ppm and

decided that the methine protons are in *cis*-relationship. Thus, the absolute configurations of (+)-**127** (*cis*-1,3) was determined as (3*S*,4*aR*).

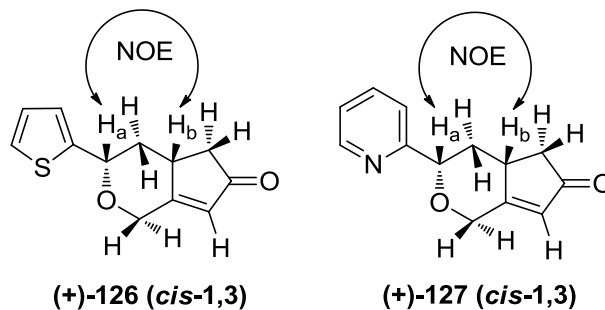


Figure 21. NOE correlations observed between H_a and H_b protons of (+)-**126** (*cis*-1,3) and (+)-**127** (*cis*-1,3).

Since compound (+)-**125** was properly crystallized, X-ray diffraction analysis has been done and confirmed the absolute configuration of the newly created stereogenic centers at the fused position of cyclopenta[*c*]pyran ring as (3*S*,4*aR*) (Figure 22).

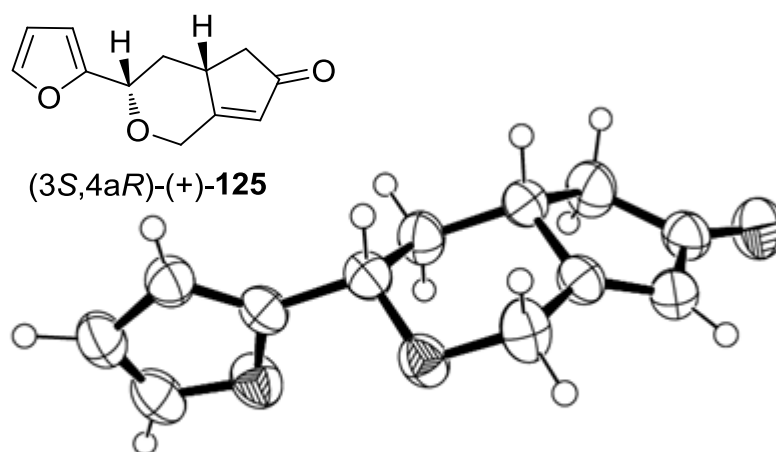
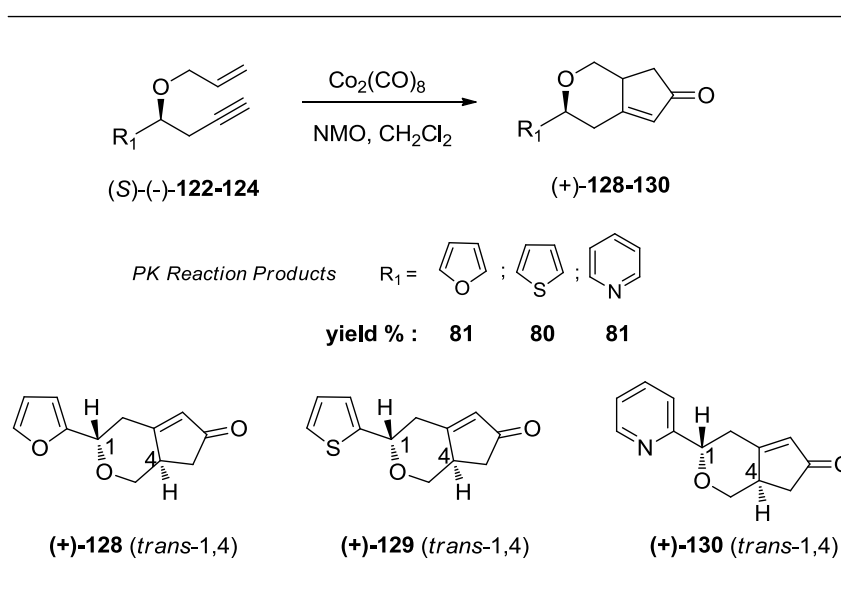


Figure 22. X-ray structure of compounds (3*S*,4*aR*)-(+)-**125**.

The differential NOE results of cyclopentenone-pyran products (+)-**126-127** and X-ray structures of (+)-**125** (*cis*-1,3) provided an explanation to question why enynes (*S*)-(-)-**116-118** afforded single diastereomers. In all products, the new stereogenic centers located at the fused position of cyclopentenone-pyran rings possess an (*R*)-configuration since the pyran rings are in the most favored chair conformation as expected.

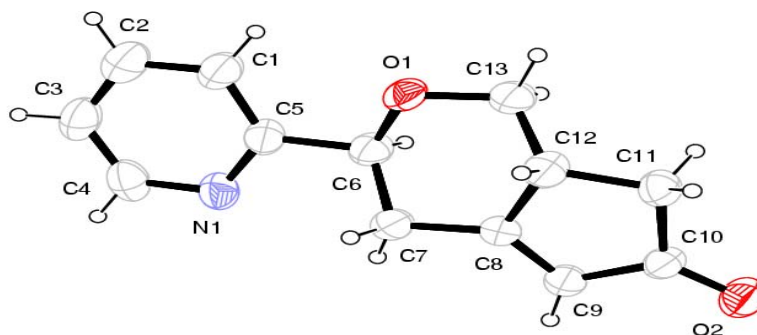
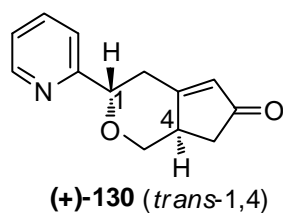
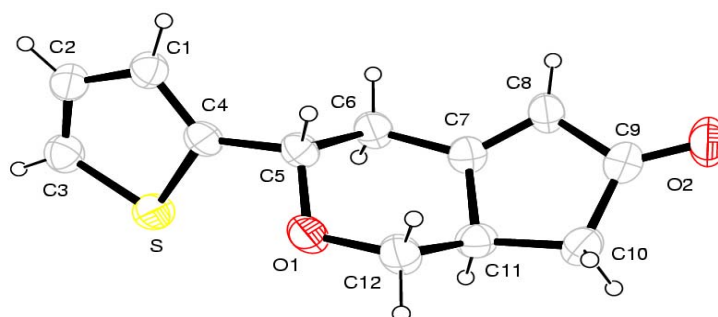
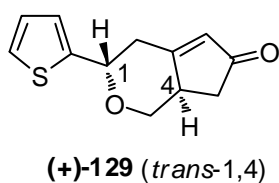
2.4.2 Synthesis of Cyclopenta[*c*]pyran Bicyclic Compounds Derived from Homopropargyl Alcohol Backbone

The applicability and the remote control property on stereoselectivity of the intramolecular PKR on chiral enynes has been examined by changing the main chiral backbone from homoallyl to homopropargyl unit. For this purpose, the compounds (*S*)-(-)-**122-124** were subjected to the PKR under the same conditions mentioned in previous section to afford corresponding cyclopenta[*c*]pyran derivatives (+)-**128-130** (Scheme 31).



Scheme 31. Synthesis of PK products from chiral enynes derived from homopropargylic alcohols.

In all three cases, single diastereomeric products have been isolated and characterized. The structure elucidations of (+)-**128-130** were done by ^1H , ^{13}C NMR and also with full NMR analysis including DEPT, COSY, HSQC and HMBC (Figure A65-A70). As a representative example, ^1H NMR of (+)-**129** shows characteristic olefinic proton of cyclopentenone unit constructed as a result of PKR at 5.95 ppm as a singlet. In ^{13}C NMR spectrum of (+)-**129**, the characteristic ketone carbonyl signal was observed at 206.3 ppm. The other compounds (+)-**128** and (+)-**129** also show similar signals. Absolute configuration determination of all products (+)-**128-130** has been done by single crystal X-ray diffraction method. X-ray results showed that compounds (+)-**128-130** have trans-1,4 relation between the stereogenic methine protons and absolute configurations are found as (3*S*,7*aR*) for all products. (Figure 24).



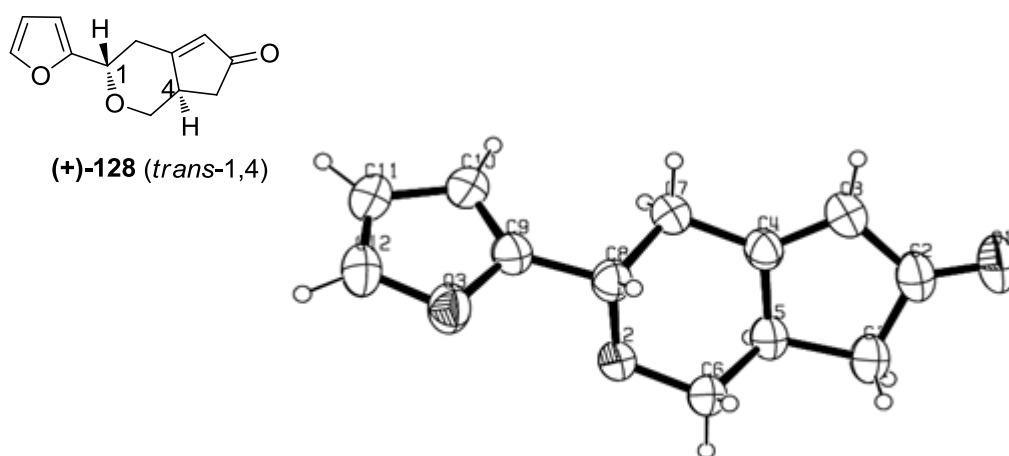


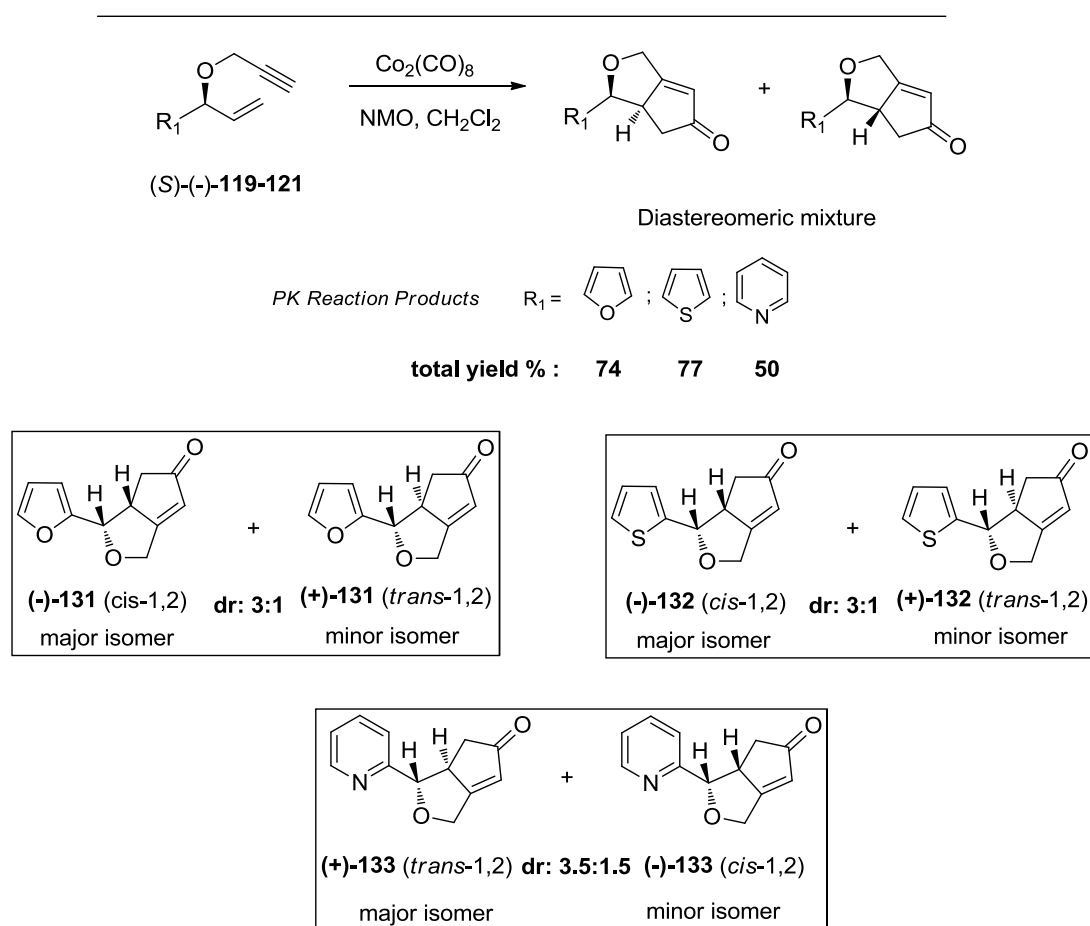
Figure 23. X-ray structure of compounds (+)-**128** (*trans*-1,4), (+)-**129** (*trans*-1,4) and (+)-**130** (*trans*-1,4).

X-ray results of (+)-**128-130** (*trans*-1,4) provided a same explanation to question why enynes (*S*)-(-)-**122-124** afforded single diastereomers regarding other cyclopentenone fused PK products. Since, pyran rings are in the most favored chair conformation as mentioned before. Similarly, the new stereogenic centers located at the fused position of cyclopentenone-pyran rings possess again an (*R*)-configuration in all products as well, regarding other cyclopenta[*c*]pyran bicyclic compounds.

2.4.3 Synthesis of Cyclopenta[*c*]furan Bicyclic Compounds Derived from Allylic Alcohol Backbone

As a last class of PKR studies of heteroaryl substituted chiral enynes, diastereoselectivity during the construction of cyclopentenone-furan ring systems was explored. For this purpose, the enynes compounds (*S*)-(-)-**119-121** having chiral allylic alcohol backbone were subsequently subjected to intramolecular PKR by following the procedure given above. In contrast to pyran fused cyclic systems,

chiral enynes leading to furan fused cyclopentenone frameworks afforded diastereomeric mixtures (Scheme 32). This was presumably due to the less conformational effect of furan rings on the diastereoselectivity comparing with the most favored chair conformation of pyran rings. The diastereomeric mixtures were separated by flash column chromatography and product ratio was determined by ^1H NMR.



Scheme 32. Synthesis of PK products from chiral enynes derived from allylic alcohols.

The structure elucidations of (+)-**131-133** and (-)-**131-133** were done by ^1H , ^{13}C NMR and full NMR analysis including DEPT, COSY, HSQC and HMBC. The olefinic proton of the (-)-**131** resonates at 6.04 ppm as a broad singlet. The

characteristic ketone carbonyl signal was observed at 207.7 ppm in ^{13}C NMR. The relative configurations of (-)-**131** and (+)-**131** were determined by comparing coupling constant values (J) of the methine protons attached to stereogenic centers. ^1H -NMR spectrum of (-)-**131** shows a doublet at 4.36 ppm with $J = 10.7$ Hz for the methine proton of stereogenic center and a multiplet at 3.50-3.54 for the methine proton of newly created stereogenic center, whereas the same set of protons of minor product (+)-**131** appears as doublet at 5.24 ppm with $J = 8.3$ Hz and a multiplet at 3.54-3.59 ppm, respectively. These coupling constant values are in accordance with the literature data indicated as $J = 10.7$ and $J = 8.3$ Hz for *cis* and *trans* coupling of methine protons, respectively [160-161]. Thus, the absolute configurations of (-)-**131** (*cis*-1,2) and (+)-**131** (*trans*-1,2) could be determined as (3*S*,3*aR*) and (3*S*,3*aS*), respectively by using the known absolute configuration of chiral allylic alcohol backbone. We followed the same route for the absolute configuration determination of (-)-**132** and (+)-**132** diastereomers. ^1H -NMR spectrum of (-)-**132** shows a doublet at 4.56 ppm with $J = 10.3$ Hz for the methine proton of furan ring and a multiplet at 3.23-3.28 for the methine proton attached to newly formed stereogenic carbon center, whereas the minor (+)-**132** gives a doublet at 5.55 ppm with $J = 8.3$ Hz and a multiplet at 3.60-3.64 ppm for the corresponding methine protons, respectively. According to these results, the absolute configurations of (-)-**132** (*cis*-1,2) and (+)-**132** (*trans*-1,2) were determined as (3*S*,3*aR*) and (3*S*,3*aS*), respectively. In contrast to the intramolecular PKR results of furyl and thiophenyl substituted (*S*)-(-)-**119** and **120** derivatives, pyridine substituted substrate (*S*)-(-)-**121** afforded (+)-**133** (*trans*-1,2) isomer as major and (-)-**133** (*cis*-1,2) as minor product with the diastereomeric ratio of 3.5:1.5 which was determined by ^1H -NMR. This result can be attributed to the high coordination tendency of the pyridine ring nitrogen to the alkyne- $\text{Co}_2(\text{CO})_6$ complex and may predominantly direct the *trans*-isomer formation as the major over the *cis*-isomer. The preferred conformers of the alkyne- $\text{Co}_2(\text{CO})_6$ complex can be regarded as **A** and **B**, with and without nitrogen coordination, respectively, as shown in Figure 25. In ^1H -NMR spectrum of (+)-**133**, the methine proton of furan ring and newly generated stereogenic center methine proton resonate at 5.39 ppm as doublet with $J = 8.3$ Hz and at 3.74-3.80 ppm as multiplet, respectively, whereas, the same set of (-)-**133** protons resonate at 4.48 ppm as doublet with $J = 10.4$ Hz and at 3.30-3.37 ppm as multiplet, respectively. Depending upon these results, we deduce the

relative configurations of (+)-**133** and (-)-**133** as *trans*-1,2 and *cis*-1,2, respectively. Thus, the absolute configurations of (+)-**133** (*trans*-1,2) and (-)-**133** (*cis*-1,2) were determined as (3*S*,3*aS*) and (3*S*,3*aR*), respectively.

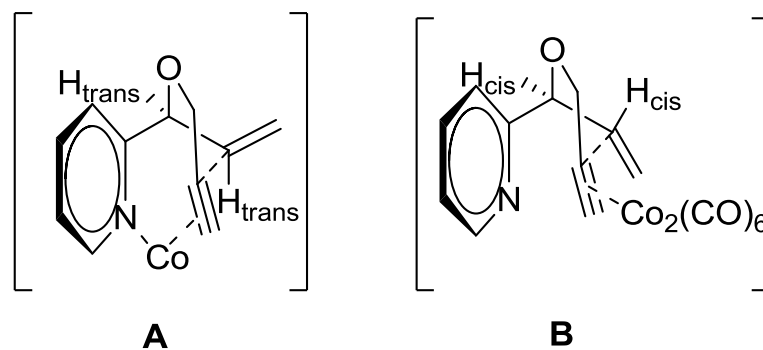


Figure 24. Proposed intermediate conformers in PKR.

2.5. Chiral Spirocyclic Compounds via Pauson Khand Reaction

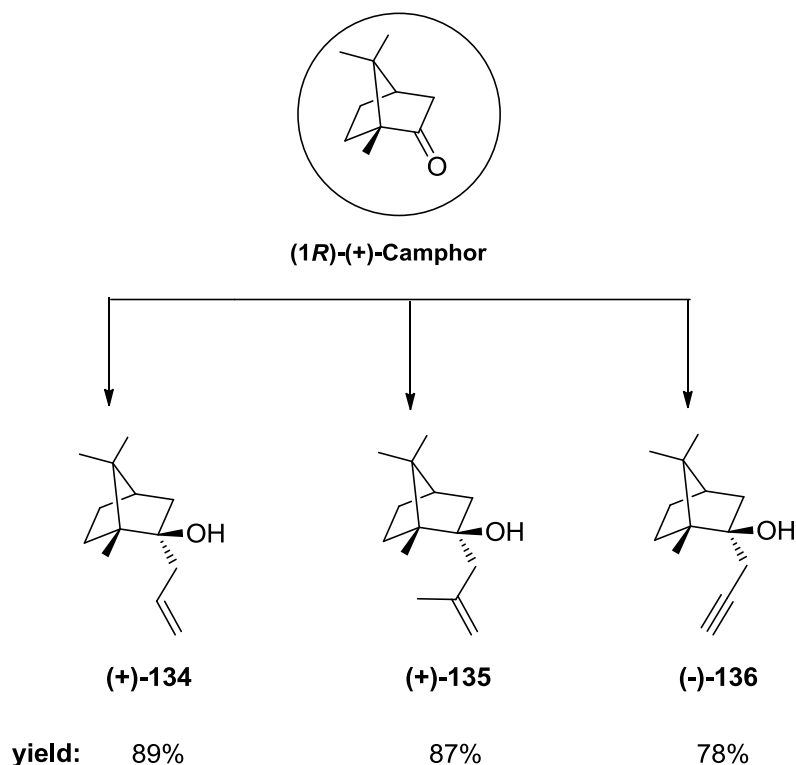
Spirocyclic [162-163] compounds have recently been of considerable interest, because the design of scaffolds can be inspired by natural products or by the application of novel reactions [164]. In particular, spiroketals are widespread structural units in many natural products [165]. The stereocontrolled construction of spiro moieties has attracted considerable attention in recent times [166-169]. The most applicable methods to prepare spiro unit utilize a ring closing metathesis (RCM) and Pauson-Khand reaction (PKR) using carbohydrates as chiral templates [170-172]. The intramolecular PKR is often a convenient route to cyclopentenone fused pyran ring systems [173-179]. The utility of this reaction in the construction of chiral ring skeletons has been used most commonly [180-185].

In previous chapters, we have described a detailed study on the intramolecular PKR of chiral enyne systems tethered to chiral 2-heteroarylcarbinol scaffolds leading to chiral other cyclopenta[*c*]pyran fused ring systems with an excellent diastereoselectivity due to high conformational control on the remote stereocenters. In line with this purpose, here in, the applicability of the

intramolecular PKR of enynes tethered to camphor and the remote stereochemistry control of newly created stereogenic center in the synthesis of spiro other cyclopenta[*c*]pyran ring skeletons were studied. The reasons for choosing camphor as a starting compound are depending upon the readily availability of the substance and high *endo*-face organometallic attacking susceptibility of the ketone functionality and in addition, available potent precursor for the construction of spiro moieties on the carbonyl group.

2.5.1 Synthesis of Tertiary Alcohols

The parent tertiary homoallylic alcohol (+)-**134** and homomethallylic alcohol (+)-**135** were prepared by addition of allylmagnesium bromide and methallylmagnesium bromide to commercially available (1*R*)-(+)-camphor in ether, respectively, as shown in Scheme 33. However, tertiary homopropargylic alcohol (-)-**136** could not be obtained with the same procedure. Another approach was used to overcome this problem indicated in section 2.1 as Reformatsky type reaction in which the addition of propargyl bromide to a carbonyl group proceeds readily by using a Zn–Cu couple. Unfortunately, the desired product was not obtained with this way. Lastly, the use of catalytic amount of HgCl₂ under Grignard condition afforded the desired product in 78% yield. It is well known that Grignard reagents prefer the sterically less crowded *endo*-face of camphor ketone moiety [164, 186]. Dimitrov et al. explained the *endo* selectivities with different groups on (1*R*)-(+)-camphor [186]. In our case, the addition of allyl, methallyl and propargylmagnesium bromide showed excellent *endo*-face diastereoselectivity as expected.



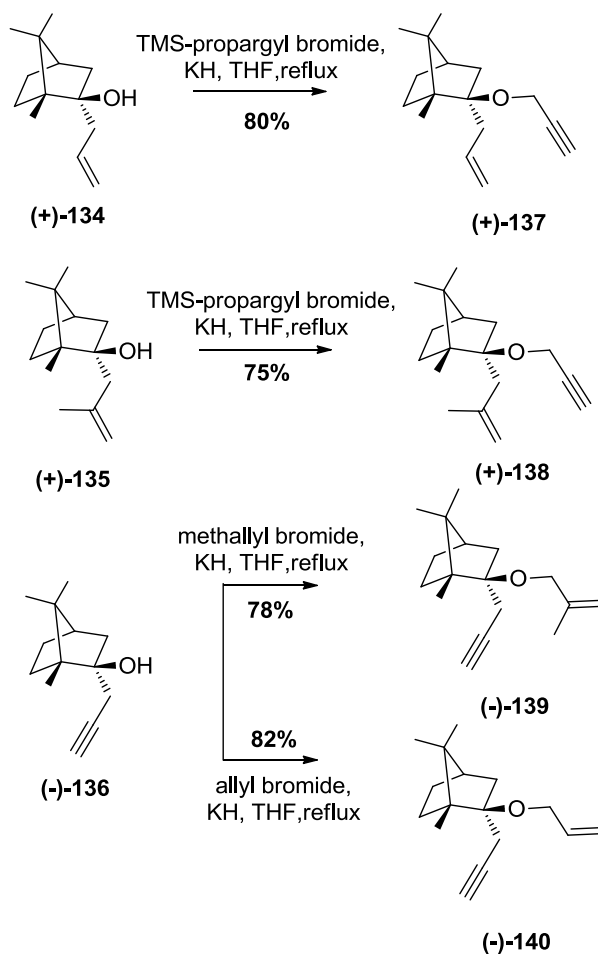
Scheme 33. Synthesis of tertiary alcohols.

The structure elucidation of all homoallylic, homomethallylic and homopropargylic alcohols were done with ^1H and ^{13}C NMR spectroscopy and homoallylic and methallylic ones are in accordance with literature data [186]. In ^1H NMR of compound (-)-**136**, propargylic methylene protons having AB systems, appear as doublet of doublets at 2.40 and 2.34 ppm with the coupling constant values $J = 16.4$ and 2.4 Hz due to the geminal coupling and the coupling with terminal acetylenic proton. In addition, other characteristic NMR signal of terminal acetylenic proton resonates at 2.15 ppm as broad singlet.

2.5.2. Construction of Enyne Systems

The purpose of this part is to synthesize chiral enyne systems for PK cyclization like other enyne systems indicated in previous chapters. Camphor tethered enyne systems were built on optically pure tertiary homoallylic and homopropargylic alcohol skeletons by *O*-propargylation, *O*-methallylation and *O*-

allylation using TMS-propargyl bromide, methallyl bromide and allyl bromide with KH in THF, respectively (Scheme 34). Firstly, NaH was used for the abstraction of proton, however, it did not afford any desired product. KH was used as an alternative base and afforded acceptable yields in short reaction times. In propargylation reactions, TMS-protected propargyl bromide was used to avoid side reactions with KH. At the end of the reaction, TMS group was easily removed after quenching.



Scheme 34. Synthesis of enyne systems derived from tertiary alcohols.

The structure characterization of enyne systems was done with ^1H and ^{13}C NMR spectroscopy. In ^1H NMR of compound (+)-137, the methylene and terminal acetylenic protons of newly attached propargyl unit appear as doublet at 3.98 ppm with $J = 1.7$ Hz and 2.26 ppm as broad singlet, respectively. ^1H NMR of compound (+)-138, shows the characteristic methylene and methine protons regarding propargyl

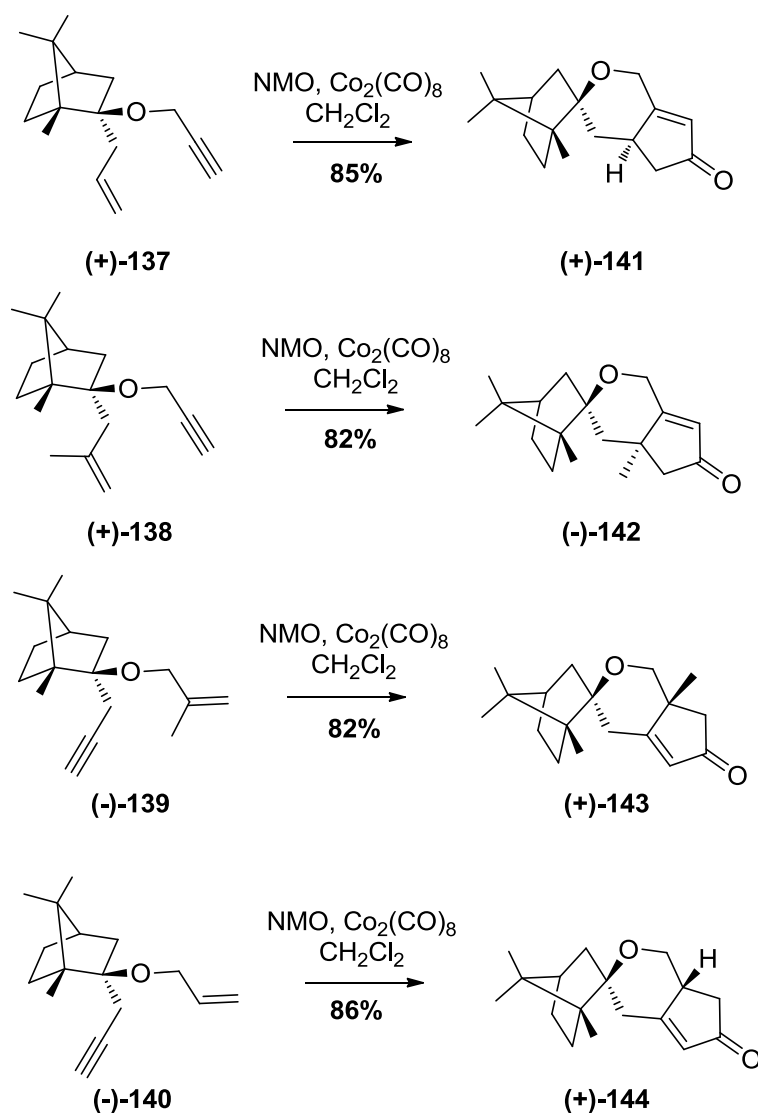
unit as doublet at 4.11 and 2.37 ppm ($J = 2.4$ Hz) and triplet ($J = 2.4$ Hz) respectively.

In ^1H NMR spectrum of compound (-)-**140**, allylic methylene protons appears as multiplet at 3.80-3.90 ppm. The other characteristic signal anchored allyl unit belonging to methine proton resonates at 5.81-5.92 ppm as multiplet, whereas olefinic methylene protons gives the signals at 5.23 and 5.01 ppm as doublet of doublets, with the coupling constant values $J = 18.2, 1.5$ Hz and $J = 11.5, 1.5$ Hz, respectively. In addition, ^{13}C NMR shows the signals for olefinic carbons at 135.8 and 114.9 ppm. Methallyl attached enyne derivative (-)-**139** shows the characteristic olefinic protons at 4.95 and 4.74 ppm and the methyl group protons attached to olefinic unit at 1.67 ppm as singlet. The methallylic diastereotopic protons resonates at 3.73 ppm as doublet ($J = 12.2$ Hz) and 3.68 as doublet ($J = 12.2$ Hz).

^1H and ^{13}C NMR spectra are shown in appendix part (Figure A85-A91).

2.5.3 Synthesis of PK Products

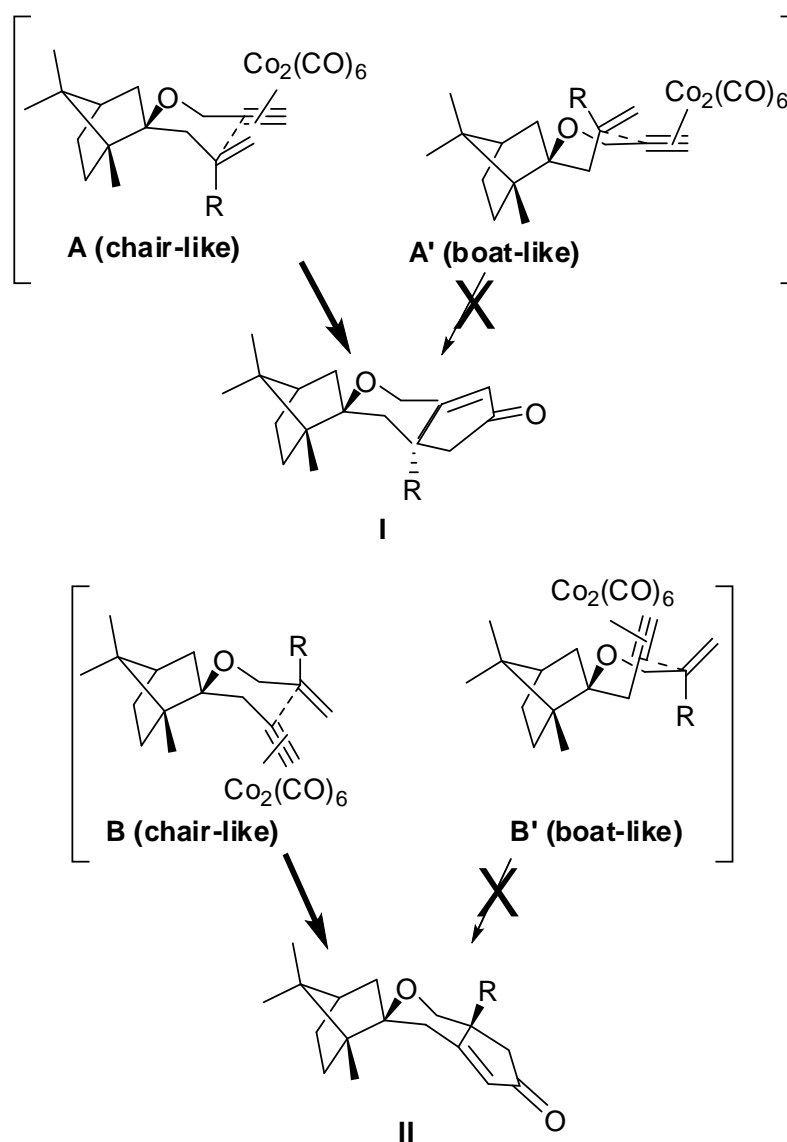
In order to study the applicability and the remote control property on stereoselectivity of the intramolecular PKR on camphor derived chiral enynes, compounds (+)-**137-138** and (-)-**139-140** were subjected to [2+2+1] cycloaddition reaction under same condition mentioned in previous sections. In all cases, single diastereomeric products (+)-**141**, (-)-**142**, (+)-**143**, (+)-**144**, have been isolated and characterized (Scheme 35).



Scheme 35. Synthesis of spirobicyclic PK products.

^1H and ^{13}C NMR spectra obviously confirmed the formation of single diastereomeric products. As a representative example, ^1H NMR of (-)-142 shows characteristic olefinic proton of newly constructed cyclopentenone unit at 5.85 ppm as a singlet. Pyran ring diastereotopic methylene protons next to the oxygen resonate at 4.41 and 4.26 ppm as doublets with the identical coupling constants ($J_{\text{AB}} = 13.6$ Hz) due to the geminal coupling. Quaternary center attached methyl protons are observed at 1.40 ppm as singlet. ^{13}C NMR shows the characteristic ketone carbonyl signal at 206.9 ppm which also strongly supports the construction of cyclopentenone moiety. The other spirobicyclic compounds (+)-141, (+)-143 and (+)-144 also

The excellent diastereoselectivity observed in the Pauson–Khand reactions may also be explained by considering the relative stability of the intermediates that lead to (+)-**141**, (-)-**142** and (+)-**143**, (+)-**144** as the sole product on the basis of the accepted Pauson–Khand mechanism [93,187-188]. The preferred conformers of the alkyne- $\text{Co}_2(\text{CO})_6$ complex can be regarded as **A** and **B**, respectively (Scheme 36). A weaker repulsion in **A** than **A'** and **B** than **B'** favors cyclization through the conformers **A** and **B**, respectively.



Scheme 36. Plausible conformations of the intermediates in the Pauson Khand reaction
80

CHAPTER 3

CONCLUSION

In this study, new 2-heteroaryl substituted chiral fused cyclopenta[*c*]pyran, cyclopenta[*c*]furan and camphor fused spiro cyclopenta[*c*]pyran derivatives were successfully synthesized. Homoallylic, allylic, homopropargylic secondary alcohols and 3 different camphor based chiral tertiary alcohols are valuable candidates for preparing chiral scaffolds for target heterocycles and synthesized in high yields. The enzyme catalyzed resolution of these secondary alcohols has been accomplished in high ee values. In particular, resolution of allylic alcohols is firstly succeeded in very short time. Absolute configurations of all alcohols were determined as (*S*) according to specific rotations reported in literature. After synthesis of target chiral alcohols, new enantiomerically enriched 2-furyl-, thiophenyl- and pyridinyl substituted enynes anchored to homoallyl and homopropargyl alcohol backbones have been synthesized. Their intramolecular PKR showed a high conformational control on the new stereocenter formed in the cyclopentenone-pyran ring system and all afforded single diastereomer indicated by NMR. The absolute configurations of the products synthesized from homoallylic- and homopropargylic-based enynes have been determined by differential NOE experiments and X-ray analysis, respectively. Enantiomerically enriched 2-heteroarylsubstituted enynes tethered to allyl alcohol backbones, which were subjected to intramolecular PKR, were also synthesized. In contrast to the cyclopentenone- pyran-fused ring systems, the resultant cyclopentenone-furan- fused ring systems were isolated as *cis:trans* isomers with acceptable diastereoselectivities. The absolute configurations of them have been determined by ¹H NMR. The role of the conformational control of pyrans was found to have a drastic influence on the diastereoselectivity in comparison with the furan ring systems.

For spirocyclic compounds, chiral tertiary alcohols were subjected to propargylation and allylation reactions, respectively to afford the corresponding enynes. Their intramolecular PKR also showed a high conformational control and in all cases, single diastereomeric products were obtained. The absolute configurations of the spirocyclic products have been determined by X-ray analysis. The results of X-ray analysis showed that the newly formed stereogenic centers located at the fused position of all cyclopenta[*c*]pyran rings have (*R*) configuration that is presumably due to the most favorable chair conformation of pyran ring.

CHAPTER 4

EXPERIMENTAL

All experiments were carried out in pre-dried glassware (1 h, 150 °C) under an inert atmosphere of Argon. The following reaction solvents were distilled from the indicated drying agents: dichloromethane (P_2O_5), tetrahydrofuran (sodium, benzophenone) 1H -NMR and ^{13}C -NMR spectra were recorded in $CDCl_3$ on Bruker Spectrospin Avance DPX-400 spectrometer. 1H (400 MHz) and ^{13}C NMR were recorded in $CDCl_3$ and the chemical shift as were expressed in ppm relative to $CDCl_3$ (δ 7.26 and 77.0 for 1H and ^{13}C NMR, respectively) as the internal standard. Standard COSY, HETCOR and DEPT experiments were performed to establish NMR assignments.

Infrared spectra were recorded on a Thermo Nicolet IS10 ATR-FT-IR spectrophotometer. The mass spectra were recorded on Thermo Scientific DSQ II Single Quadrupole GC/MS. HRMS data were obtained via LC-MS analysis performed with APCI-Q-TOF II (Waters, Milford, MA, USA) at Mass Spectrometry Facility Center for Functional Genomics University at Albany. Optical rotations were measured employing a Rudolph research analytical, autopol III automatic polarimeter. Melting points were obtained on a Thomas Hoover capillary melting point apparatus and are uncorrected.

Flash column chromatography was performed by using thick-walled glass columns with a flash grade (Merc Silica Gel 60). Reactions were monitored by thin layer chromatography using precoated silica gel plates (Merc Silica Gel PF-254), visualized by UV-light and polymolybden phosphoric acid in ethanol as

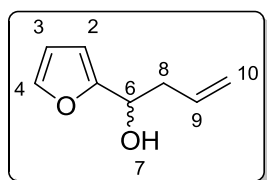
appropriate. All extracts were dried over anhydrous magnesium sulphate and solutions were concentrated under vacuum by using rotary evaporator.

Only characterization data of novel compounds are given in experimental section and related literature is cited.

4.1. General Procedure for Synthesis of Racemic Homoallylic Alcohols, *rac*-95-97

To a stirred solution of Mg turnings (15 mmol) and iodine (2 pieces) in dry diethyl ether (7 mL) at 25 °C equipped with a reflux condenser was added dropwise a mixture of allylbromide (11 mmol) in anhydrous diethyl ether (5 mL). The mixture was allowed to reflux for 30 min. The mixture was cooled down to 0 °C and then corresponding aldehyde (10 mmol) in dry diethylether (3 mL) was added dropwise. The resultant mixture was stirred for 2 h. The reaction mixture was hydrolyzed with saturated ammonium chloride solution (10 mL) and then with 1 M HCl (2 mL). The resultant mixture was extracted with diethylether (3 x 30 mL). The combined organic phase was washed with brine (20 mL) and dried over MgSO₄ and evaporated in vacuo. The crude products were purified by flash column chromatography with a mixture of solvents of ethyl acetate and hexane at a ratio of 1:10 for *rac*-95, 1:8 for *rac*-96 and 1:1 for *rac*-97.

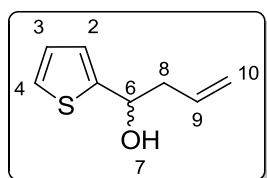
4.1.1 1-(Furan-2-yl)but-3-en-1-ol, (\pm)-*rac*-95



Colorless oil (yield 75%). ¹H-NMR δ (CDCl₃): 7.29 (brs, 1H, *H*₄), 6.25 (dd, *J* = 1.8 and 3.1 Hz, 1H, *H*₃), 6.17 (d, *J* = 3.1 Hz, 1H, *H*₂), 5.79-5.67 (m, 1H, *H*₉), 5.04-5.12 (m, 2H, *H*₁₀), 4.66 (q, *J* = 5.67, 1H, *H*₆), 2.52-2.56 (m, 2H, *H*₈), 2.10 (brs, 1H, *H*₇).

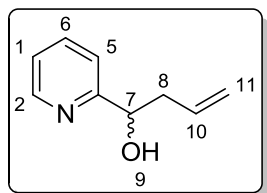
$^{13}\text{C-NMR } \delta$ (CDCl_3): 156.10, 141.94, 133.76, 118.40, 110.13, 106.08, 66.94, 40.06.
(Figure A1-A2)

4.1.2 1-(Thiophen-2-yl)but-3-en-1-ol, (\pm)-rac-96



Colorless oil (yield 80%). $^1\text{H-NMR } \delta$ (CDCl_3): 7.16 (dd, $J = 1.2$ and 4.6 Hz, 1H, H_4), 6.88–6.90 (m, 2H, H_3, H_2), 5.70–5.80 (m, 1H, H_9), 5.07–5.13 (m, 2H, H_{10}), 4.88–4.92 (m, 1H, H_6), 2.54 (t, $J = 6.8$ Hz, 2H, H_8), 2.15 (brs, 1H, H_7). $^{13}\text{C-NMR } \delta$ (CDCl_3): 147.90, 133.90, 126.63, 124.54, 123.70, 118.70, 69.42, 43.37. (Figure A3-A4).

4.1.3 1-(Pyridin-2-yl)but-3-en-1-ol, (\pm)-rac-97

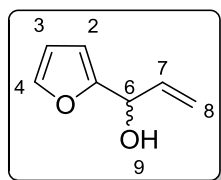


Colorless oil (yield 78%). $^1\text{H-NMR } \delta$ (CDCl_3): 8.47 (d, $J = 4.5$ Hz, 1H, H_2), 7.61 (t, $J = 7.6$ Hz, 1H, H_6), 7.21 (d, $J = 7.8$ Hz, 1H, H_5), 7.08–7.15 (m, 1H, H_1), 5.70–5.85 (m, 1H, H_{10}), 4.98–5.10 (m, 2H, H_{11}), 4.70–4.80 (m, 1H, H_7), 3.98–4.08 (m, 1H, H_9), 2.52–2.63 (m, 1H, H_8), 2.38–2.48 (m, 1H, H_8). $^{13}\text{C-NMR } \delta$ (CDCl_3): 161.38, 148.20, 136.46, 134.06, 122.21, 120.30, 117.84, 72.20, 42.80. (Figure A5-6).

4.2 General Procedure for Synthesis of Racemic Allylic Alcohols, *rac*-99-101

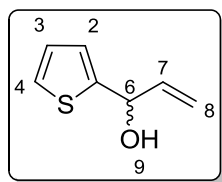
To a stirred solution of vinyl magnesium bromide (1.0 N stock solution, 12 mmol) was added dropwise a mixture of aldehyde (10 mmol) in anhydrous diethyl ether (1 mmol ald. for 5 mL) at 0 °C. The mixture was stirred under argon atmosphere until all the aldehyde was consumed (controlled by TLC) at room temperature. The reaction mixture was hydrolyzed with saturated ammonium chloride solution (10 mL) and then with 1 M HCl (2 mL). The resultant mixture was extracted with diethylether (3 x 30 mL). The combined organic phase was washed with brine (20 mL) and dried over MgSO₄ and evaporated in vacuo. The crude products were purified by flash column chromatography with a mixture of solvents of ethyl acetate and hexane at a ratio of 1:19 for *rac*-99, 1:7 for *rac*-100 and 1:1 for *rac*-101.

4.2.1 1-(Furan-2-yl)prop-2-en-1-ol, (±)-*rac*-99



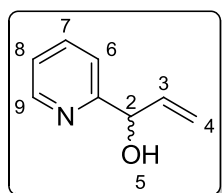
Yellow oil (yield 85%). ¹H-NMR δ (CDCl₃): 7.39 (brs, 1H, *H*₄), 6.31-6.34 (m, 1H, *H*₃), 6.24 (d, *J* = 3.2 Hz, 1H, *H*₂), 6.06-6.15 (m, 1H, *H*₇), 5.41 (d, *J* = 17.1 Hz, 1H, *H*₈), 5.26 (d, *J* = 10.4 Hz, 1H, *H*₈), 5.20 (d, *J* = 5.6 Hz, 1H, *H*₆), 2.33 (brs, 1H, *H*₉). ¹³C-NMR δ (CDCl₃): 155.08, 142.41, 136.85, 116.45, 110.28, 106.68, 68.58. (Figure A7-8).

4.2.2 1-(Thiophen-2-yl)prop-2-en-1-ol, (±)-rac-100



Yellow oil (yield 80%). $^1\text{H-NMR}$ δ (CDCl_3): 7.16-7.19 (m, 1H, H_4), 6.80-6.90 (m, 2H, H_3 , H_2), 6.00-6.08 (m, 1H, H_7), 5.28-5.38 (m, 2H, H_8), 5.12-5.19 (m, 1H, H_6). $^{13}\text{C-NMR}$ δ (CDCl_3): 146.64, 139.36, 126.80, 125.27, 124.41, 115.70, 71.03. (Figure A9-10).

4.2.3 1-(pyridin-2-yl)prop-2-en-1-ol, (±)-rac-101



Yellow oil (yield 84%). $^1\text{H NMR}$ δ (CDCl_3): 8.47 (d, $J = 4.8$ Hz, 1H, H_9), 7.62 (td, $J = 1.7$ and 7.6 Hz, 1H, H_7), 7.21 (d, $J = 8.0$ Hz, 1H, H_6), 7.13-7.15 (m, 1H, H_8), 5.83-5.92 (m, 1H, H_3), 5.38 (dt, $J = 1.3$ and 17.0 Hz, 1H, H_4), 5.17 (dt, $J = 1.3$ and 10.1 Hz, 1H, H_4), 5.08-5.10 (d, $J = 6.7$ Hz, 1H, H_2). $^{13}\text{C-NMR}$ δ (CDCl_3): 160.4, 148.4, 139.9, 137.1, 122.7, 121.2, 116.7, 74.5. (Figure A11-12).

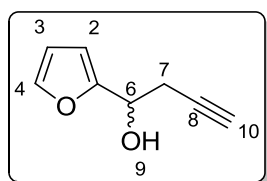
4.3. General Procedure for Synthesis of Racemic 2-Furyl and 2-thienyl substituted Homopropargylic Alcohols, rac-103-105

Zn-Cu couple preparation was performed in an oxygen-free environment. Zinc dust (6.5 g, 100 mmol) was suspended in distilled water (10 mL). Acidic cupric chloride solution (0.15 M in 5% hydrochloric acid, 22 mL) was added with vigorous magnetic stirring. When the evolution of gas ceased the suspension was filtered and

the black solid was washed with water until the wash gave a negative test with 6% silver nitrate solution. The Zn-Cu was then washed twice with acetone.

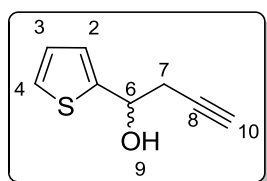
To a stirred mixture of aldehyde (72 mmol) and freshly prepared Zn-Cu couple (1.03 g, 79.6 mmol) in THF (20 mL), propargyl bromide (0.21 g, 79.6 mmol, 80% solution in toluene) was added dropwise at 0 °C. The mixture was refluxed for 6h (TLC monitoring). The resultant mixture was hydrolyzed with 1N HCl (8 mL) and extracted with ether (3 x 30 mL), dried over MgSO₄ and evaporated in vacuo. The crude products were purified by flash column chromatography with a mixture of solvents of ethyl acetate and hexane at a ratio of 1:9 for *rac*-**103** and 1:7 for *rac*-**104**.

4.3.1 1-(Furan-2-yl)but-3-yn-1-ol, (±)-*rac*-103



Yellow oil (yield 70%). ¹H-NMR δ (CDCl₃): 7.37 (brs, 1H, *H*₄), 6.31-6.34 (m, 2H, *H*₂, *H*₃), 4.84 (bt, *J* = 5.6 Hz, 1H, *H*₆), 2.81-2.87 (m, 2H, *H*₇), 2.06 (brs, 1H, *H*₁₀). ¹³C-NMR δ (CDCl₃): 154.8, 142.2, 110.1, 106.6, 80.0, 71.1, 66.1, 26.0. (Figure A13-14).

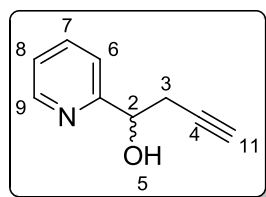
4.3.2 1-(Thiophen-2-yl)but-3-yn-1-ol, (±)-*rac*-104



Yellow oil (yield 72%). $^1\text{H-NMR}$ δ (CDCl_3): 7.11 (d, $J = 5.0$ Hz, 1H, H_4), 6.88 (d, $J = 3.2$ Hz, 1H, H_3), , 6.81-6.84 (m, 1H), 4.91 (t, $J = 6.2$ Hz, 1H, H_6), 3.18 (brs, 1H, H_9), 2.58 (dd, $J = 2.5$ and 6.3 Hz, 2H, H_7), 1.96 (t, $J = 2.5$ Hz, 1H, H_{10}). $^{13}\text{C-NMR}$ δ (CDCl_3): 146.4, 126.7, 124.9, 124.2, 80.5, 71.6, 68.5, 29.4. (Figure A15-16).

4.3.3 Procedure for Synthesis of 1-(pyridin-2-yl)but-3-yn-1-ol, (\pm)-rac-105

To a stirred suspension of Mg turnings (28 mmol) and iodine (two crystals) and HgCl_2 (9 mg) turnings in dry diethyl ether (10 mL) at 25 °C equipped with a reflux condenser was added dropwise a mixture of propargylbromide (25 mmol) in anhydrous diethyl ether (5 mL). The mixture was allowed to reflux for 30 min. The mixture was cooled down to °C and then picolinaldehyde (10 mmol) in dry diethylether (3 mL) was added dropwise. The resultant mixture was stirred for 5 h. The reaction mixture was hydrolyzed with saturated ammonium chloride solution (10 mL) and with 1 N HCl (2 mL). The resultant mixture was extracted with diethylether (3 x 30 mL). The combined organic phase was washed with brine (20 mL), dried over MgSO_4 , and evaporated in vacuo. The crude product was purified by flash column chromatography using mixture of ethyl acetate and hexane as eluent at ratio of 1:1.



Yellow oil (yield 81%). $^1\text{H-NMR}$ δ (CDCl_3): 8.48 (d, $J = 4.7$ Hz, 1H, H_9), 7.63 (t, $J = 7.7$ Hz, 1H, H_7), 7.34 (d, $J = 7.8$ Hz, 1H, H_6), 7.12-7.17 (m, 1H, H_8), 4.82 (t, $J = 6.1$ Hz, 1H, H_2), 4.34 (s, 1H, H_5), 2.64 (dd, $J = 2.4$ and 6.1 Hz, 2H, H_3), 1.94 (t, $J = 2.6$ Hz, 1H, H_{11}). $^{13}\text{C-NMR}$ δ (CDCl_3): 160.0, 148.4, 136.7, 122.8, 120.8, 80.5, 71.1, 70.8, 28.4. (Figure A17-18).

4.4. General Procedure for Enzymatic Resolution of Homoallylic, Allylic and Homopropargylic Alcohols

To a solution of the *rac*-**95-97**, *rac*-**99-101**, *rac*-**103-105** (3 mmol) in anhydrous co-solvent (THF for PS-C II and CAL-B, DIPE for Lipozyme) (3 mL) and vinyl acetate (2.7 mL) in a 25 mL round bottom flask, was added lipase (1 equiv. w/w). The reaction mixture was stirred at constant temperature and monitored by TLC and recording on HPLC. At the desired conversion, the reaction mixture was filtered off, the solid was washed with Et₂O, and the solvent was evaporated under vacuum to give a residue that was purified by column chromatography on silica gel. Experiments were repeated at least twice.

4.4.1 (S)-(-)-1-(2-Furyl)but-3-en-1-ol, (S)-(-)-95 as a yellow oil; $[\alpha]_D^{29} = -40.0$ (*c* 5.0, CH₂Cl₂) for 99% ee. The absolute configuration and enantiomeric purity of the product were determined by HPLC analysis (Daicel Chiralcel OJ-H, hexane/*i*-PrOH 96:4, flow rate=1 mLmin⁻¹, $\lambda=230$ nm), $t_R=11.20$ min (*R* isomer), $t_R=12.64$ min (*S* isomer) in comparison with the racemic sample).

4.4.1.1 (R)-(+)-1-(2-Furyl)but-3-en-1-yl acetate, (R)-(+)-107 as a yellow oil; $[\alpha]_D^{29} = +22.20$ (*c* 1.02, CH₂Cl₂) for 96% ee. The absolute configuration and enantiomeric purity of the product were determined by HPLC analysis (Whelk, hexane/*i*PrOH 96:4, flow rate=1 mLmin⁻¹, $\lambda=230$ nm), $t_R=5.49$ min, $t_R=6.25$ in comparison with the racemic sample).

4.4.2 (S)-(-)-1-(Thiophen-2-yl)but-3-en-1-ol, (S)-(-)-96 as a yellow oil; $[\alpha]_D^{27} = -17.1$ (*c* 1.2, CH₂Cl₂) for 99% ee. The enantiomeric purity of the product was determined by HPLC analysis (Daicel Chiralcel OJ-H, hexane/*i*-PrOH 96:4, flow rate=1 mL min⁻¹, $\lambda=230$ nm), $t_R=12.98$ min (*S* isomer), $t_R=15.01$ min (*R* isomer) in comparison with the racemic sample.

4.4.2.1 (R)-(+)-1-(Thiophen-2-yl)but-3-enyl acetate, (R)-(+)-108 as a yellow oil; $[\alpha]_D^{29} = +84.0$ (*c* 1, CH₂Cl₂) for 91% ee. The enantiomeric purity of the product was determined by HPLC analysis (Daicel Chiralcel OJ-H, hexane/*i*-PrOH 96:4, flow rate=1 mLmin⁻¹, $\lambda=230$ nm), $t_R=8.58$ min (*S* isomer), $t_R=19.86$ min (*R* isomer) in comparison with the racemic sample.

4.4.3 (S)-(-)-1-(Pyridin-2-yl)but-3-en-1-ol, (S)-(-)-97 as a yellow oil; $[\alpha]_D^{29} = -42.9$ (*c* 0.86, CH₂Cl₂) for 98% ee. The enantiomeric purity of the product was determined by HPLC analysis (Daicel Chiralcel OJ-H, hexane/*i*-PrOH 99:1, flow rate = 0.3 mLmin⁻¹, $\lambda=254$ nm), $t_R=58.75$ min (*S* isomer), $t_R=63.74$ min (*R* isomer) in comparison with the racemic sample.

4.4.3.1 (R)-(+)-1-(Pyridin-2-yl)but-3-enyl acetate, (R)-(+)-109 as a yellow oil; $[\alpha]_D^{30} = +49.7$ (*c* 0.5, CH₂Cl₂) for 95% ee. The enantiomeric purity of the product was determined by HPLC analysis after conversion to alcohol.

4.4.4 (S)-(+)-1-(Furan-2-yl)prop-2-en-1-ol, (S)-(+)-99 as a yellow oil; $[\alpha]_D^{28} = +1.1$ (*c* 2.24, CHCl₃) for 98% ee. The enantiomeric purity of the product was determined by HPLC analysis (Daicel Chiralcel OJ-H, hexane/*i*-PrOH 96:4, flow rate = 1 mLmin⁻¹, $\lambda=230$ nm), $t_R=18.26$ min (*S* isomer), $t_R=19.75$ min (*R* isomer) in comparison with the racemic sample.

4.4.5 (S)-(-)-1-(Thiophen-2-yl)prop-2-en-1-ol, (S)-(-)-100 as a yellow oil; $[\alpha]_D^{28} = -2.7$ (*c* 1, CHCl₃) for 97% ee. The enantiomeric purity of the product was determined by HPLC analysis (Daicel Chiralcel OJ-H, hexane/*i*-PrOH 96:4, flow rate = 1 mLmin⁻¹, $\lambda=230$ nm), $t_R=20.93$ min (*S* isomer), $t_R=27.14$ min (*R* isomer) in comparison with the racemic sample.

4.4.6 (S)-(+)-1-(Pyridin-2-yl)prop-2-en-1-ol, (S)-(+)-101 as a yellow oil; $[\alpha]_D^{29} = +54.8$ (*c* 1.84, CHCl₃) for 90% ee. The enantiomeric purity of the product was determined by HPLC analysis after conversion to acetate (Daicel Chiralcel OJ-H, hexane/*i*-PrOH 99:1, flow rate = 1 mLmin⁻¹, $\lambda = 254$ nm), $t_R = 34.17$ min (*R* isomer), $t_R = 35.90$ min (*S* isomer) in comparison with the racemic sample.

4.4.6.1 (R)-(+)-1-(Pyridin-2-yl)allyl acetate, (R)-(+)-112 as a yellow oil; $[\alpha]_D^{27} = +36.4$ (*c* 1.84, CHCl₃) for 99% ee. The enantiomeric purity of the product was determined by HPLC analysis (Daicel Chiralcel OJ-H, hexane/*i*-PrOH 99:1, flow rate = 1 mLmin⁻¹, $\lambda = 254$ nm), $t_R = 32.40$ min (*R* isomer), $t_R = 35.10$ min (*S* isomer) in comparison with the racemic sample.

4.4.7 (S)-(+)-1-(Furan-2-yl)but-3-yn-1-ol, (S)-(+)-103 as a yellow oil; $[\alpha]_D^{29} = +6.67$ (*c* 3.1, MeOH) for 93% ee. The absolute configuration and enantiomeric purity of the product were determined by HPLC analysis (Daicel Chiralcel OD-H, hexane/*i*PrOH 96:4, flow rate=1 mLmin⁻¹, $\lambda = 230$ nm), $t_R = 16.842$ min, $t_R = 23.15$ in comparison with the authentic sample).

4.4.7.1. (R)-(+)-1-(Furan-2-yl)but-3-ynyl acetate, (R)-(+)-113 as a yellow oil; $[\alpha]_D^{29} = +54.6$ (*c* 4.0, MeOH) for 90% ee. The absolute configuration and enantiomeric purity of the product were determined by HPLC analysis (Whelk, hexane/*i*PrOH 96:4, flow rate=1 mLmin⁻¹, $\lambda = 230$ nm), $t_R = 5.89$ min, $t_R = 6.11$ in comparison with the authentic sample.

4.4.8 (S)-(+)-1-(Thiophen-2-yl)but-3-yn-1-ol, (S)-(+)-104 as a yellow oil; $[\alpha]_D^{28} = +26.5$ (*c* 1, EtOH) for 99% ee. The enantiomeric purity of the product was determined by HPLC analysis (Daicel Chiralcel OJ-H, hexane/*i*-PrOH 96:4, flow rate=1 mLmin⁻¹, $\lambda = 230$ nm), $t_R = 35.56$ min (*R* isomer), $t_R = 41.75$ min (*S* isomer) in comparison with the racemic sample.

4.4.8.1 (R)-(+)-1-(Thiophen-2-yl)but-3-ynyl acetate, (R)-(+)-114 as a yellow oil; $[\alpha]_D^{29} = +73.4$ (c 1, EtOH) for 93% ee. The enantiomeric purity of the product was determined by HPLC analysis (Daicel Chiralcel OJ-H, hexane/*i*-PrOH 96:4, flow rate=1 mLmin⁻¹, λ =230 nm), t_R =11.53 min (*S* isomer), t_R =14.31 min (*R* isomer) in comparison with the racemic sample.

4.4.9 (S)-(-)-1-(Pyridin-2-yl)but-3-yn-1-ol, (S)-(-)-105 as a yellow oil but after a short time turns black; $[\alpha]_D^{28} = -6.7$ (c 1, CH₂Cl₂) (The $[\alpha]$ value of the product was recorded immediately after resolution because of this compound has a tendency to dark while storage) for 99% ee. The enantiomeric purity of the product was determined by HPLC analysis (Daicel Chiralcel OJ-H, hexane/*i*-PrOH 99:1, flow rate = 0.3 mLmin⁻¹, λ =254 nm), t_R =90.56 min (*R* isomer), t_R =97.90 min (*S* isomer) in comparison with the racemic sample. The absolute configuration of the compound was determined by comparing α value after conversion to its saturated form [189].

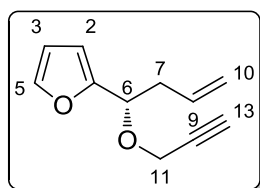
4.4.9.1 (R)-(+)-1-(Pyridin-2-yl)but-3-ynyl acetate, (R)-(+)-115 as a yellow oil but after a short time turns black; $[\alpha]_D^{27} = +44.0$ (c 0.5, CH₂Cl₂) for 75% ee. The enantiomeric purity of the product was determined by HPLC analysis (Daicel Chiralcel OJ-H, hexane/*i*-PrOH 97:3, flow rate=1 mLmin⁻¹, λ =254 nm), t_R =11.20 min (*R* isomer), t_R =12.64 min (*S* isomer) in comparison with the racemic sample.

4.5 General Procedure for *O*-allylation and *O*-propargylation

To a solution of (S)-(-)-**95-97** or (S)-(+)-**99-101** and (S)-(-)-**103-105** (1.4 mmol) in dry THF (15 mL) was added NaH (0.62 g, 60% dispersion in oil, 1.54 mmol) under argon. The solution heated at reflux until H₂ gas removing completed (nearly 45 min.). Subsequently allylbromide or propargylbromide (1.54 mmol) was added dropwise followed by tetrabutylammonium iodide (0.5 mmol). The mixture was refluxed for another 2h and hydrolyzed by the cautious addition of water (15 mL). The aqueous layer was extracted with ether (3x20 mL). The combined organic phase was dried over MgSO₄ and evaporated in vacuo. The crude product mixtures

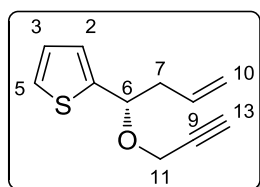
were separated by flash column chromatography using ethylacetate/hexane solvent as eluent (1:6) system for compounds (S)-(-)-116, (S)-(-)-117, (S)-(-)-119, (S)-(-)-120, (S)-(-)-122, (S)-(-)-123 and (1:1) system for compounds (S)-(-)-118, (S)-(-)-121, (S)-(-)-124. The products (S)-(-)-116, (S)-(-)-117, (S)-(-)-118, (S)-(-)-119, (S)-(-)-120, (S)-(-)-121, (S)-(-)-122, (S)-(-)-123, (S)-(-)-124, were obtained 83, 80, 89, 78, 80, 41, 79, 82, 90% yield, respectively.

4.5.1 (S)-(-)-2-(1-(Prop-2-ynyloxy)but-3-enyl)furan, (-)-116



(83% yield) as a yellow oil. $[\alpha]_D^{29} = -67.5$ (c 2.7, CH_2Cl_2). $^1\text{H-NMR}$ δ (CDCl_3): 7.32 (brs, 1H, H_5), 6.24-6.26 (m, 2H, H_2, H_3), 5.62-5.72 (m, 1H, H_9), 5.02 (dd, $J = 1.7$ and 17.1 Hz, 1H, H_{10}), 4.96 (d, 10.2 Hz, 1H, H_{10}), 4.51 (t, $J = 7.0$ Hz, 1H, H_6), 4.07 (dd, $J_{\text{AB}} = 2.4$ and 15.9 Hz, 1H, H_{11}), 3.86 (dd, $J_{\text{AB}} = 2.3$ and 15.9 Hz, 1H, H_{11}), 2.52-2.63 (m, 2H, H_7), 2.31 (t, $J = 2.4$ Hz, 1H, H_{13}). $^{13}\text{C-NMR}$ δ ($\text{CDCl}_3 + \text{CCl}_4$): 153.2, 142.8, 134.1, 117.7, 110.3, 109.3, 80.0, 74.6, 73.2, 55.8, 38.7. Anal. calcd.: C, 74.98; H, 6.86; found.: C, 74.36; H, 6.81. (Figure A37-38).

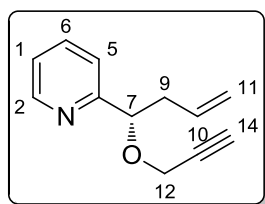
4.5.2 (S)-(-)-2-(1-(Prop-2-ynyloxy)but-3-enyl)thiophene, (S)-(-)-117



This is a yellow oil. (0.21 g, 80% yield). $[\alpha]_D^{29} = -97.6$ (c 1.35, CH_2Cl_2). $^1\text{H-NMR}$ δ (CDCl_3): 7.21 (d, $J = 5.0$ Hz, 1H, H_5), 6.93 (d, $J = 3.4$ Hz, 1H, H_3), 6.88-6.90 (m, 1H, H_2), 5.65-5.75 (m, 1H, H_9), 5.03 (ddd, $J = 1.5, 3.3$ and 17.2 Hz, 1H, H_{10}), 4.97

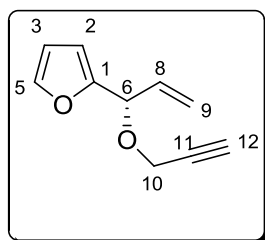
(dd, $J = 1.0$ and 10.2 Hz, 1H, H_{10}), 4.76 (t, $J = 6.8$ Hz, 1H, H_6), 4.08 (dd, $J_{AB} = 2.4$ and 15.8 Hz, 1H, H_{11}), 3.85 (dd, $J_{AB} = 2.4$ and 15.8 Hz, 1H, H_{11}), 2.60-2.67 (m, 1H, H_7), 2.43-2.50 (m, 1H, H_7), 2.32 (t, $J = 2.37$ Hz, 1H, H_{13}). $^{13}\text{C-NMR}$ δ ($\text{CDCl}_3 + \text{CCl}_4$): 144.2, 134.0, 126.4, 126.2, 125.5, 117.5, 79.7, 75.4, 74.4, 55.2, 42.4. IR (neat): 2973, 1088, 1047, 880 cm^{-1} . MS (EI) m/z (rel. intensity) 151 ($\text{M}^+ - 41$ ($^+\text{CH}_2\text{CH}=\text{CH}_2$), base). (Figure A39-40).

4.5.3 (S)-(-)-2-(1-(Prop-2-ynoxy)but-3-enyl)pyridine, (S)-(-)-118



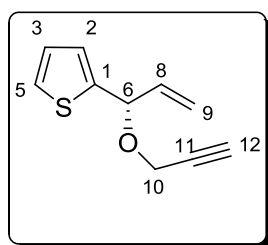
This is a yellow oil. (0.23 g, 89% yield). $[\alpha]_{\text{D}}^{29} = -136.9$ (c 3, CH_2Cl_2). $^1\text{H-NMR}$ δ (CDCl_3): 8.50 (d, $J = 4.4$ Hz, 1H, H_2), 7.62 (t, $J = 7.6$ Hz, 1H, H_6), 7.34 (d, $J = 7.8$ Hz, 1H, H_5), 7.11-7.14 (m, 1H, H_1), 5.69-5.79 (m, 1H, H_{10}), 4.93-5.00 (m, 2H, H_{11}), 4.64 (t, $J = 6.4$ Hz, 1H, H_7), 4.12 (d, $J_{AB} = 15.8$ Hz, 1H, H_{12}), 3.94 (d, $J_{AB} = 15.8$ Hz, 1H, H_{12}), 2.51-2.55 (m, 2H, H_9), 2.33 (brs, 1H, H_{14}). $^{13}\text{C-NMR}$ δ (CDCl_3): 160.7, 149.2, 136.6, 134.0, 122.6, 120.9, 117.3, 81.4, 79.6, 74.4, 56.5, 40.6. IR (neat): 2961, 1084, 797 cm^{-1} . MS (EI) m/z (rel. intensity) 146 ($\text{M}^+ - 41$ ($^+\text{CH}_2\text{CH}=\text{CH}_2$), base). Anal. Calcd. C, 76.98; H, 7.00; N, 7.48. Found: C, 76.94; H, 6.98; N, 7.39. (Figure A41-42).

4.5.4 (S)-(-)-2-(1-(Prop-2-ynoxy)allyl)furan, (S)-(-)-119



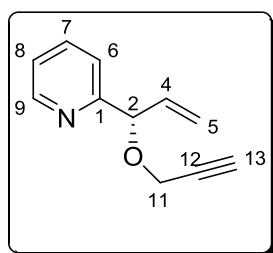
This is a yellow oil. (0.18 g, 78% yield). $[\alpha]_D^{20} = -7.1$ (c 1, CH₂Cl₂). ¹H-NMR δ (CDCl₃): 7.31-7.33 (m, 1H, *H*₅), 6.21-6.826 (m, 2H, *H*₃ ve *H*₂), 5.93 (ddd, *J* = 6.8, 10.3 and 17.2 Hz, 1H, *H*₈), 5.29-5.34 (dm, *J* = 17.2 Hz, 1H, *H*₉), 5.23-5.25 (dm, *J* = 10.3 Hz, 1H, *H*₉), 5.00 (d, *J* = 6.7 Hz, 1H, *H*₆), 4.09 (dd, *J*_{AB} = 2.4 and 15.8 Hz, 1H, *H*₁₀), 4.01 (dd, *J*_{AB} = 2.4 and 15.8 Hz, 1H, *H*₁₀), 2.34 (t, *J* = 2.4 Hz, 1H, *H*₁₂). ¹³C-NMR δ (CDCl₃): 151.5, 141.6, 133.4, 117.4, 109.1, 107.5, 78.4, 73.6, 73.0, 54.1. IR (neat): 2960, 1092, 799 cm⁻¹. MS (EI) *m/z* (rel. intensity) 162 (M⁺, 4), 107 (62), 95 (base). (Figure A43-44).

4.5.5 (S)-(-)-2-(1-(Prop-2-ynoxy)allyl)thiophene, (S)-(-)-120



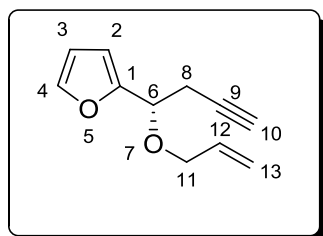
This is a yellow oil. (0.2 g, 80% yield). $[\alpha]_D^{22} = -13.4$ (c 1, CH₂Cl₂). ¹H-NMR δ (CDCl₃): 7.19 (dd, *J* = 1.2 and 5.0 Hz, 1H, *H*₅), 6.91-6.92 (dm, *J* = 3.4 Hz, 1H, *H*₃), 6.87-6.89 (m, 1H, *H*₂), 5.91 (ddd, *J* = 6.8, 10.2 and 17.0 Hz, 1H, *H*₈), 5.27-5.33 (dm, *J* = 17.1 Hz, 1H, *H*₉), 5.20-5.23 (m, 2H, *H*₉ ve *H*₆), 4.10 (dd, *J*_{AB} = 2.4 and 15.9 Hz, 1H, *H*₁₀), 4.02 (dd, *J*_{AB} = 2.4 and 15.9 Hz, 1H, *H*₁₀), 2.33 (t, *J* = 2.3 Hz, 1H, *H*₁₂). ¹³C-NMR δ (CDCl₃): 143.8, 137.4, 126.8, 126.0, 125.9, 118.0, 79.8, 76.7, 75.0, 55.3. IR (neat): 1264, 736 cm⁻¹. MS (EI) *m/z* (rel. intensity) 151 (M⁺ - 27(⁺CH=CH₂), base), 111 (30). (Figure A45-46).

4.5.6 (S)-(-)-2-(1-(Prop-2-ynoxy)allyl)pyridine, (S)-(-)-121



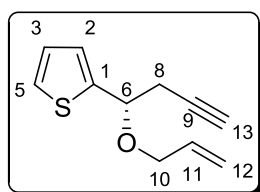
This is a yellow oil. (0.1 g, 41% yield). $[\alpha]_{\text{D}}^{22} = -18.0$ (c 1, CH_2Cl_2). $^1\text{H-NMR}$ δ (CDCl_3): 8.51 (d, $J = 4.8$ Hz, 1H, H_9), 7.64 (td, $J = 1.8$ and 7.7 Hz, 1H, H_7), 7.40 (d, $J = 7.9$ Hz, 1H, H_6), 7.12-7.15 (m, 1H, H_8), 5.90 (ddd, $J = 7.1$, 10.3 and 17.3 Hz, 1H, H_4), 5.37-5.41 (dm, $J = 17.2$ Hz, 1H, H_5), 5.25-5.28 (dm, $J = 10.3$ Hz, 1H, H_5), 5.08 (d, $J = 7.1$ Hz, 1H, H_2), 4.17 (d, $J = 2.4$ Hz, 2H, H_{11}), 2.37 (t, $J = 2.4$ Hz, 1H, H_{13}). $^{13}\text{C-NMR}$ δ (CDCl_3): 158.8, 148.2, 135.9, 135.4, 121.7, 120.2, 117.5, 81.4, 78.5, 73.6, 54.8. IR (neat): 2958, 1069, 803 cm^{-1} . MS (EI) m/z (rel. intensity) 134 ($\text{M}^+ - 39$ ($^+\text{CH}_2\text{C}\equiv\text{CH}$), 78), 118 ($\text{M}^+ - 45$ ($^+\text{OCH}_2\text{C}\equiv\text{CH}$), base). (Figure A47-48).

4.5.7 (S)-2-(1-(Allyloxy)but-3-ynyl)furan, (S)-(-)-122



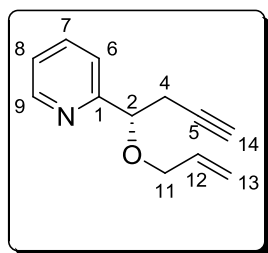
Yellow oil (80 % yield) $[\alpha]_{\text{D}}^{29} = -103.4$ (c , 1.0, CH_2Cl_2); $^1\text{H-NMR}$ δ (CDCl_3): 7.33 (t, $J = 1.2$ Hz, 1H, H_4), 6.28-6.26 (m, 2H, H_2 , H_3), 5.80 (ddt, $J = 17.0$, 10.4 and 5.2 Hz, 1H, H_{12}), 5.20 (dq, $J_{\text{trans}} = 17.2$ and 1.6 Hz, 1H, H_{13}), 5.11 (dq, $J_{\text{cis}} = 10.3$ and 1.3 Hz, 1H, $H_{13'}$), 4.45 (t, $J = 6.8$ Hz, 1H, H_6), 3.94 (ddt, $J = 12.8$, 5.2 and 1.5 Hz, 1H, H_{11}), 3.82 (ddt, $J = 12.8$, 6.2 and 1.3 Hz, 1H, $H_{11'}$), 2.70 (t, $J = 2.4$ Hz, 1H, H_8), 2.68 (t, $J = 2.6$ Hz, 1H, H_8'), 1.86 (t, $J = 2.4$ Hz, 1H, H_{10}); $^{13}\text{C-NMR}$ δ (CDCl_3): 151.9, 141.4, 133.3, 116.3, 109.0, 107.4, 79.1, 71.3, 68.9, 68.7, 23.5 IR(neat) cm^{-1} : 3301, 1725, 1685, 1077, 733. (Figure A49-50).

4.5.8 (S)-(-)-2-(1-(Allyloxy)but-3-ynyl)thiophene, (S)-(-)-123



This is a yellow oil. (0.22 g, 82% yield). $[\alpha]_D^{29} = -33.1$ (c 1.3, CH_2Cl_2). $^1\text{H-NMR}$ δ (CDCl_3): 7.17-7.24 (m, 1H, H_5), 6.94-6.96 (m, 1H, H_3), 6.89-6.91 (m, 1H, H_2), 5.77-5.87 (m, 1H, H_{11}), 5.18-5.22 (dm, $J = 15.7$ Hz, 1H, H_{12}), 5.10-5.12 (dm, $J = 10.3$ Hz, 1H, H_{12}), 4.68 (t, $J = 6.6$ Hz, 1H, H_6), 3.97 (dd, $J_{\text{AB}} = 5.0$ and 12.8 Hz, 1H, H_{10}), 3.83 (dd, $J_{\text{AB}} = 6.3$ and 12.8 Hz, 1H, H_{10}), 2.72 (ddd, $J_{\text{AB}} = 2.8, 6.5$ and 16.5 Hz, 1H, H_8), 2.59 (ddd, $J_{\text{AB}} = 2.8, 6.7$ and 16.7 Hz, 1H, H_8), 1.92 (t, $J = 2.5$ Hz, 1H, H_{13}). $^{13}\text{C-NMR}$ δ (CDCl_3): 144.5, 134.4, 126.5, 125.7, 125.3, 117.5, 80.4, 75.0, 70.4, 69.8, 28.5. IR (neat): 2972, 1081, 1039, 879 cm^{-1} . MS (EI) m/z (rel. intensity) 153 ($\text{M}^+ - 39$ ($^+\text{CH}_2\text{C}\equiv\text{CH}$), base). (Figure A51-52).

4.5.9 .(S)-(-)-2-(1-(Allyloxy)but-3-ynyl)pyridine, (S)-(-)-124

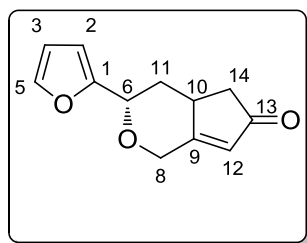


This is a yellow oil. (0.23 g, 90% yield). $[\alpha]_D^{29} = -63.6$ (c 0.9, CH_2Cl_2). $^1\text{H-NMR}$ δ (CDCl_3): 8.49 (d, $J = 4.61$ Hz, 1H, H_9), 7.63 (t, $J = 7.5$ Hz, 1H, H_7), 7.41 (d, $J = 7.84$ Hz, 1H, H_6), 7.06-7.18 (m, 1H, H_8), 5.85 (ddd, $J = 5.5, 10.8$ and 16.3 Hz, 1H, H_{12}), 5.19-5.23 (dm, $J = 17.2$ Hz, 1H, H_{13}), 5.08-5.11 (dm, $J = 10.4$ Hz, 1H, H_{13}), 4.57 (t, $J = 6.0$ Hz, 1H, H_2), 3.99 (dd, $J = 5.2$ and 12.8 Hz, 1H, H_{11}), 3.91 (dd, $J = 5.7$ and 12.8 Hz, 1H, H_{11}), 2.73 (ddd, $J = 2.5, 5.5$ and 16.8 Hz, 1H, H_4), 2.64 (dd, $J = 6.4$ and 16.8 Hz, 1H, H_4), 1.86 (t, $J = 2.6$ Hz, 1H, H_{14}). $^{13}\text{C-NMR}$ δ (CDCl_3): 160.3, 149.1, 136.5, 134.4, 122.7, 121.0, 117.2, 80.4, 80.0, 70.5, 70.1, 26.2. Anal. Calcd. C, 76.98; H, 7.00; N, 7.48. Found: C, 77.12; H, 7.21; N, 7.33. (Figure A53-54).

4.6 General Procedure for Pauson-Khand Reaction

To a solution of (*S*)-(-)-**116-118**, (*S*)-(-)-**119-121** and (*S*)-(-)-**122-124** (1 mmol) in CH₂Cl₂ (10 mL) was added Co₂(CO)₈ (1.7 mmol), and stirred for 2h (TLC monitoring). Then, NMO (9 mmol) was added and stirred for 24h. The products (+)-**125-127**, (+)-**128-130**, and diastereomeric couples of (+)-**131**/(-)-**131**, (+)-**132**/(-)-**132**, (+)-**133**/(-)-**133** were purified by flash column chromatography using ethylacetate/hexane solvent as eluent (1:1 system for compounds (+)-**125**, (+)-**126**, (+)-**128**, (+)-**129** and 10:1 system for compounds (+)-**127**, (+)-**130**). The products (+)-**125**, (+)-**126**, (+)-**127**, (+)-**128**, (+)-**129**, (+)-**130**, were obtained 75, 76, 80, 81, 80 and 81% yield, respectively. Diastereomeric mixtures obtained from compounds (*S*)-(-)-**119-121** were purified by flash column chromatography using ethylacetate/hexane solvent as eluent (1:1 system for couples (+)-**131**/(-)-**131**, (+)-**132**/(-)-**132** and 10:1 system for couple (+)-**133**/(-)-**133**). The total yields of couples (+)-**131**/(-)-**131**, (+)-**132**/(-)-**132** and (+)-**133**/(-)-**133** are 74, 77, 50% yield, respectively.

4.6.1 (3*S*,4*aR*)-(+)-3-(Furan-2-yl)-3,4,4*a*,5-tetrahydrocyclopenta[*c*]pyran-6(1*H*)-one, (+)-**125**

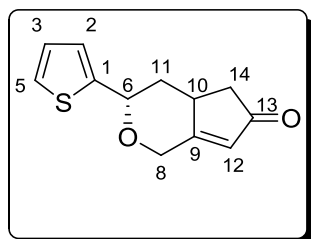


(0.18 g, 75% yield) as a white solid; mp 89 °C. $[\alpha]_D^{29} = +35.5$ (*c* 1.7, CH₂Cl₂)

¹H-NMR δ (CDCl₃): 7.33 (d, *J* = 1.0 Hz, 1H), 6.29 (m, 1H), 6.24 (d, *J* = 3.2 Hz, 1H), 5.94 (s, 1H), 4.74 (d, *J* = 13.5 Hz, 1H), 4.63 (dd, *J* = 1.3 and 11.5 Hz, 1H), 4.35 (d, *J* = 13.5 Hz, 1H), 2.97-3.00 (m, 1H), 2.62 (dd, *J* = 6.5 and 18.8 Hz, 1H), 2.36 (dd, *J* = 5.8 and 13.0 Hz, 1H), 2.08 (dd, *J* = 2.8 and 18.6 Hz, 1H), 1.80 (dd, *J* = 12.2 and 24.4 Hz, 1H) ¹³C-NMR δ (CDCl₃): 207.4, 174.2, 153.0, 142.6, 127.8, 110.3, 107.1, 72.2, 67.0, 41.8, 39.0, 37.9. IR (KBr): 1702, 1622, 1403 cm⁻¹. Anal. calcd.: C, 70.57; H,

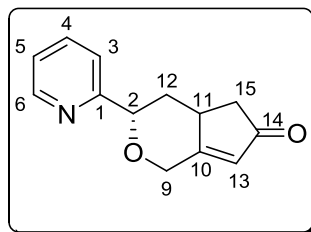
5.92; found.: C, 70.36; H, 5.78. (Figure A55-60).

4.6.2 (3*S*,4*aR*)-(+)-3-(Thiophen-2-yl)-3,4,4*a*,5-tetrahydrocyclopenta[*c*]pyran-6(1*H*)-one, (3*S*,4*aR*)-(+)-126



This is a white solid. Mp: 104-105 °C, (0.17 g, 80% yield). $[\alpha]_D^{29} = +53.4$ (*c* 1.6, CH₂Cl₂). ¹H-NMR δ (CDCl₃): 7.19-7.20 (m, 1H, *H*₅), 6.90-6.93 (m, 2H, *H*₃ ve *H*₂), 5.94 (s, 1H, *H*₁₂), 4.82 (d, *J* = 11.1 Hz, 1H, *H*₆), 4.77 (d, *J*_{AB} = 13.5 Hz, 1H, *H*₈), 4.36 (d, *J*_{AB} = 13.5 Hz, 1H, *H*₈), 3.00-3.03 (m, 1H, *H*₁₀), 2.61 (dd, *J* = 6.5 and 18.6 Hz, 1H, *H*₁₄), 2.44 (dd, *J* = 5.5 and 13.0 Hz, 1H, *H*₁₁), 2.06 (dd, *J* = 2.7 and 18.6 Hz, 1H, *H*₁₄), 1.70 (q, *J* = 12.3 Hz, 1H, *H*₁₁). ¹³C-NMR δ (CDCl₃): 206.3, 173.1, 142.8, 126.8, 125.6, 124.1, 123.0, 73.9, 66.2, 40.9, 40.7, 38.2. IR (neat): 1708, 1629, 1072, cm⁻¹. HRMS, Calculated [M]⁺ 221.0636, Measured [M]⁺ 221.0632. (Figure A61-62).

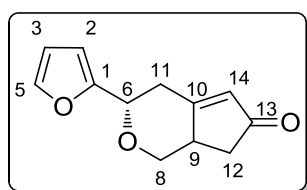
4.6.3 (3*S*,4*aR*)-(+)-3-(Pyridin-2-yl)-3,4,4*a*,5-tetrahydrocyclopenta[*c*]pyran-6(1*H*)-one, (3*S*,4*aR*)-(+)-127



This is a yellow thick liquid. (0.16 g, 76% yield). $[\alpha]_D^{29} = +33.6$ (*c* 1, CH₂Cl₂). ¹H-NMR δ (CDCl₃): 8.48 (d, *J* = 4.07 Hz, 1H, *H*₆), 7.63 (t, *J* = 7.3 Hz, 1H, *H*₄), 7.38 (d, *J* = 7.8 Hz, 1H, *H*₃), 7.12-7.15 (m, 1H, *H*₅), 5.95 (s, 1H, *H*₁₃), 4.83 (d, *J*_{AB} = 13.4 Hz,

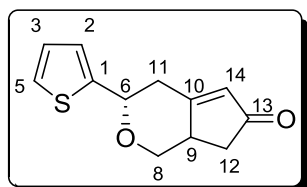
1H, H_9), 4.68 (d, $J = 11.1$ Hz, 1H, H_2), 4.39 (d, $J_{AB} = 13.4$ Hz, 1H, H_9), 3.03-3.09 (m, 1H, H_{11}), 2.54-2.64 (m, 2H, H_{15}), 2.03 (dd, $J = 2.2$ and 18.7 Hz, 1H, H_{12}), 1.45-1.46 (q, $J_{AB} = 12.1$ Hz, 1H, H_{12}). ^{13}C -NMR δ (CDCl_3): 207.5, 174.6, 160.0, 148.9, 136.8, 127.6, 122.7, 120.1, 79.6, 67.1, 41.8, 40.7, 39.4. HRMS, Calculated $[\text{M}]^+$ 216.1024, Measured $[\text{M}]^+$ 216.1021. (Figure A63-64).

4.6.4 (3*S*,7*aR*)-(+)-3-(Furan-2-yl)-3,4,7,7*a*-tetrahydrocyclopenta[*c*]pyran-6(1*H*)-one, (+)-128



(0.19 g, 81% yield) as a white solid; mp 81-82 °C. $[\alpha]_{\text{D}}^{29} = +99.1$ (c 3.6, MeOH). ^1H -NMR δ (CDCl_3): 7.37 (brs, 1H), 6.31 (brs, 2H), 5.95 (s, 1H), 4.32-4.39 (m, 3H), 3.21 (t, $J = 11.0$ Hz, 1H), 2.98 (d, $J = 13.3$ Hz, 1H), 2.86 (t, $J = 12.4$ Hz, 1H), 2.45 (dd, $J = 6.6$ and 18.8 Hz, 1H), 1.89 (d, $J = 18.8$ Hz, 1H). ^{13}C -NMR δ (CDCl_3): 207.5, 178.4, 152.7, 142.9, 128.1, 110.4, 107.6, 73.3, 73.2, 40.9, 37.0, 35.3. IR (KBr): 1704, 1618, 1381 cm^{-1} . ION MODE; FAB+ MS (m/z) exact mass; 205.0786 (M+1); observed; 205.0802 (M+1). (Figure A65-66).

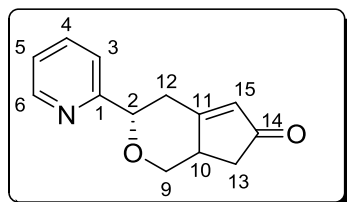
4.6.5 (3*S*,7*aR*)-(+)-3-(Thiophen-2-yl)-3,4,7,7*a*-tetrahydrocyclopenta[*c*]pyran-6(1*H*)-one, (3*S*,7*aR*)-(+)-129



This is a white solid. Mp:132-133 °C, (0.17g, 80% yield). $[\alpha]_{\text{D}}^{29} = +250$ (c 0.45, MeOH). ^1H -NMR δ (CDCl_3): 7.19-7.25 (m, 1H, H_5), 6.93-6.97 (m, 2H, H_3 ve H_2),

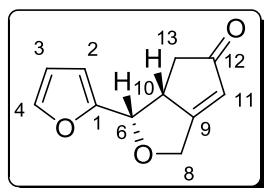
5.95 (s, 1H, H_{14}), 4.58 (d, $J = 11.0$ Hz, 1H, H_6), 4.37 (dd, $J = 6.4$ and 10.7 Hz, 1H, H_8), 3.23 (t, $J = 10.9$ Hz, 1H, H_8), 3.10 (d, $J = 13.5$ Hz, 1H, H_{11}), 2.95-3.05 (m, 1H, H_9), 2.71 (t, $J = 11.8$ Hz, 1H, H_{11}), 2.45 (dd, $J_{AB} = 6.6$ and 18.8 Hz, 1H, H_{12}), 1.89 (d, $J_{AB} = 18.8$ Hz, 1H, H_{12}). $^{13}\text{C-NMR}$ δ (CDCl_3): 206.7, 177.6, 143.3, 127.4, 126.2, 124.9, 123.7, 75.6, 73.1, 40.3, 38.8, 36.5. IR (neat): 2926, 1691, 1000, 706 cm^{-1} . MS (EI) m/z (rel intensity) 220 (base). HRMS, Calculated $[\text{M}]^+$ 221.0636, Measured $[\text{M}]^+$ 221.0632. (Figure A67-68).

4.6.6 (3*S*,7*aR*)-(+)-3-(Pyridin-2-yl)-3,4,7,7a-tetrahydrocyclopenta[*c*]pyran-6(1*H*)-one, (3*S*,7*aR*)-(+)-130



This is a white solid. Mp: 90-92 °C. (0.17 g, 81% yield). $[\alpha]_{\text{D}}^{29} = +126.1$ (c 1, MeOH). $^1\text{H-NMR}$ δ (CDCl_3): 8.52 (d, $J = 4.34$ Hz, 1H, H_6), 7.67 (t, $J = 7.6$ Hz, 1H, H_4), 7.43 (d, $J = 7.8$ Hz, 1H, H_3), 7.16-7.21 (m, 1H, H_5), 5.97 (s, 1H, H_{15}), 4.41-4.45 (m, 2H, H_2 ve H_9), 3.26 (t, $J = 11.0$ Hz, 1H, H_9), 3.20 (bd, $J = 13.8$ Hz, 1H, H_{12}), 2.98-3.04 (m, 1H, H_{10}), 2.60 (t, $J = 12.3$ Hz, 1H, H_{12}), 2.45 (dd, $J_{AB} = 6.7$ and 18.7 Hz, 1H, H_{13}), 1.90 (bd, $J_{AB} = 18.7$ Hz, 1H, H_{13}). $^{13}\text{C-NMR}$ δ (CDCl_3): 207.3, 179.1, 159.5, 149.1, 136.9, 127.9, 123.0, 120.5, 80.6, 73.7, 40.9, 37.6, 37.1. IR (neat): 2917, 1082, 796 cm^{-1} . MS (EI) m/z (rel intensity) 215 (M^+ , 4), 106 (base). HRMS, Calculated $[\text{M}]^+$ 216.1024, Measured $[\text{M}]^+$ 216.1021. (Figure A69-70).

4.6.7 (3*S*,3*aR*)-(+)-3-(Furan-2-yl)-3a,4-dihydro-1*H*-cyclopenta[*c*]furan-5(3*H*)-one, (3*S*,3*aR*)-(-)-131

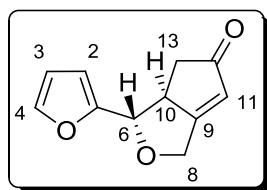


(0.14 g, 74% total yield for (-)-**131** and (+)-**131**).

This is a thick liquid. $[\alpha]_D^{18} = -30.1$ (c 1, CH_2Cl_2).

Discernable NMR Data: $^1\text{H-NMR}$ δ (CDCl_3): 7.38 (d, $J = 1.03$ Hz, 1H, H_4), 6.30-6.34 (m, 2H, H_2 ve H_3), 6.04 (brs, 1H, H_{11}), 4.80 (d, $J_{\text{AB}} = 15.7$ Hz, 1H, H_8), 4.60 (d, $J_{\text{AB}} = 15.8$ Hz, 1H, H_8), 4.36, (d, $J = 10.7$ Hz, 1H, H_6), 3.50-3.54 (m, 1H, H_{10}), 2.56 (dd, $J_{\text{AB}} = 6.5$ and 17.9 Hz, 1H, H_{13}), 2.13 (dd, $J_{\text{AB}} = 3.5$ and 17.8 Hz, 1H, H_{13}). $^{13}\text{C-NMR}$ δ (CDCl_3): 207.7, 182.7, 150.9, 143.2, 125.1, 110.5, 109.1, 76.7, 66.0, 49.1, 38.7. HRMS, Calculated $[\text{M}]^+$ 191.0708, Measured $[\text{M}]^+$ 191.0700. (Figure A71-72).

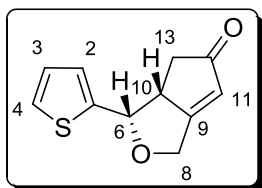
4.6.8 (3*S*,3*aS*)-(-)-3-(Furan-2-yl)-3*a*,4-dihydro-1*H*-cyclopenta[*c*]furan-5(3*H*)-one, (3*S*,3*aS*)-(+)-**131**



This is a thick liquid. $[\alpha]_D^{20} = +39.8$ (c 0.83, CH_2Cl_2).

Discernable NMR Data: $^1\text{H-NMR}$ δ (CDCl_3): 7.23 (d, $J = 1.1$ Hz, 1H, H_4), 6.22 (dd, $J = 1.8$ and 3.2 Hz, 1H, H_3), 6.10 (d, $J = 3.2$ Hz, 1H, H_2), 6.04 (brs, 1H, H_{11}), 5.24 (d, $J = 8.3$ Hz, 1H, H_6), 4.71 (d, $J = 6.4$ Hz, 2H, H_8), 3.54-3.59 (m, 1H, H_{10}), 2.45 (dd, $J_{\text{AB}} = 6.5$ and 17.8 Hz, 1H, H_{13}), 1.78 (dd, $J_{\text{AB}} = 3.8$ and 17.8 Hz, 1H, H_{13}). $^{13}\text{C-NMR}$ δ (CDCl_3): 207.4, 180.9, 151.1, 141.7, 123.6, 109.1, 107.5, 73.2, 64.4, 47.9, 37.0. IR (neat): 2916, 1011, 748 cm^{-1} . MS (EI) m/z (rel intensity) 190 (M^+ , 31), 94 (base), 66 (50). HRMS, Calculated $[\text{M}]^+$ 191.0708, Measured $[\text{M}]^+$ 191.0700. (Figure A73-74).

4.6.9 (3*S*,3*aR*)-(+)-3-(Thiophen-2-yl)-3*a*,4-dihydro-1*H*-cyclopenta[*c*]furan-5(3*H*)-one, (3*S*,3*aR*)-(-)-132

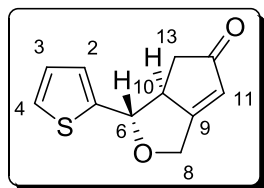


(0.15 g, 77% total yield for (-)-**132** and (+)-**132**).

This is a thick liquid. $[\alpha]_D^{22} = -32.0$ (*c* 1, CH₂Cl₂).

Discernable NMR Data: ¹H-NMR δ (CDCl₃): 7.25 (dd, *J* = 1.2 and 5.0 Hz, 1H, *H*₄), 6.98 (dm, *J* = 3.4 Hz, 1H, *H*₃), 6.91 -6.95 (m, 1H, *H*₂), 6.03 (dd, *J* = 2.1 and 3.6 Hz, 1H, *H*₁₁), 4.84 (dm, *J* = 15.9 Hz, 1H, *H*₈), 4.64 (d, *J* = 1.2 Hz, 1H, *H*₈), 4.56 (d, *J* = 10.3 Hz, 1H, *H*₆), 3.23-3.28 (m, 1H, *H*₁₀), 2.56 (dd, *J*_{AB} = 6.4 and 17.7 Hz, 1H, *H*₁₃), 2.17 (dd, *J*_{AB} = 3.61 and 17.7 Hz, 1H, *H*₁₃). ¹³C-NMR δ (CDCl₃): 206.4, 181.7, 140.8, 125.7, 124.6, 124.2, 124.1, 79.6, 65.2, 52.2, 37.5. HRMS, Calculated [M]⁺ 207.0480, Measured [M]⁺ 207.0470. (Figure A75-76).

4.6.10 (3*S*,3*aS*)-(-)-3-(Thiophen-2-yl)-3*a*,4-dihydro-1*H*-cyclopenta[*c*]furan-5(3*H*)-one, (3*S*,3*aS*)-(+)-132

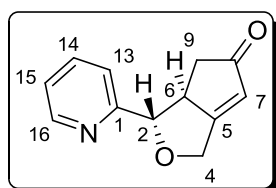


This is a thick liquid. $[\alpha]_D^{22} = +128.2$ (*c* 1, CH₂Cl₂).

Discernable NMR Data: ¹H-NMR δ (CDCl₃): 7.13 (d, *J* = 5.0 Hz, 1H, *H*₄), 6.87-6.89 (m, 1H, *H*₃), 6.76 (d, *J* = 3.4 Hz, 1H, *H*₂), 6.08 (s, 1H, *H*₁₁), 5.55 (d, *J* = 8.3 Hz, 1H, *H*₆), 4.77 (d, *J*_{AB} = 15.6 Hz, 1H, *H*₈), 4.69 (d, *J*_{AB} = 15.8 Hz, 1H, *H*₈), 3.60-3.64 (m, 1H, *H*₁₀), 2.542 (dd, *J*_{AB} = 6.6 and 17.6 Hz, 1H, *H*₁₃), 1.80 (dd, *J*_{AB} = 3.6 and

17.9 Hz, 1H, H_{13}). $^{13}\text{C-NMR } \delta$ (CDCl_3): 207.3, 179.5, 140.0, 125.7, 124.8, 124.3, 76.2, 64.1, 48.5, 37.1, 28.7. IR (neat): 2360, 1091, 798 cm^{-1} . MS (EI) m/z (rel intensity) 206 (M^+ , 34), 94 (base), 66 (48). HRMS, Calculated $[\text{M}]^+$ 207.0480, Measured $[\text{M}]^+$ 207.0470. (Figure A77-78).

4.6.11 (3*S*,3*aS*)-(+)-3-(Pyridin-2-yl)-3*a*,4-dihydro-1*H*-cyclopenta[*c*]furan-5(3*H*)-one, (3*S*,3*aS*)-(+)-133

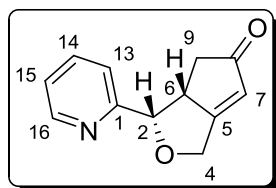


(0.1 g, 50% total yield for (+)-**133** and (-)-**133**).

This is a thick liquid. $[\alpha]_{\text{D}}^{24} = +85.5$ (c 1, CH_2Cl_2).

Discernable NMR Data: $^1\text{H-NMR } \delta$ (CDCl_3): 8.47 (dm, $J = 4.7$ Hz, 1H, H_{16}), 7.58 (td, $J = 1.7$ and 7.7 Hz, 1H, H_{14}), 7.10 (dd, $J = 4.8$ and 6.6 Hz, 1H, H_{13}), 7.05 (bd, $J = 7.8$ Hz, 1H, H_{15}), 5.98 (s, 1H, H_7), 5.39 (d, $J = 8.3$ Hz, 1H, H_2), 4.94 (d, $J_{\text{AB}} = 15.4$ Hz, 1H, H_4), 4.80 (d, $J_{\text{AB}} = 15.4$ Hz, 1H, H_4), 3.74-3.80 (m, 1H, H_6), 2.49 (dd, $J_{\text{AB}} = 6.6$ and 18.2 Hz, 1H, H_9), 1.78 (dd, $J_{\text{AB}} = 3.7$ and 18.2 Hz, 1H, H_9). $^{13}\text{C-NMR } \delta$ (CDCl_3): 207.6, 179.7, 157.5, 148.2, 135.5, 123.8, 121.5, 119.8, 79.4, 65.2, 48.3, 37.1. HRMS, Calculated $[\text{M}]^+$ 201.0790, Measured $[\text{M}]^+$ 201.0784. (Figure A79-80).

4.6.12 (3*S*,3*aR*)-(-)-3-(Pyridin-2-yl)-3*a*,4-dihydro-1*H*-cyclopenta[*c*]furan-5(3*H*)-one, (3*S*,3*aR*)-(-)-133



This is a thick liquid $[\alpha]_{\text{D}}^{18} = -27.6$ (c 0.5, CH_2Cl_2)

Discernable NMR Data: $^1\text{H-NMR}$ δ (CDCl_3): 8.52 (d, $J = 4.3$ Hz, 1H, H_{16}), 7.67 (td, $J = 1.3$ and 7.7 Hz, 1H, H_{14}), 7.43 (d, $J = 7.7$ Hz, 1H, H_{13}), 7.18-7.21 (m, 1H, H_{15}), 6.06 (s, 1H, H_7), 4.89 (d, $J_{\text{AB}} = 15.7$ Hz, 1H, H), 4.69 (d, $J_{\text{AB}} = 15.7$ Hz, 1H, H_4), 4.48 (d, $J = 10.4$ Hz, 1H, H_2), 3.30-3.37 (m, 1H, H_6), 2.61 (dd, $J_{\text{AB}} = 6.4$ and 17.9 Hz, 1H, H_9), 2.63 (dd, $J_{\text{AB}} = 3.5$ and 17.9 Hz, 1H, H_9). $^{13}\text{C-NMR}$ δ (CDCl_3): 207.0, 181.9, 157.5, 148.2, 135.7, 124.1, 122.1, 119.7, 83.9, 65.3, 50.7, 38.4. HRMS, Calculated $[\text{M}]^+ 201.0790$, Measured $[\text{M}]^+ 201.0784$. (Figure A81-82).

4.7 X-Ray Structure Determination of Compound (+)-125 and (+)-128

For the crystal structure determination, the single-crystal of the compounds $\text{C}_{12}\text{H}_{12}\text{O}_3$ ((+)-125:cis) and $\text{C}_{12}\text{H}_{12}\text{O}_3$ ((+)-128:trans) was used for data collection on a four-circle Rigaku R-AXIS RAPID-S diffractometer equipped with a two-dimensional area IP detector. The graphite-monochromatized Mo $K\alpha$ radiation ($\lambda=0.71073$ Å) and oscillation scans technique with $\Delta\omega=5^\circ$ for one image were used for data collection. Images for (+)-125:cis and (+)-128:trans were taken successfully by varying ω with three sets of different χ and ϕ values. For each compounds the 108 images for six different runs covering about 99.8 % of the Ewald spheres were performed. The lattice parameters were determined by the least-squares methods on the basis of all reflections with $F^2 > 2\sigma(F^2)$. Integration of the intensities, correction for Lorentz and polarization effects and cell refinement was performed using CrystalClear software [190]. The structures were solved by direct methods (SHELXS-97) and non-H atoms were refined by full-matrix least-squares method with anisotropic temperature factors (SHELXL-97) [191].

4.7.1 Crystal Data for Compound (+)-125:cis

$\text{C}_{12}\text{H}_{12}\text{O}_3$, crystal system, space group: monoclinic, P21/c; (no:14); unit cell dimensions: $a = 5.5093(3)$, $b = 18.8250(6)$, $c = 10.2240(5)$ Å, $\beta = 105.466(2)^\circ$; volume: $1021.96(6)$ Å³; $Z=4$; calculated density: 1.33 mg/m³; absorption coefficient: 0.095 mm⁻¹; $F(000)$: 432; crystal size: $0.031 \times 0.025 \times 0.012$ mm³; θ range for data collection $2.2 - 30.5^\circ$; completeness to θ : 30.5° , 99.8 %; refinement method: full-matrix least-

square on F^2 ; data/restraints/parameters: 3117/0/160; goodness-of-fit on F^2 : 1.386; final R indices [$I > 2\sigma(I)$]: $R_1 = 0.073$, $wR_2 = 0.183$; R indices (all data): $R_1 = 0.074$, $wR_2 = 0.183$; extinction coefficient: 0.00; largest diff. peak and hole: 0.226 and -0.239 $e \text{ \AA}^{-3}$.

4.7.2 Crystal Data for Compound (+)-128:trans

$C_{12}H_{12}O_3$, crystal system, space group: orthorhombic, P212121; (no:14); unit cell dimensions: $a = 7.8398(8)$, $b = 11.4097(8)$, $c = 11.9476(9)$ \AA , $\beta = 90^\circ$; volume: 1068.71(2) \AA^3 ; $Z = 4$; calculated density: 1.27 mg/m^3 ; absorption coefficient: 0.091 mm^{-1} ; $F(000)$: 432; crystal size: $0.021 \times 0.015 \times 0.012$ mm^3 ; θ range for data collection 2.5-30.6°; completeness to θ : 30.6°, 99.7 %; refinement method: full-matrix least-square on F^2 ; data/restraints/parameters: 3275/0/138; goodness-of-fit on F^2 : 1.139; final R indices [$I > 2\sigma(I)$]: $R_1 = 0.076$, $wR_2 = 0.150$; R indices (all data): $R_1 = 0.130$, $wR_2 = 0.171$; extinction coefficient: 0.0090; largest diff. peak and hole: 0.132 and -0.123 $e \text{ \AA}^{-3}$.

Crystallographic data (excluding structure factors) for the structures of (+)-125:cis and (+)-128:trans in this thesis have been deposited with the Cambridge Crystallographic Data center as supplementary publication numbers CCDC 622252 and 622253, respectively. Copies of the data can be obtained, free of charge, on application to CCDC, 12 Union Road, Cambridge CB2 1EZ, UK [fax: +44 1223 336033 or e-mail:deposit@ccdc.cam.ac.uk]

4.8. X-Ray Structure Determination of Compound (+)-129 and (+)-130

For the crystal structure determination, the single-crystals of the compounds (3*S*,7*aR*)-(+)-129 and (3*S*,7*aR*)-(+)-130 were used for data collection on a four-circle Rigaku R-AXIS RAPID-S diffractometer (equipped with a two-dimensional area IP detector). The graphite-monochromatized Mo K_α radiation ($\lambda = 0.71073$ \AA) and oscillation scans technique with $\Delta\omega = 5^\circ$ for one image were used for data collection. The lattice parameters were determined by the least-squares methods on the basis of all reflections with $F^2 > 2\sigma(F^2)$. Integration of the intensities, correction for Lorentz

and polarization effects and cell refinement was performed using CrystalClear (Rigaku/MSI Inc., 2005) software [190]. The structures were solved by direct methods using SHELXS-97 and refined by a full-matrix least-squares procedure using the program SHELXL-97 [191]. H atoms were positioned geometrically and refined using a riding model, fixing the aromatic C–H distances at 0.93 Å, methine C–H distances at 0.98 Å and methylene C–H distances at 0.97 Å [$U_{\text{iso}}(\text{H})=1.2U_{\text{eq}}(\text{C})$]. The final difference Fourier maps showed no peaks of chemical significance.

4.8.1 Crystal Data for Compound (3S,7aR)- (+)-129

$\text{C}_{12}\text{H}_{12}\text{O}_2\text{S}$, crystal system, space group: monoclinic, P21; (no:4); unit cell dimensions: $a= 9.1316(4)$, $b= 6.8573(3)$, $c=9.3837(4)$ Å, $\alpha=90$ $\beta=111.46(2)$, $\gamma=90^\circ$; volume: $546.86(4)$ Å³; $Z=2$; calculated density: 1.34 mg/m³; absorption coefficient: 0.272 mm^{-1} ; $F(000)$: 232; θ range for data collection $2.3 - 30.6^\circ$; refinement method: full-matrix least-square on F^2 ; data/parameters: 2594/137; goodness-of-fit on F^2 : 1.114; final R indices [$I > 2\sigma(I)$]: $R_1= 0.047$, $wR_2=0.117$; R indices (all data): $R_1=0.061$, $wR_2=0.140$; largest diff. peak and hole: 0.166 and $-0.231 \text{ e } \text{Å}^{-3}$; CCDC-762198.

4.8.2. Crystal Data for Compound (3S,7aR)- (+)-130

$\text{C}_{13}\text{H}_{13}\text{NO}_2$, crystal system, space group: orthorhombic, P212121; (no:19); unit cell dimensions: $a= 7.0938(2)$, $b= 7.0233(2)$, $c= 44.0534(9)$ Å, $\alpha=90$ $\beta=90$, $\gamma=90^\circ$; volume: $2194.82(2)$ Å³; $Z=8$; calculated density: 1.30 mg/m³; absorption coefficient: 0.088 mm^{-1} ; $F(000)$: 912; θ range for data collection $2.8 - 26.5^\circ$; refinement method: full-matrix least-square on F^2 ; data/parameters: 4500/289; goodness-of-fit on F^2 : 1.039; final R indices [$I > 2\sigma(I)$]: $R_1= 0.070$, $wR_2=0.144$; R indices (all data): $R_1=0.140$, $wR_2=0.173$; largest diff. peak and hole: 0.232 and $-0.187 \text{ e } \text{Å}^{-3}$; CCDC-762052.

4.9 Synthesis of Spiro Compounds

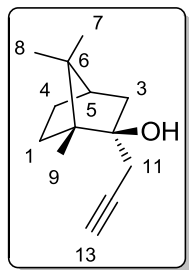
4.9.1 Synthesis of Homoallyl and Homomethallyl Alcohols

To a stirred solution of Mg and iodide (2 pieces) turnings (15 mmol) in dry diethyl ether (10 mL) at 25°C equipped with a reflux condenser was added dropwise a mixture of allylbromide (11 mmol) and methallyl bromide (11 mmol) in anhydrous diethyl ether (5 mL). The mixture was allowed to reflux for 30 min. The mixture was cooled down to 0°C and then, camphor (10 mmol) in dry diethylether (3 mL) was added dropwise. The resultant mixture was stirred 5h. The reacting mixture was hydrolyzed with saturated ammonium chloride solution (10 ml) and with 1N HCl (2 mL). The resultant mixture was extracted with diethylether (3x30 mL). The combined organic phase was washed with brine (20 mL) and dried over $MgSO_4$ and evaporated *in vacuo*. The crude products were purified flash column chromatography with mix solvent of ethyl acetate and hexane at ratio of 1:6 for (+)-**134**, 1:15 for (+)-**135** [186].

4.9.2 Synthesis of Homopropargyl Alcohol

To a stirred solution of Mg (28 mmol), iodine (2 pieces) and $HgCl_2$ (9 mg) turnings in dry diethyl ether (10 ml) at 25°C equipped with a reflux condenser was added dropwise a mixture of propargylbromide (25 mmol) in anhydrous diethyl ether (5 mL). The mixture was allowed to reflux for 30 min. The mixture was cooled down to 0°C and then, camphor (10 mmol) in dry diethylether (3 mL) was added dropwise. The resultant mixture was stirred 5h. The reacting mixture was hydrolyzed with saturated ammonium chloride solution (10 mL) and with 1N HCl (2 mL). The resultant mixture was extracted with diethylether (3x30 mL). The combined organic phase was washed with brine (20 mL) and dried over $MgSO_4$ and evaporated *in vacuo*. The crude products were purified flash column chromatography with mix solvent of ethyl acetate and hexane at ratio of 1:30.

4.9.2.1 (1R,2S)-1,7,7-trimethyl-2-(prop-2-ynyl)bicyclo[2.2.1]heptan-2-ol, (-)-136

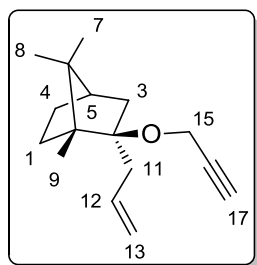


This is a colorless oil (78% yield). $[\alpha]_D^{25} = -3.6$ (c 1.75, CH_2Cl_2). $^1\text{H-NMR}$ δ (CDCl_3): 2.40 (dd, $J_{\text{AB}} = 2.4$ and 16.4 Hz, 1H, H_{11}), 2.34 (dd, $J_{\text{AB}} = 2.4$ and 16.4 Hz, 1H, H_{11}), 2.15 (brs, 1H, H_{13}), 1.97-2.01 (m, 1H), 1.60-1.70 (m, 2H), 1.22-1.43 (m, 3H), 1.05 (s, 3H), 0.90-0.97 (m, 1H), 0.87 (s, 3H), 0.79 (s, 3H). $^{13}\text{C-NMR}$ δ (CDCl_3): 81.8, 79.1, 71.1, 52.2, 49.6, 46.2, 45.0, 30.8, 30.4, 26.9, 21.2, 20.9, 10.5. (Figure A83-84).

4.9.3 General Procedure for *O*-allylation, *O*-methallylation and *O*-propargylation

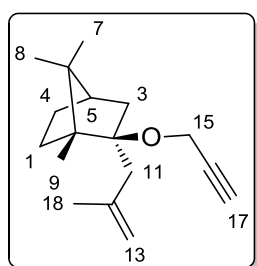
To a solution of (+)-**134** or (+)-**135** or (-)-**136** (5 mmol) in dry THF (20 mL) was added KH (35% dispersion in oil, 10 mmol) under argon allylbromide, methallylbromide or TMS-propargylbromide (10 mmol) was then added dropwise followed by tetrabutylammonium iodide (0.5 mmol). The mixture was refluxed for overnight and hydrolyzed by the cautious addition of water (15 mL). The aqueous layer was extracted with ether (3x20 mL). The combined organic phase was dried over MgSO_4 and evaporated in vacuo. The crude product mixture was separated by flash column chromatography using ethylacetate/hexane (1:20) as the eluent to afford the product.

4.9.3.1 (1R,2R)-2-allyl-1,7,7-trimethyl-2-(prop-2-ynyloxy)bicyclo[2.2.1]heptane, (+)-137



This is a colorless oil (80% yield). $[\alpha]_D^{25} = +3.56$ (*c* 1.7, CH₂Cl₂). ¹H-NMR δ (CDCl₃): 5.88-5.99 (m, 1H, *H*₁₂), 4.99 (d, *J* = 18.1 Hz, 1H, *H*₁₃), 4.95 (d, *J* = 10.8 Hz, 1H, *H*₁₃), 3.98 (d, *J* = 1.7 Hz, 2H, *H*₁₅), 2.55 (dd, *J* = 13.8 and *J* = 2.06 Hz, 1H), 2.26 (brs, 1H, *H*₁₇), 2.10-2.16 (m, 2H), 1.60-1.69 (m, 2H), 1.43-1.49 (m, 1H), 1.27-1.36 (m, 1H), 0.97 (s, 3H), 0.90-0.93 (m, 2H), 0.85 (s, 3H), 0.76 (s, 3H). ¹³C-NMR δ (CDCl₃): 134.9, 114.8, 85.8, 81.0, 71.7, 52.2, 49.2, 48.2, 44.0, 41.0, 39.8, 29.5, 26.0, 20.0, 11.0. Anal. Calcd: C, 82.70; H, 10.41. Found: C, 82.71; H, 10.46. (Figure A85-88).

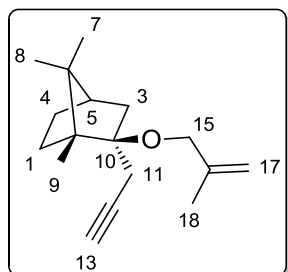
4.9.3.2 (1R,2S)-1,7,7-trimethyl-2-(2-methylallyl)-2-(prop-2-ynyloxy)bicyclo[2.2.1]heptane, (+)-138



This is a colorless oil (75% yield). $[\alpha]_D^{26} = 22.8$ (*c* 1, CH₂Cl₂). ¹H-NMR δ (CDCl₃): 4.88 (t, *J* = 1.2 Hz, 2H, *H*₁₃), 4.11 (d, *J* = 2.4 Hz, 2H, *H*₁₅), 2.51 (d, *J* = 15.4 Hz, 1H), 2.37 (t, *J* = 2.4 Hz, 1H, *H*₁₇), 2.24-2.31 (m, 2H), 1.94 (s, 3H), 1.72-1.81 (m, 3H), 1.09 (s, 3H), 1.02-1.07 (m, 2H), 1.01 (s, 3H), 0.87 (s, 3H). ¹³C-NMR δ (CDCl₃): 138.3, 114.8, 87.7, 81.4, 72.7, 53.7, 50.0, 49.0, 44.9, 42.9, 41.9, 29.8, 26.7, 22.5,

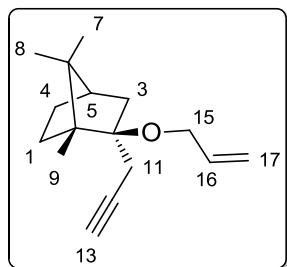
21.1, 20.7, 20.7. Anal. Calcd: C, 82.84; H, 10.42. Found: C, 82.87; H, 10.3. (Figure A87).

4.9.3.3 (1R,2S)-1,7,7-trimethyl-2-(2-methylallyloxy)-2-(prop-2-ynyl)bicyclo[2.2.1]heptane, (-)-139



This is a colorless oil (82% yield). $[\alpha]_D^{26} = -19.02$ (c 1, CH_2Cl_2). $^1\text{H-NMR}$ δ (CDCl_3): 4.95 (s, 1H, H_{17}), 4.74 (s, 1H, H_{17}), 3.73 (d, $J_{\text{AB}} = 12.2$ Hz, 1H, H_{15}), 3.68 (d, $J_{\text{AB}} = 12.2$ Hz, 1H, H_{15}), 2.67 (dd, $J_{\text{AB}} = 2.5$ and 17.9 Hz, 1H), 2.21 (dd, $J_{\text{AB}} = 2.5$ and 17.9 Hz, 1H), 2.11 (dt, $J = 3.5$ and 12.9 Hz, 1H), 1.87-1.88 (m, 1H), 1.67 (s, 3H, H_{18}), 1.60-1.63 (m, 2H), 1.37-1.54 (m, 3H), 1.01 (s, 3H), 0.95-0.98 (m, 1H), 0.94 (s, 3H), 0.78 (s, 3H). $^{13}\text{C-NMR}$ δ (CDCl_3): 143.1, 110.3, 84.2, 82.5, 69.7, 64.6, 53.7, 50.0, 45.0, 40.6, 31.0, 26.9, 25.1, 21.2, 20.9, 19.9, 11.4. Anal. Calcd: C, 82.87; H, 10.64. Found: C, 82.87; H, 10.38. (Figure A88-89).

4.9.3.4 (1R,2S)-2-(allyloxy)-1,7,7-trimethyl-2-(prop-2-ynyl)bicyclo[2.2.1]heptane, (-)-140



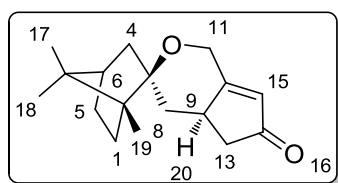
This is a colorless oil (78% yield). $[\alpha]_D^{25} = -16.1$ (c 1.6, CH_2Cl_2). $^1\text{H-NMR}$ δ (CDCl_3): 5.81-5.92 (m, 1H, H_{16}), 5.23 (dd, $J = 18.2$ and 1.5 Hz, 1H, H_{17}), 5.01 (dd, J

= 11.1 and 1.5 Hz, 1H, H_{17}), 3.80-3.90 (m, 2H, H_{15}), 2.65 (dd, $J = 17.8$ and 2.5 Hz, 1H), 2.22 (dd, $J = 17.8$ and 2.5 Hz, 1H), 2.10 (dt, $J = 12.9$ and 3.4 Hz, 1H), 1.89 (t, $J = 2.5$ Hz, 1H), 1.58-1.69 (m, 2H), 1.36-1.51 (m, 3H), 1.01 (s, 3H), 0.97-0.99 (m, 1H), 0.95 (s, 3H), 0.78 (s, 3H). $^{13}\text{C-NMR } \delta$ (CDCl_3): 134.8, 114.0, 83.4, 81.4, 68.7, 61.0, 52.6, 49.0, 44.0, 40.0, 30.0, 25.9, 24.3, 20.1, 19.9, 10.5. Anal. Calcd: C, 82.70; H, 10.41. Found: C, 82.72; H, 10.43. (Figure A90-91).

4.9.4 General Procedure for The Pauson-Khand Reaction

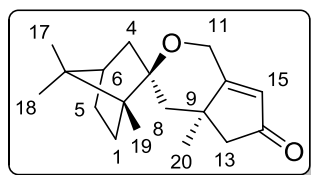
To a solution of compound (+)-**137**, (+)-**138**, (-)-**139**, (-)-**140** (1 mmol) in CH_2Cl_2 (20 mL) was added $\text{Co}_2(\text{CO})_8$ (1.7 mmol), and stirred for 2h (TLC monitoring). Then, NMO (*N*-Methylmorpholine-*N* Oxide) (9 mmol) was added and stirred for further 24h. The crude products were purified by flash column chromatography (EtOAc: Hexane, 1:1 for (+)-**141**, (-)-**142**, (+)-**143**; 1:2 for (+)-**144**).

4.9.4.1 (1R,2R,4a'R)-1,7,7-trimethyl-4a',5'-dihydro-1'H-spiro[bicyclo[2.2.1]heptane-2,3'-cyclopenta[c]pyran]-6'(4'H)-one, (+)-**141**



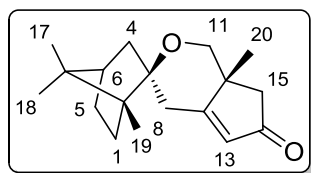
This is a white solid (85%). mp 115-117 °C. $[\alpha]_D^{29} = +22.9$ (c 0.75, CH_2Cl_2). $^1\text{H-NMR } \delta$ (CDCl_3): 5.83 (s, 1H, H_{15}), 4.27(dd, $J = 13.9$ and 31.0 Hz, 2H, H_{11}), 2.87-2.90 (m, 1H), 2.56 ($J = 6.4$ and 18.6 Hz, 1H), 2.19-2.23 (m, 1H), 1.93-1.99 (m, 1H), 1.88 (dd, $J = 5.7$ and 12.3 Hz, 1H), 1.64-1.71 (m, 2H), 1.53 (brs 1H), 1.34-1.44 (m, 2H), 1.17-1.23 (m, 2H), 0.96 (s, 3H), 0.81 (s, 3H), 0.75 (s, 3H). $^{13}\text{C-NMR } \delta$ (CDCl_3): 206.9, 176.2, 125.2, 82.4, 58.3, 52.1, 47.9, 44.4, 41.4, 40.0, 37.5, 35.8, 29.4, 26.1, 20.5, 19.9, 9.3. Anal. Calcd: C, 78.42; H, 9.29. Found: C, 78.42; H, 9.31. IR (KBr): 1704, 1691 cm^{-1} . (Figure A92-93).

4.9.4.2 (1R,2S,4a'R)-1,4a',7,7-tetramethyl-4a',5'-dihydro-1'H-spiro[bicyclo[2.2.1]heptane-2,3'-cyclopenta[c]pyran]-6'(4'H)-one, (-)-142



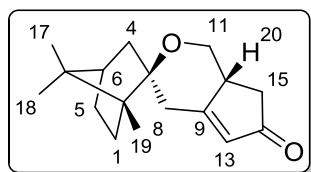
This is a white solid (82%). mp 99 – 101 °C. $[\alpha]_D^{20} = -177.4$ (*c* 1, CHCl₃). ¹H-NMR δ (CDCl₃): 5.85 (s, 1H, *H*₁₅), 4.41, (d, *J*_{AB} = 13.6 Hz, 1H, *H*₁₁), 4.26 (d, *J*_{AB} = 13.6 Hz, 1H, *H*₁₁), 2.36 (d, *J*_{AB} = 18.1 Hz, 1H), 2.25 (d, *J*_{AB} = 13.6 Hz, 1H), 1.44-1.83 (m, 5H), 1.40 (s, 3H, *H*₂₀) 1.28-1.39 (m, 2H), 1.03 (s, 3H), 0.96-1.00 (m, 2H), 0.86 (s, 3H), 0.79 (s, 3H), ¹³C-NMR δ (CDCl₃): 208.2, 181.6, 125.7, 82.6, 56.7, 54.0, 53.9, 47.9, 46.5, 45.4, 41.5, 41.0, 29.6, 27.2, 27.0, 21.3, 20.5, 10.0. Anal. Calcd: C, 78.79; H, 9.55. Found: C, 78.56; H, 9.27. IR (KBr): 1709, 1595 cm⁻¹. (Figure A94-95).

4.9.4.3 (1R,2S,7a'R)-1,7,7,7a'-tetramethyl-7',7a'-dihydro-1'H-spiro[bicyclo[2.2.1]heptane-2,3'-cyclopenta[c]pyran]-6'(4'H)-one, (+)-143



This is a white solid (82%). mp 126 – 128 °C. $[\alpha]_D^{20} = +93.30$ (*c* 1, CHCl₃). ¹H-NMR δ (CDCl₃): 5.80 (s, 1H, *H*₁₃), 3.53 (d, *J*_{AB} = 10.9 Hz, 1H, *H*₁₁), 3.21 (d, *J*_{AB} = 10.9 Hz, 1H, *H*₁₁), 2.61 (d, *J*_{AB} = 12.5 Hz, 1H), 2.31 (d, *J*_{AB} = 12.5 Hz, 1H), 2.09 (d, *J*_{AB} = 18.6 Hz, 1H), 2.02 (d, *J*_{AB} = 18.6 Hz, 1H), 1.85-1.89 (m, 1H), 1.67-1.70 (m, 2H), 1.33-1.42 (m, 2H), 1.26 (s, 3H), 1.19 (brs, 1H), 0.96-0.98 (m, 1H), 0.92 (s, 3H), 0.88 (s, 3H), 0.82 (s, 3H). ¹³C-NMR δ (CDCl₃): 206.0, 183.8, 126.7, 85.1, 69.8, 52.5, 48.1, 45.3, 44.4, 42.6, 38.6, 35.0, 29.1, 25.8, 21.4, 20.2, 19.9, 9.2. Anal. Calcd: C, 78.79; H, 9.55. Found: C, 78.90; H, 9.53. IR (KBr): 1704 cm⁻¹. (Figure A96-97).

4.9.4.4 (1R,2S,7a'R)-1,7,7-trimethyl-7',7a'-dihydro-1'H-spiro[bicyclo[2.2.1]heptane-2,3'-cyclopenta[c]pyran]-6'(4'H)-one, (+)-144



This is a white solid (86%). mp 129 - 131°C. $[\alpha]_D^{25} = 222.6$ (*c* 0.68, CH₂Cl₂). ¹H-NMR δ (CDCl₃): 5.88 (s, 1H, *H*₁₃), 3.90 (dd, *J* = 10.9 and 6.79 Hz, 1H, *H*₁₁), 3.07 (t, *J* = 10.9 Hz, 1H, *H*₁₁), 2.73-2.79 (m, 1H), 2.44-2.49 (m, 2H), 2.33-2.40 (m, 1H), 1.79-1.89 (m, 2H), 1.61-1.71 (m, 2H), 1.47 (s, 1H), 1.37-1.41 (s, 2H), 0.95-0.98 (m, 2H), 0.91 (s, 3H), 0.85 (s, 3H), 0.82 (s, 3H). ¹³C-NMR δ (CDCl₃): 206.9, 180.5, 127.3, 84.4, 65.0, 52.4, 48.1, 44.4, 40.0, 38.4, 37.9, 36.4, 29.1, 25.8, 20.2, 19.9, 9.3. Anal. Calcd: C, 78.42; H, 9.29. Found: C, 78.51; H, 9.27. IR (KBr): 1704, 1627 cm⁻¹. (Figure A98-99).

4.9.5 X-ray Structure Analysis

Data for all X-ray structures ((+)-141, (-)-142, (+)-143 and (+)-144) were collected using a four-circle Rigaku R-Axis RAPID-S diffractometer with graphite monochromated MoK α radiation ($\lambda=0.71073\text{\AA}$) at room temperature. The lattice parameters were determined by the least-squares methods on the basis of all reflections with $F^2 > 2\sigma(F^2)$. Integration of intensities, correction of Lorentz and polarization effects and cell refinement were performed using CrystalClear software [190]. The structures were solved by direct methods SHELXS-97 and non-H atoms were refined by full-matrix least-squares method with anisotropic temperature factors SHELXL-97 [191].

4.9.5.1 Crystal Data for (+)-141

$C_{17}H_{24}O_2$, crystal system, space group: orthorhombic, $P2_12_12_1$; (no:19); unit cell dimensions: $a=7.4740(4)$, $b=9.6040(5)$, $c=20.3370(6)$ Å, $\beta=90^\circ$; volume: $1459.8(3)$ Å³; $Z=4$; calculated density: 1.18 mg/m³; absorption coefficient: 0.075 mm⁻¹; $F(000)$: 568; θ range for data collection 2.3 – 30.5° ; refinement method: full-matrix least-square on F^2 ; data/parameters: 4460/176; goodness-of-fit on F^2 : 0.900; final R indices [$I>2\sigma(I)$]: $R_1=0.049$, $wR_2=0.140$; R indices (all data): $R_1=0.079$, $wR_2=0.169$; largest diff. peak and hole: 0.164 and -0.115 eÅ⁻³; CCDC- 696281.

4.9.5.2 Crystal Data for (-)-142

$C_{18}H_{26}O_2$, crystal system, space group: orthorhombic, $P2_12_12_1$; (no:19); unit cell dimensions: $a=7.3488(2)$, $b=12.1080(4)$, $c=17.7416(5)$ Å, $\beta=90^\circ$; volume: $1578.63(1)$ Å³; $Z=4$; calculated density: 1.15 mg/m³; absorption coefficient: 0.073 mm⁻¹; $F(000)$: 600; θ range for data collection 2.8 – 25° ; refinement method: full-matrix least-square on F^2 ; data/parameters: 2785/185; goodness-of-fit on F^2 : 1.488; final R indices [$I>2\sigma(I)$]: $R_1=0.076$, $wR_2=0.146$; R indices (all data): $R_1=0.076$, $wR_2=0.146$; largest diff. peak and hole: 0.113 and -0.122 e Å⁻³; CCDC- 696633.

4.9.5.3 Crystal Data for (+)-143

$C_{18}H_{26}O_2$, crystal system, space group: monoclinic, $P2_1$; (no:4); unit cell dimensions: $a=7.0389(3)$, $b=11.2919(5)$, $c=19.9882(6)$ Å, $\beta=98.28(2)^\circ$; volume: $1572.13(6)$ Å³; $Z=4$; calculated density: 1.16 mg/m³; absorption coefficient: 0.073 mm⁻¹; $F(000)$: 600; θ range for data collection 2.7 – 25.1° ; refinement method: full-matrix least-square on F^2 ; data/parameters: 5561/368; goodness-of-fit on F^2 : 1.056; final R indices [$I>2\sigma(I)$]: $R_1=0.046$, $wR_2=0.099$; R indices (all data): $R_1=0.058$, $wR_2=0.114$; largest diff. peak and hole: 0.112 and -0.160 e Å⁻³; CCDC- 696622.

4.9.5.4 Crystal Data for (+)-144

$C_{17}H_{24}O_2$, crystal system, space group: monoclinic, P21; (no:4); unit cell dimensions: $a= 6.9320(5)$, $b=9.5090(5)$, $c=11.5680(6)$ Å, $\beta=102.73(3)^\circ$; volume: $743.8(1)$ Å³; $Z=2$; calculated density: 1.16 mg/m³; absorption coefficient: 0.074 mm⁻¹; $F(000)$: 284; θ range for data collection 2.8 – 31.1° ; refinement method: full-matrix least-square on F^2 ; data/parameters: 4571/177; goodness-of-fit on F^2 : 0.975; final R indices [$I>2\sigma(I)$]: $R_1= 0.076$, $wR_2=0.229$; R indices (all data): $R_1=0.143$, $wR_2=0.315$; largest diff. peak and hole: 0.187 and -0.241 e Å⁻³; CCDC- 696632.

REFERENCES

- [1]. Richardson, G. M. *The Foundation of Stereochemistry* (Am. Book Co., New York), Ed. **1901**.
- [2]. Kelvin, W. T. The second Robert Boyer lecture, *J. Oxford Univ. Junior Sci. Club* **1884**, 18, 25.
- [3]. Noyori, R. *Asymmetric Catalysis in Organic Synthesis*, Wiley, New York, 1994.
- [4]. Lin, G.; Li, Y.; Albert, S. C. *Principles and Applications of Asymmetric Synthesis*, John Wiley & Sons Ltd. 2001.
- [5]. Malnic, B.; Hirono, J.; Sato, T.; Buck, L. B. *Cell* **1999**, 96, 713.
- [6]. Zozulya, S.; Echeverri, F.; Nguyen, T. *Genome Biol.* **2001**, 6, 2.
- [7]. Pasteur, L. *Comptes Rend. Acad. Sci. Paris* **1858**, 46, 615
- [8]. Leffingwell, J. C. Chirality and Odour Perception, www.leffingwell.com/chirality/chirality.htm 2007.
- [9]. Riehl, J. P. *Mirror-Image Asymmetry: An Introduction to The Origin and Consequences of Chirality*, John Wiley & Sons Ltd, 2010.
- [10]. Owens, M. J.; McConathy, J. *J. Clin. Psychiatry* **2003**, 5, 70.
- [11]. Caner, H.; Groner, E.; Levy L.; Agranat, I. *Drug Discov. Today* **2004**, 9, 105.
- [12]. Thayer, A. N. *Chem. Eng. News* **2007**, 85, 11.
- [13]. Fromherz, K. *Deutsche Med. Wochenschrift* **1923**, 49, 814.
- [14]. Blaschke, G.; Kraft, H. P.; Fickentscher, K.; Kohler, F. *Arzneimittel-Forschung* **1979**, 29, 1640.
- [15]. Cannarsa, M. J. *Chem. Ind.* **1996**, 10, 374.

- [16]. Stinson, S. C. *Chem. Eng. News* **1997**, 75, 38.
- [17]. Stinson, S. C. *Chem. Eng. News* **1998**, 76, 83.
- [18]. Stinson, S. C. *Chem. Eng. News* **1999**, 77, 101.
- [19]. Sheldon, R. A. *Chirotechnology: Industrial synthesis of optically active compounds*, 2nd ed., Marcel Dekker, Inc. New York 1993.
- [20]. Sherk, A. E.; Fraser, R. B. *J. Org. Chem.* **1982**, 47, 932.
- [21]. Jacques J.; Collet, A.; Wilen, S. H. *Enantiomers, Racemates and Resolutions* Wiley-Interscience, New York 1981.
- [22]. Newman, P. *Optical resolution procedures for chemical compounds*, Optical Resolution Information Center, Manhattan College, Riverdale, New York 1978.
- [23]. Kagan, H. B.; Fiaud, J. C. *Top. Stereochem.* **1988**, 18, 249.
- [24]. Sih, C. J.; Wu, S. H. *Top. Stereochem.* **1989**, 19, 63.
- [25]. Keith, J. M.; Larrow, J. F.; Jacobsen, E. N. *Adv. Synth. Catal.* **2001**, 343, 5.
- [26]. Bovara, R.; Carrea, G.; Ferrara, L.; Riva, S. *Tetrahedron: Asymmetry* **1991**, 2, 931.
- [27]. Ruble, J. C.; Latham, H. A.; Fu, G. C. *J. Am. Chem. Soc.* **1997**, 119, 1492.
- [28]. Spivey, A. C.; Fekner, T.; Spey, S. E. *J. Org. Chem.* **2000**, 65, 3154.
- [29]. Ruble, J. C.; Tweddell, J.; Fu, G. C. *J. Org. Chem.* **1998**, 63, 2794.
- [30]. Trost, B. M. *Angew. Chem. Int. Ed.* **1995**, 34, 259.
- [31]. Larsson, A. L. E.; Persson, B. A.; Backvall, J. E. *Angew. Chem. Int. Ed.* **1997**, 36, 1211.
- [32]. Brooks, D. W.; Wilson, M.; Webb, M. *J. Org. Chem.* **1987**, 52, 2244.
- [33]. Nicolaou, K.C.; Sorensen, E. *Classics in Total Synthesis* Wiley-VCH 1996.
- [34]. Clayden, J. *Organic Chemistry*, Oxford, 2000, 1224.

- [35]. Berkessel, A.; Groeger, H. *Asymmetric Organocatalysis: from Biomimetic Concepts to Applications in Asymmetric Synthesis* Wiley-VCH 2005.
- [36]. Ahrendt, K. A.; Borths, C. J.; MacMillan, D. W. C. *J. Am. Chem. Soc.* **2000**, *122*, 4243.
- [37]. Wakchaure, V. N.; List, B. *Angew. Chem. Int. Ed.* **2010**, *49*, 4136.
- [38]. Illanes, A. *Enzyme biocatalysis: Principles and Applications* Springer, 2008.
- [39]. Anastas, P. T.; Kirchhoff, M. M. *Acc.Chem. Res.* **2002**, *35*, 686.
- [40]. Sheldon, R. A. *Acad. Sci. Paris, IIC, Chimie/Chemistry* **2000**, *3*, 541.
- [41]. Anastas, P. T.; Warner, J. C. *Green Chemistry: Theory and Practice*, Oxford University Press, Oxford, 1998.
- [42]. Anastas, P. T.; Williamson (Eds.), T. C. *Green Chemistry: Frontiers in Chemical Synthesis and Processes*, Oxford University Press, Oxford, 1998.
- [43]. Anastas, P. T.; Heine, L.G.; Williamson (Eds.), T. C. *Green Chemical Syntheses and Processes*, American Chemical Society, Washington DC, 2000.
- [44]. Powell, K. A.; Ramer, S. W.; Del Cardayré, S. B.; Stemmer, W. P. C.; Tobin, M. B.; Longchamp, P. F.; Huisman, G. *Angew. Chem. Int. Ed.* **2001**, *40*, 3948.
- [45]. Bommarius, A. S.; Riebel, B. R. *Biocatalysis: Fundamentals an applications*. Wiley-VCH, Weinheim 2004.
- [46]. Panke, S.; Held, M.; Wubbolts, M. *Curr. Op. Biotechnol.* **2004**, *15*, 272.
- [47]. Dakin, H. D.; *J. Physiol.* **1905**, *32*, 199.
- [48]. Schmid, R. D.; Verger, R. *Angew. Chem.* **1998**, *110*, 1694.
- [49]. Krishna, S. H.; Karanth, N. G. *Catalysis Reviews* **2002**, *44*, 499.
- [50]. Hu, C. H.; Brinck, T. *International Journal of Quantum Chemistry* **1997**, *89*.
- [51]. Hedstrom, L. *Chem. Rev.* **2002**, *102*, 4501.

- [52]. Kazlauskas, R. J.; Weissfloch, A. N. E.; Rappaport A. T.; Cuccia L. A. *J. Org. Chem.* **1991**, *56*, 2656.
- [53]. Xie, Z. F. *Tetrahedron: Asymmetry* **1991**, *2*, 773.
- [54]. Janssen, A. J. M.; Klunder, A. J. H.; Zwanenburg, B. *Tetrahedron* **1991**, *47*, 7645.
- [55]. Burgess, K.; Jennings, L. D. *J. Am. Chem. Soc.* **1991**, *113*, 6129.
- [56]. Mezzetti A.; Schrag, J. D.; Cheong, C. S.; Kazlauskas, R. J. *Chem. Biol.* **2005**, *12*, 427.
- [57]. Magnusson, A. O.; Takwa, M.; Hamberg, A.; Hult, K.; *Angew. Chem. Int. Ed.* **2005**, *44*, 4582.
- [58]. Weissfloch, A. N. E.; Kazlauskas, R. J. *J. Org. Chem.* **1995**, *60*, 6959.
- [59]. Chen, C. S; Wu, S. H; Girdaukas, G.; Sih, C. J. *J. Am. Chem. Soc.* **1987**, *109*, 2812.
- [60]. Chen, C. S.; Sih, C. J. *Angew. Chem. Int. Ed.* **1989**, *28*, 695.
- [61]. Bommarius, A. S.; Riebel, B. R. *Biocatalysis*; Wiley-VCH: Weinheim, 2004.
- [62]. Ghanem, A.; Eboul-Enein, H. Y. *Tetrahedron: Asymmetry* **2004**, *15*, 3331.
- [63]. Cotterill, I. C.; Sutherland, A. G.; Robert, S. M.; Grobbauer, R.; Spreitz, J.; Faber, K. J. *J. Chem. Soc., Perkin Trans. I* **1991**, 1365.
- [64]. Bornscheuer, U. T.; Kazlauskas, R. J. *Hydrolases in Organic Synthesis*. Wiley-VCH: Weinheim 1999.
- [65]. Hanefeld, U. *Org. Biomol. Chem.* **2003**, *1*, 2405.
- [66]. Rouhi, A. M. *Chem. Eng. News* **2004**, *82*, 47.
- [67]. Suginaka, K.; Hayashi, Y.; Yamamoto, Y. *Tetrahedron: Asymmetry* **1996**, *7*, 1153.

- [68]. Hamada, H.; Shiromoto, M.; Funahashi, M.; Itoh, T.; Nakamura, K. *J. Org. Chem.* **1996**, *61*, 2332, correction, p. 9635.
- [69]. Trolisas, M.; Orrenius, C.; Sahlén, F.; Gedde, U. W.; Norin, T.; Hult, A.; Hermann, D.; Rudquist, P.; Komitov, L.; Lagerwall, S. T.; Lindström, J. *J. Am. Chem. Soc.* **1996**, *118*, 8542.
- [70]. Uenishi, J.; Hiraoka, T.; Hata, S.; Nishiwaki, K.; Yonemitsu, O.; Nakamura, K.; Tsukube, H. *J. Org. Chem.* **1998**, *63*, 2481.
- [71]. Uenishi, J.; Nishiwaki, K.; Hata, S.; Nakamura, K. *Tetrahedron Lett.* **1994**, *35*, 7973.
- [72]. Kato, K.; Katayama, M.; Gautam, R. K.; Fujii, S.; Kimoto, H. *Biosci. Biotechnol. Biochem.* **1994**, *58*, 1353.
- [73]. Kato, K.; Katayama, M.; Fujii, S.; Kimoto, H. *J. Ferment. Bioeng.* **1996**, *82*, 355.
- [74]. Partali, V.; Waagen, V.; Alvik, T.; Anthonsen, T. *Tetrahedron: Asymmetry* **1993**, *4*, 961.
- [75]. Johnson, C. R.; Sakaguchi, H. *Synlett* **1992**, 813.
- [76]. Van Rantwijk, F.; Sheldon, R. A. *Tetrahedron* **2004**, *60*, 501.
- [77]. Smidt, H.; Fischer, A.; Fischer, P.; Schmid, R. D. *Biotechnol. Techn.* **1996**, *10*, 335.
- [78]. Gotor, V.; Menendez, E.; Mouloungui, Z.; Gaset, A. *J. Chem. Soc., Perkin Trans. 1* **1993**, 2453.
- [79]. Jaeger, K. E.; Liebeton, K.; Zonta, A.; Schimossek, K.; Reetz, M. T. *Appl. Microbiol. Biotechnol.* **1996**, *46*, 99.
- [80]. Kanerva, L. T.; Csomos, P.; Sundholm, O.; Bernath, G.; Fulop, F. *Tetrahedron: Asymmetry* **1996**, *7*, 1705.
- [81]. Puertas, S.; Brieva, R.; Rebolledo, F.; Gotor, V. *Tetrahedron* **1993**, *49*, 4007.

- [82]. Sánchez, V. M.; Rebolledo, F.; Gotor, V. *Tetrahedron: Asymmetry* **1997**, *8*, 37.
- [83]. Hieber, G.; Ditrich, K. *Chimi. Oggi* **2001**, *19*, 16.
- [84]. Stead, P.; Marley, H.; Mahmoudian, M.; Webb, G.; Noble, D.; Ip, Y. T.; Piga, E.; Rossi, T.; Roberts, S.; Dawson, M. J. *Tetrahedron: Asymmetry* **1996**, *7*, 2247.
- [85]. Patel, R. N.; Banerjee, A.; Ko, R. Y.; Howell, J. M.; Li, W. S.; Comezoglu, F. T.; Partyka, R. A.; Szarka, L. *Biotechnol. Appl. Biochem.* **1994**, *20*, 23.
- [86]. MacKeith, R. A.; McCague, R.; Olivo, H. F.; Palmer, C. F.; Roberts, S. M. *J. Chem. Soc., Perkin Trans. I* **1993**, 313.
- [87]. MacKeith, R. A.; McCague, R.; Olivo, H. F.; Roberts, S. M.; Taylor, S. J. C.; Xiong, H. *Bioorg. Med. Chem.* **1994**, *2*, 387.
- [88]. Cvetovich, R. J.; Chartrain, M.; Hartner, F.W.; Roberge, C.; Amato, J. S.; Grabowski, E. J. *J. Org. Chem.* **1996**, *61*, 6575.
- [89]. Beller, M.; Bolm, C. *Transition Metals for Organic Synthesis. Building Blocks and Fine Chemicals*; Eds.; Wiley-VCH: Weinheim, Germany, **1998**; Vol. 2, p 3.
- [90]. Khand, I. U.; Knox, G. R.; Pauson, P. L.; Watts, W. E. *J. Chem. Soc., Perkin Trans. I* **1971**, 36.
- [91]. Khand, I. U.; Knox, G. R.; Pauson, P. L.; Watts, W. E.; Foreman, M. I. *J. Chem. Soc., Perkin Trans. I* **1973**, 977.
- [92]. Schore, N. E.; Croudace, M. C. *J. Org. Chem.* **1981**, *46*, 5436.
- [93]. Magnus, P.; Principe, L. M. *Tetrahedron Lett.* **1985**, *26*, 4851.
- [94]. Shambayati, S.; Crowe, W. E.; Schreiber, S. L. *Tetrahedron Lett.* **1990**, *31*, 5289.
- [95]. Jeong, N.; Chung, Y. K.; Lee, B. Y.; Lee, S. H.; Yoo, S. E. *Synlett* **1991**, 204.
- [96]. Pérez-Serrano, L.; Casarrubios, L.; Domínguez, G.; Pérez-Castells. *J. Org. Lett.* **1999**, *1*, 1187.

- [97]. Pérez-Serrano, L.; Blanco-Urgoiti, J.; Casarrubios, L.; Domínguez, G.; Pérez-Castells, J. *J. Org. Chem.* **2000**, *65*, 3513.
- [98]. Sugihara, T.; Yamada, M.; Ban, H.; Yamaguchi, M.; Kaneko, C. *Angew. Chem. Int. Ed.* **1997**, *36*, 2801.
- [99]. Rajesh, T.; Periasamy, M. *Tetrahedron Lett.* **1998**, *39*, 117.
- [100]. Simonian, S. O.; Smit, W. A.; Gybin, A. S.; Shashkov, A. S.; Mikaelian, G. S.; Tarasov, V. A.; Ibragimov, I. I.; Caple, R.; Froen, D. E. *Tetrahedron Lett.* **1986**, *27*, 1245.
- [101]. Sugihara, T.; Yamada, M.; Yamaguchi, M.; Nishizawa, M. *Synlett* **1999**, 771.
- [102]. Mukai, C.; Kim, J. S.; Uchiyama, M.; Hanaoka, M. *Tetrahedron Lett.* **1998**, *39*, 7909.
- [103]. Mukai, C.; Kim, J. S.; Sonobe, H.; Hanaoka, M. *J. Org. Chem.* **1999**, *64*, 6822.
- [104]. Fonquerna, S.; Rios, R.; Moyano, A.; Pericás, M.; Riera, A. *Eur. J. Org. Chem.* **1999**, 3459.
- [105]. Fonquerna, S.; Moyano, A.; Pericás, M.; Riera, A. *J. Am. Chem. Soc.* **1997**, *119*, 10225.
- [106]. Adrio, J.; Carretero, J. C. *J. Am. Chem. Soc.* **1999**, *121*, 7411.
- [107]. Verdaguer, X.; Moyano, A.; Pericás, M. A.; Riera, A. *J. Am. Chem. Soc.* **1994**, *116*, 2153.
- [108]. Montenegro, E.; Poch, M.; Moyano, A.; Pericás, M. A.; Riera, A. *Tetrahedron Lett.* **1998**, *39*, 335.
- [109]. Hay, A. M.; Kerr, W. J.; Kirk, G. G.; Middlemiss, D. *Organometallics* **1995**, *14*, 4986.
- [110]. Castro, J.; Moyano, A.; Pericás, M. A.; Riera, A.; Alvarez-Larena, A.; Piniella, J. F. *J. Am. Chem. Soc.* **2000**, *122*, 7944.

- [111]. Hiroi, K.; Watanabe, T.; Kawagashi, R.; Abe, I. *Tetrahedron Lett.* **2000**, *41*, 891.
- [112]. Rutherford, D. T.; Christie, S. D. R. *Tetrahedron Lett.* **1998**, *39*, 9805.
- [113]. Fletcher, A. J.; Rutherford, D. T.; Christie, S. D. R. *Synlett* **2000**, 1040.
- [114]. Kerr, W. J.; Kirk, G. G.; Middlemiss, D. *Synlett* **1995**, 1085.
- [115]. Derdau, V.; Laschat, S.; Jones, P. G. *Heterocycles* **1998**, *48*, 1445.
- [116]. Ingate, S. T.; Contelles, M. *Org. Prep. Proced. Int.* **1998**, *30*, 121.
- [117]. Geis, O.; Schmalz, H. G. *Angew. Chem. Int. Ed.* **1998**, *37*, 911.
- [118]. Chung, Y. K. *Coord. Chem. Rev.* **1999**, *188*, 297.
- [119]. Brummond, K. M.; Kent, J. L. *Tetrahedron* **2000**, *56*, 3263.
- [120]. Gibson, S. E.; Stevanazzi, A. *Angew. Chem. Int. Ed.* **2003**, *42*, 1800.
- [121]. Bonaga, L. V. R.; Krafft, M. E. *Tetrahedron* **2004**, *60*, 9795.
- [122]. Laschat, S.; Becheanu, A.; Bell, T.; Baro, A. *Synlett* **2005**, 2547.
- [123]. Gibson, S. E.; Mainolfi, N. *Angew. Chem. Int. Ed.* **2005**, *44*, 3022.
- [124]. Park, K. H.; Chung, Y. K. *Synlett* **2005**, 545.
- [125]. Denmark, S. E.; Fu, J. *Chem. Rev.* **2003**, *103*, 2763.
- [126]. Castro, J.; Sorensen, H.; Riera, A.; Moyano, A.; Pericas, M. A.; Greene, A. E. *J. Am. Chem. Soc.* **1990**, *112*, 9388.
- [127]. Takano, S.; Inomata, K.; Ogasawara, K. *J. Chem. Soc., Chem. Commun.* **1992**, 169.
- [128]. Rowley, E. G.; Schore, N. E. *J. Org. Chem.* **1992**, *57*, 6853.
- [129]. Pallerla, M. K.; Fox, J. M. *Org. Lett.* **2007**, *26*, 5625.

- [130]. Jamison, T. F.; Shambayati, S.; Crowe, W. E.; Schreiber, S. L. *J. Am. Chem. Soc.* **1997**, *119*, 4353.
- [131]. Honda, T.; Kaneda, K. *J. Org. Chem.* **2007**, *72*, 6541.
- [132]. Min, S. J.; Danishefsky, S. J. *Angew. Chem Int. Ed.* **2007**, *46*, 2199.
- [133]. Kozaka, T.; Miyakoshi, N.; Mukai, C. *J. Org. Chem.* **2007**, *72*, 10147.
- [134]. Nicholas, K. M. *Acc. Chem. Res.* **1987**, *20*, 207.
- [135]. Wu, Y.; Chang, F. R.; Duh, C. Y.; Wang, S. K. *Heterocycles* **1992**, *34*, 667.
- [136]. Myint, S. H.; Cortes, A.; Laurens, A.; Hocquemiller, R.; Leboeuf, M.; Cave', A.; Cotte, J.; Que'ro, A. M. *Phytochemistry* **1991**, *30*, 3335.
- [137]. Joesang, A.; Dubaele, B.; Cave', A.; Bartoli, M. H.; Be'riel, H. *J. Nat. Prod.* **1991**, *54*, 967.
- [138]. Cow, D.; Myint, S. H.; Hocquemiuer, R. *Tetrahedron* **1991**, *47*, 8195.
- [139]. Scholz, G.; Tochtermann, W. *Tetrahedron Lett.* **1991**, *32*, 5535.
- [140]. Wakabaywhi, N.; Spencer, S. L.; Waters, R. M.; Lusby, W. R. *J. Nat. Prod.* **1991**, *54*, 1419.
- [141]. Rieser, M. J.; Kozolowski, J. F.; Wood, K. V.; McLaughlin, J. L. *Tetrahedron Lett.* **1991**, *32*, 1137.
- [142]. Fang, X. P.; Rupprecht, J. K.; Alkofahi, A.; Hui, Y. H.; Liu, Y. M.; Smith, D. L.; Wood, K. V.; McLaughlin, J. L. *Heterocycles* **1991**, *32*, 11.
- [143]. Tanyeli, C.; Akhmedov, I. M.; Özdemirhan, D. *Enantiomer* **2001**, 259.
- [144]. Sezer, S.; Ozdemirhan, D.; ğahin, E.; Tanyeli, C. *Tetrahedron:Asymmetry* **2006**, *17*, 2981.
- {145}. Son, S. U.; Yoon, Y. A.; Choi, D. S.; Park, J. K.; Kim, B. M.; Chung, Y. K. *Org. Lett.* **2001**, *3*, 1065.

- [146]. Son, S. U.; Paik, S.-J.; Lee, S. I.; Chung, Y. K. *J. Chem. Soc., Perkin Trans. 1* **2000**, 141.
- [147]. Hong, S. H.; Kim, J. W.; Choi, D. S.; Chung, Y. K.; Lee, S.-G. *J. Chem. Soc., Chem. Commun.* **1999**, 2099.
- [148]. Son, S. U.; Choi, D. S.; Chung, Y. K. *Org. Lett.* **2000**, 2, 2097.
- [149]. Deeter, J.; Frazier, J.; Staten, G.; Staszak, M.; Wiegel, L. *Tetrahedron Lett.* **1990**, 31, 7101.
- [150]. Farr, R. A.; Peet, N. P.; Kang, M. S. *Tetrahedron Lett.* **1990**, 31, 7109.
- [151]. Soai, K.; Hori, H.; Niwa, S. *Heterocycles* **1989**, 29, 2065.
- [152]. Kusakabe, M.; Kitano, Y.; Kobayashi, Y.; Sato, F. *J. Org. Chem.* **1989**, 54, 2085.
- [153]. Brown, H. C.; Randad, R. S.; Bhat, K. S.; Zaidelwicz, M.; Racheria, U. S. *J. Am. Chem. Soc.* **1990**, 112, 2389.
- [154]. Racheria, U. S.; Brown, H. C. *J. Org. Chem.* **1991**, 56, 401.
- [155]. Racheria, U. S.; Liao, Y.; Brown, H. C. *J. Org. Chem.* **1992**, 57, 6614.
- [156]. Denmark, S. E.; Fu, J. *Chem. Rev.* **2003**, 103, 2763.
- [157]. Tanyeli, C.; Demir, A. S.; Arkin, H.; Akhmedov, I. M. *Enantiomer* **1997**, 2, 433.
- [158]. Sezer, S. Sahin, E. Tanyeli, C. *Tetrahedron: Asymmetry* **2010**, 21, 476.
- [159]. Sing, S.; Kumar S.; Chimni S. S.; *Tetrahedron:Asymmetry* **2002**, 13, 2679.
- [160]. Abraham, R. J.; Parry, K.; Thomas, W. A. *J. Chem. Soc. B* **1971**, 446.
- [161]. Günther, H.; Jikeli, G. *Chem. Rev.* **1977**, 77, 599.
- [162]. Sannigrahi, M. *Tetrahedron* **1999**, 55, 9007.
- [163]. Perron, F.; Albizati, K. F. *Chem. Rev* **1989**, 89, 1617.

- [164]. Dixon, D. J.; Horan, R. A. J.; Monck, N. J. T. *Org. Lett.* **2004**, *6*, 4423.
- [165]. Mead, K. T.; Brewer, B. N. *Curr. Org. Chem.* **2003**, *7*, 227.
- [166]. Ghosh, S. K.; Hsung, R. P.; Liu, J. *J. Am. Chem. Soc.* **2005**, *127*, 8260.
- [167]. Balbuena, P.; Rubio, E. M.; Melet, C. O.; Fernandez, M.G. *Chem Commun.* **2006**, 2610.
- [168]. Hotha, S.; Maurya, S. K.; Gurjar, M.; K. *Tetrahedron Lett.* **2005**, *46*, 5329.
- [169]. Leeuwenburgh, M. A.; Appeldoorn, C. C. M.; Van Hooft, P. A. V.; Overkleef, H. S.; Van Der Marel, G. A.; Van Boom, J. H. *Eur. J. Org. Chem.* **2000**, 873.
- [170]. Leeuwenburgh, M. A.; Appeldoorn, C. C. M.; Van Hooft, P. A. V.; Overkleef, H. S.; Van Der Marel, G. A.; Van Boom, J. H. *Eur. J. Org. Chem.* **2000**, 873.
- [171]. Pai, A.; Bhattacharjya, A. *J. Org. Chem.* **2001**, *66*, 9071.
- [172]. Hotha, S.; Maurya, S. K.; Gurjar, M. K. *Tetrahedron Lett.* **2005**, *46*, 5329.
- [173]. Schore, N. E.; Croudace, M. C. *J. Org. Chem.* **1981**, *46*, 5436.
- [174]. Exon, C.; Magnus, P. *J. Am. Chem. Soc.* **1983**, *105*, 2477.
- [175]. Sugihara, T.; Yamada, M.; Yamaguchi, M.; Nishizawa, M. *Synlett* **1999**, 771.
- [176]. Sugihara, T.; Yamada, M.; Ban, H.; Yamaguchi, M.; Kaneko, C. *Angew. Chem. Int. Ed.* **1997**, *36*, 2801.
- [177]. Pe´rez-Serrano, L.; Casarrubios, L.; Domi´nguez, G.; Pe´rez-Castells, *Org. Lett.* **1999**, *1*, 1187.
- [178]. Blanco-Urogaiti, J.; Casarrubios, L.; Domi´nguez, G.; Pe´rez- Castells, J. *Tetrahedron Lett.* **2002**, *43*, 5763.
- [179]. Krafft, M. E.; Bon˜aga, L. V. R.; Hirosawa, C. *J. Org. Chem.* **2002**, *67*, 1233.
- [180]. Ghosh, S. K.; Hsung, R. P.; Liu, J. *J. Am. Chem. Soc.* **2005**, *127*, 8260.
- [181]. Pal, A.; Bhattacharjya, A. *J. Org. Chem.* **2001**, *66*, 9071.

- [182]. Subburaj, K.; Okamoto, S.; Sato, F. *J. Org. Chem.* **2002**, *67*, 1024.
- [183]. Brummond, K. M.; Kerekes, A. D.; Wan, H. *J. Org. Chem.* **2002**, *67*, 5156.
- [184]. Marchueta, I.; Montenegro, E.; Panov, D.; Poch, M.; Verdaguer, X.; Moyano, A.; Perica's, M. A.; Riera, A. *J. Org. Chem.* **2001**, *66*, 6400.
- [185]. Rivero, M. R.; Adrio, J.; Carretero, J. C. *Eur. J. Org. Chem.* **2002**, 2881.
- [186]. Dimitrov, V.; Simova, S.; Kostova, K. *Tetrahedron* **1996**, *52*, 1699.
- [187]. Mukai, C.; Kim, J. S.; Sonobe, H.; Hanaoka, M. *J. Org. Chem.* **1999**, *64*, 6822.
- [188]. Cassayre, J.; Gagosz, F.; Zard, S. Z. *Angew. Chem.Int. Ed.* **2002**, *41*, 1783.
- [189]. Busto, E.; Fernandez, F.G.; Gotor, V. *Tetrahedron:Asymmetry* **2005**, *16*, 3427.
- [190]. Rigaku (2005), *CrystalClear*, Version 1.3.6. Rigaku American Corporation, 9009 New Trails Drive, The woodlands, TX 77381-5209, USA.
- [191]. Sheldrick, G. M., *SHELXS97* and *SHELXL97*, University of Göttingen, Germany, **1997**.

APPENDIX A

SUPPORTING INFORMATION

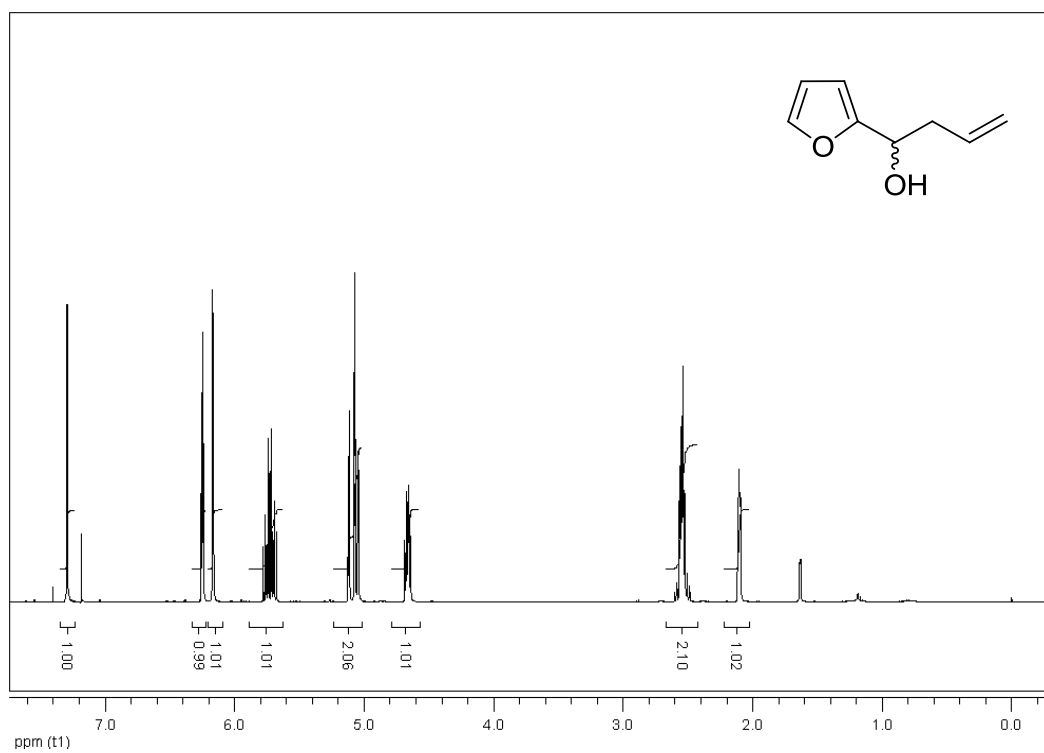


Figure A1. ^1H NMR spectrum of *rac-95*

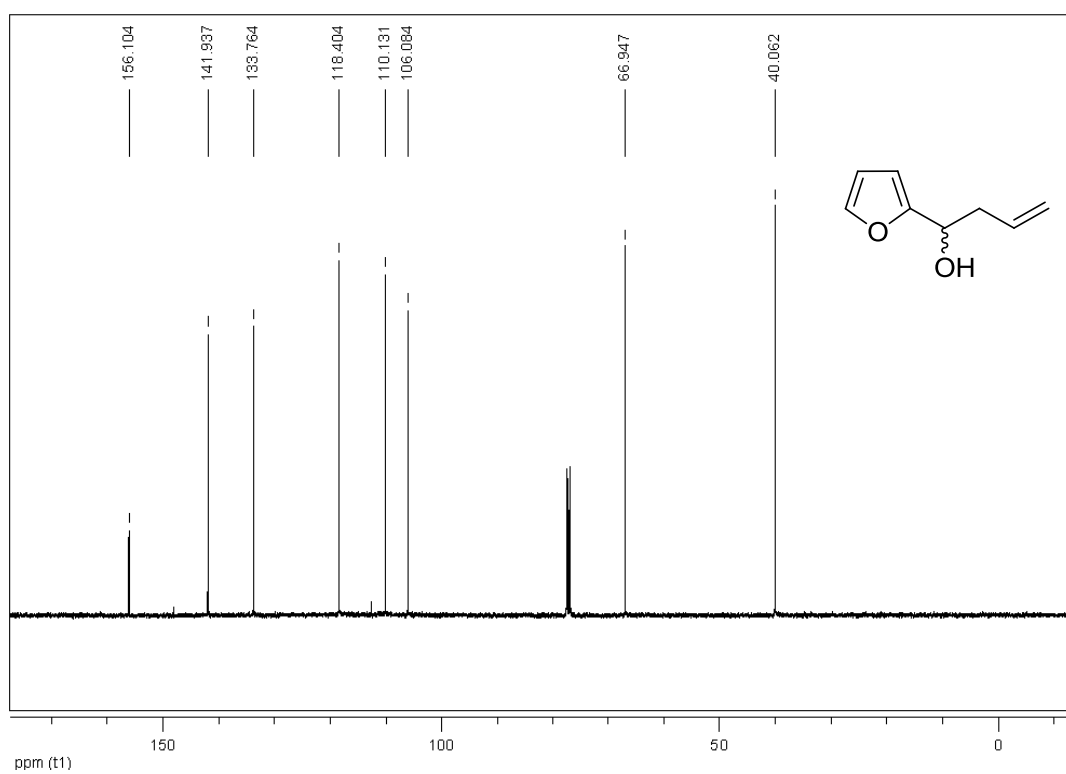


Figure A2. ^{13}C NMR spectrum of *rac-95*

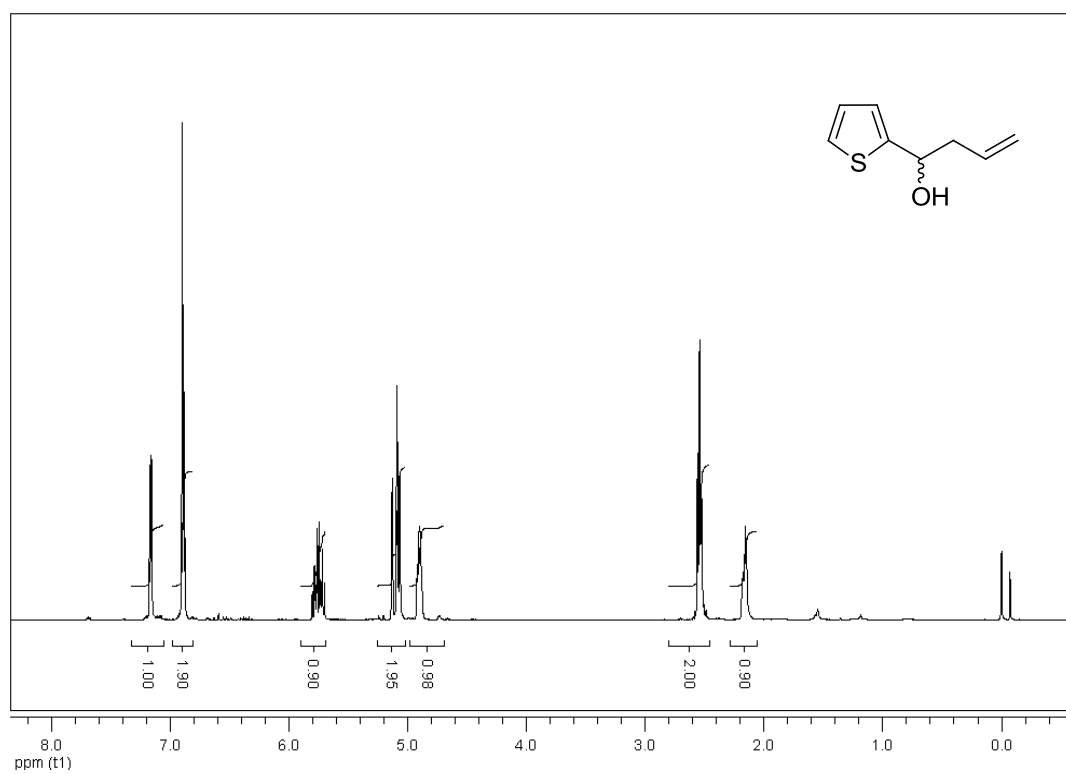


Figure A3. ^1H NMR spectrum of *rac-96*

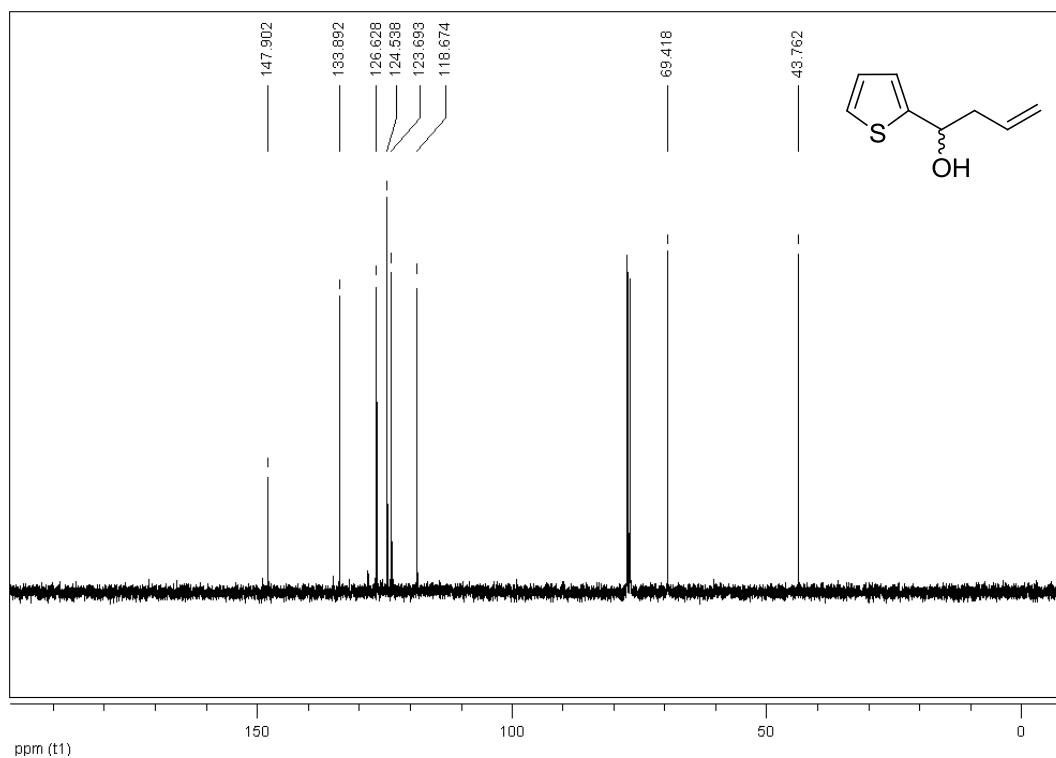


Figure A4. ^{13}C NMR spectrum of *rac-96*

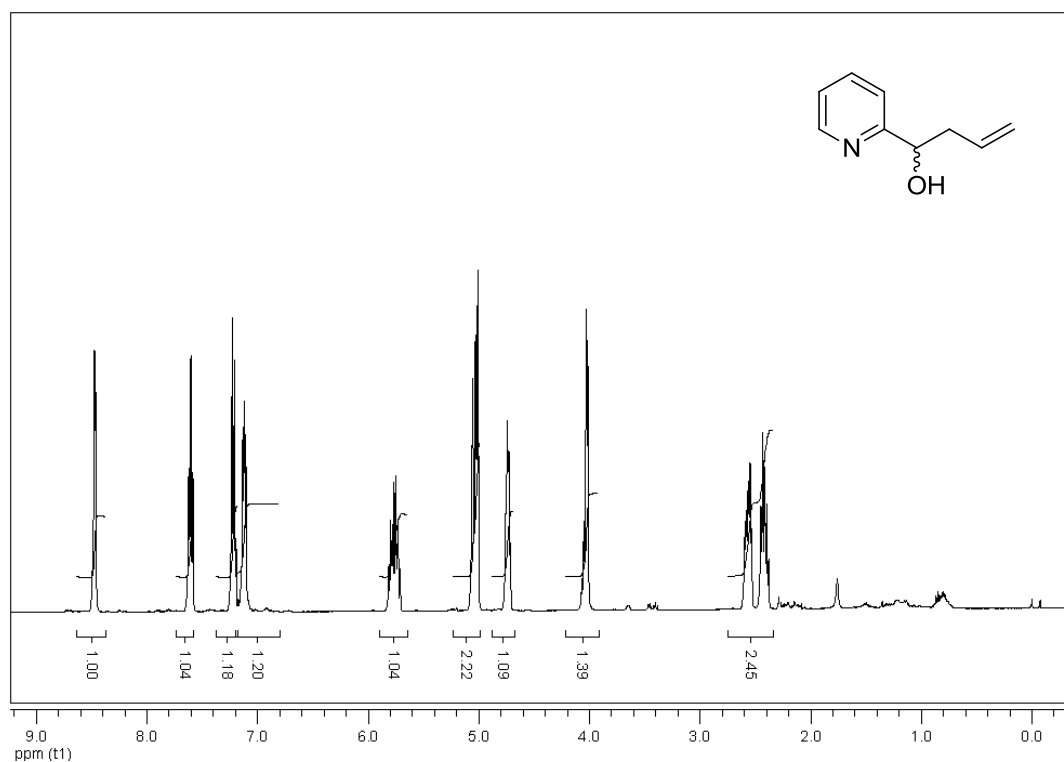


Figure A5. ^1H NMR spectrum of *rac-97*

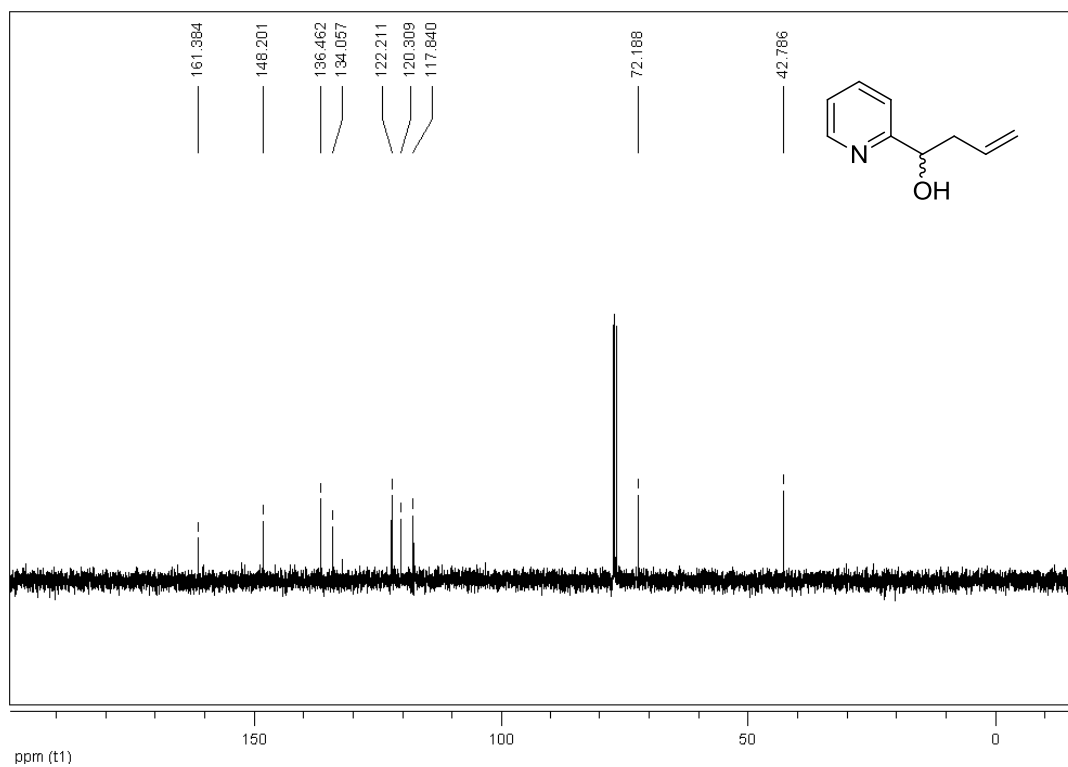


Figure A6. ^{13}C NMR spectrum of *rac-97*

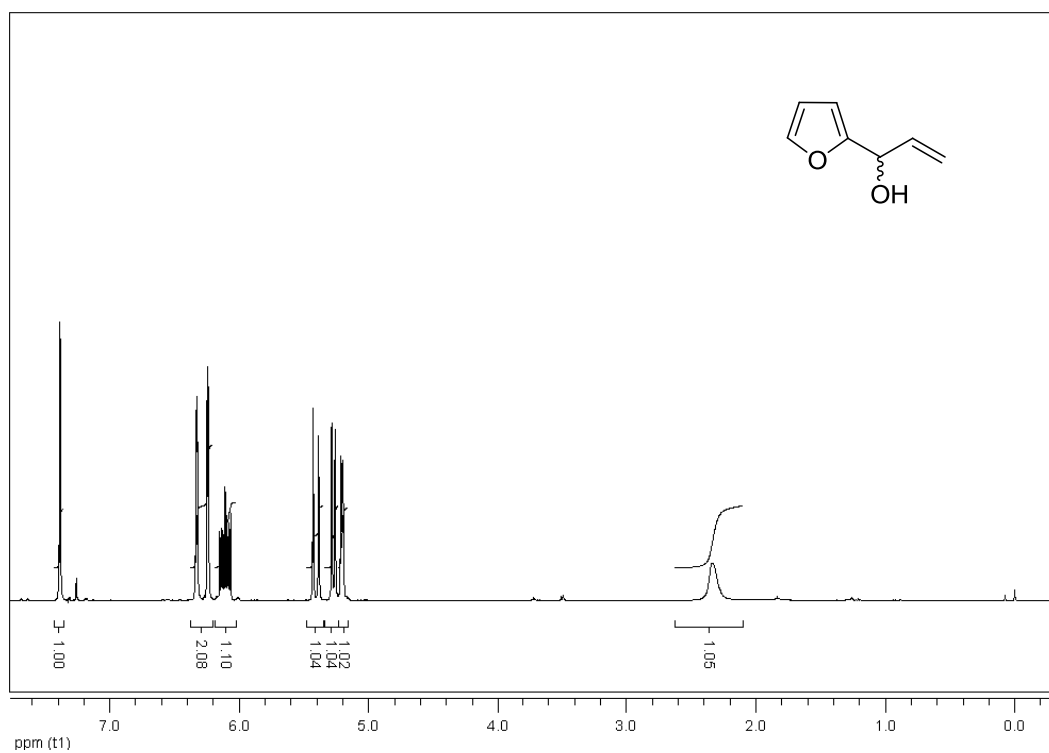


Figure A7. ^1H NMR spectrum of *rac-99*

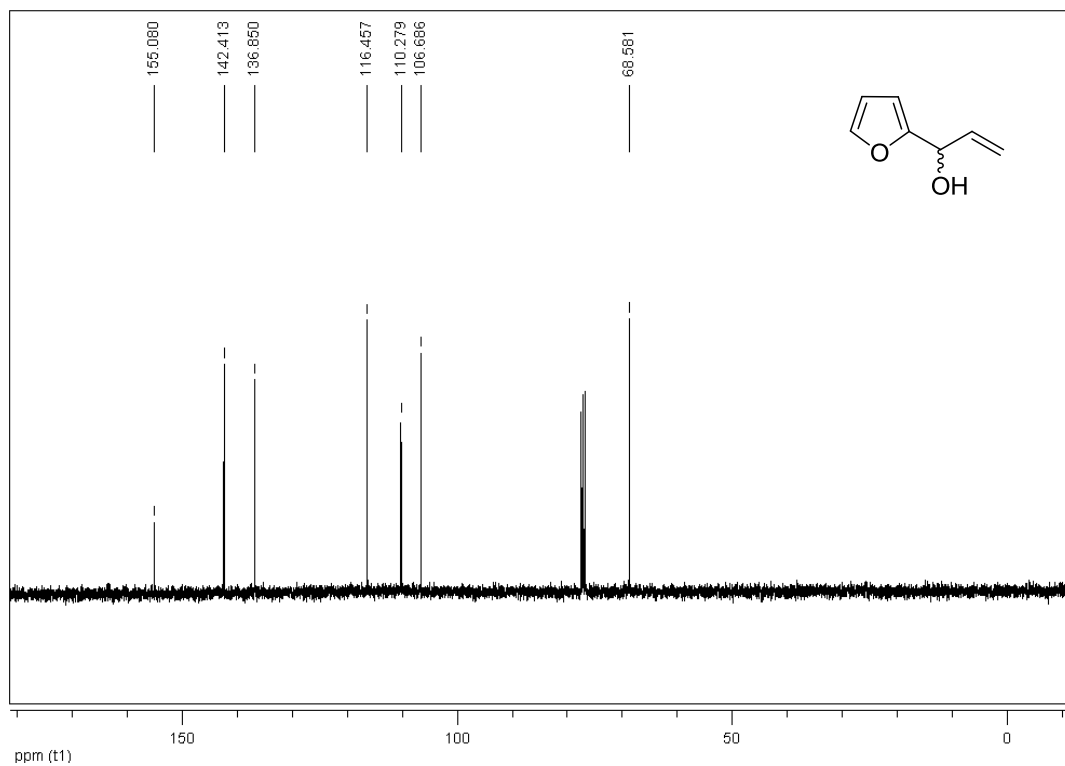


Figure A8. ^{13}C NMR spectrum of *rac*-99

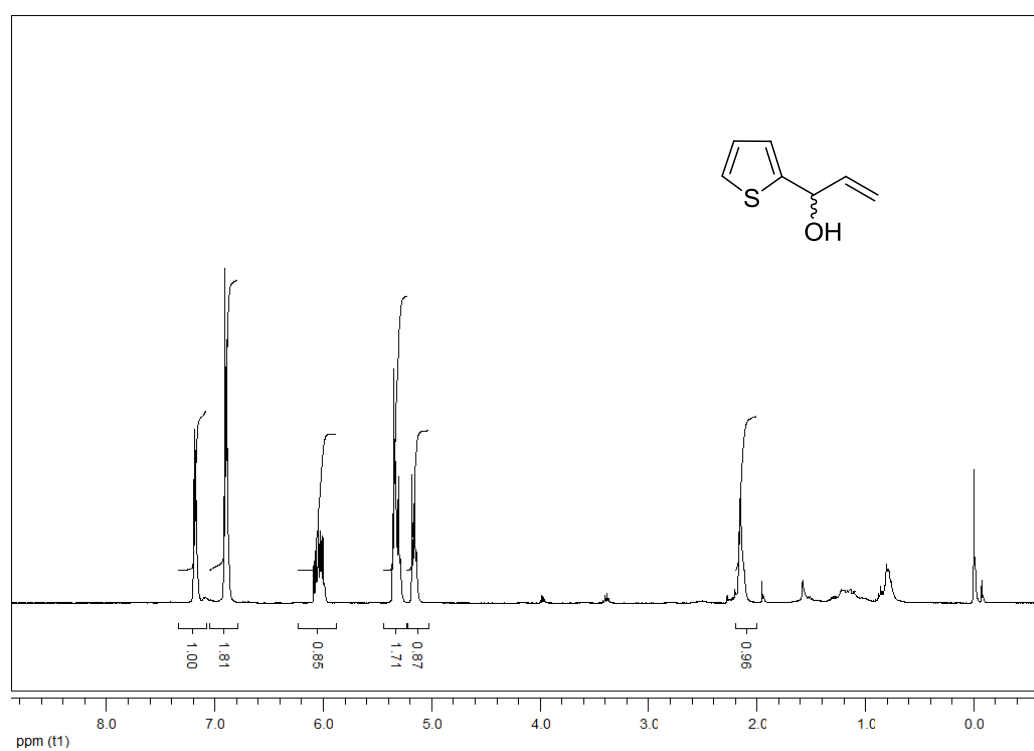


Figure A9. ^1H NMR spectrum of *rac*-100

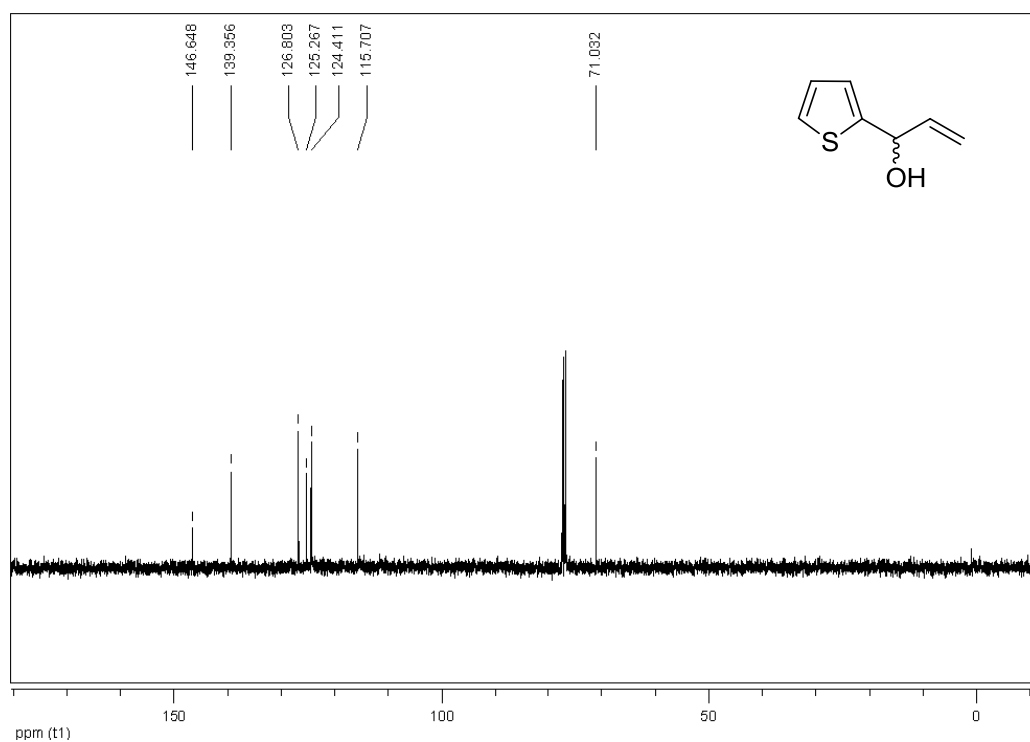


Figure A10. ¹³C NMR spectrum of *rac*-100

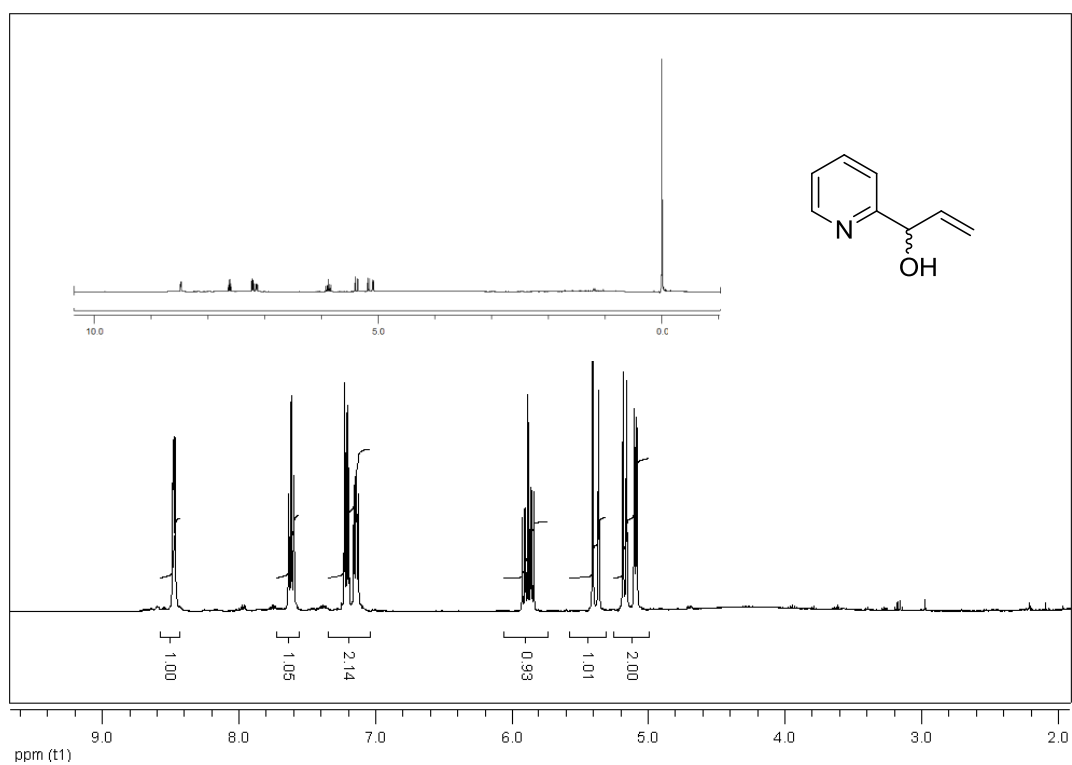


Figure A11. ¹H NMR spectrum of *rac*-101

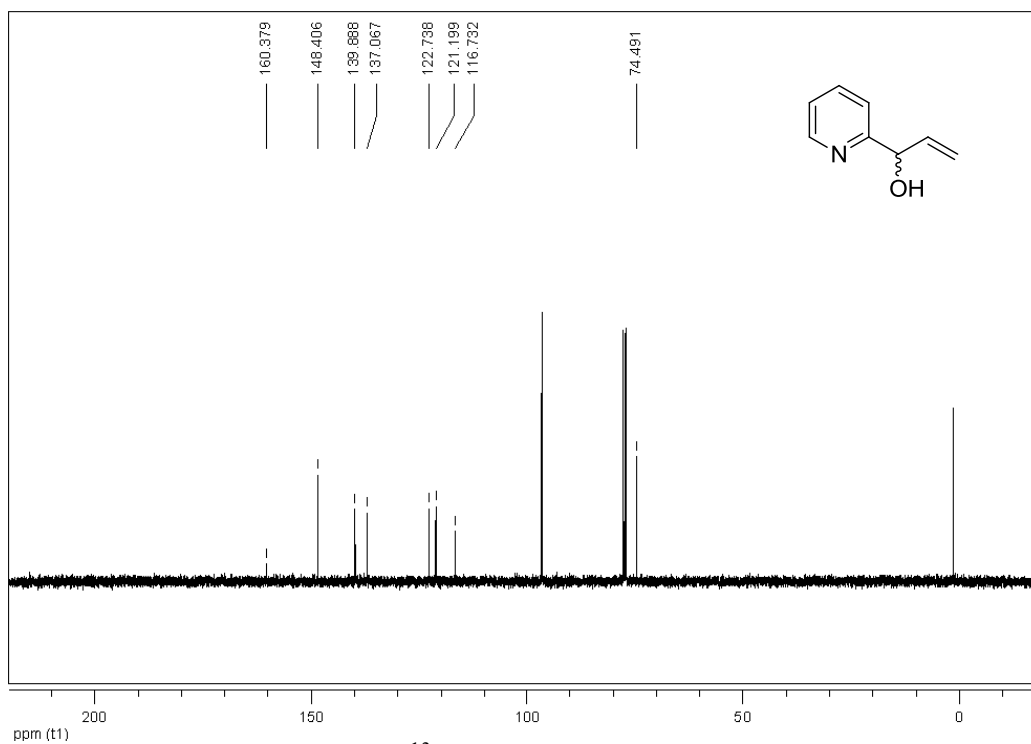


Figure A12. ^{13}C NMR spectrum of *rac*-101

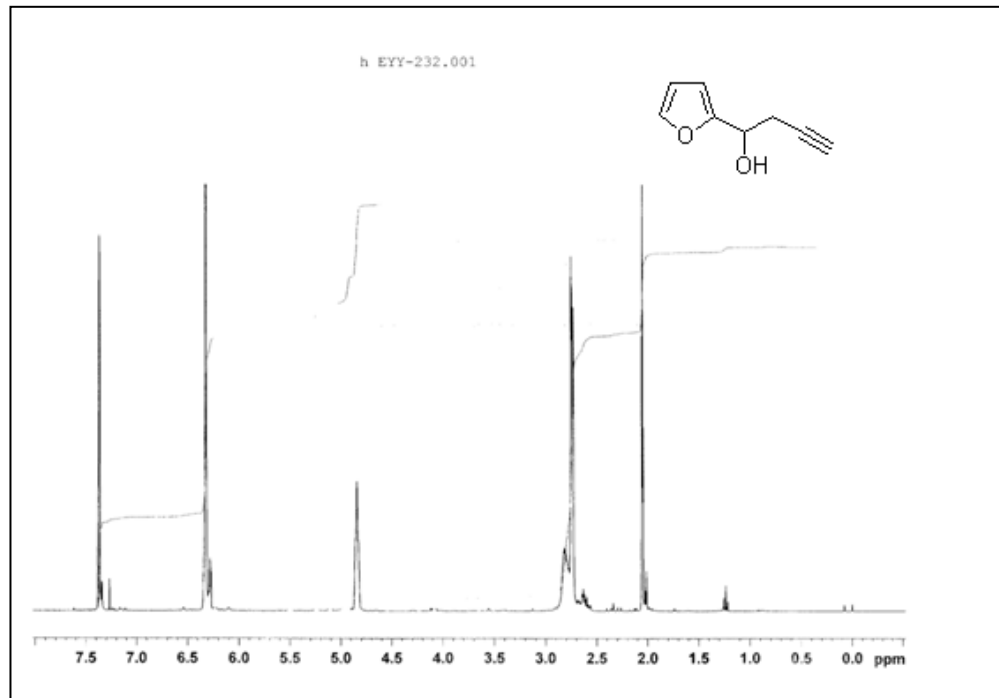


Figure A13. ^1H NMR spectrum of *rac*-103

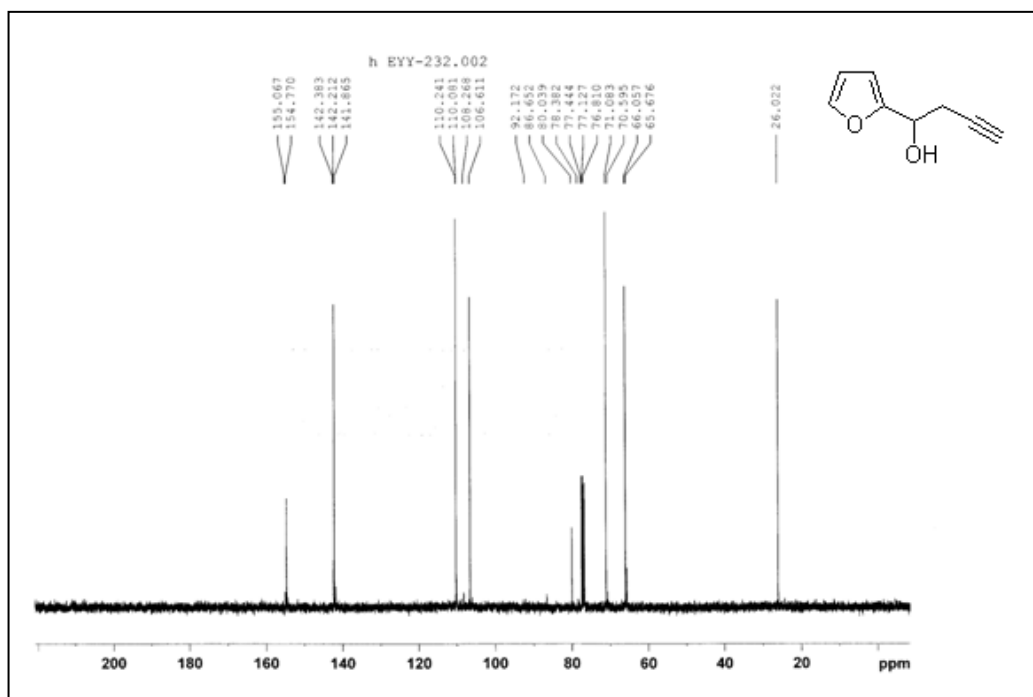


Figure A14. ^{13}C NMR spectrum of *rac*-103

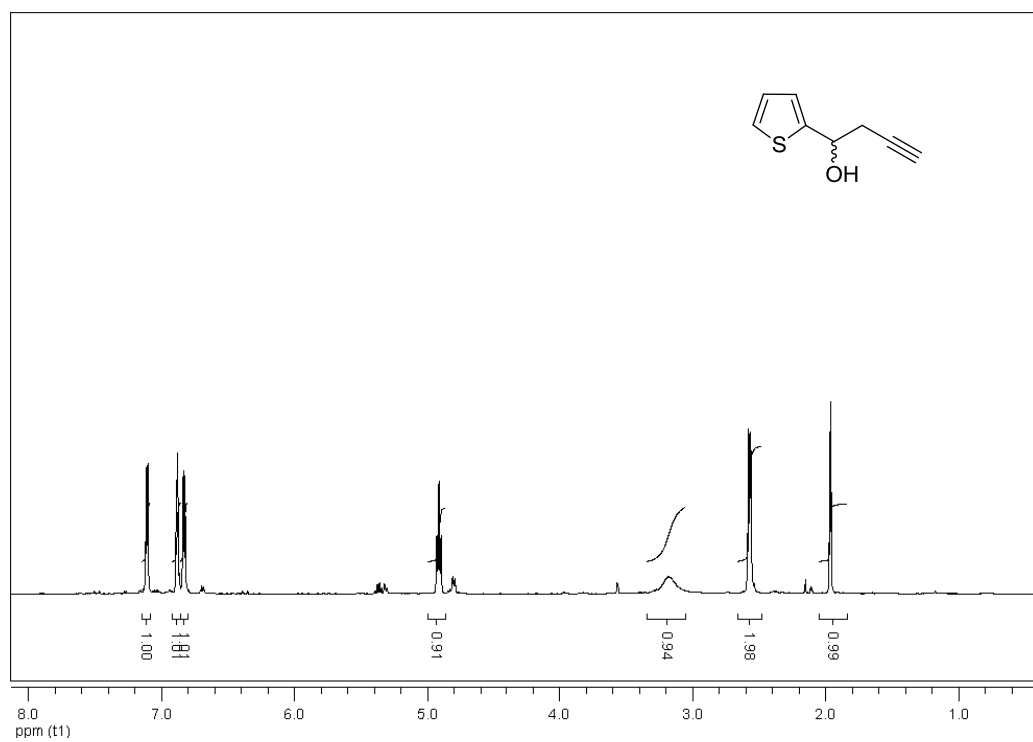


Figure A15. ^1H NMR spectrum of *rac*-104

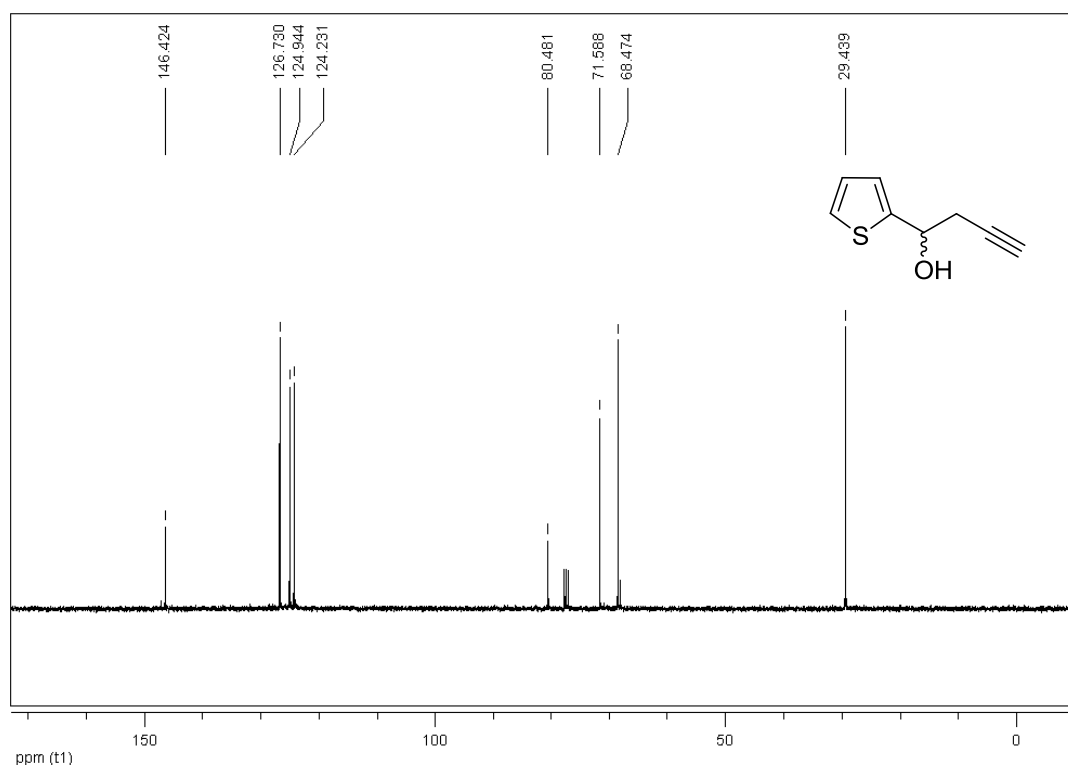


Figure A16. ^{13}C NMR spectrum of *rac*-104

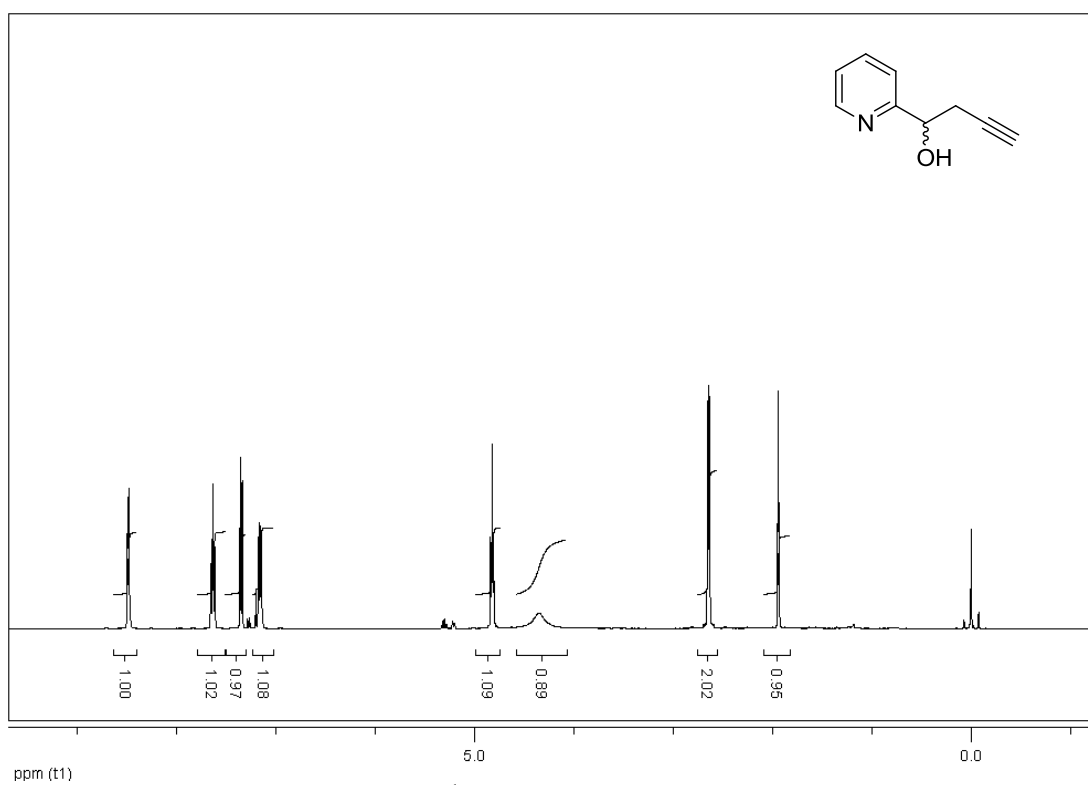


Figure A17. ^1H NMR spectrum of *rac*-105

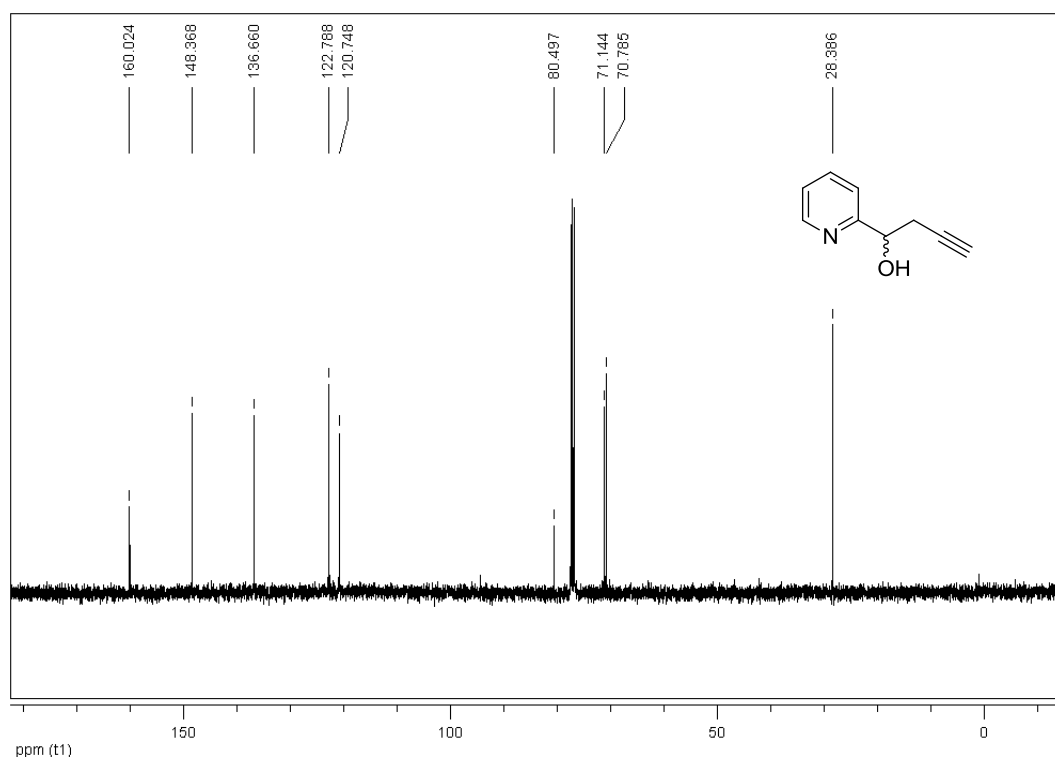


Figure A18. ^{13}C NMR spectrum of *rac*-105

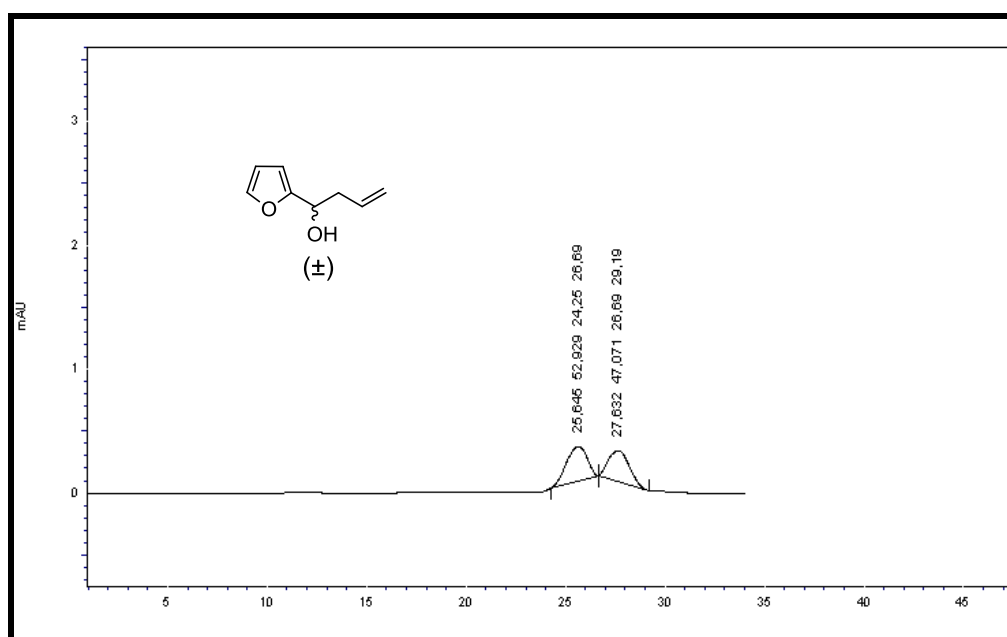


Figure A19. HPLC chromatogram of *rac*-95

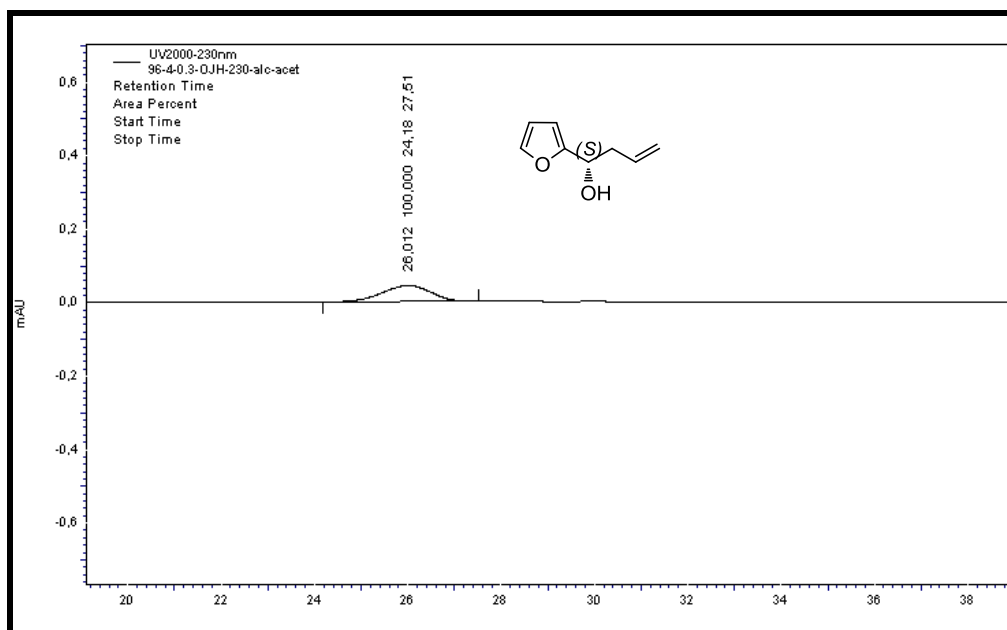


Figure A20. HPLC chromatogram of (*S*)-(-)-95

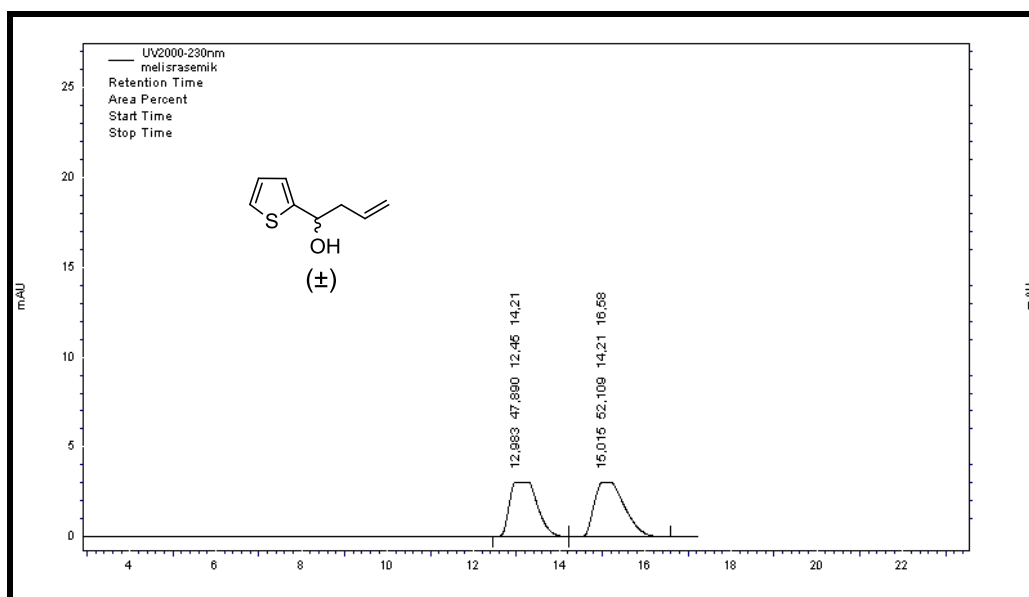


Figure A21. HPLC chromatogram of *rac*-96

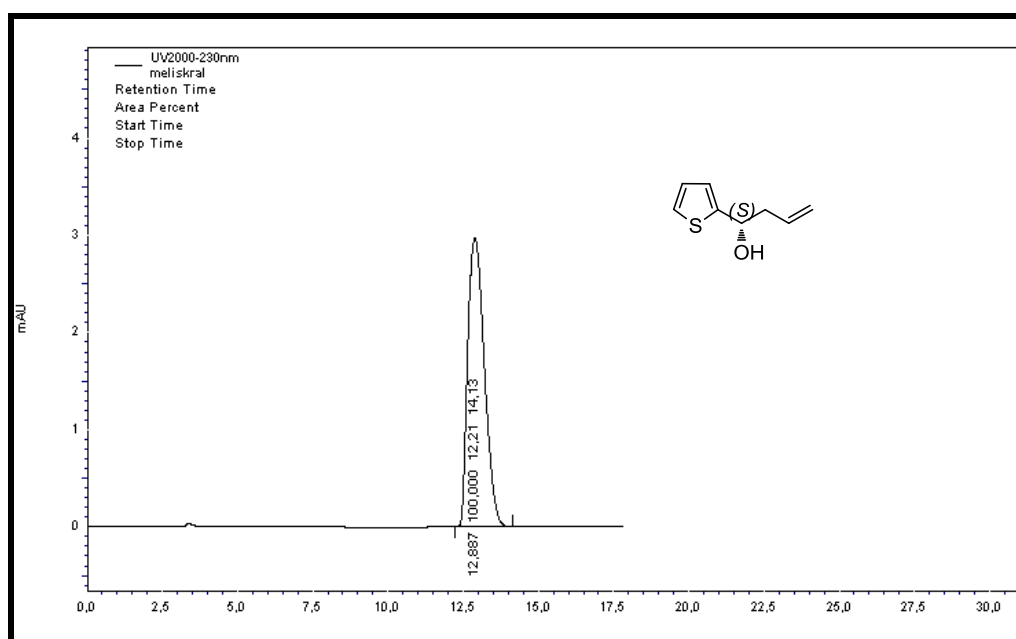


Figure A22. HPLC chromatogram of (*S*)-(-)-96

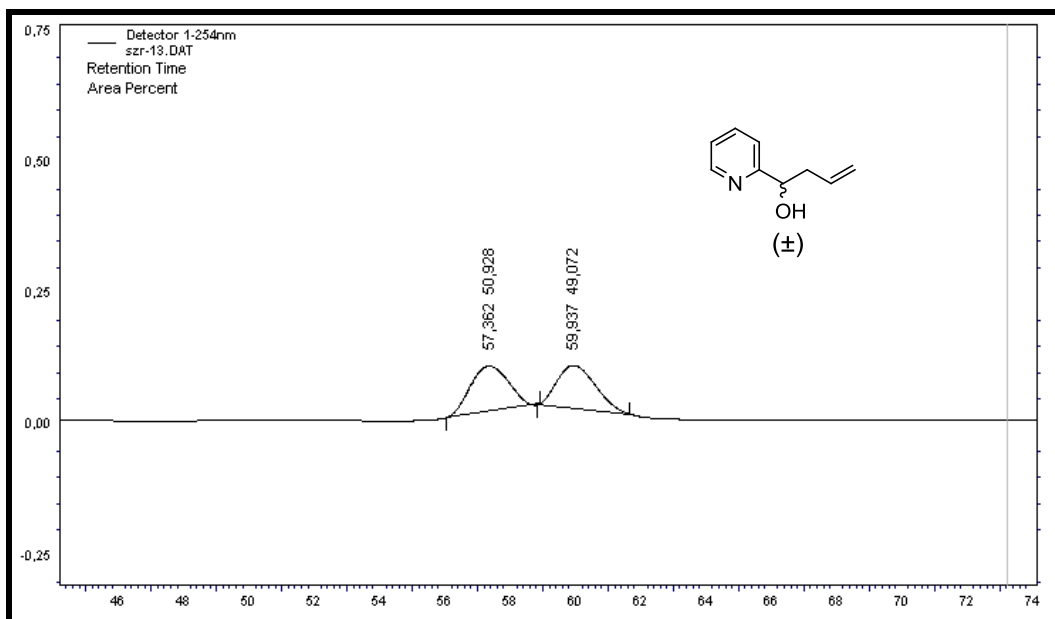


Figure A23. HPLC chromatogram of *rac*-97

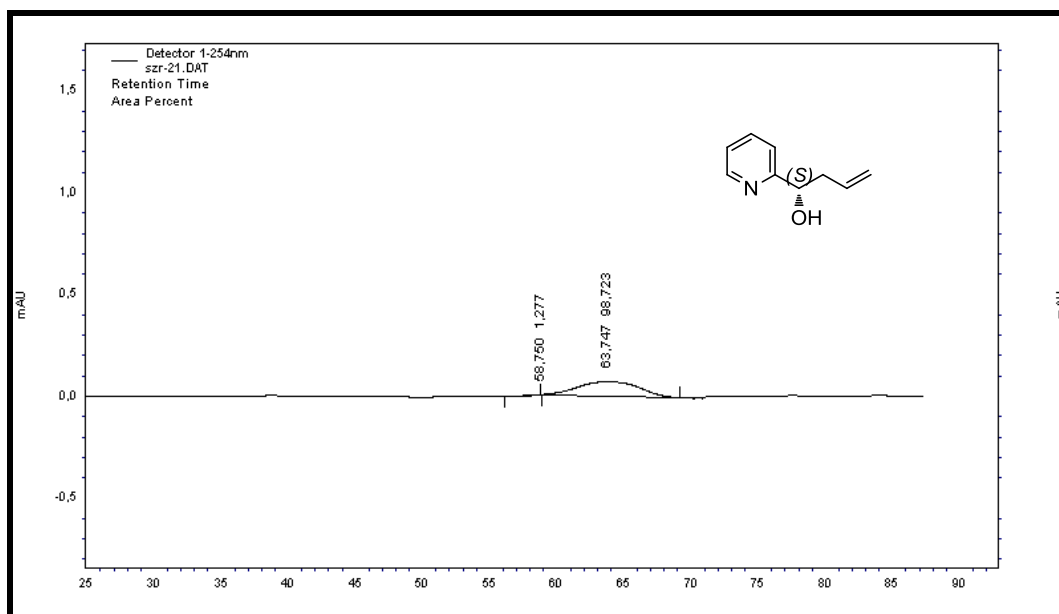


Figure A24. HPLC chromatogram of (*S*)-(-)-97

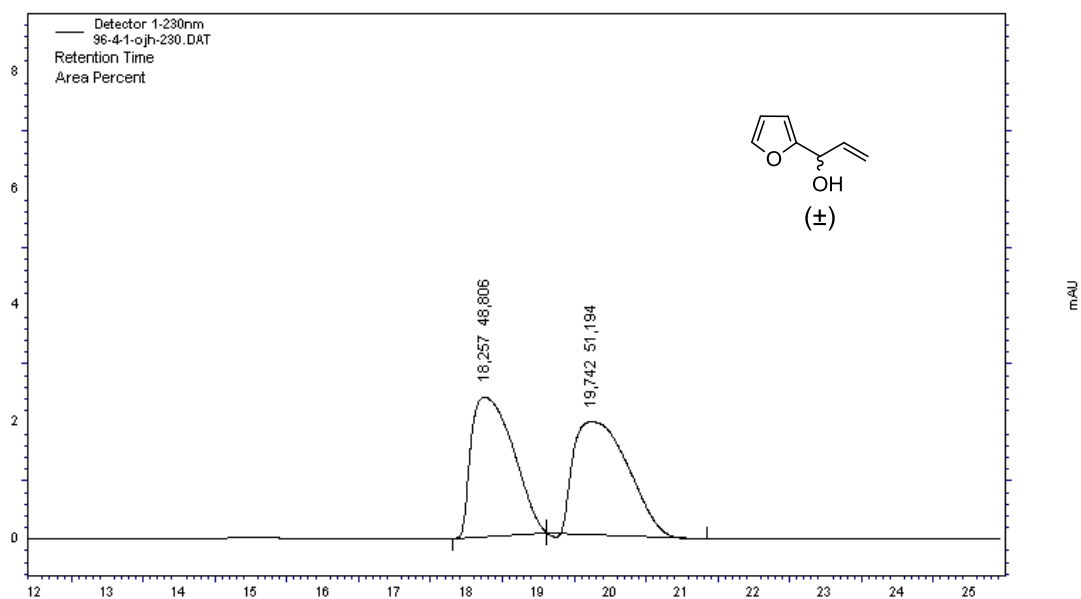


Figure A25. HPLC chromatogram of *rac*-99

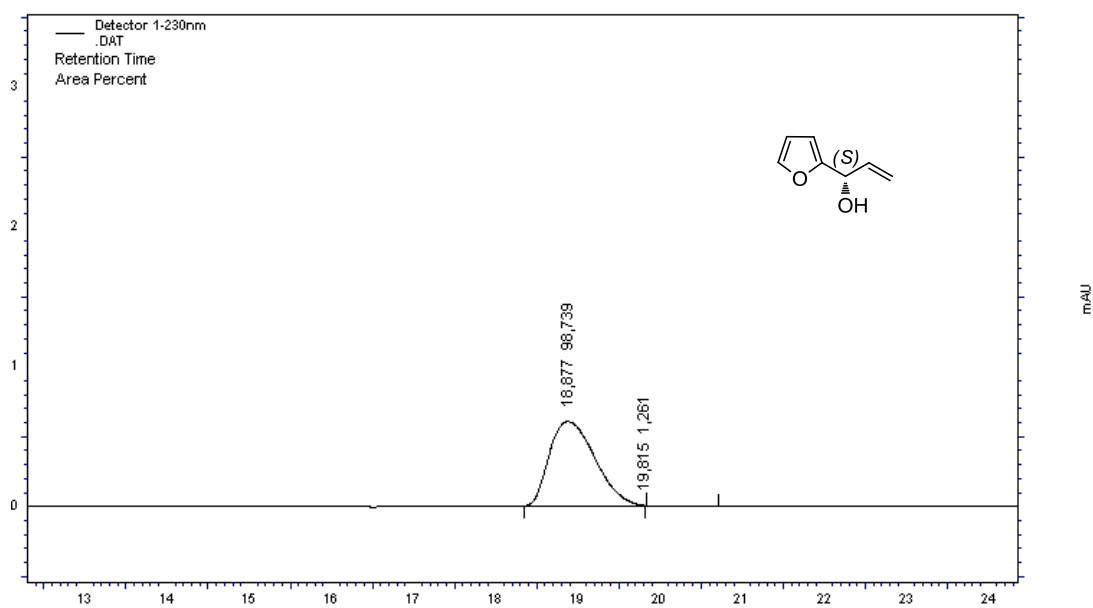


Figure A26. HPLC chromatogram of (*S*)-(+)-99

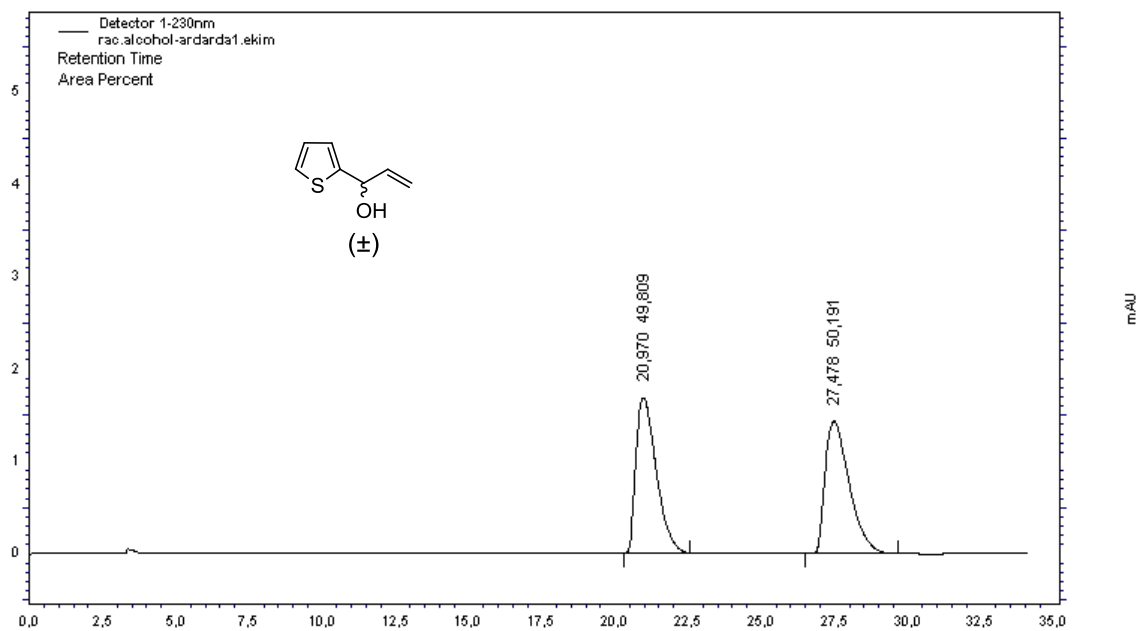


Figure A27. HPLC chromatogram of *rac*-100

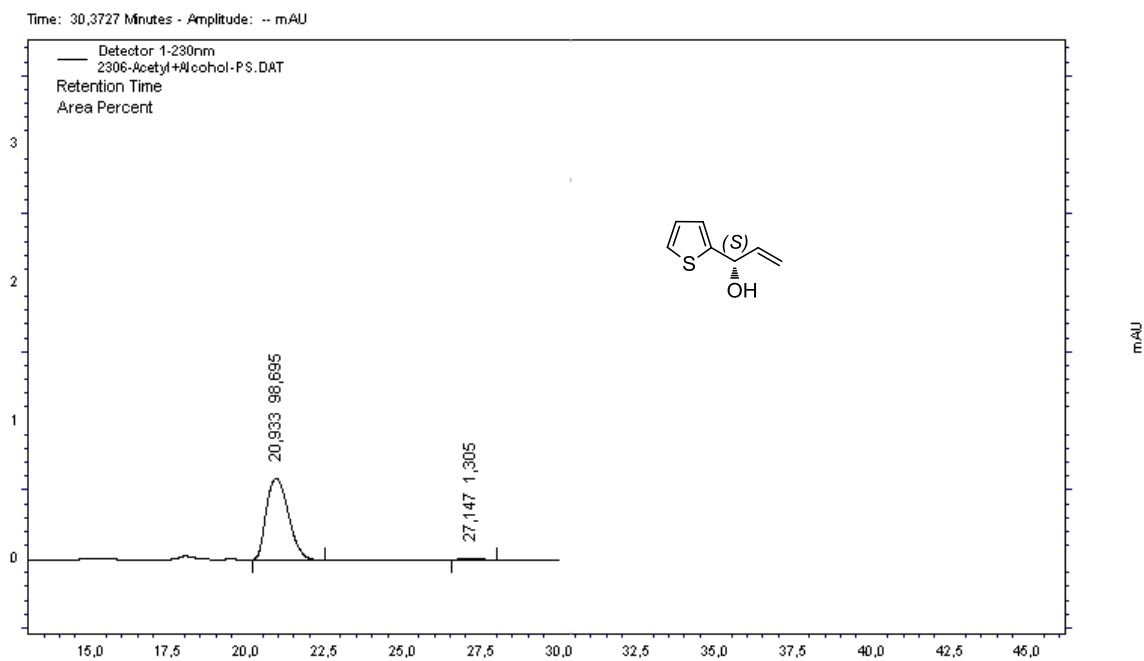


Figure A28. HPLC chromatogram of (*S*)-(-)-100

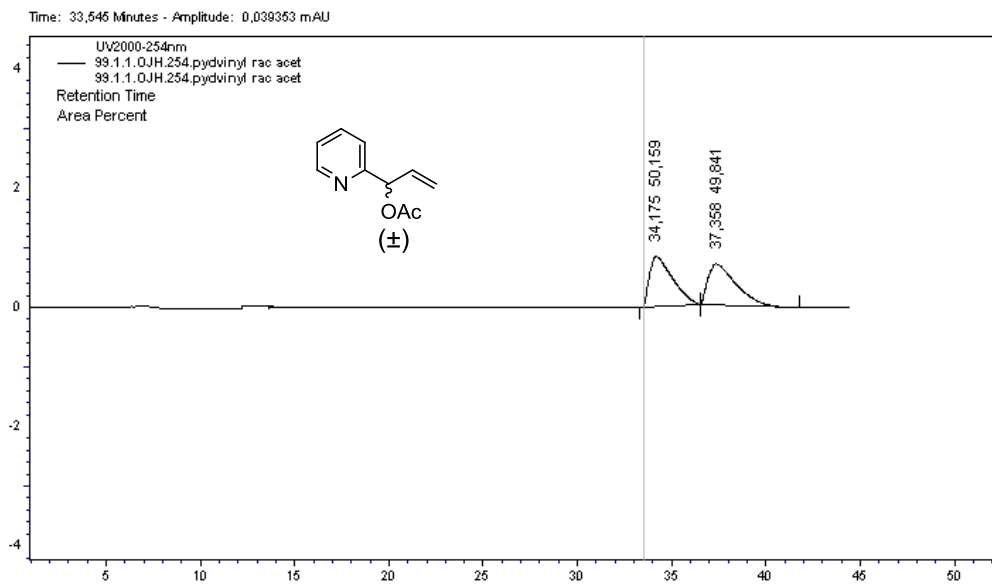


Figure A29. HPLC chromatogram of *rac*-112

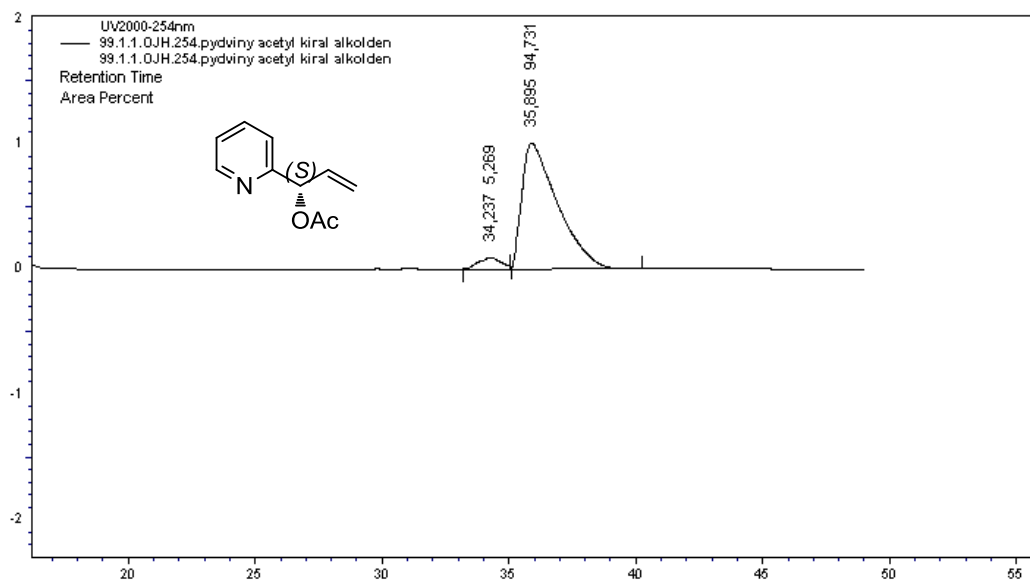


Figure A30. HPLC chromatogram of (*S*)-(+)-112

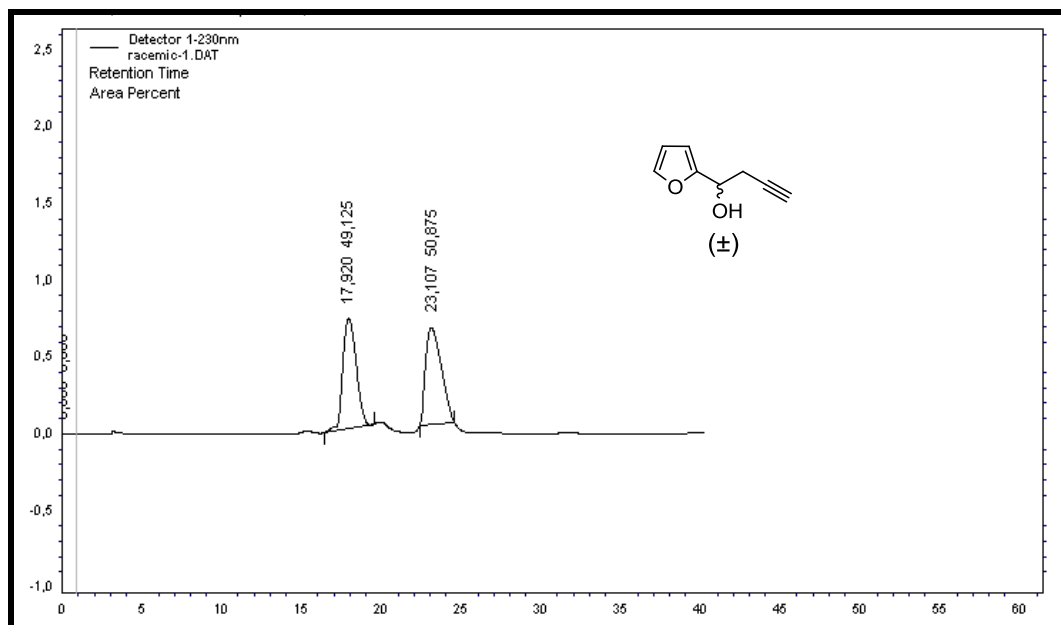


Figure A31. HPLC chromatogram of *rac*-103

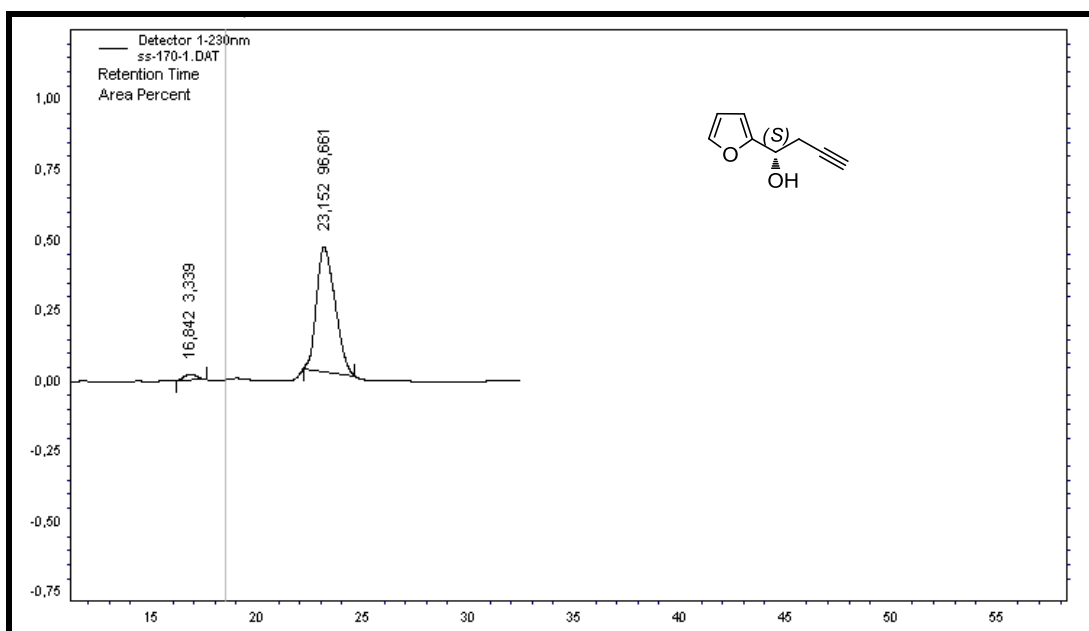


Figure A32. HPLC chromatogram of (*S*)-(+)-103

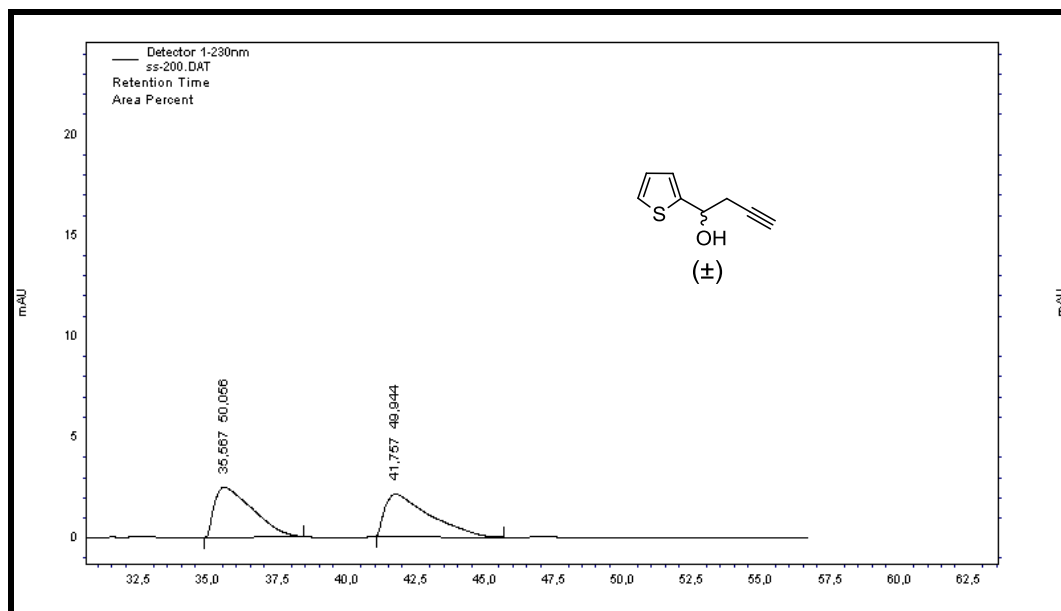


Figure A33. HPLC chromatogram of *rac*-104

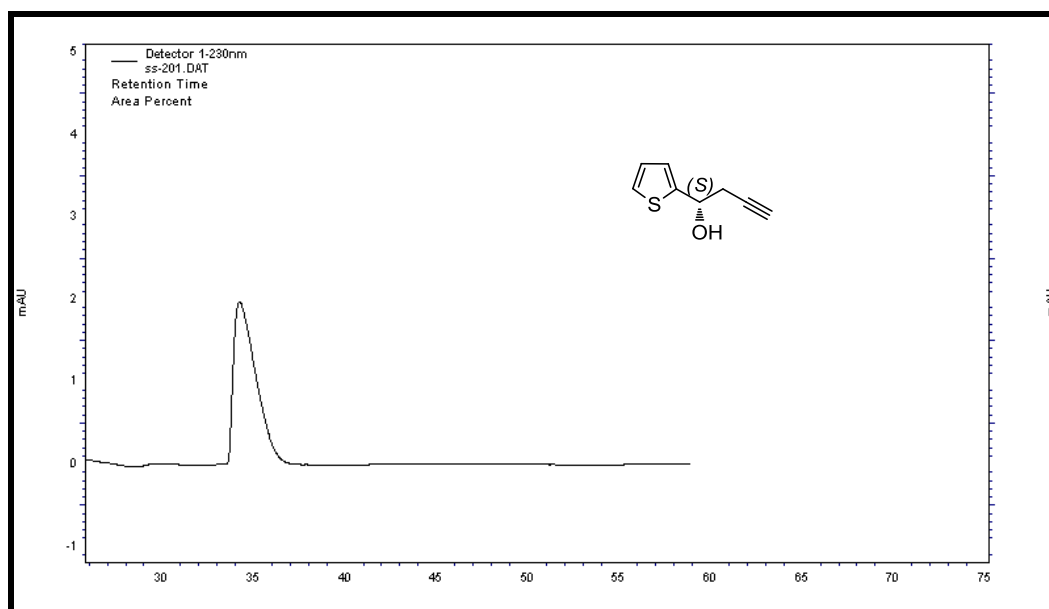


Figure A34. HPLC chromatogram of (*S*)-(+)-104

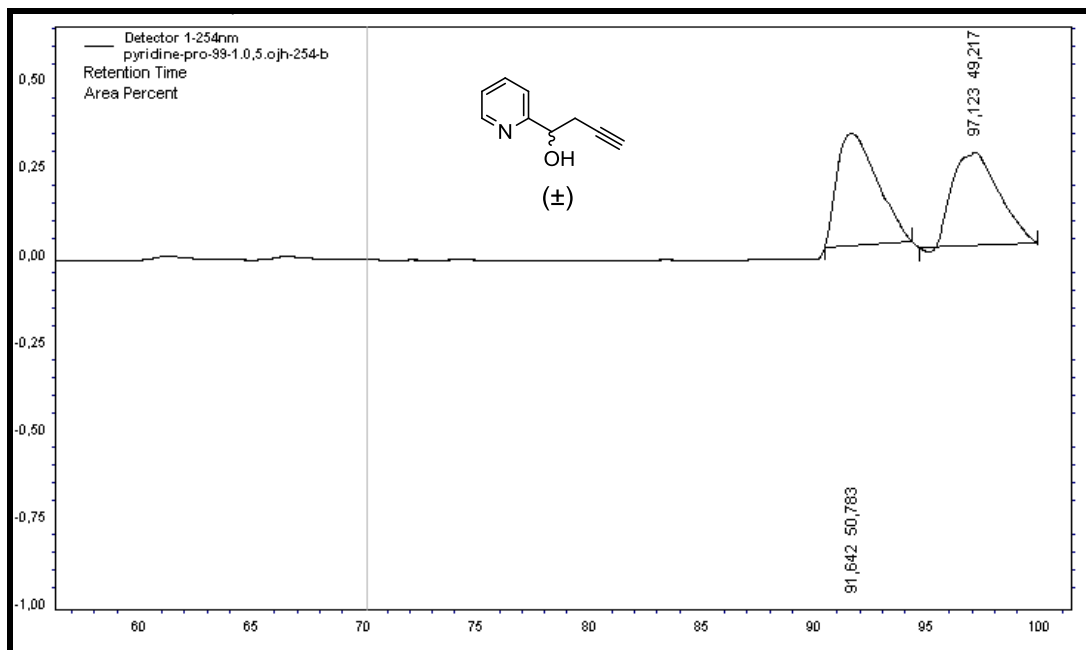


Figure A35. HPLC chromatogram of *rac*-105

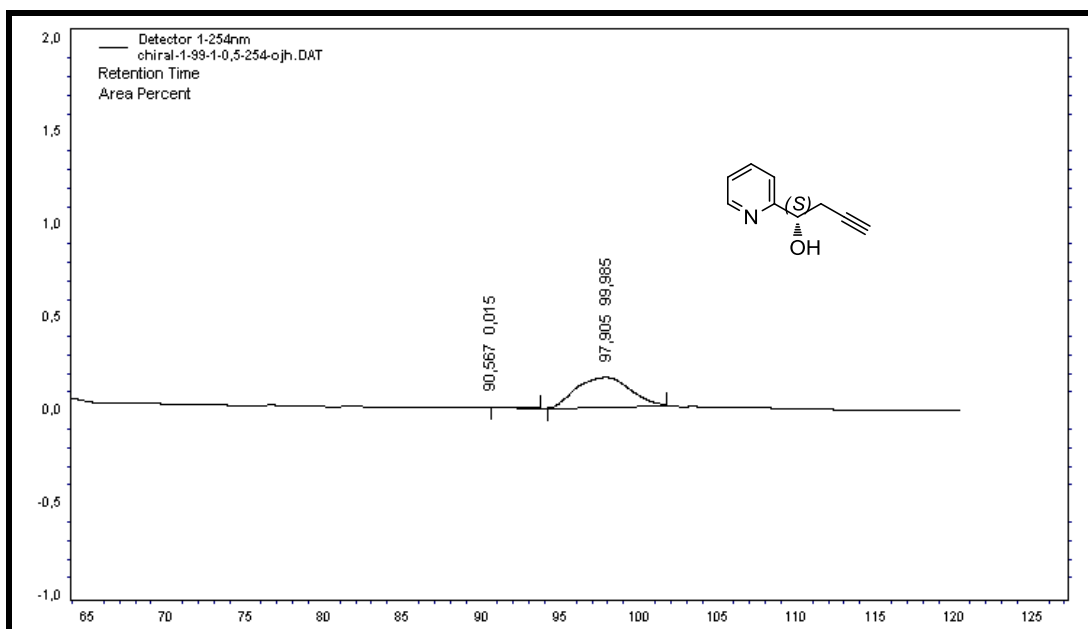


Figure A36. HPLC chromatogram of (*S*)-(-)-105

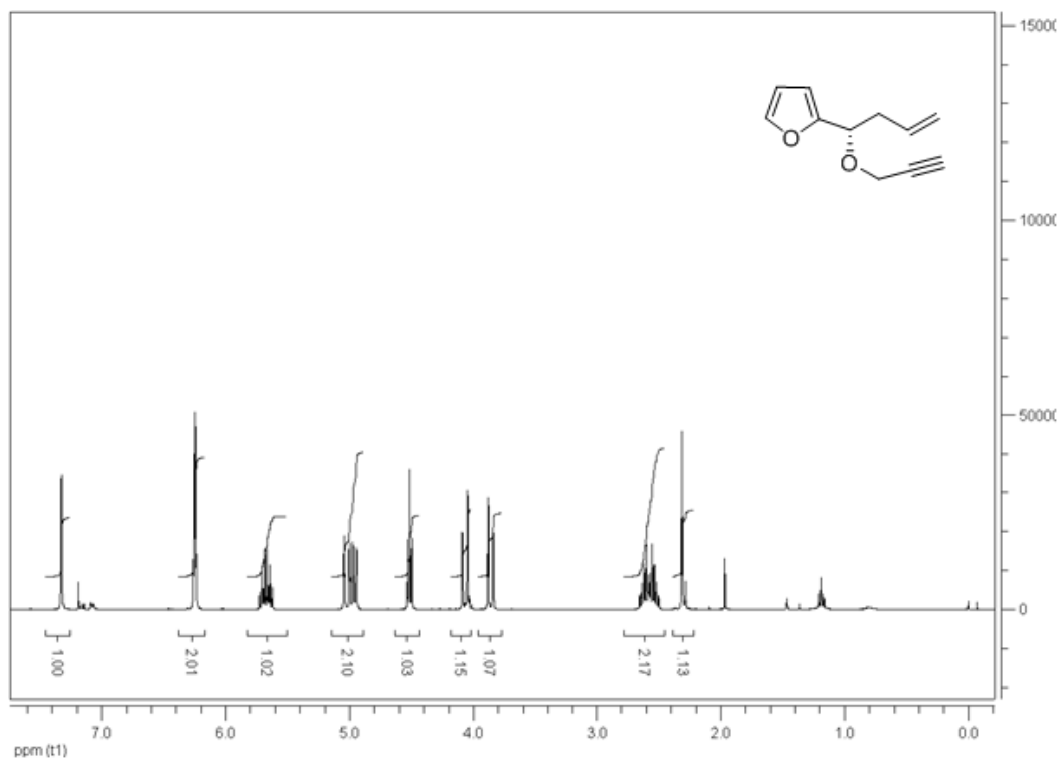


Figure A37. ^1H NMR spectrum of (S)-(-)-116

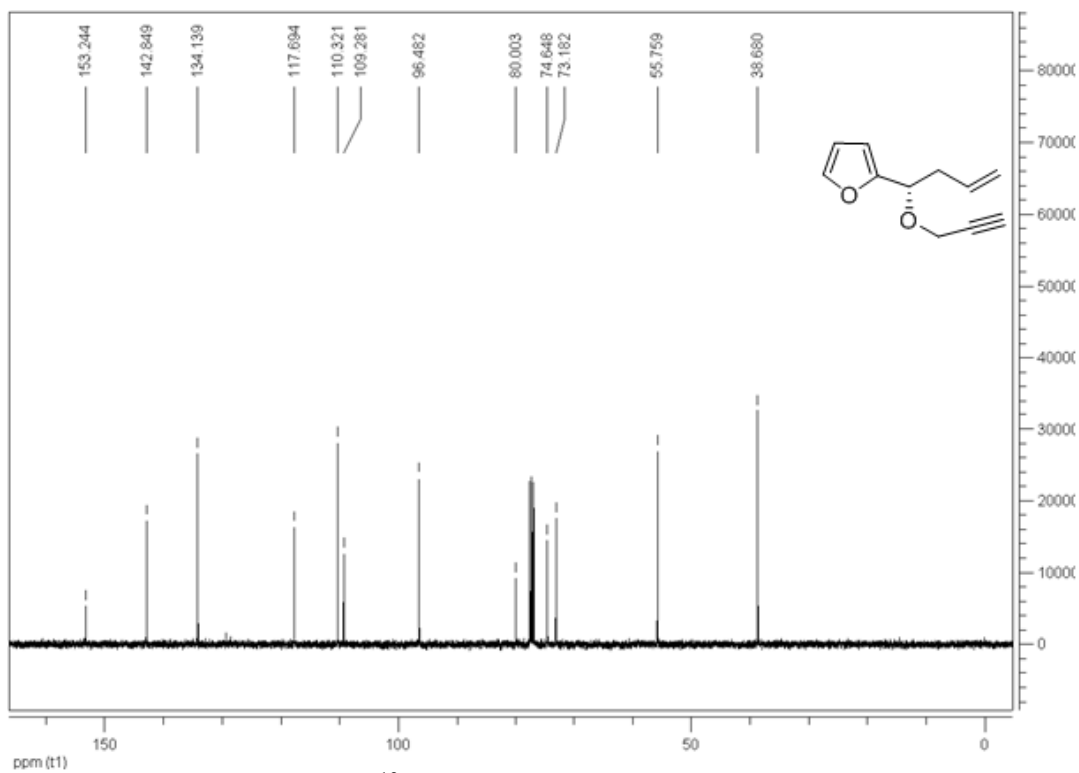


Figure A38. ^{13}C NMR spectrum of (S)-(-)-116

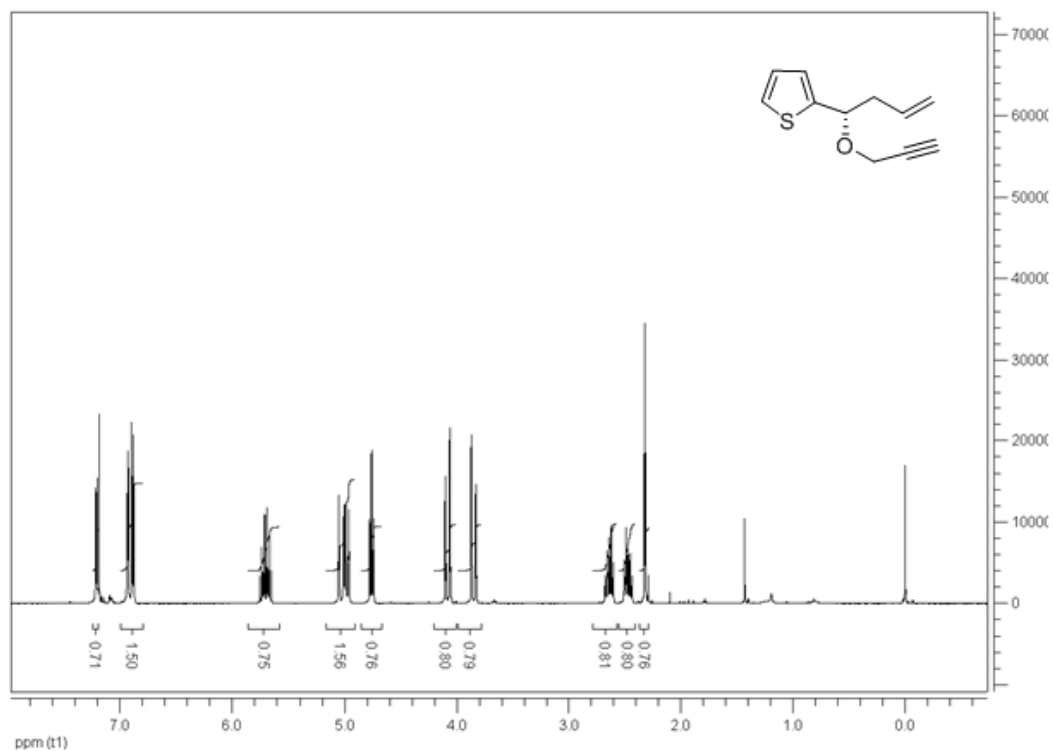


Figure A39. ^1H NMR spectrum of (S)-(-)-117

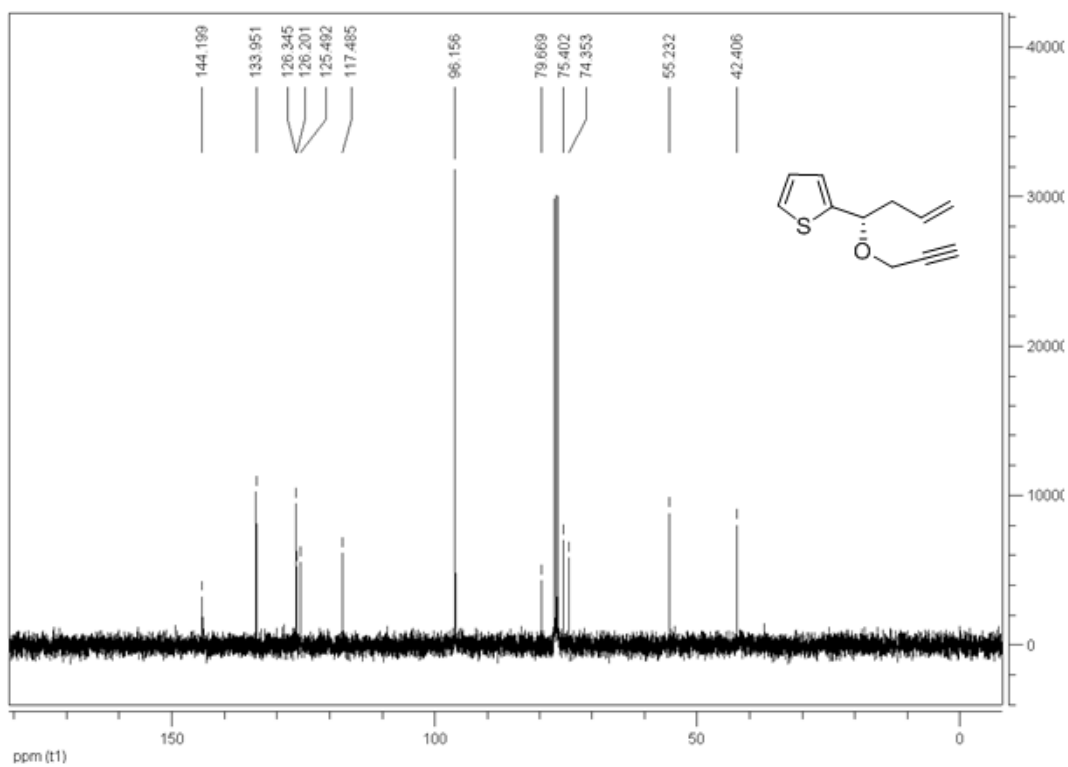


Figure A40. ^{13}C NMR spectrum of (S)-(-)-117

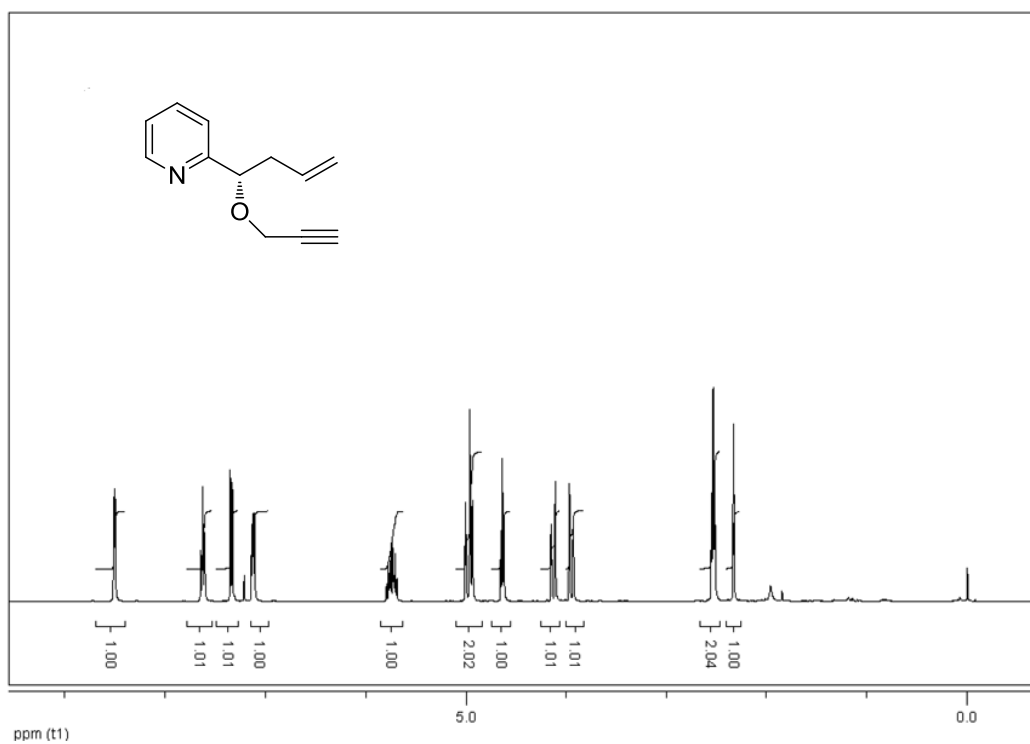


Figure A41. ¹H NMR spectrum of (S)-(-)-118

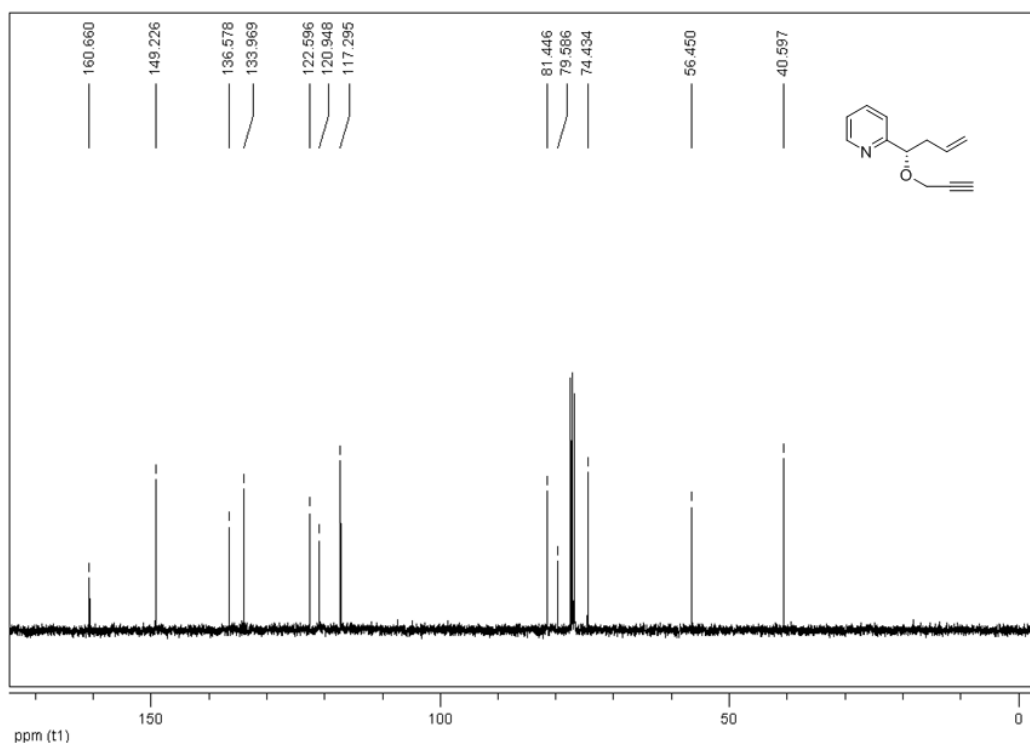


Figure A42. ¹³C NMR spectrum of (S)-(-)-118

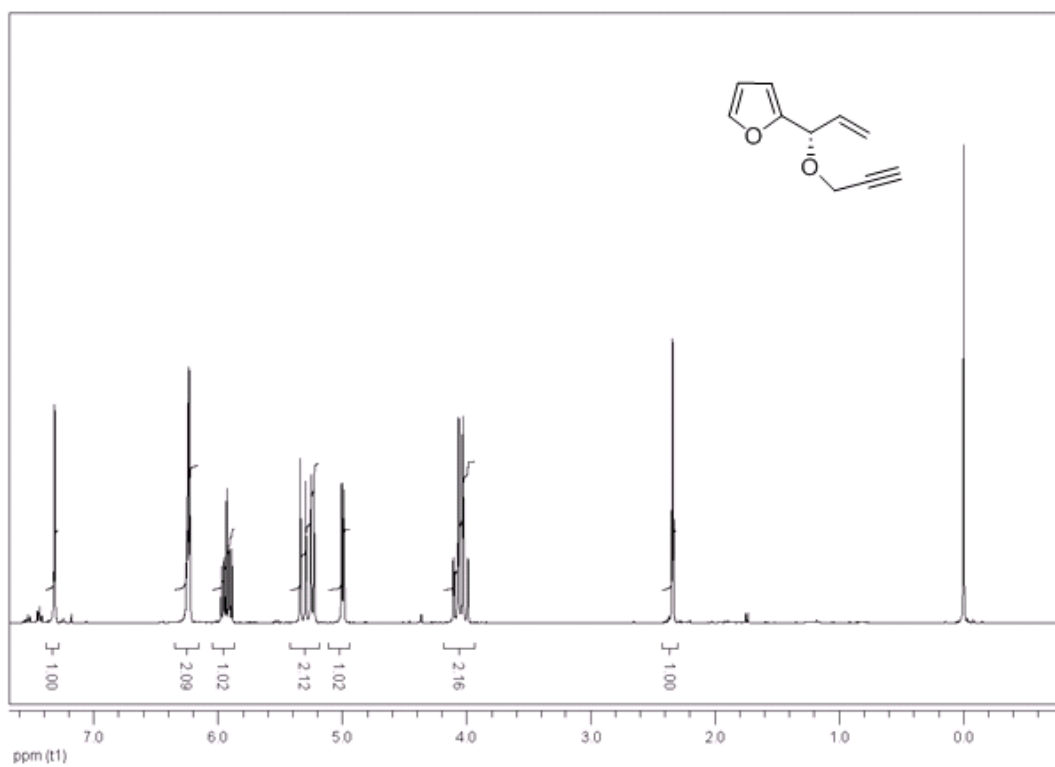


Figure A43. ¹H NMR spectrum of (S)-(-)-119

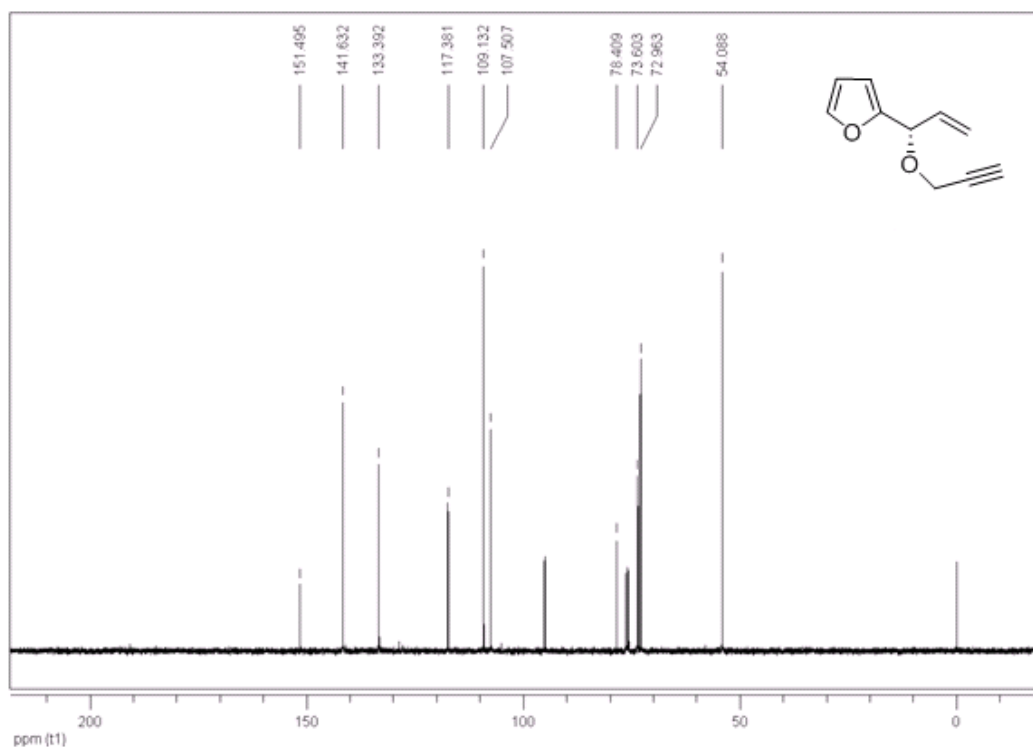


Figure A44. ¹³C NMR spectrum of (S)-(-)-119

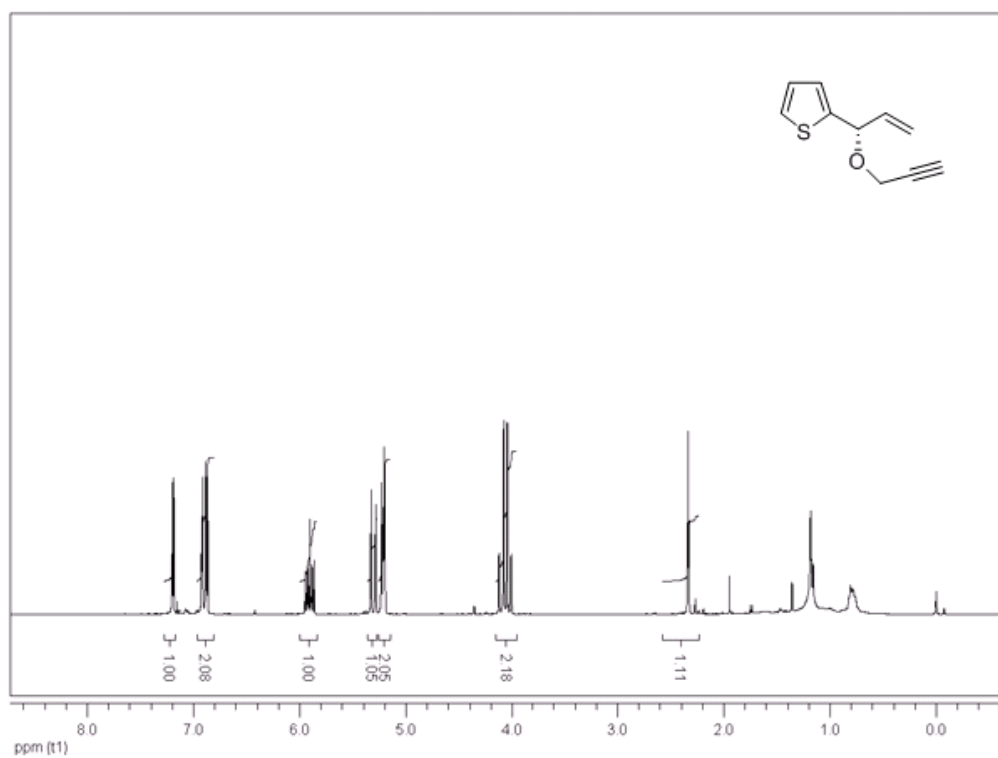


Figure A45. ^1H NMR spectrum of (S)-(-)-120

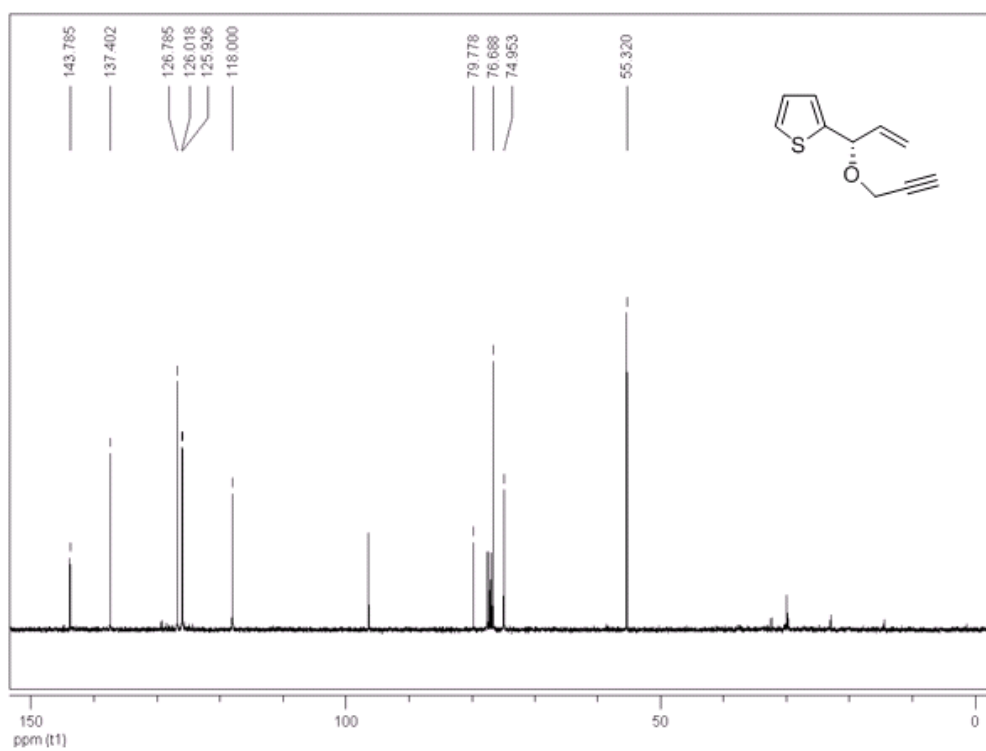


Figure A46. ^{13}C NMR spectrum of (S)-(-)-120

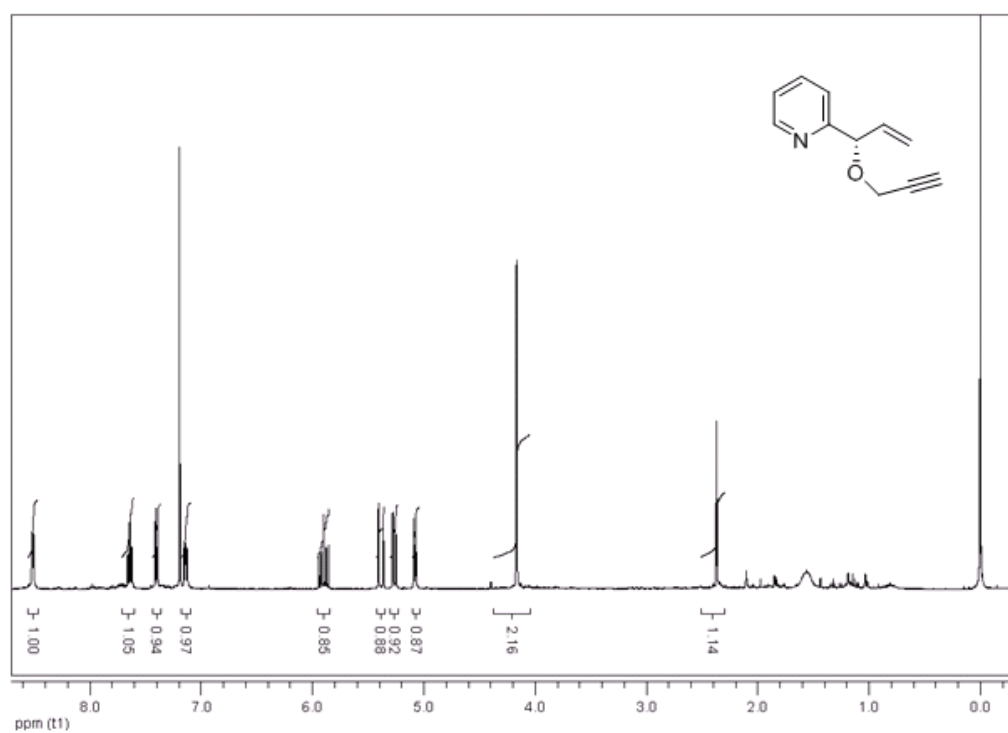


Figure A47. ¹H NMR spectrum of (S)-(-)-121

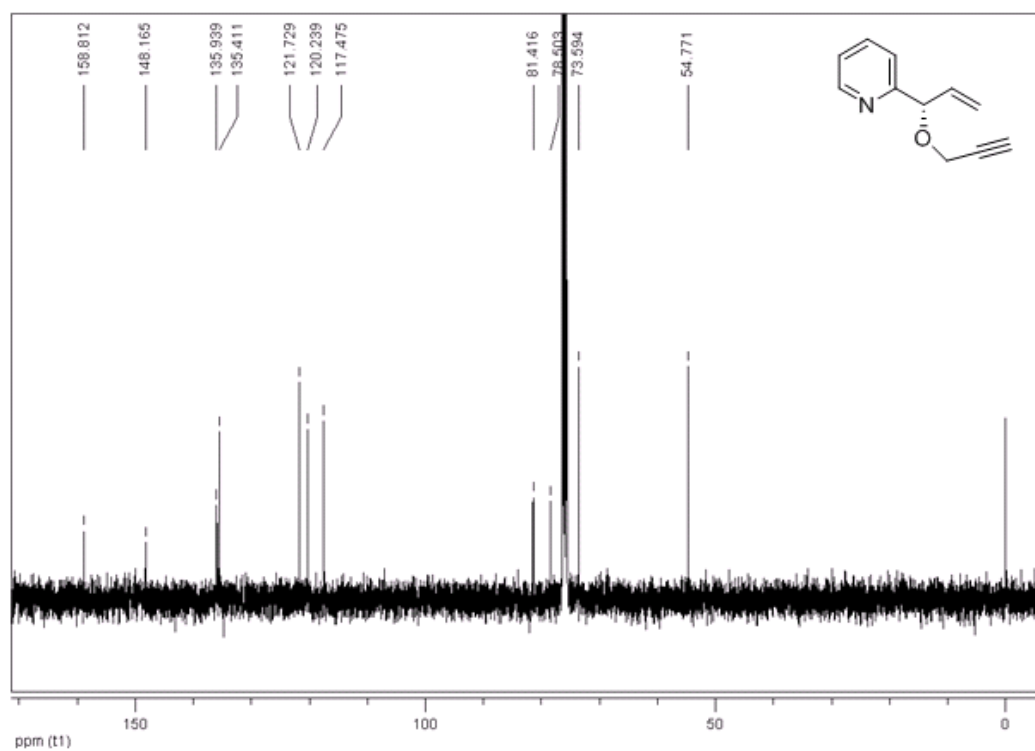


Figure A48. ¹³C NMR spectrum of (S)-(-)-121

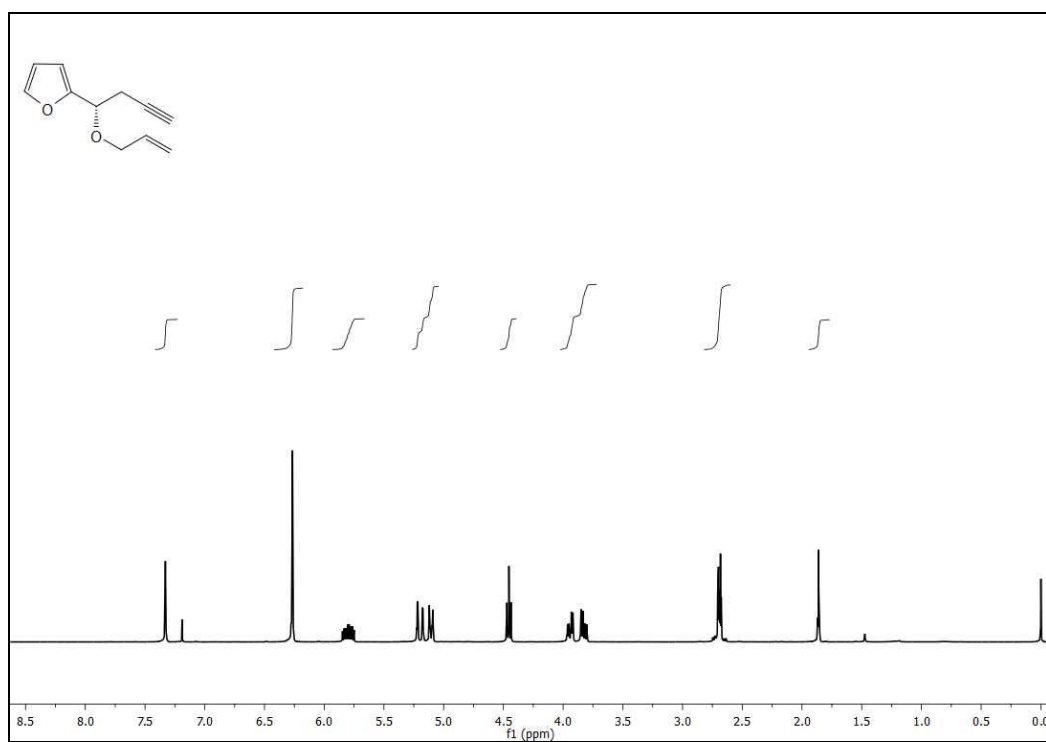


Figure A49. ¹H NMR spectrum of (S)-(-)-122

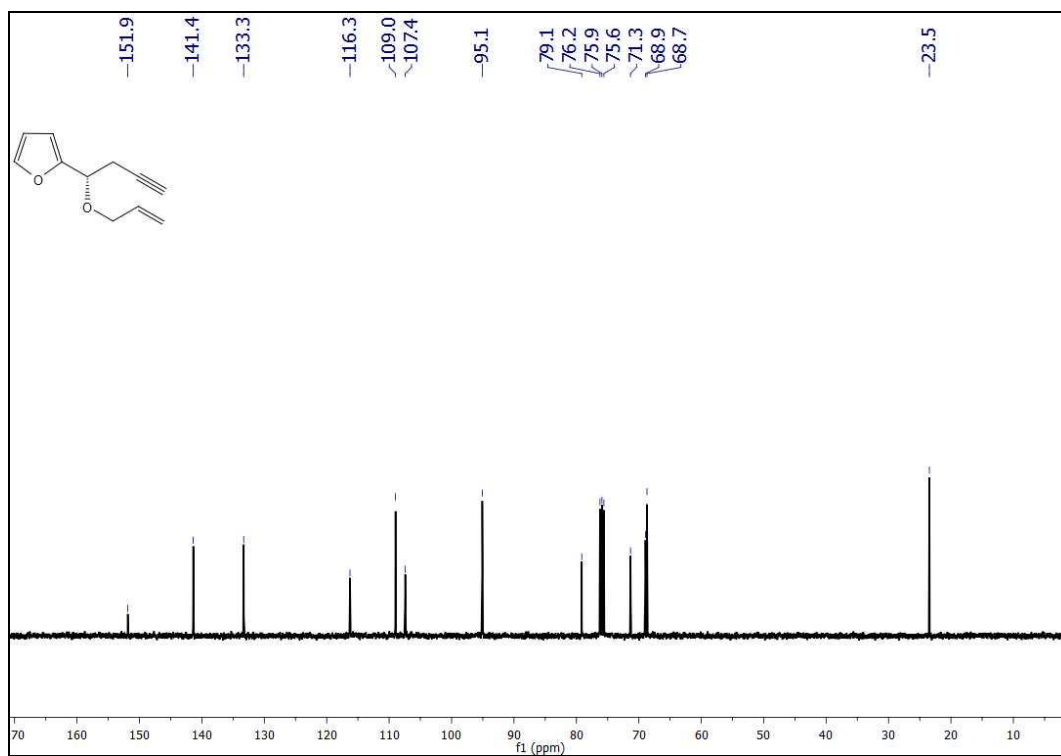


Figure A50. ¹³C NMR spectrum of (S)-(-)-122

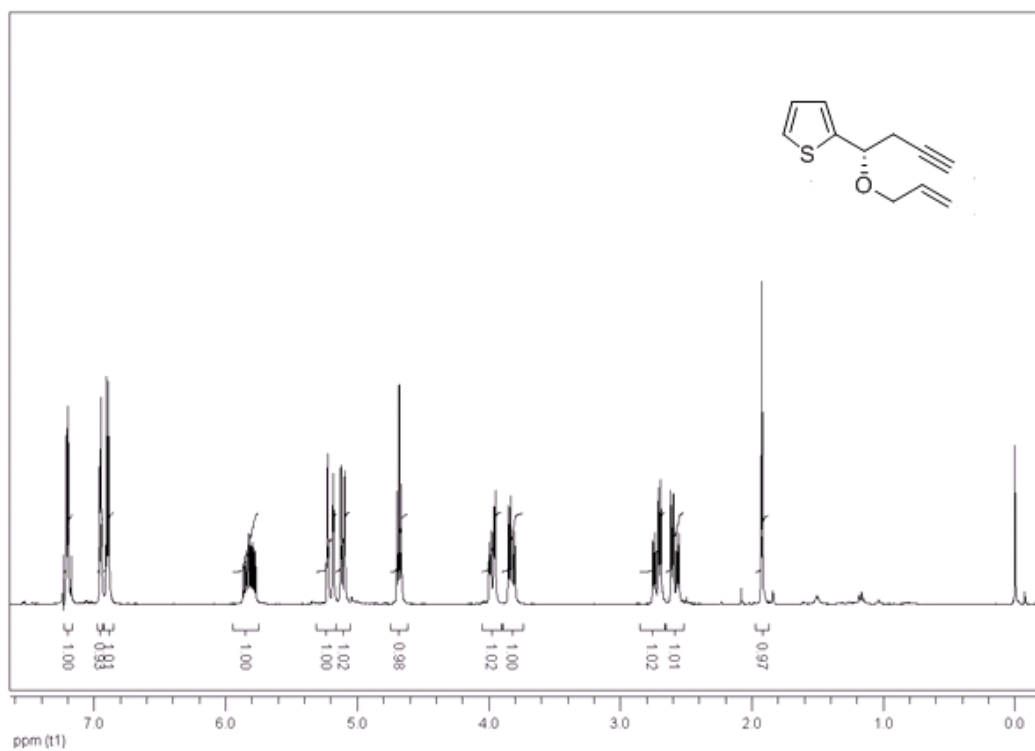


Figure A51. ¹H NMR spectrum of (S)-(-)-123

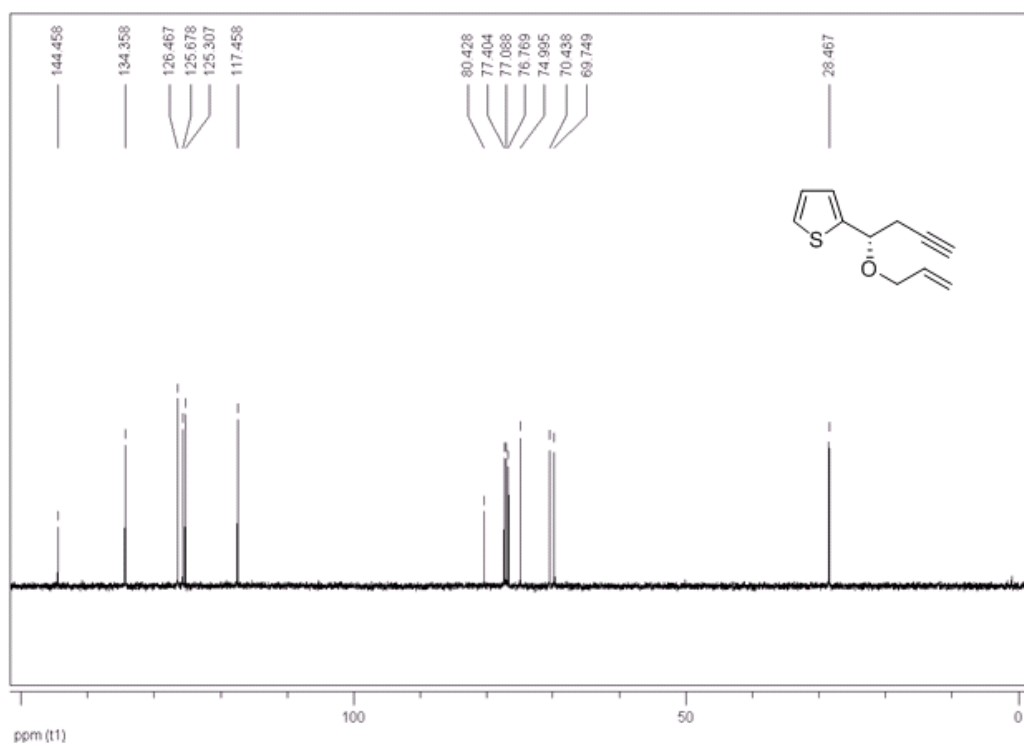


Figure A52. ¹³C NMR spectrum of (S)-(-)-123

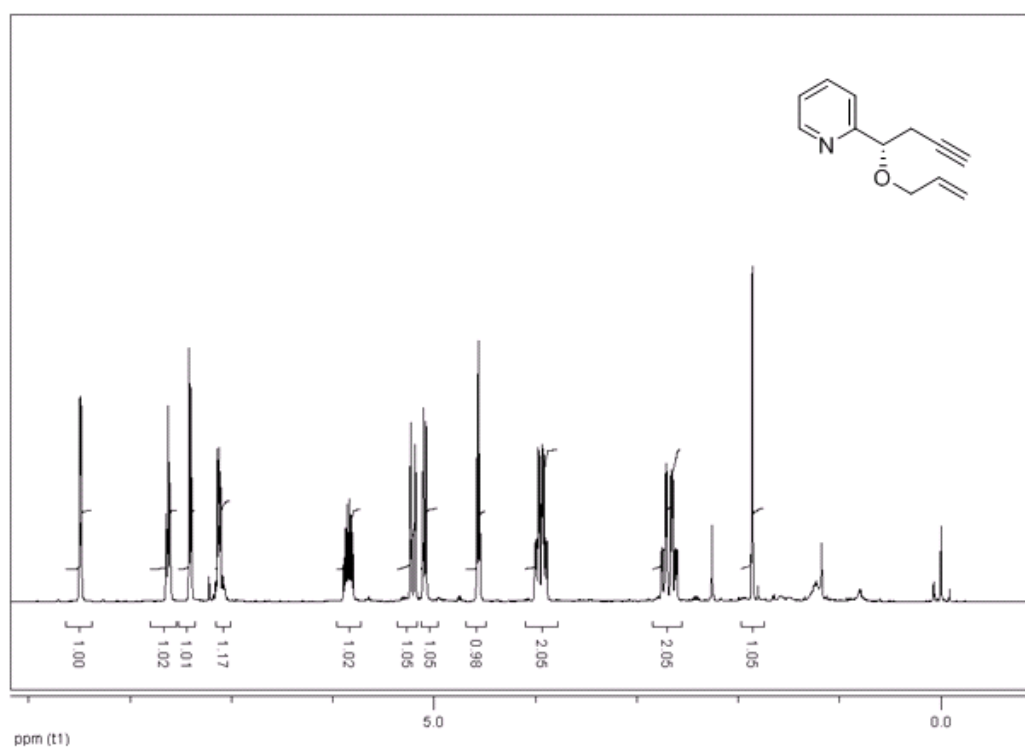


Figure A53. ^1H NMR spectrum of (S)-(-)-124

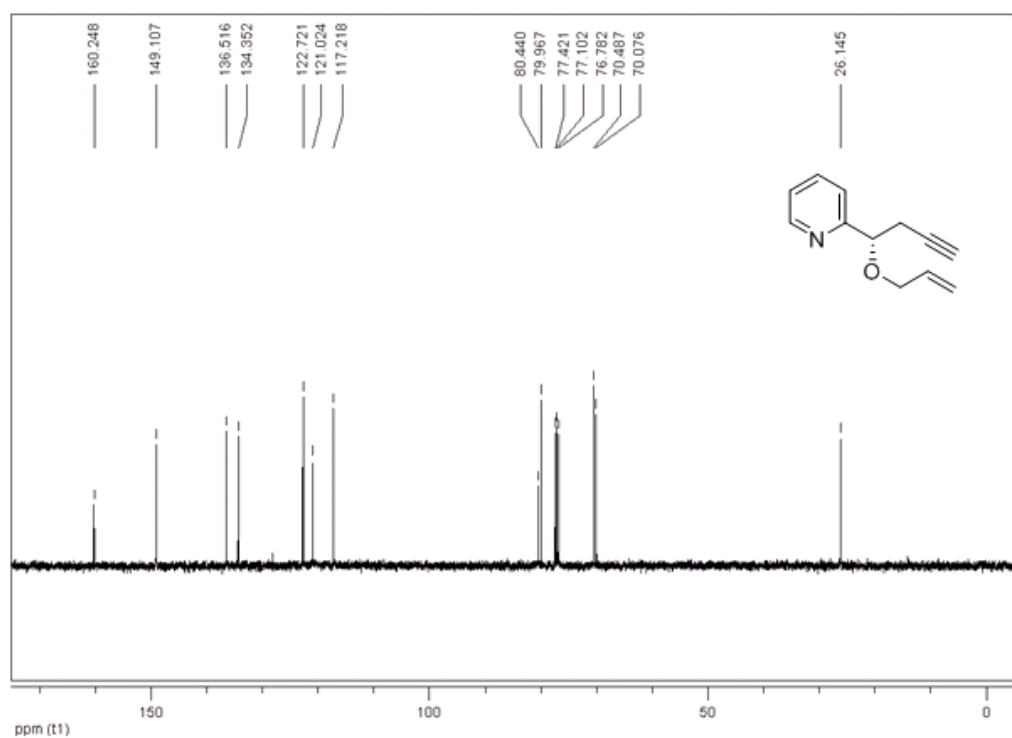


Figure A54. ^{13}C NMR spectrum of (S)-(-)-124

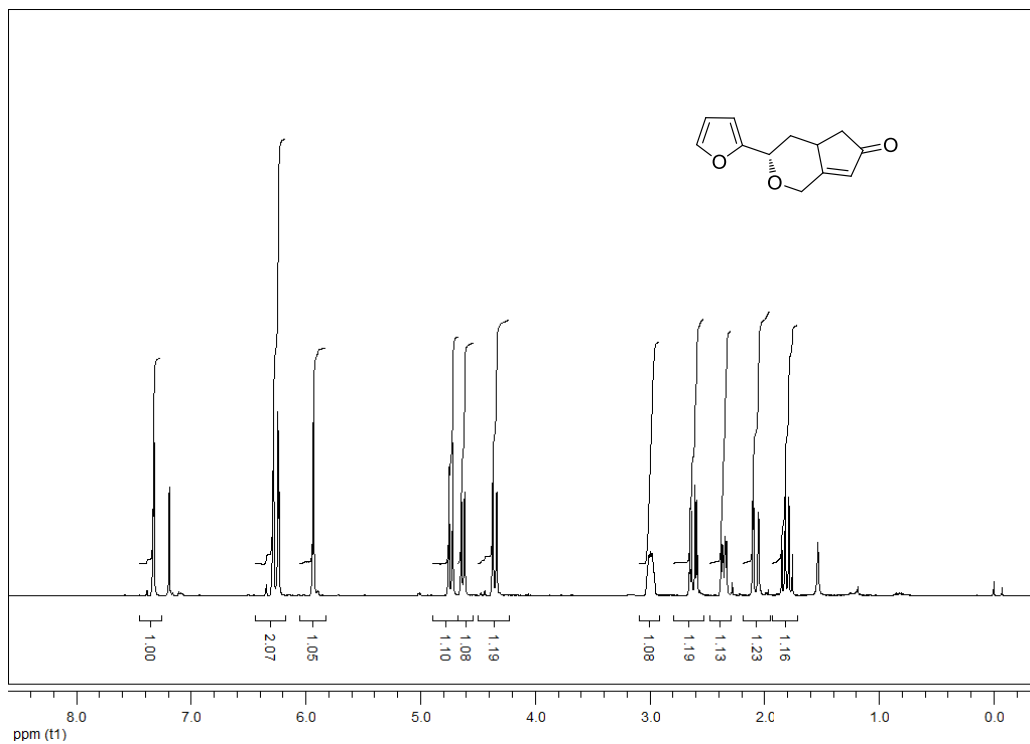


Figure A55. ^1H NMR spectrum of (+)-125

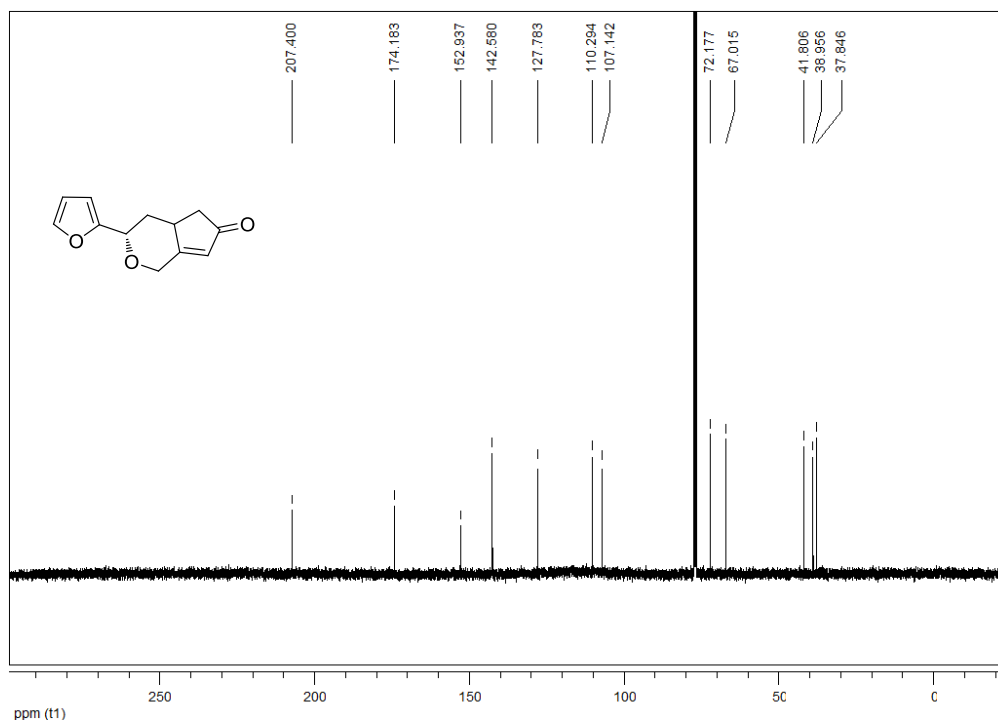


Figure A56. ^{13}C NMR spectrum of (+)-125

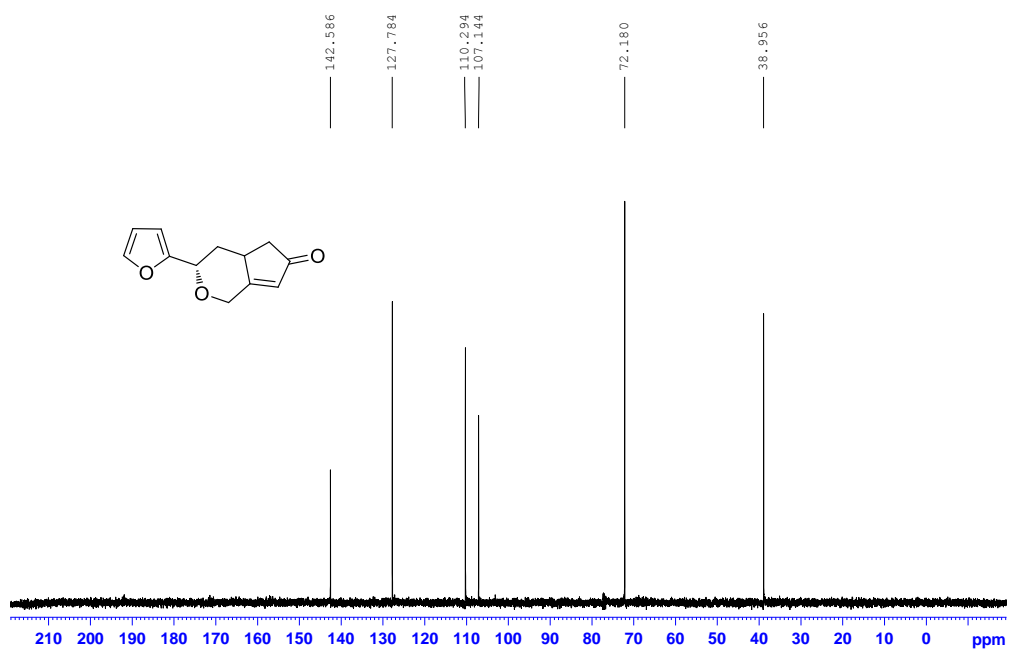


Figure A57. Dept-90 NMR spectrum of (+)-125

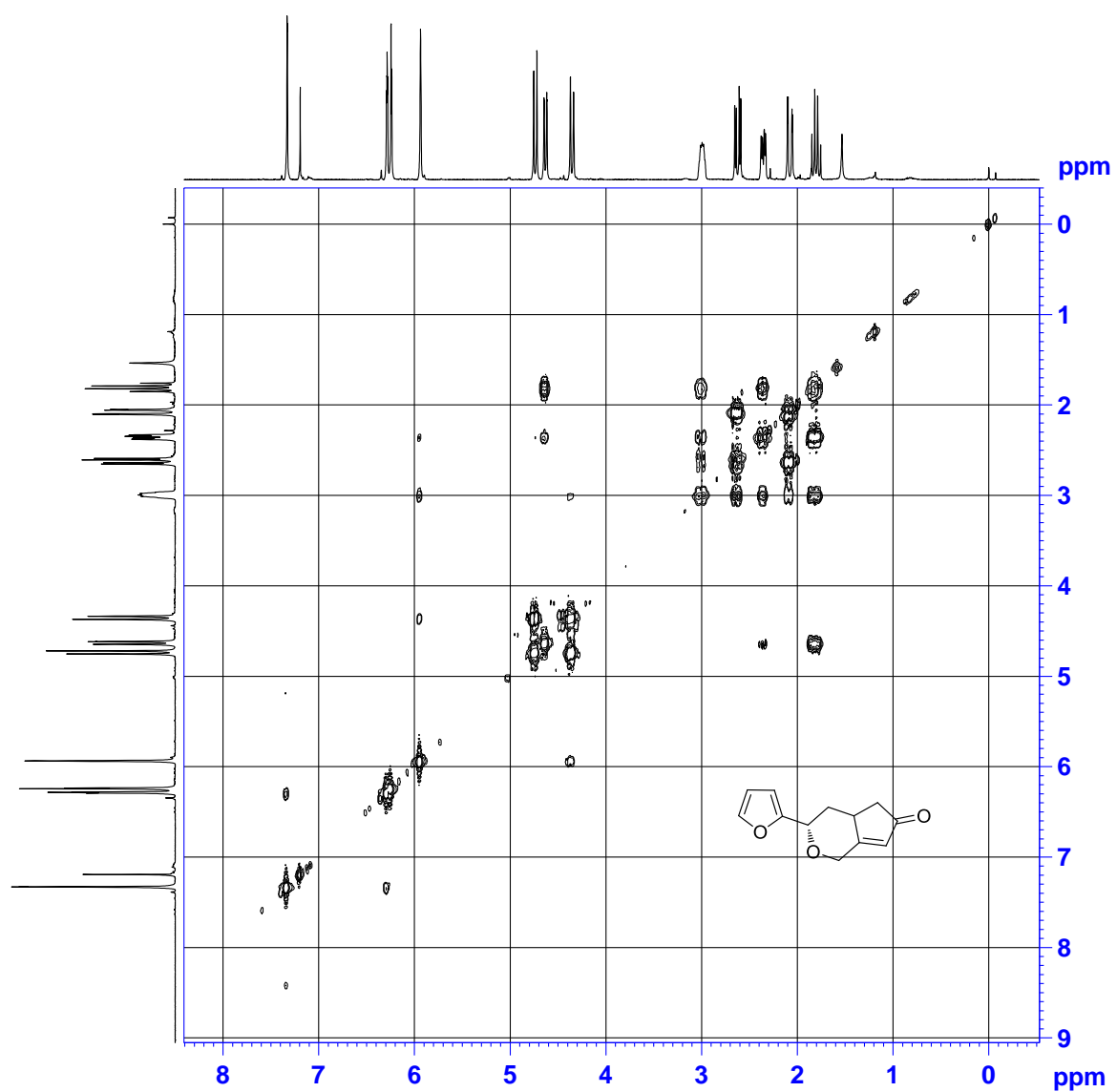


Figure A58. Cosy NMR spectrum of (+)-125

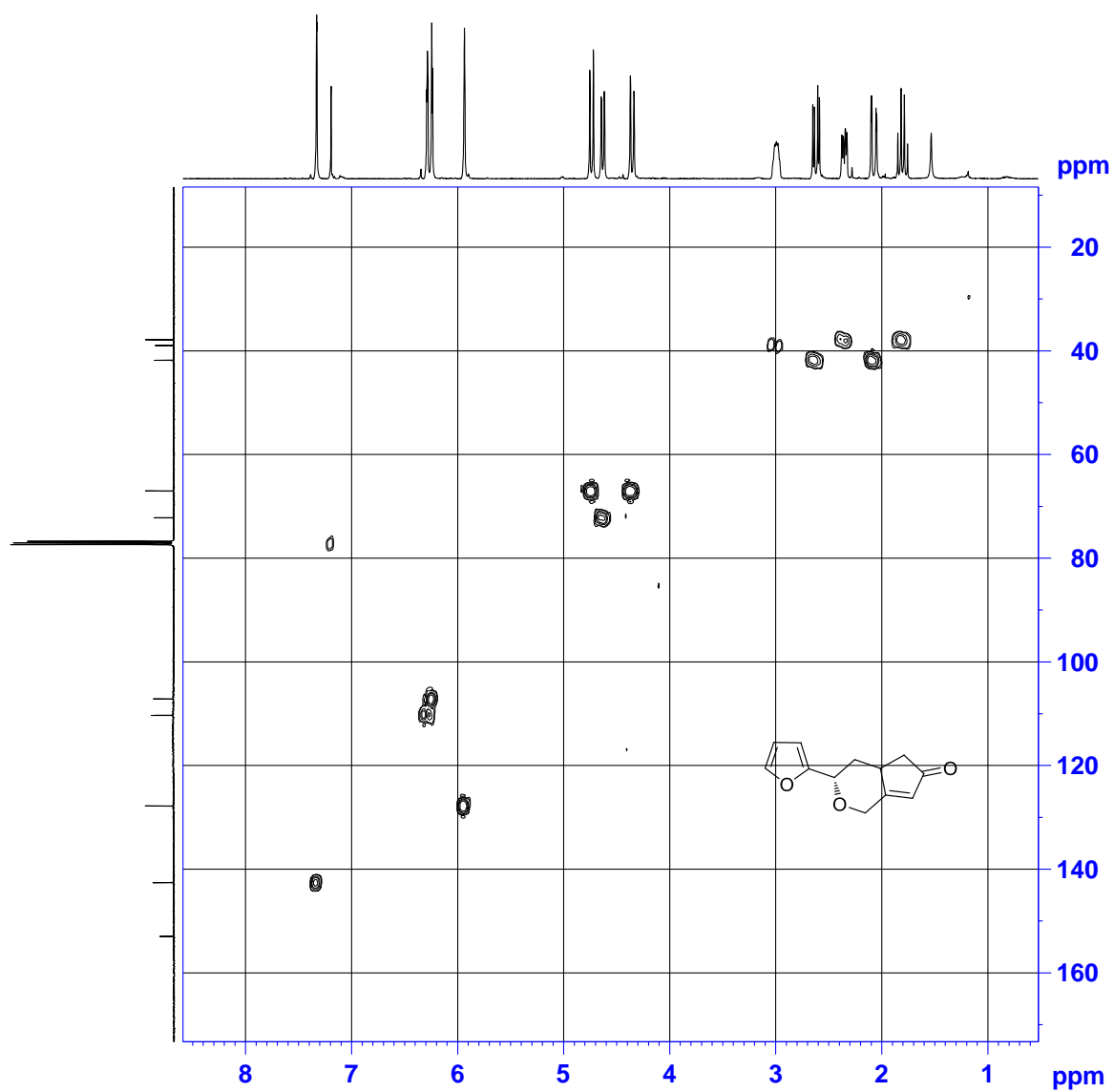


Figure A59. HMQC NMR spectrum of (+)-125

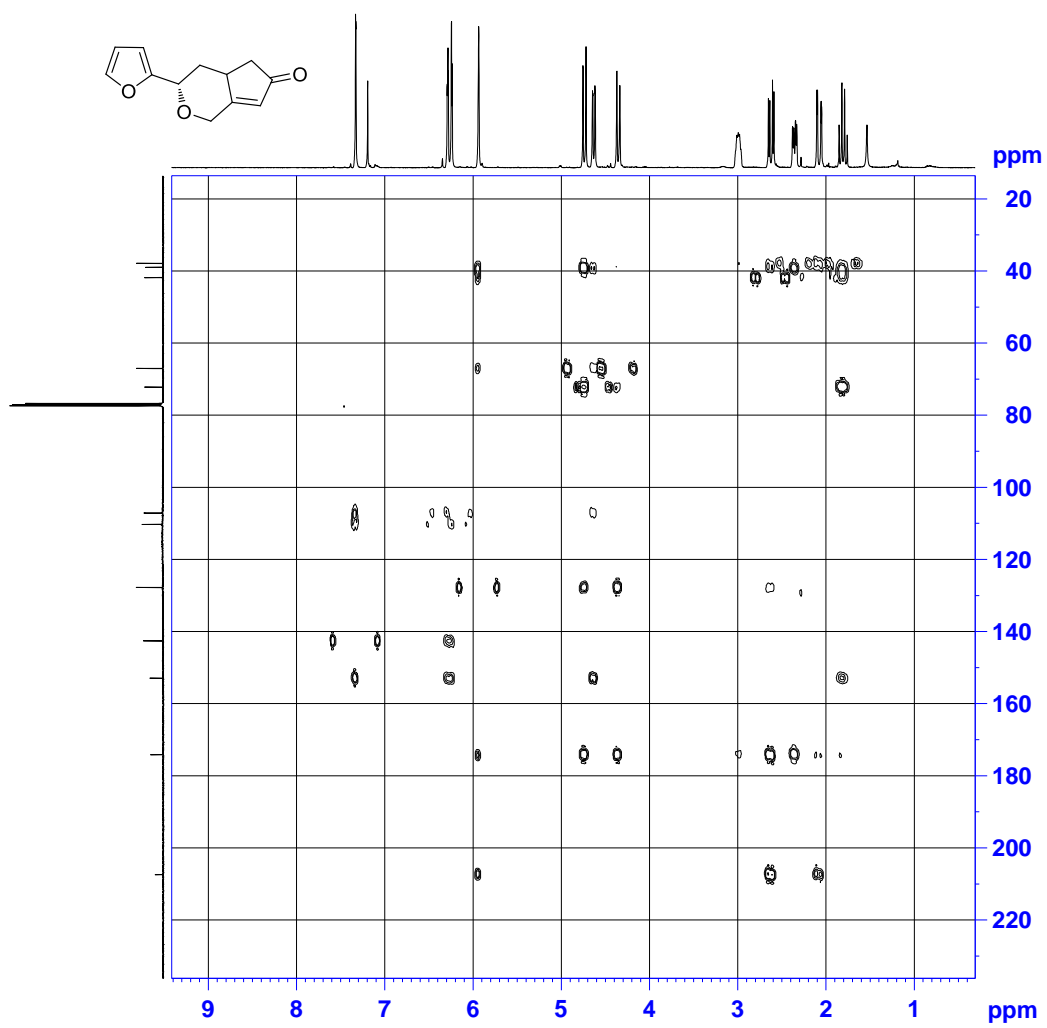


Figure A60. HMBC NMR spectrum of (+)-125

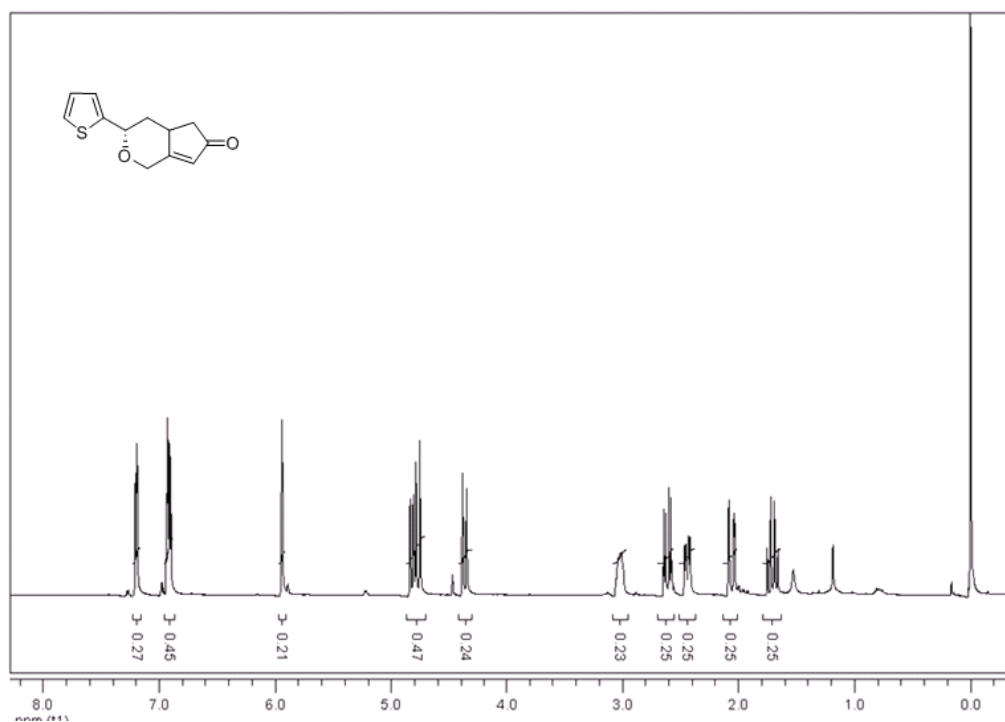


Figure A61. ^1H NMR spectrum of (+)-126

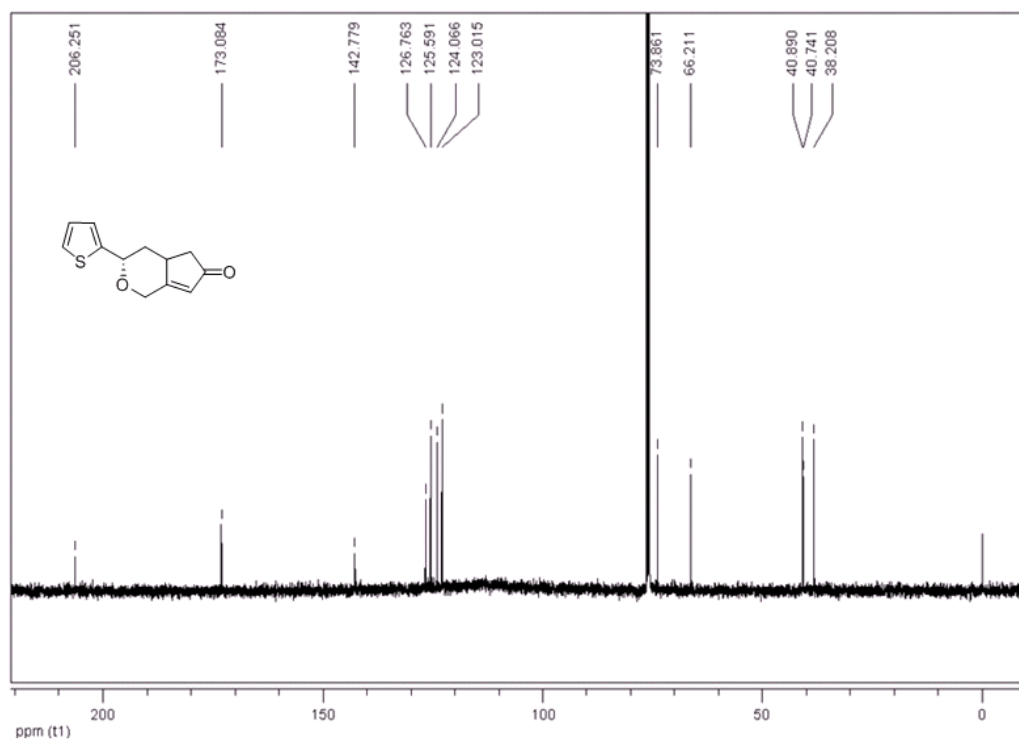


Figure A62. ^{13}C NMR spectrum of (+)-126

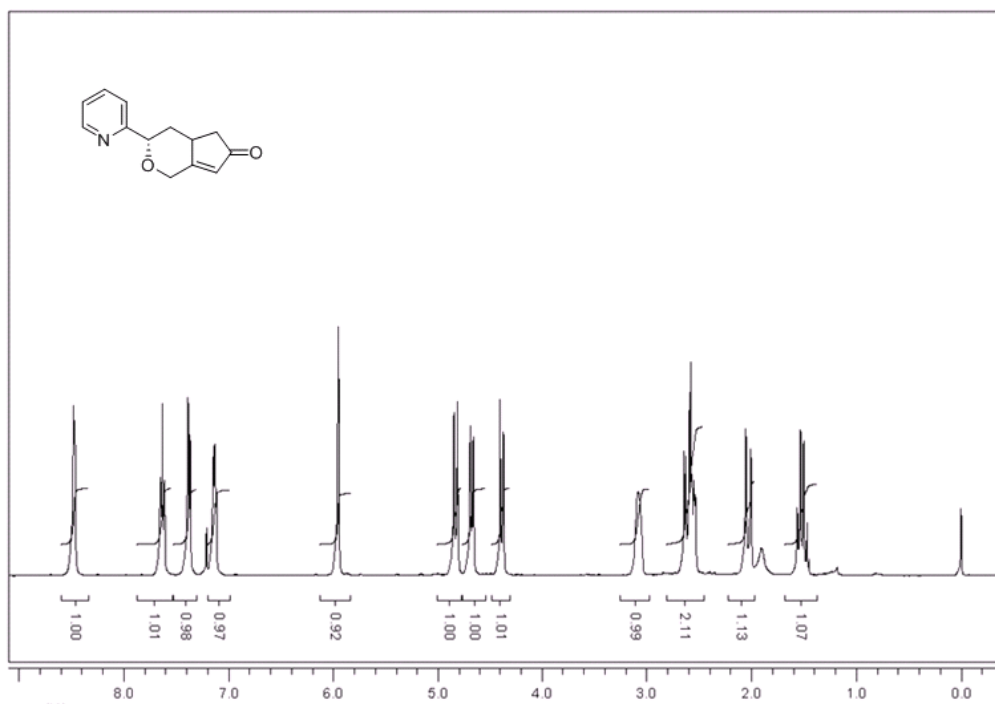


Figure A63. ¹H NMR spectrum of (+)-127

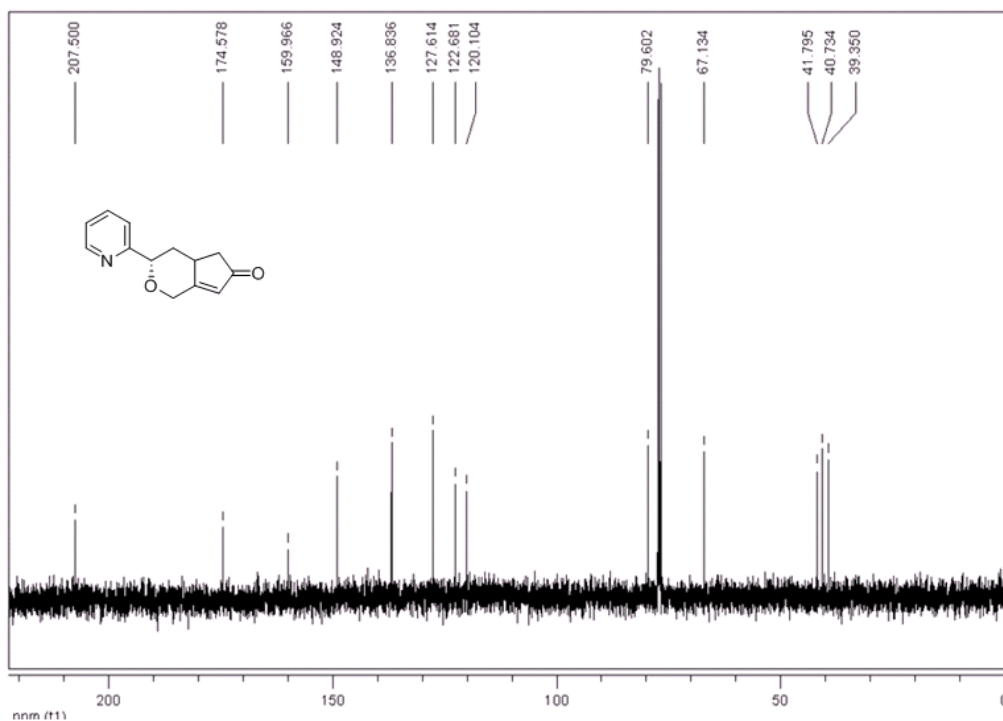


Figure A64. ¹³C NMR spectrum of (+)-127

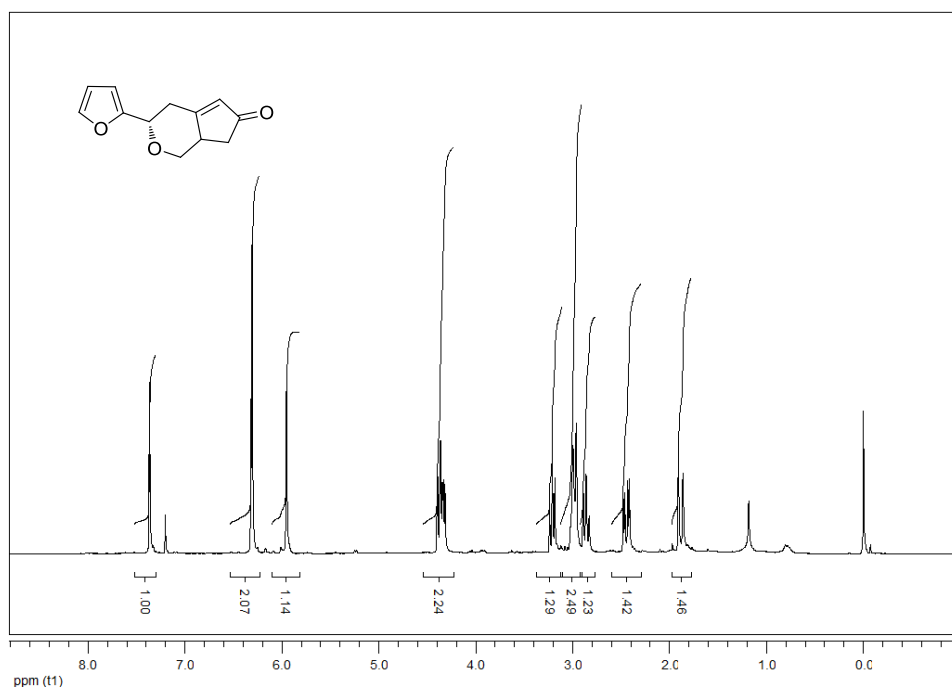


Figure A65. ^1H NMR spectrum of (+)-128

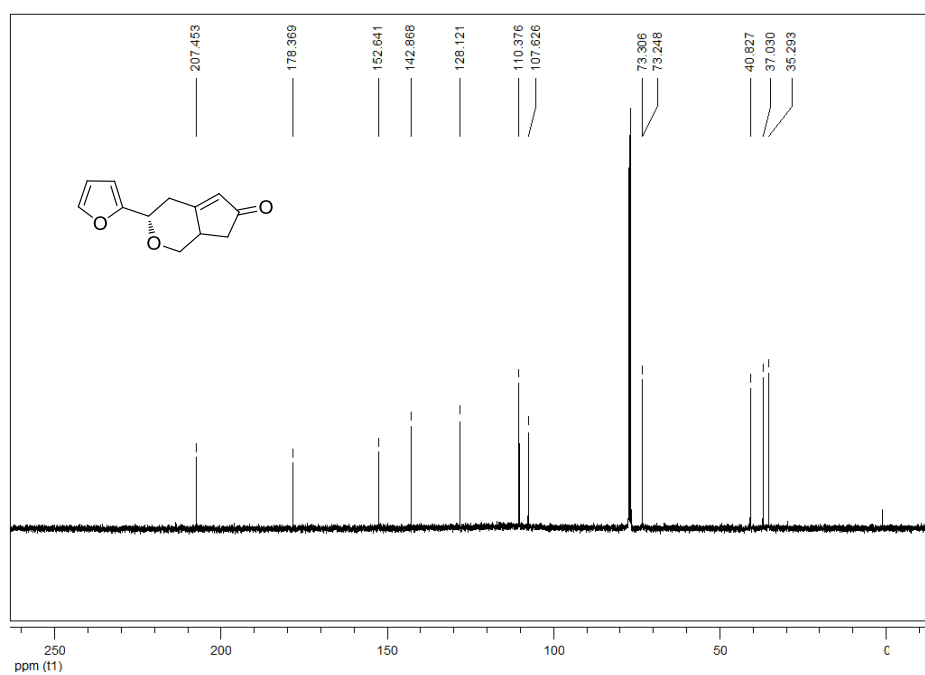


Figure A66. ^{13}C NMR spectrum of (+)-128

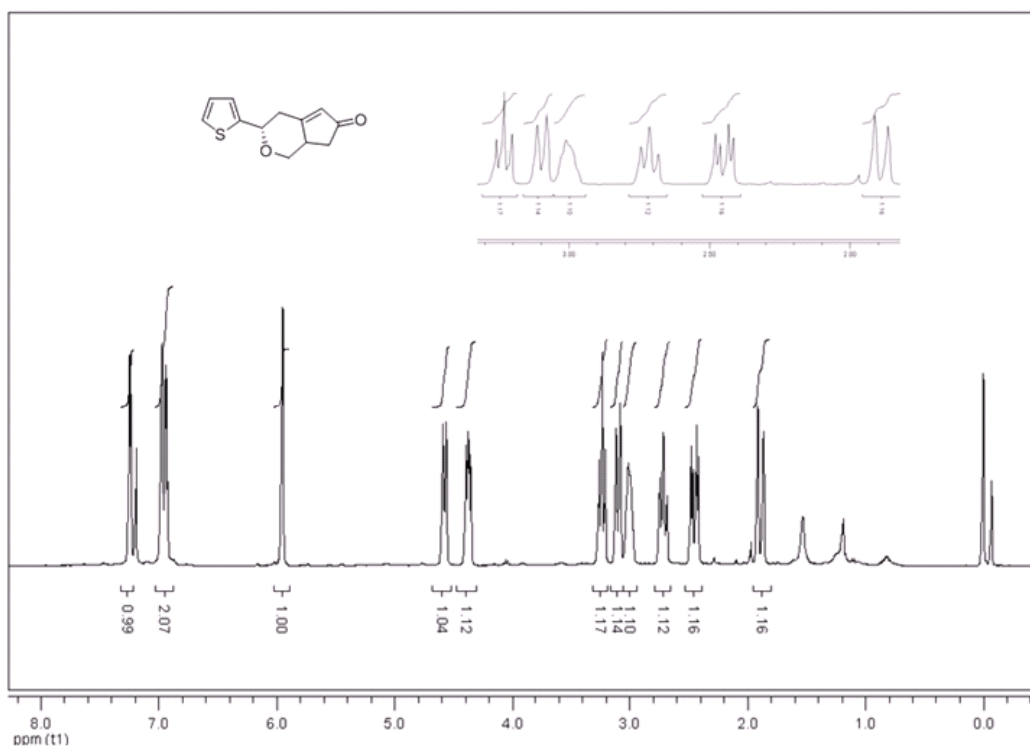


Figure A67. ¹H NMR spectrum of (+)-129

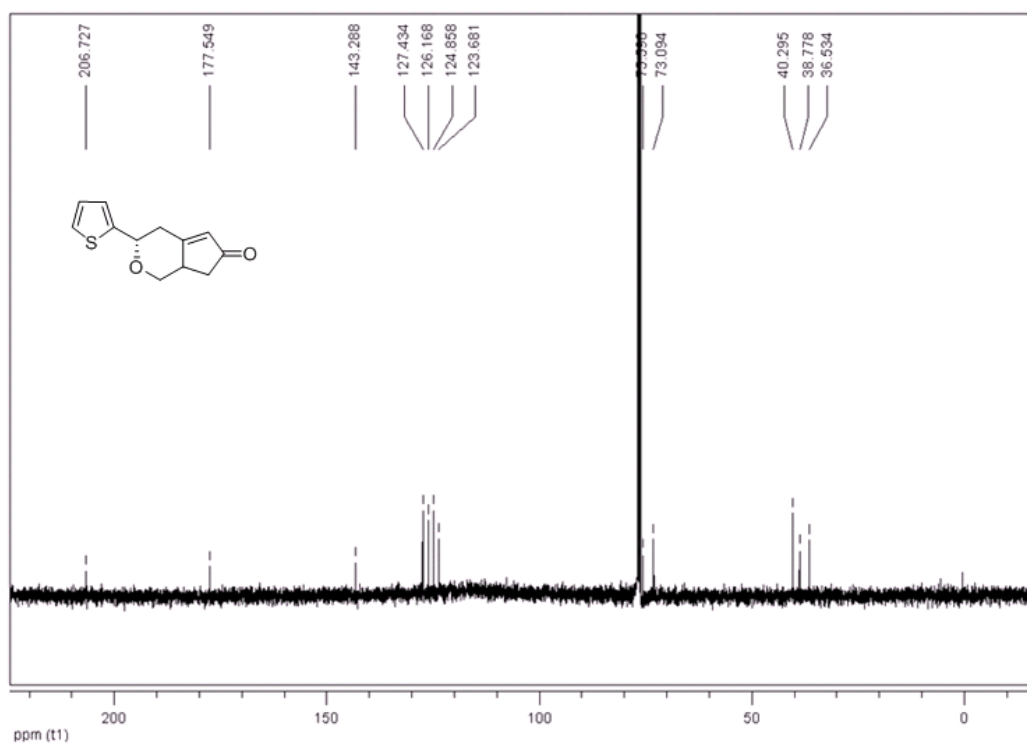


Figure A68. ¹³C NMR spectrum of (+)-129

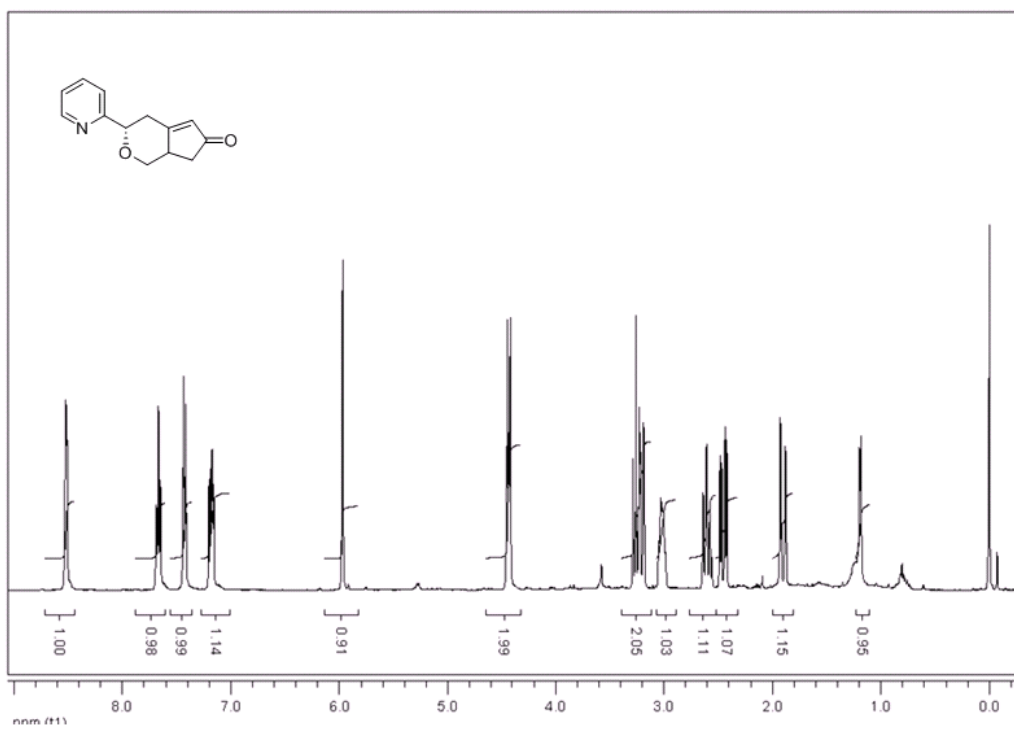


Figure A69. ¹H NMR spectrum of (+)-130

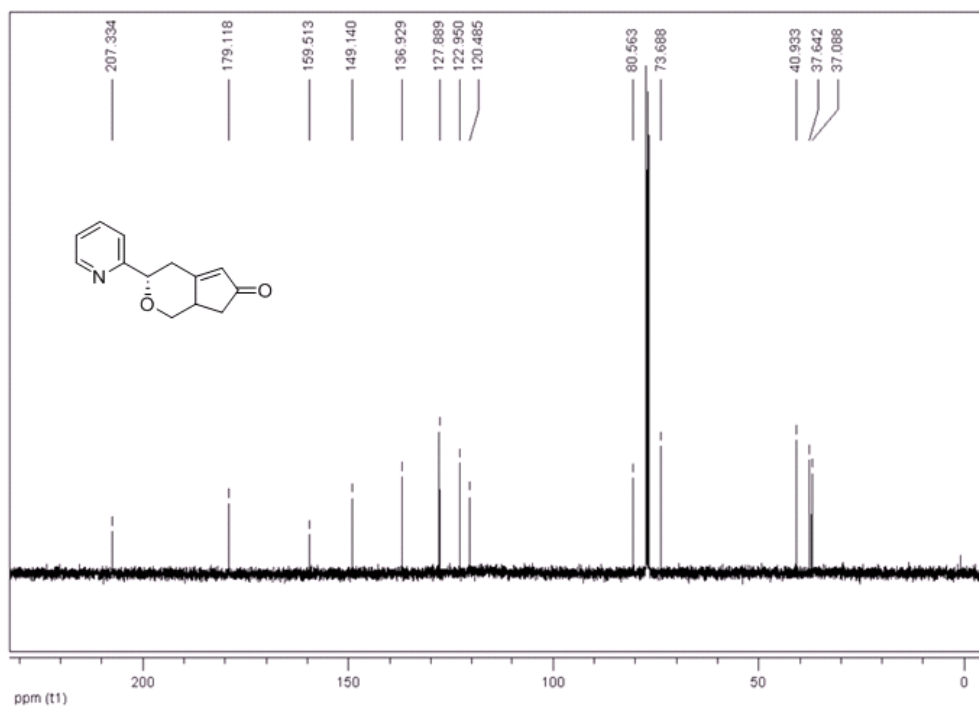


Figure A70. ¹³C NMR spectrum of (+)-130

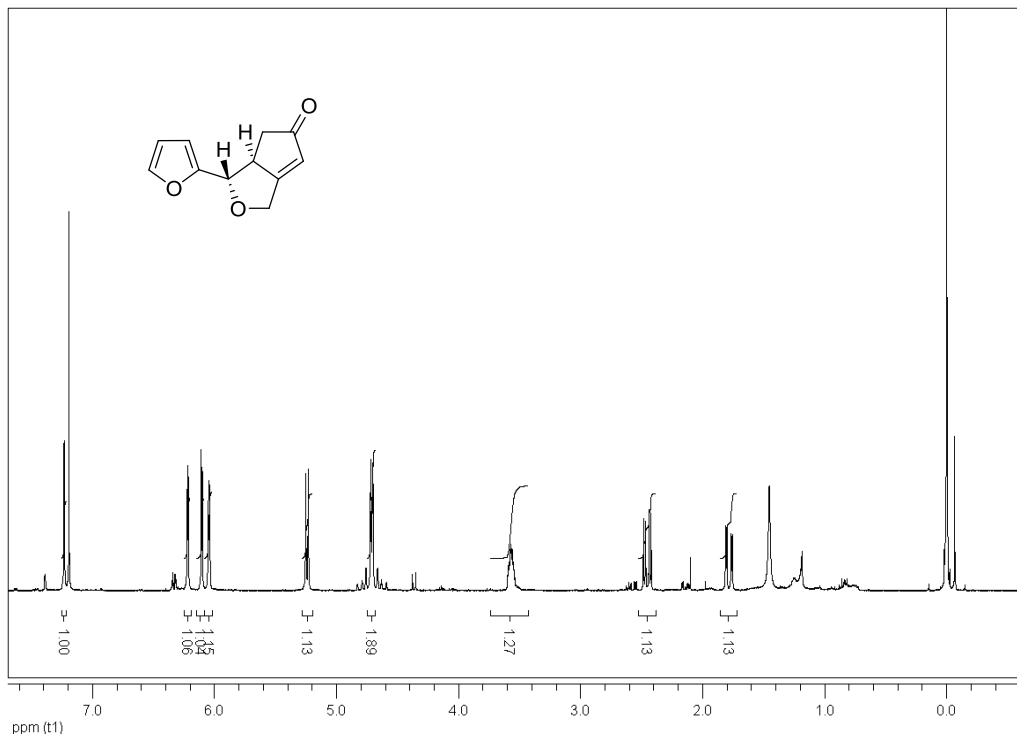


Figure A73. ¹H NMR spectrum of (+)-131

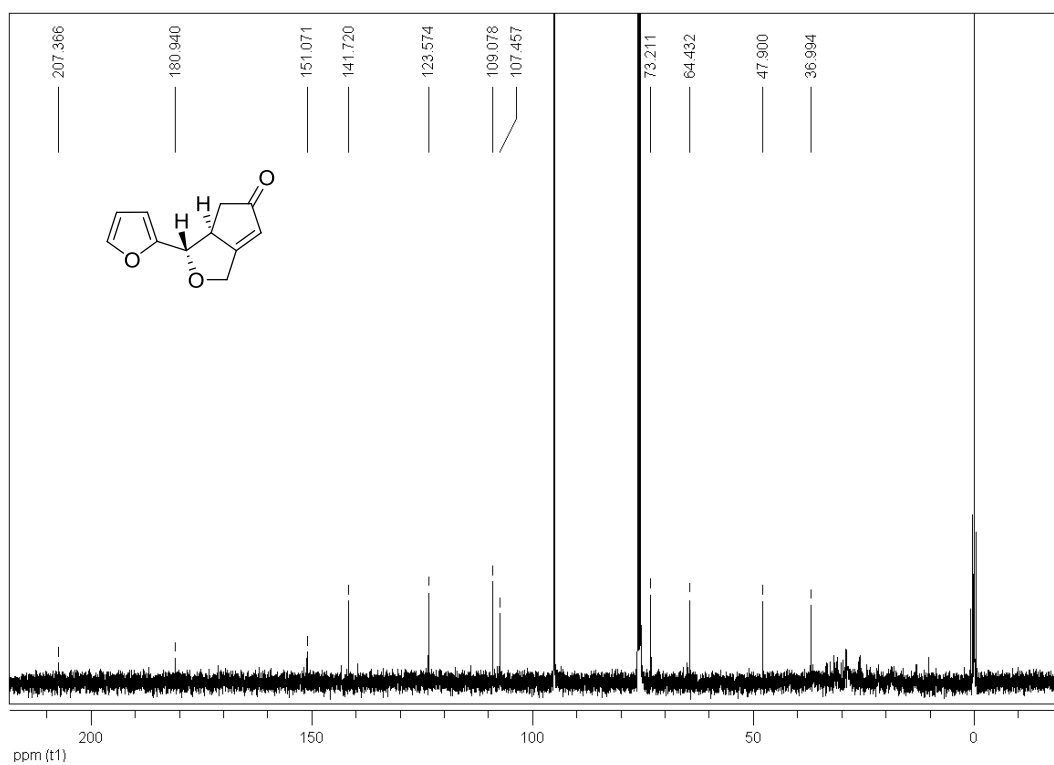


Figure A74. ¹³C NMR spectrum of (+)-131

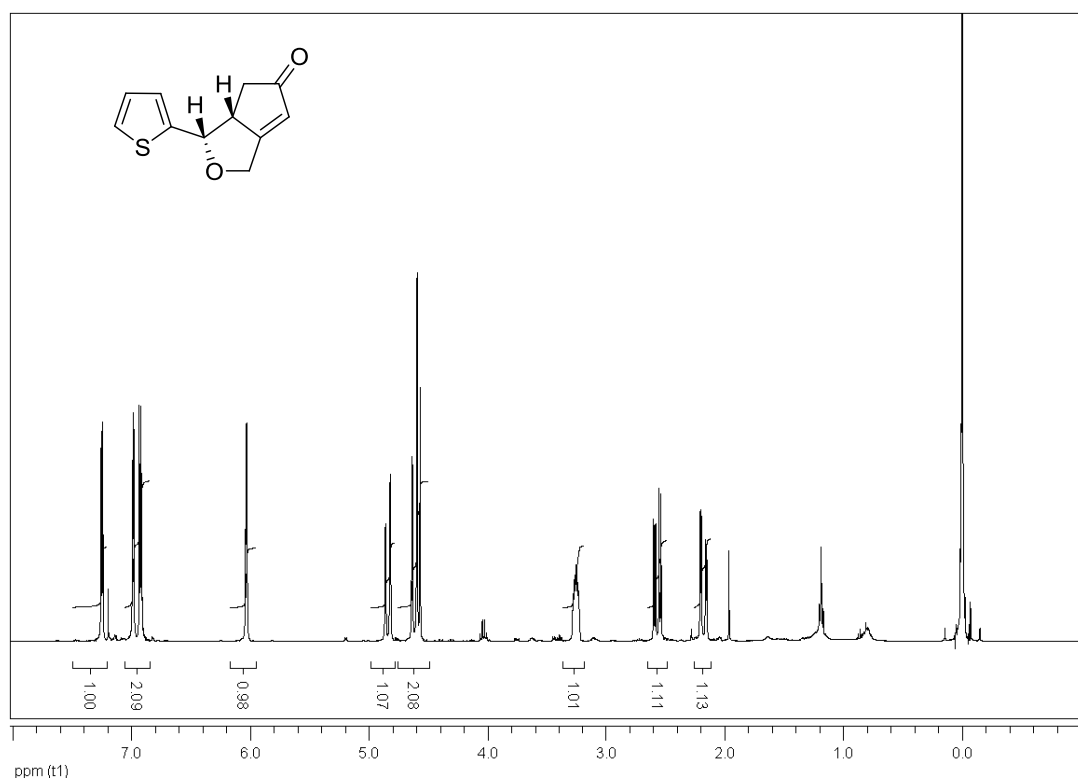


Figure A75. ¹H NMR spectrum of (-)-132

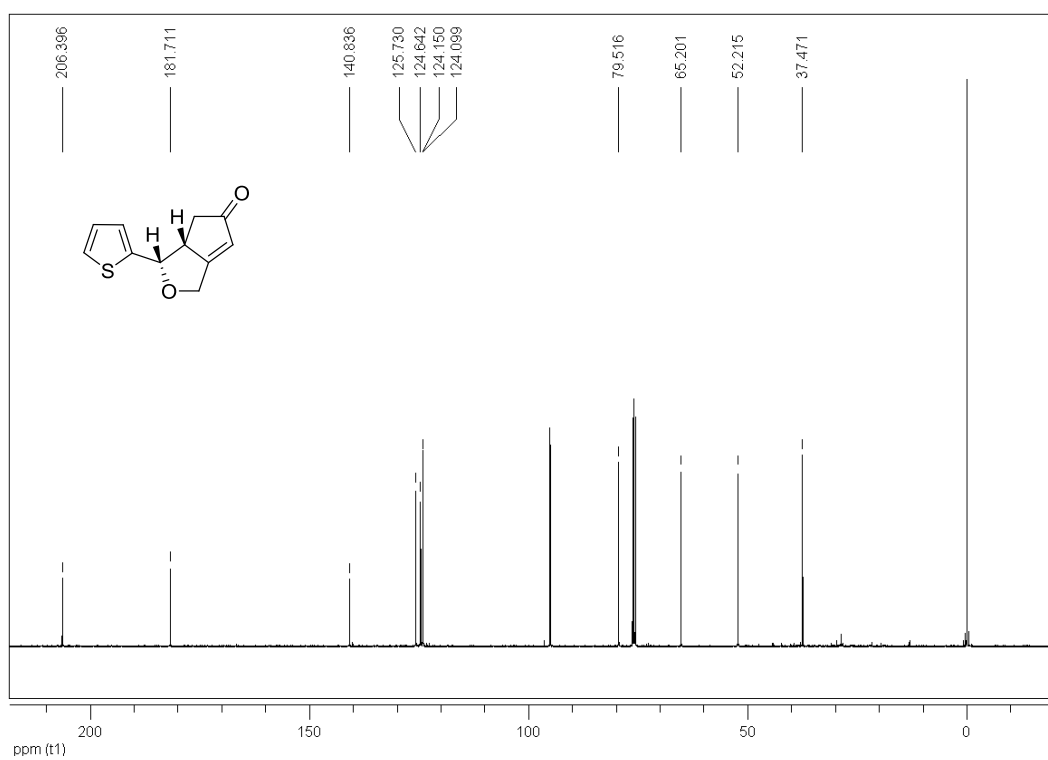


Figure A76. ¹³C NMR spectrum of (-)-132

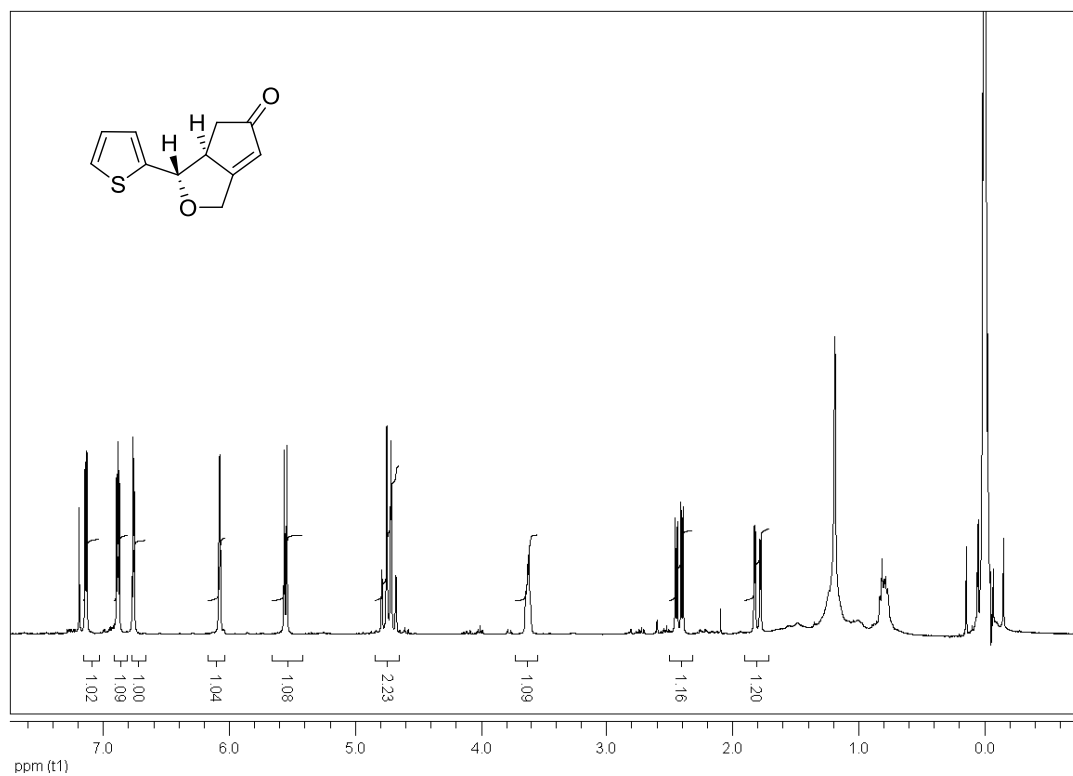


Figure A77. ¹H NMR spectrum of (+)-132

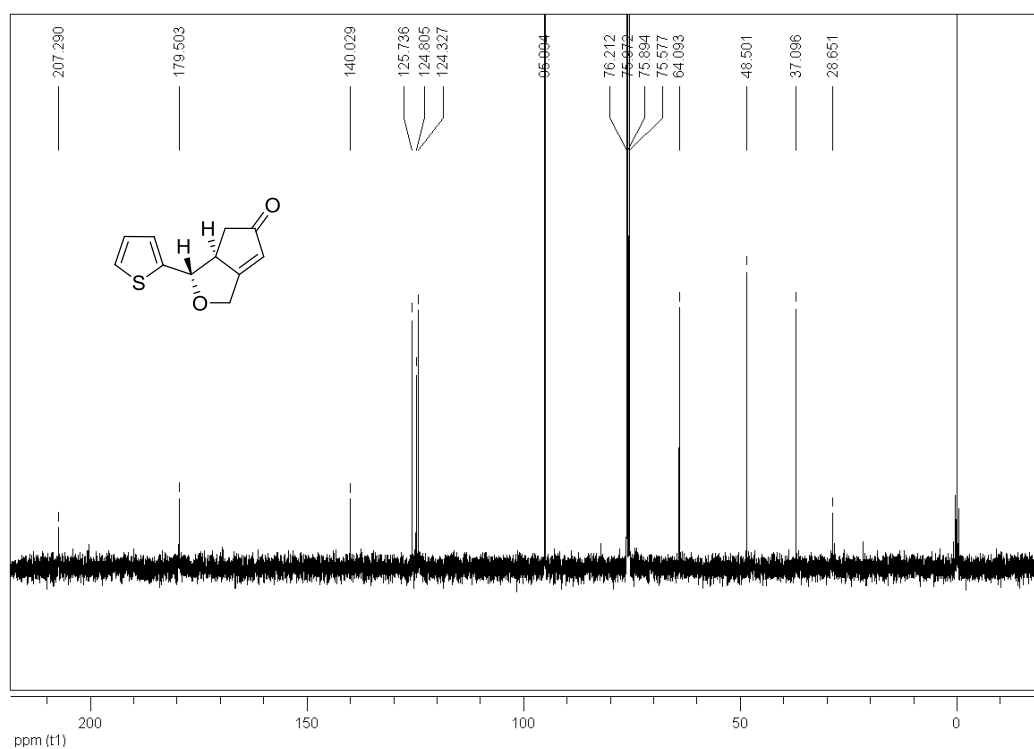


Figure A78. ¹³C NMR spectrum of (+)-132

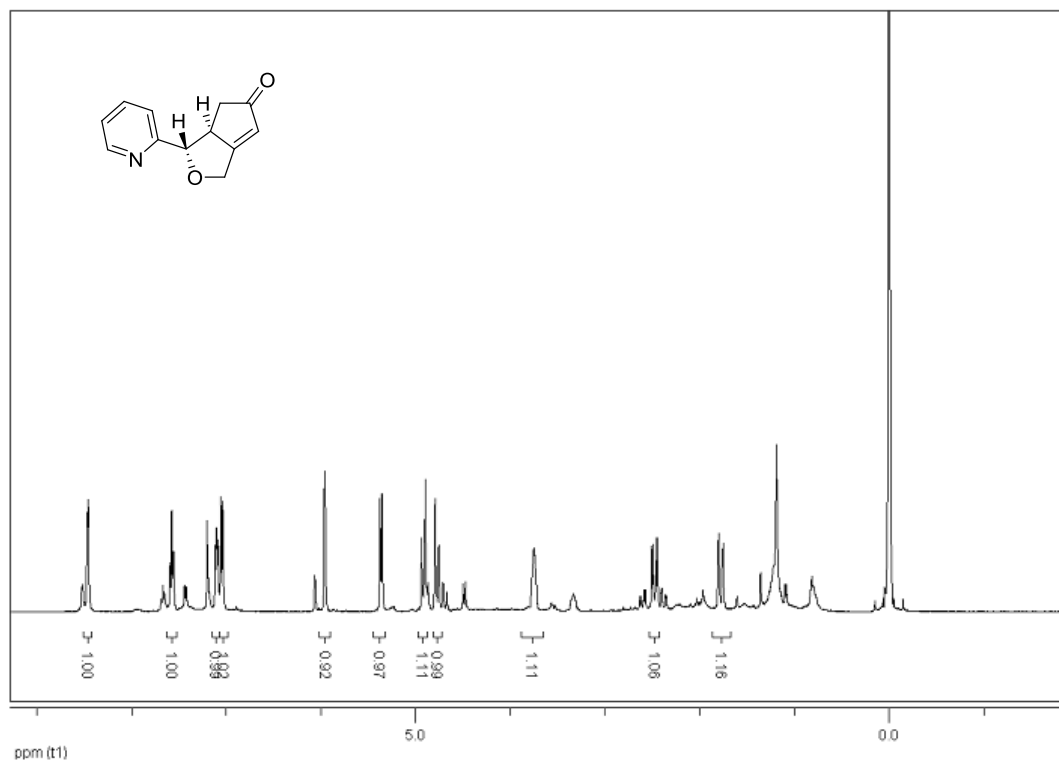


Figure A79. ¹H NMR spectrum of (+)-133

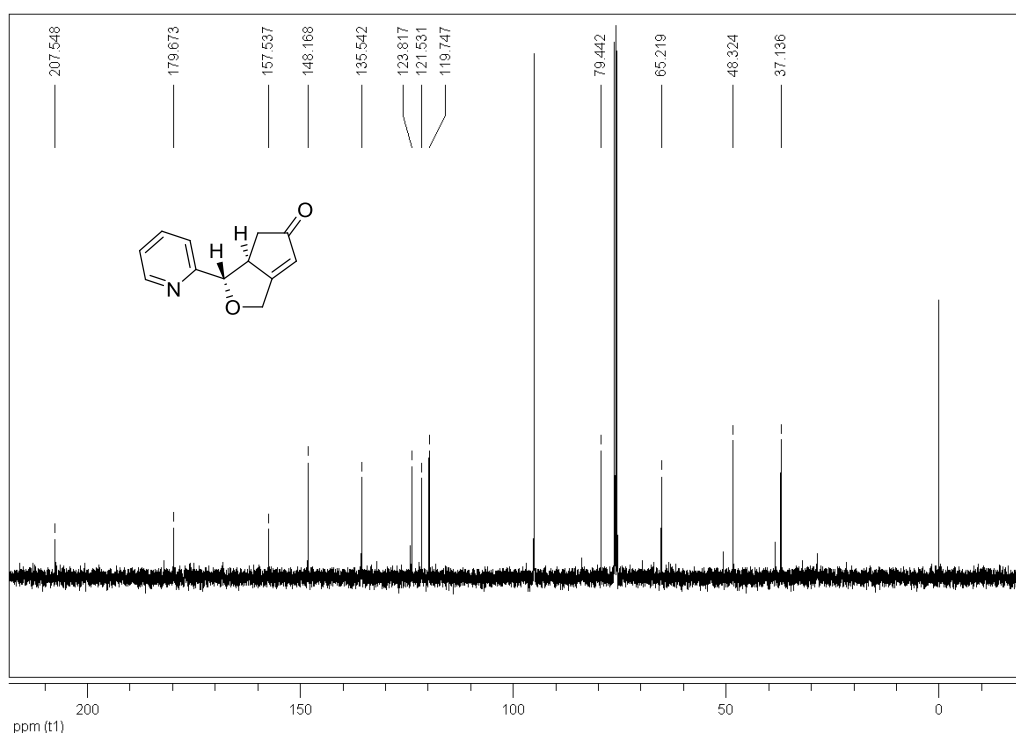


Figure A80. ¹³C NMR spectrum of (+)-133

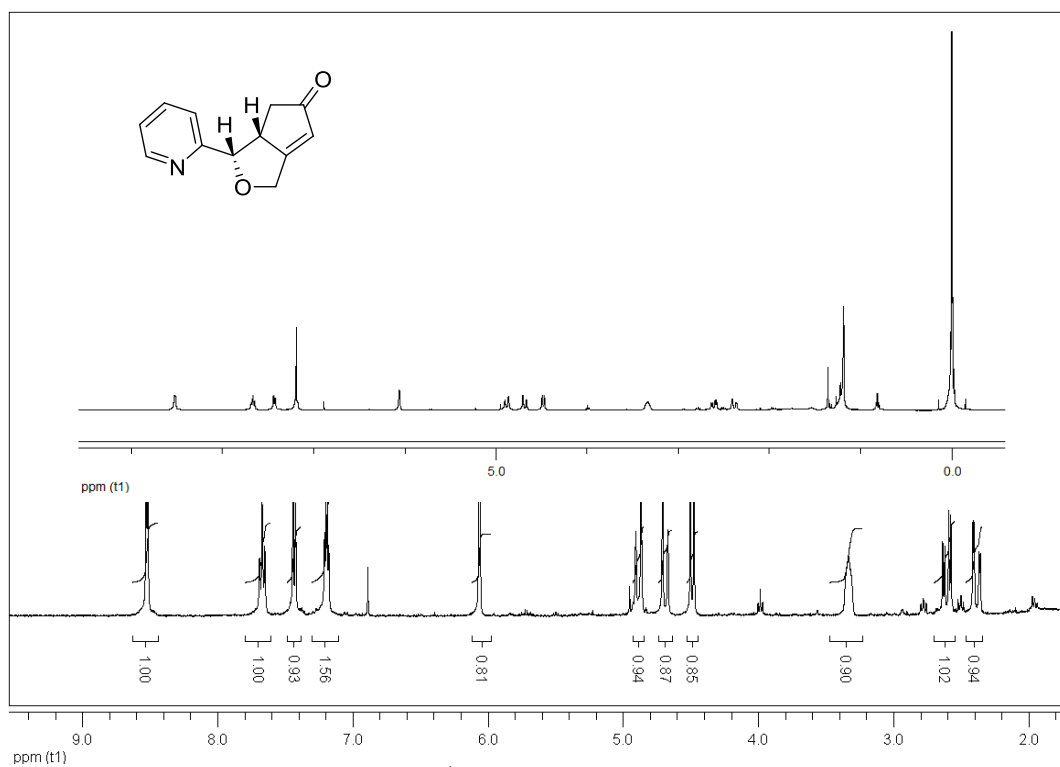


Figure A81. ¹H NMR spectrum of (-)-133

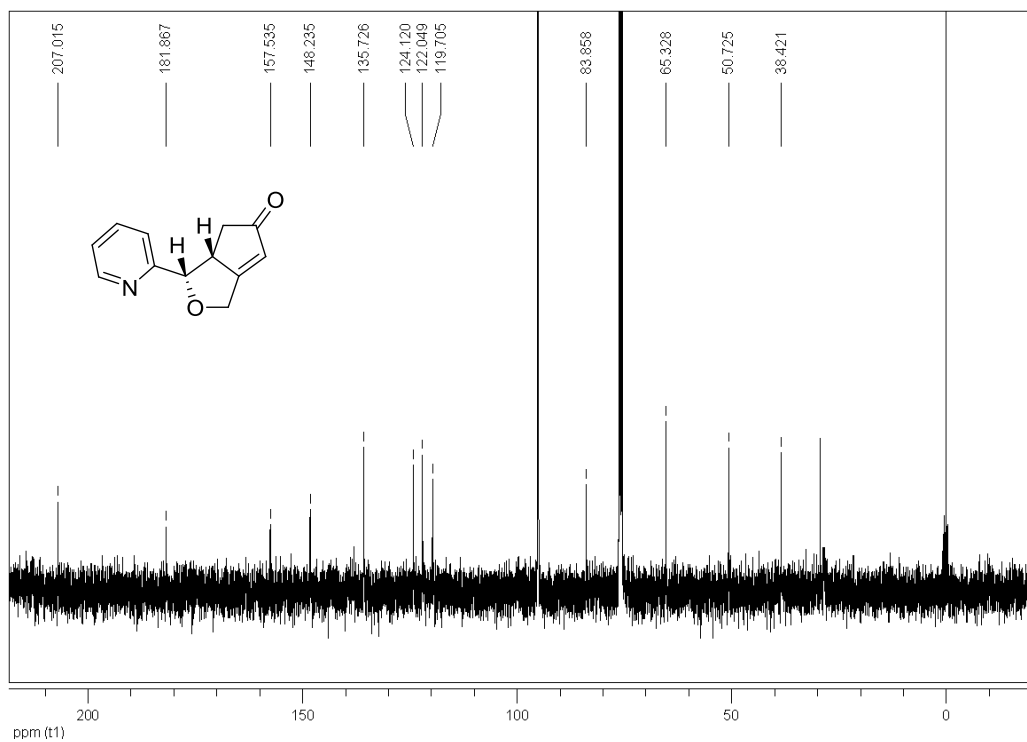


Figure A82. ¹³C NMR spectrum of (-)-133

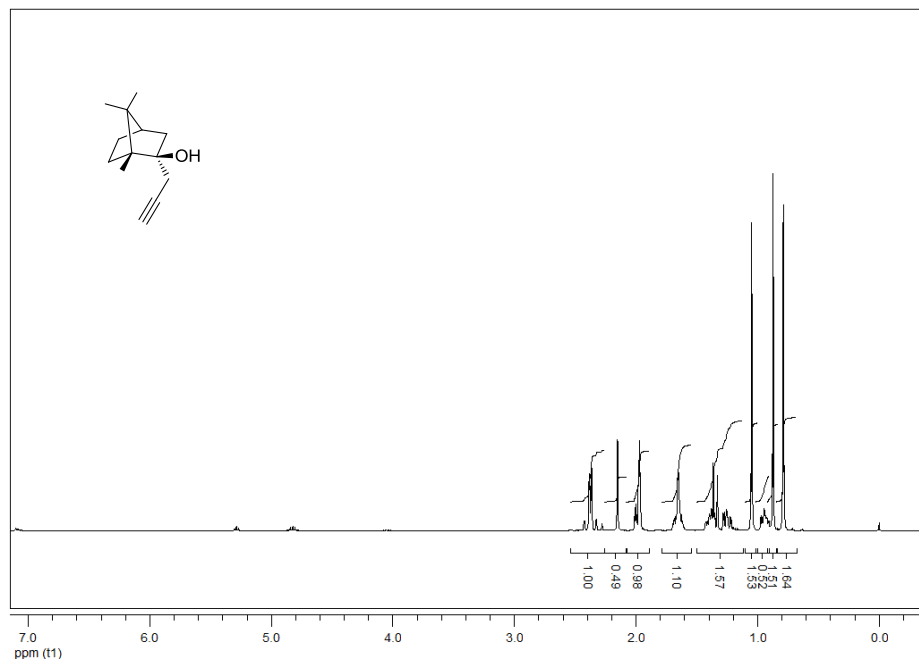


Figure A83. ¹H NMR spectrum of (-)-136

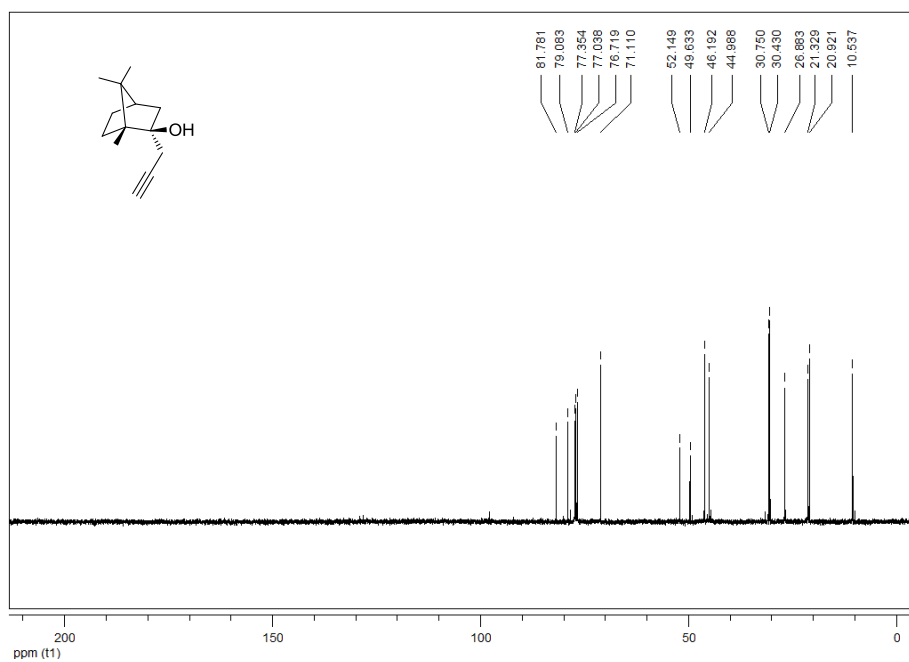


Figure A84. ¹³C NMR spectrum of (-)-136

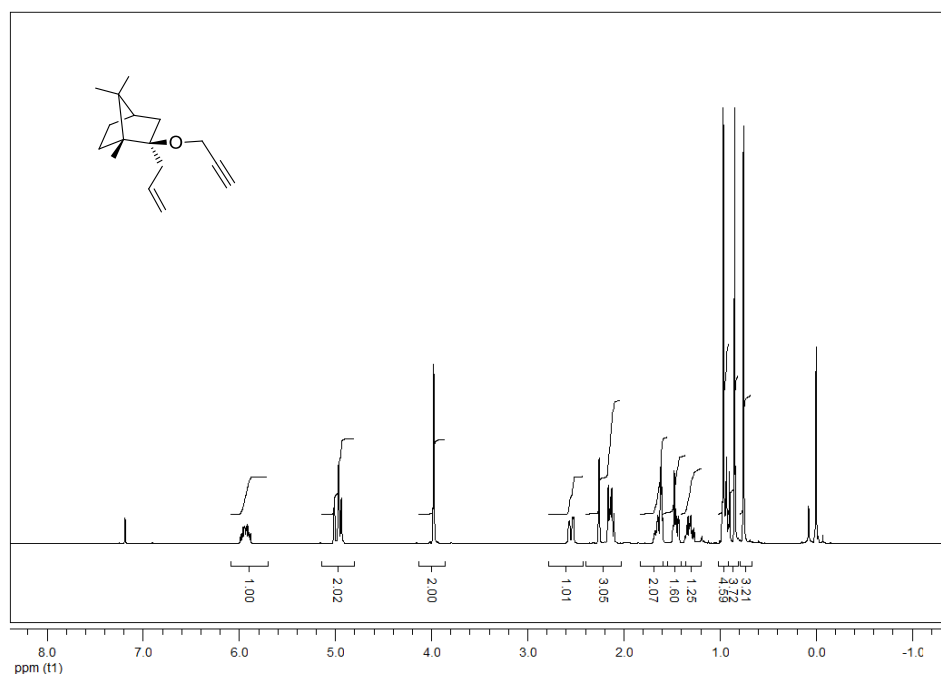


Figure A85. ¹H NMR spectrum of (+)-137

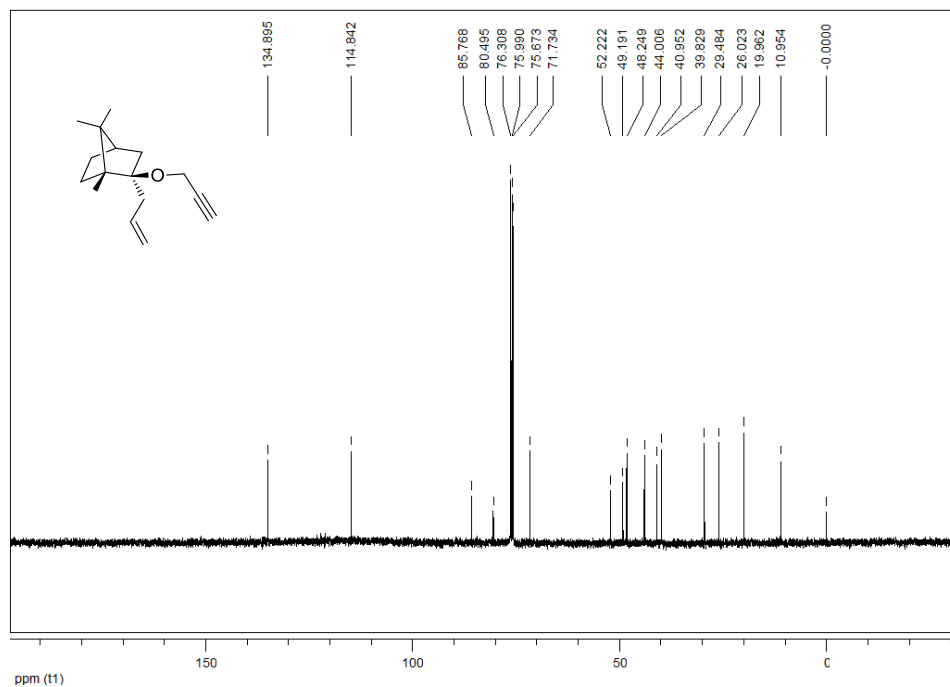


Figure A86. ¹³C NMR spectrum of (+)-137

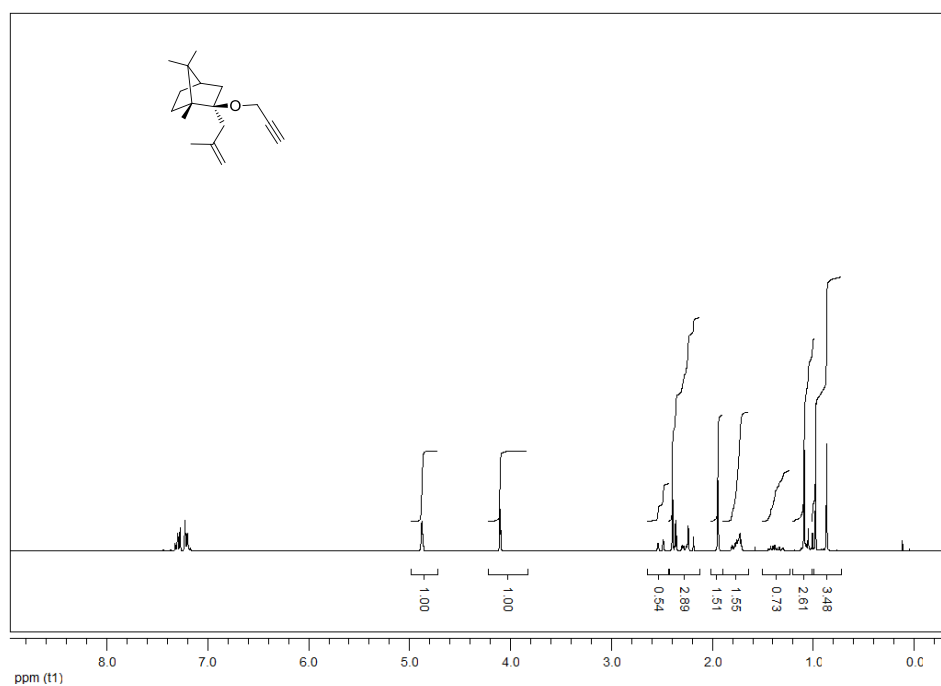


Figure A87. ^1H NMR spectrum of (+)-138

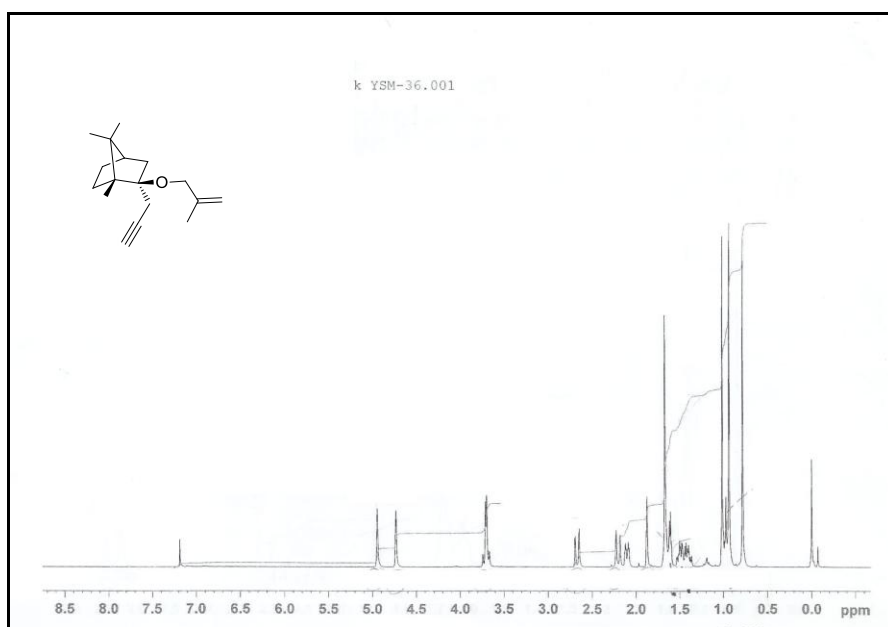


Figure A88. ^1H NMR spectrum of (-)-139

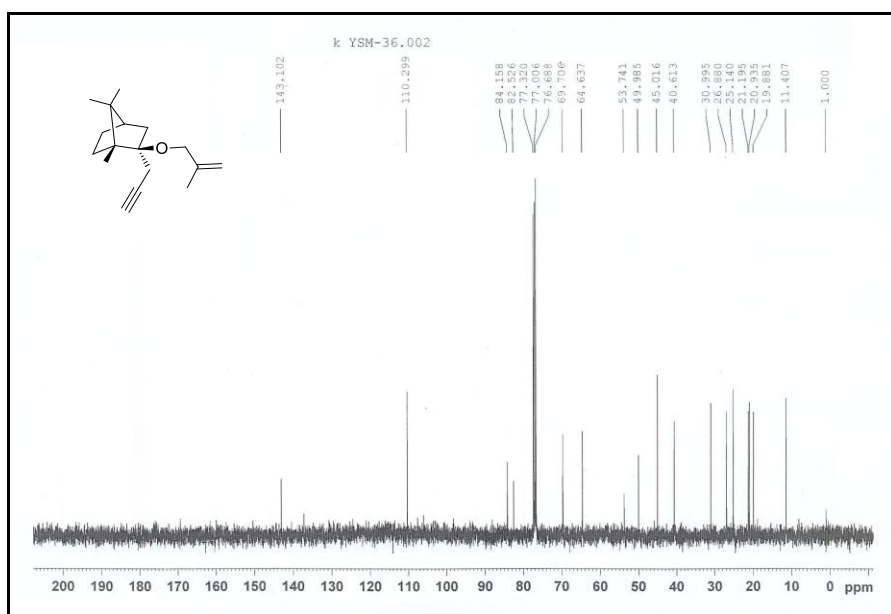


Figure A89. ¹³C NMR spectrum of (-)-139

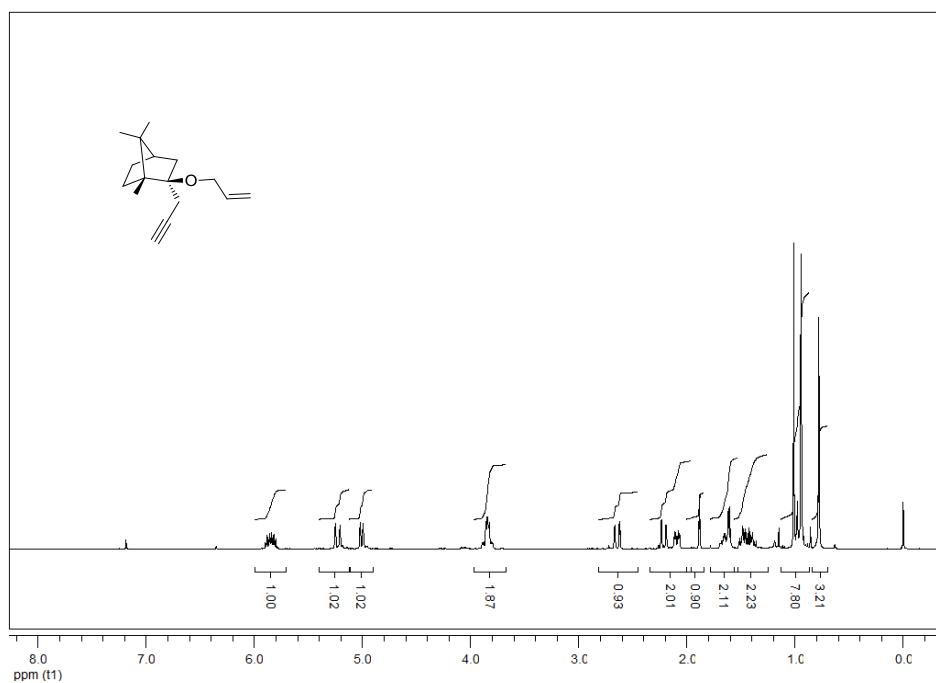


Figure A90. ¹H NMR spectrum of (-)-140

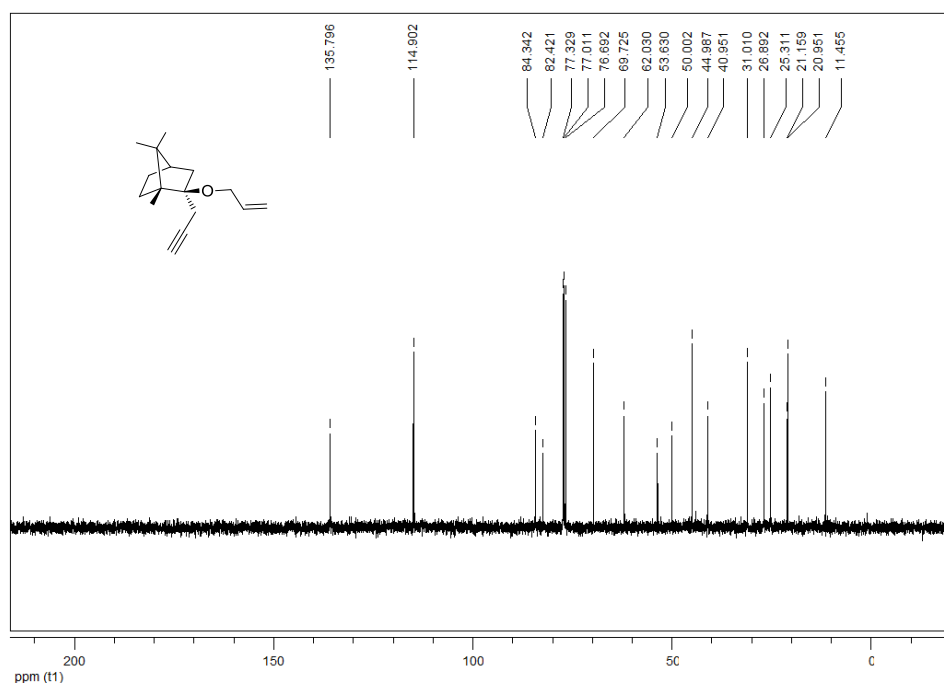


Figure A91. ¹³C NMR spectrum of (-)-140

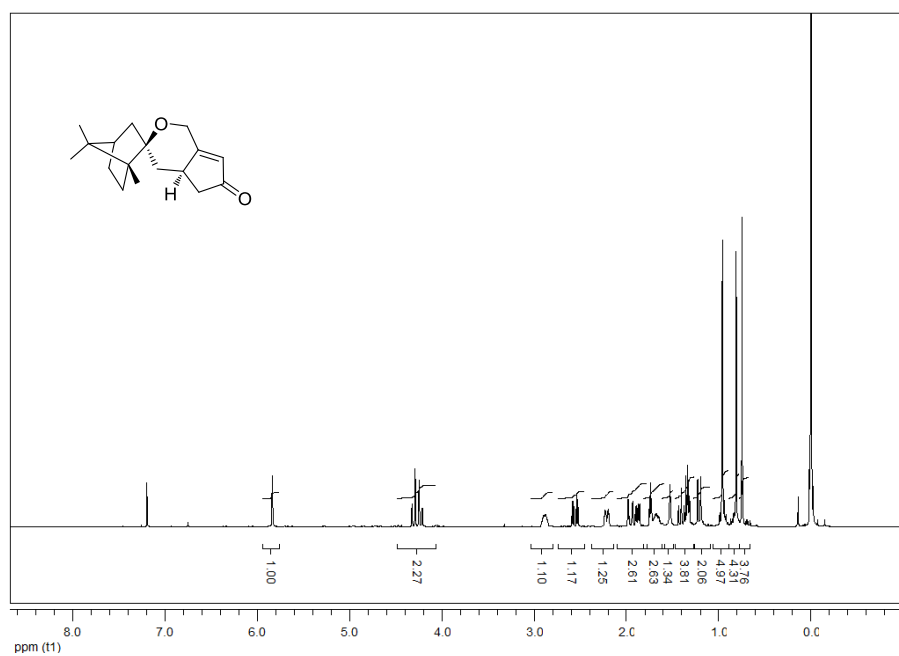


Figure A92. ¹H NMR spectrum of (+)-141

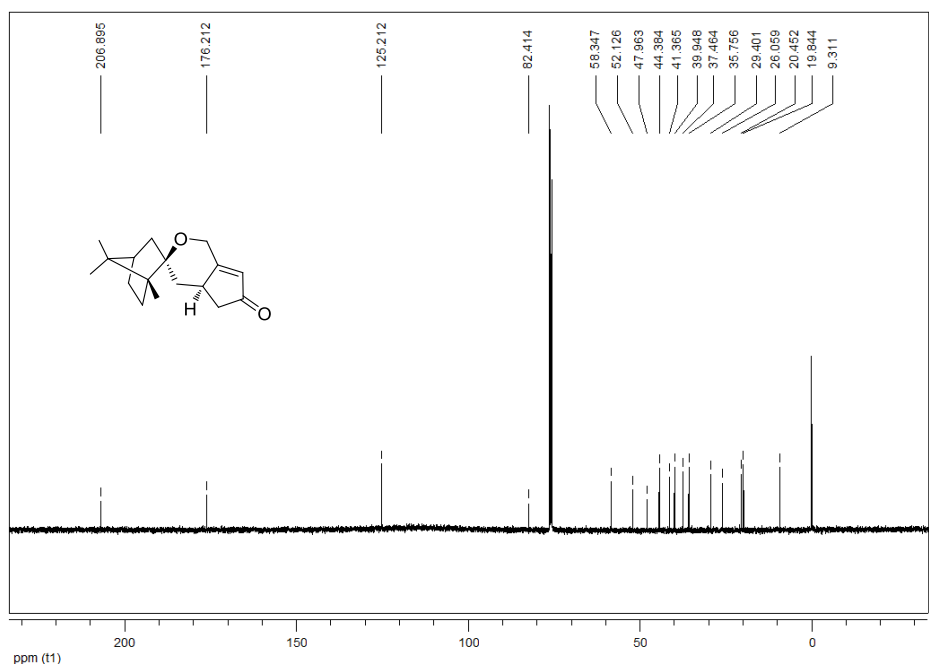


Figure A93. ^{13}C NMR spectrum of (+)-141

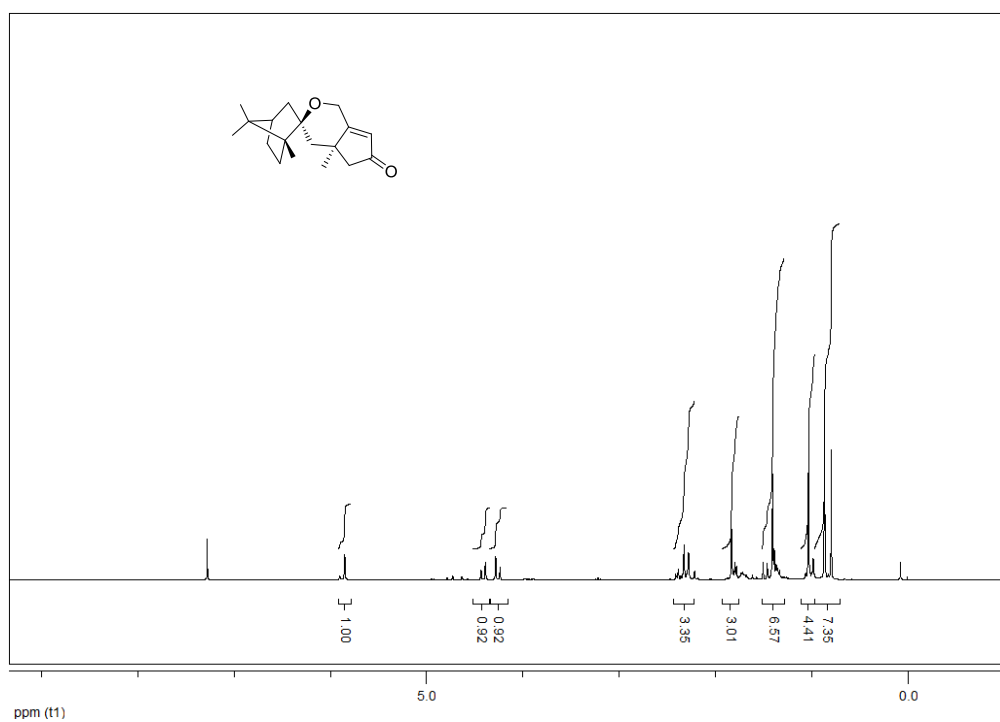


Figure A94. ^1H NMR spectrum of (-)-142

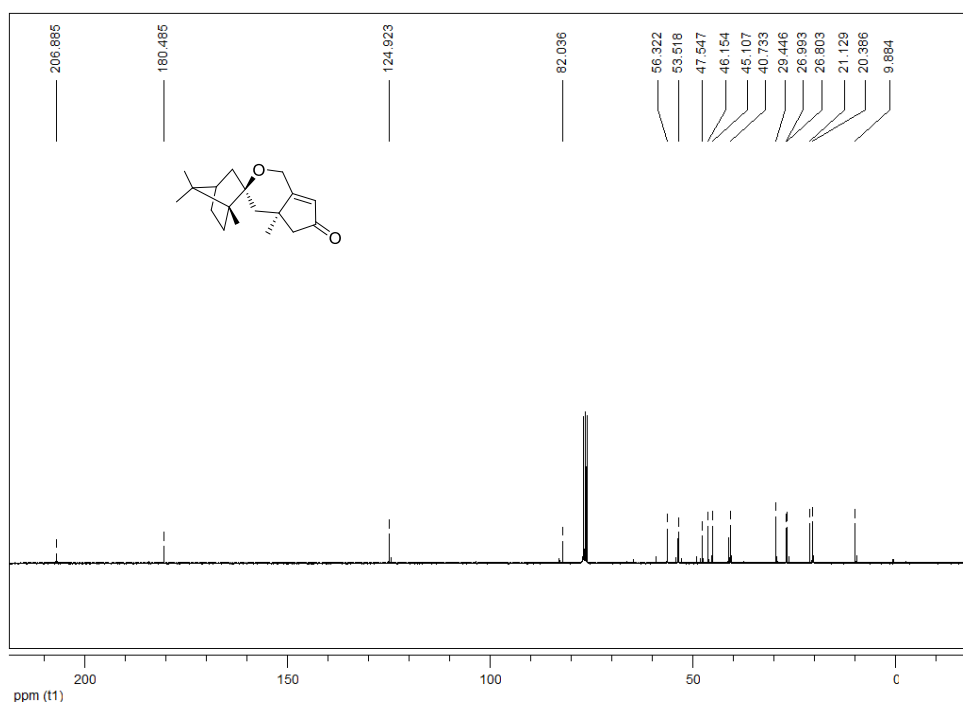


Figure A95. ^{13}C NMR spectrum of (-)-142

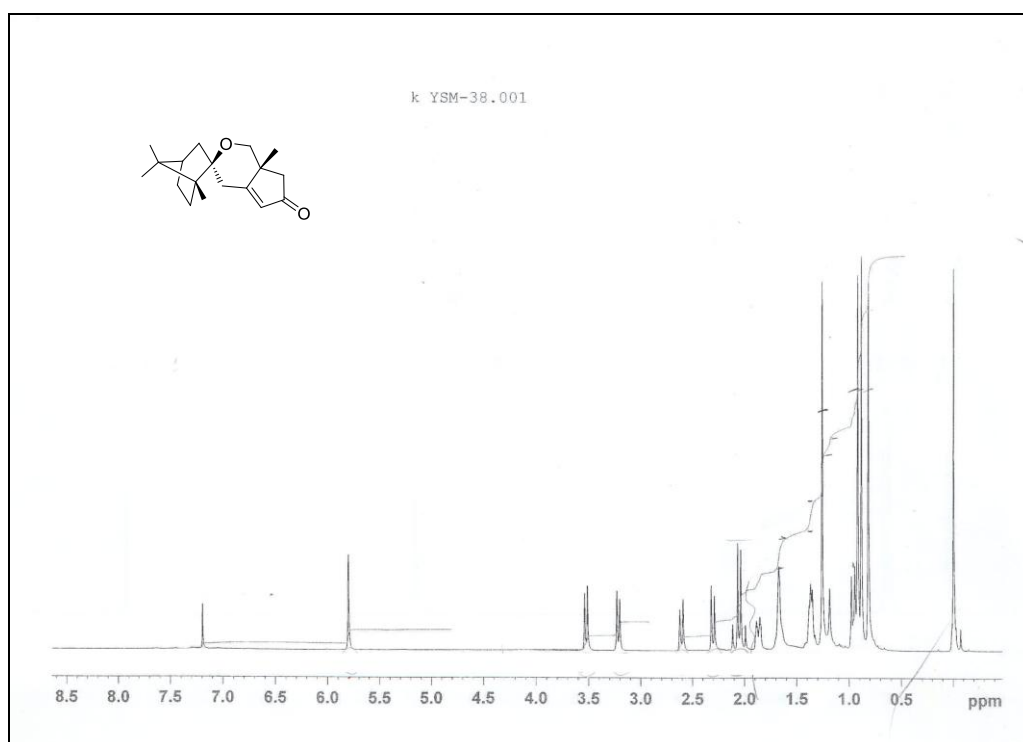


Figure A96. ^1H NMR spectrum of (+)-143

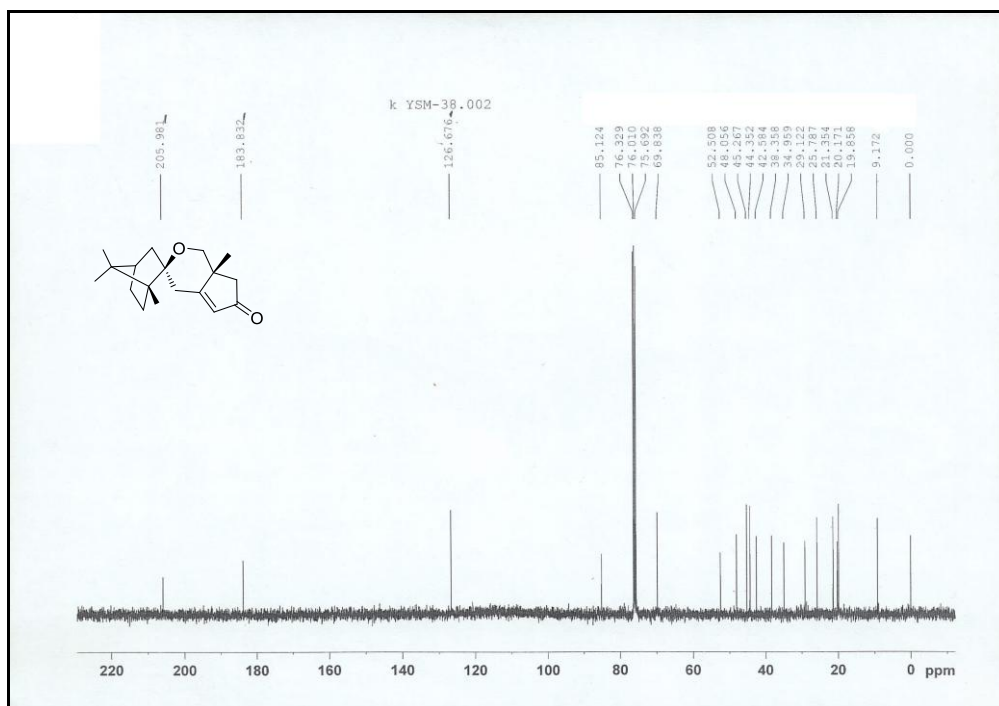


Figure A97. ^{13}C NMR spectrum of (+)-143

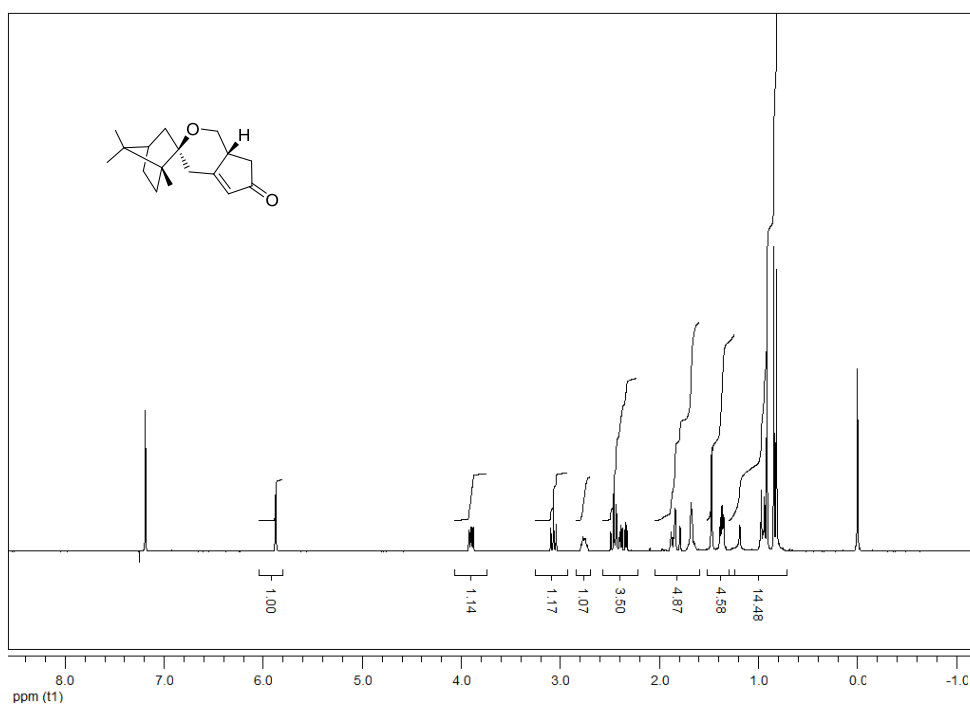


Figure A98. ^1H NMR spectrum of (+)-144

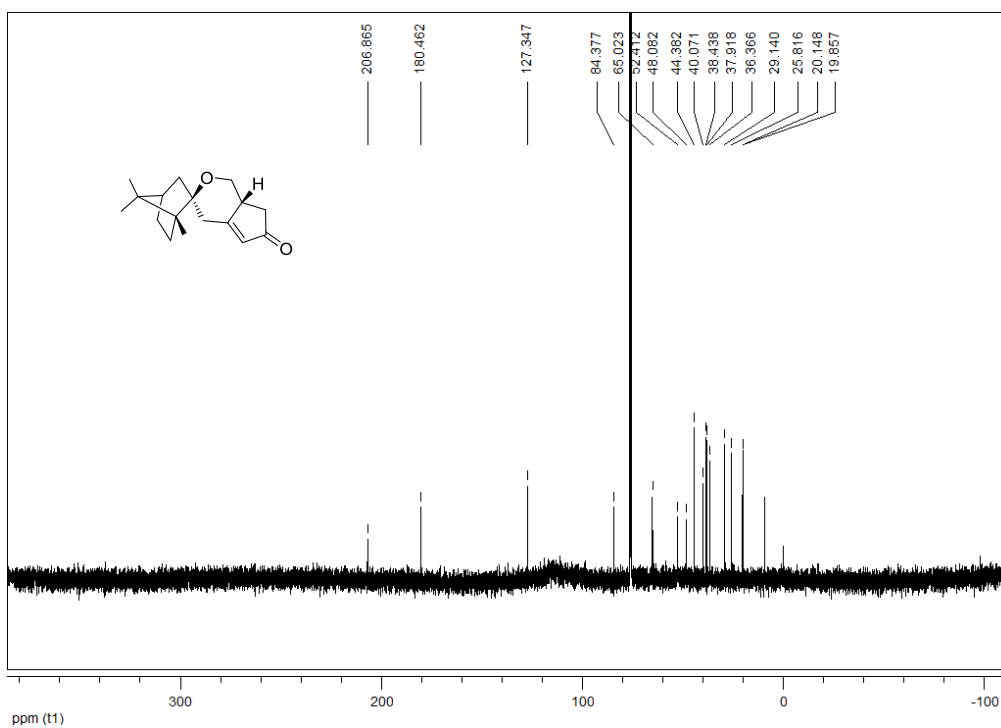


Figure A99. ^{13}C NMR spectrum of (+)-144

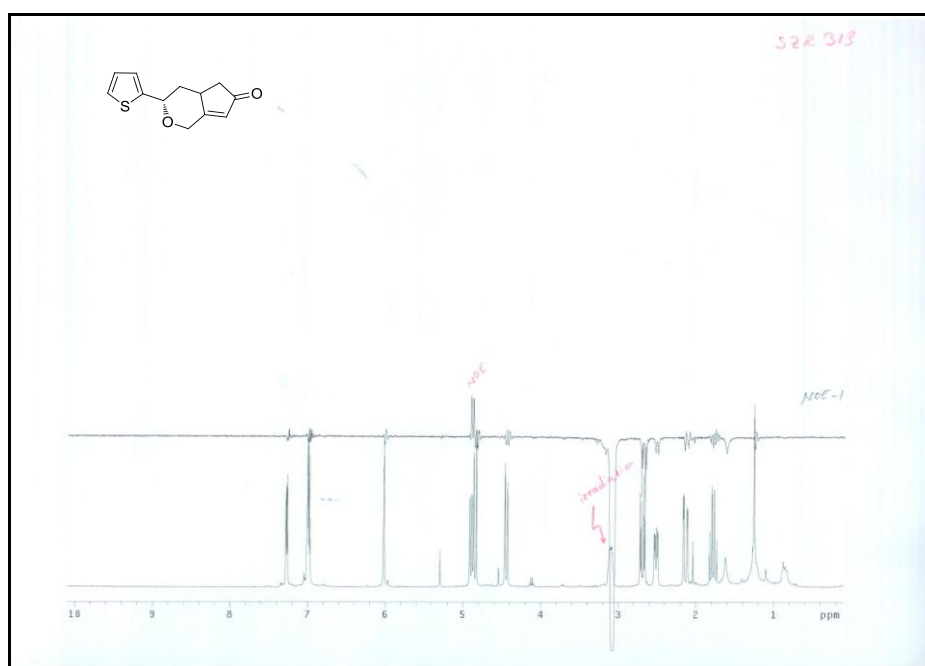


Figure A100. NOE spectrum of (+)-126

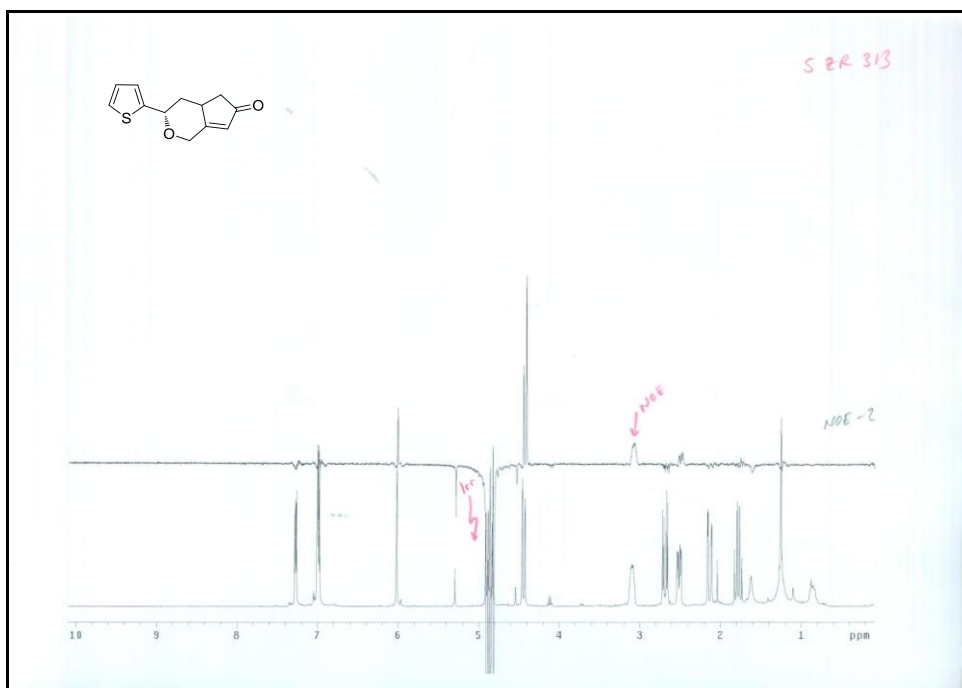


Figure A101. NOE spectrum of (+)-126



Figure A102. NOE spectrum of (+)-127

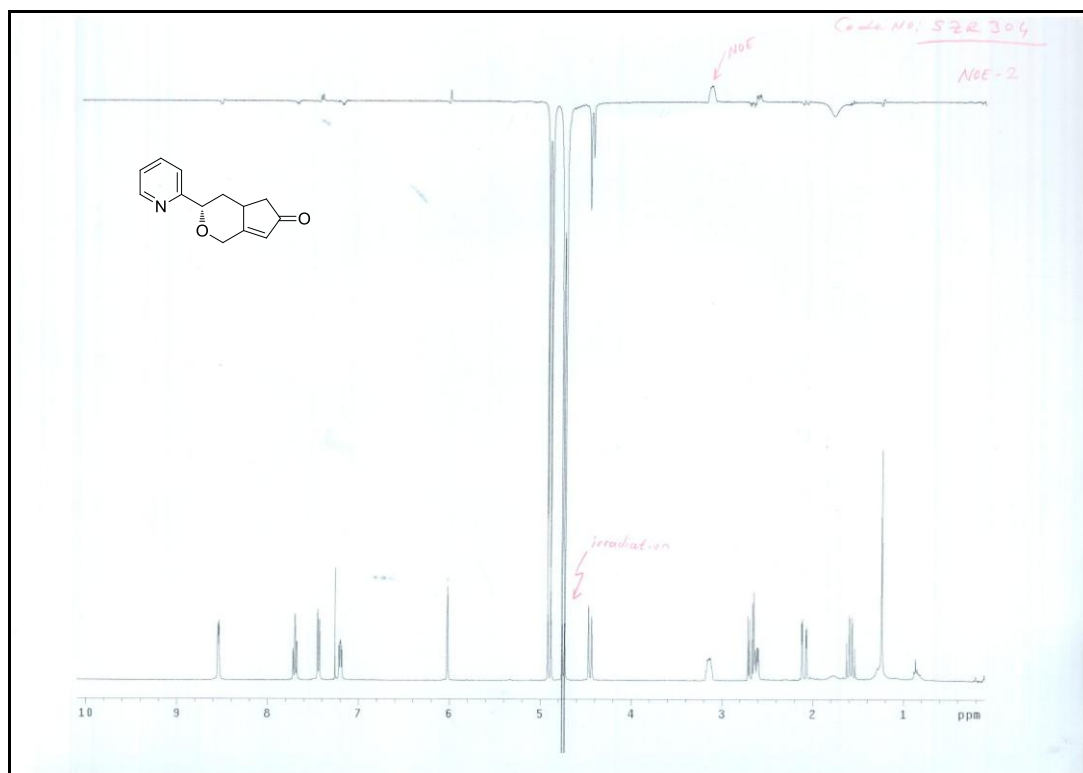


Figure A103. NOE spectrum of (+)-127

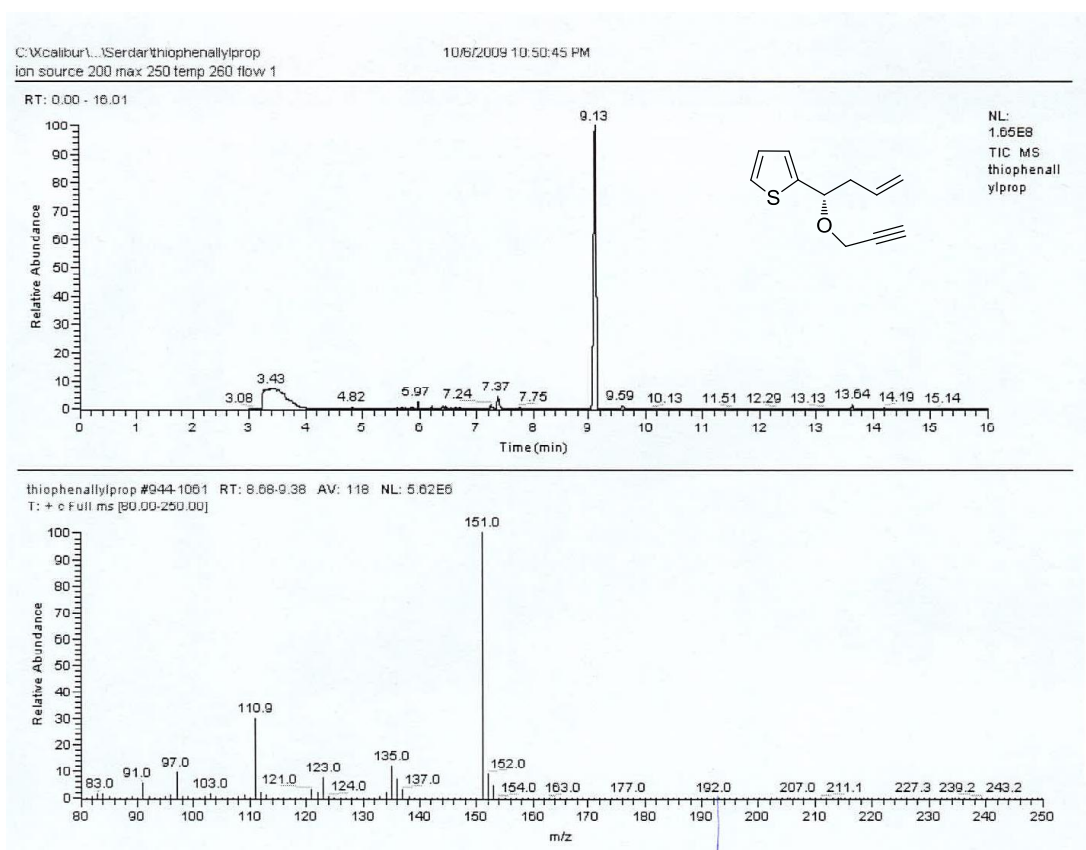
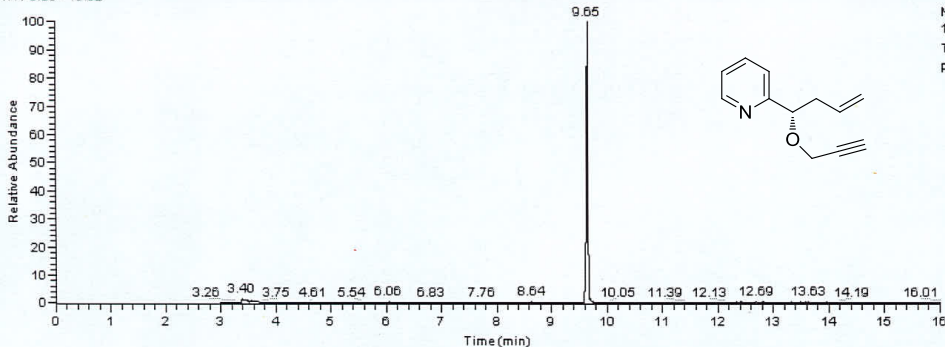


Figure A104. GC-MS spectrum of (S)-(-)-117

RT: 0.00 - 16.02



pyrallyprop #1070-1156 RT: 9.43-9.95 AV: 87 NL: 2.73E6
T: + c Full ms [90.00-250.00]

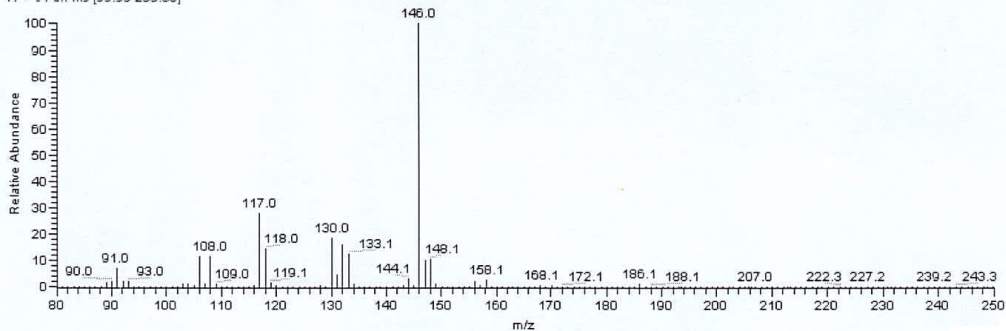
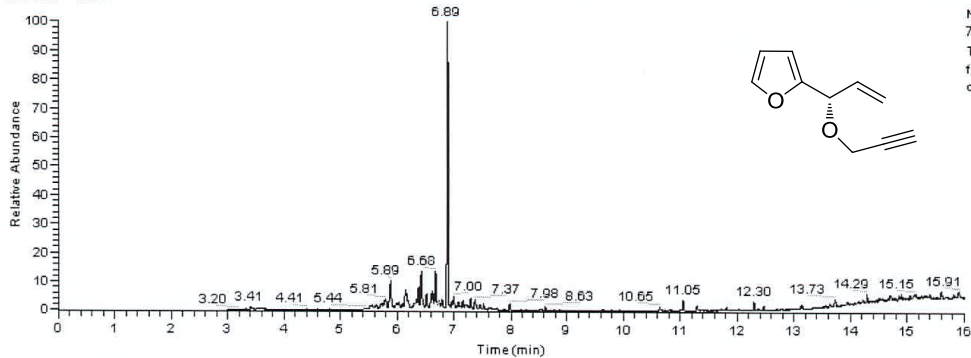


Figure A105. GC-MS spectrum of (S)-(-)-118

RT: 0.00 - 16.02



furanvinylprop #648 RT: 6.90 AV: 1 NL: 1.41E7
T: + c Full ms [90.00-250.00]

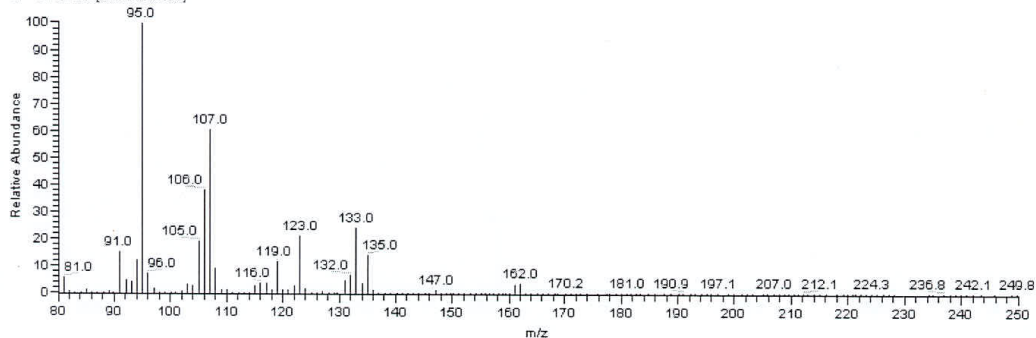


Figure A106. GC-MS spectrum of (S)-(-)-119

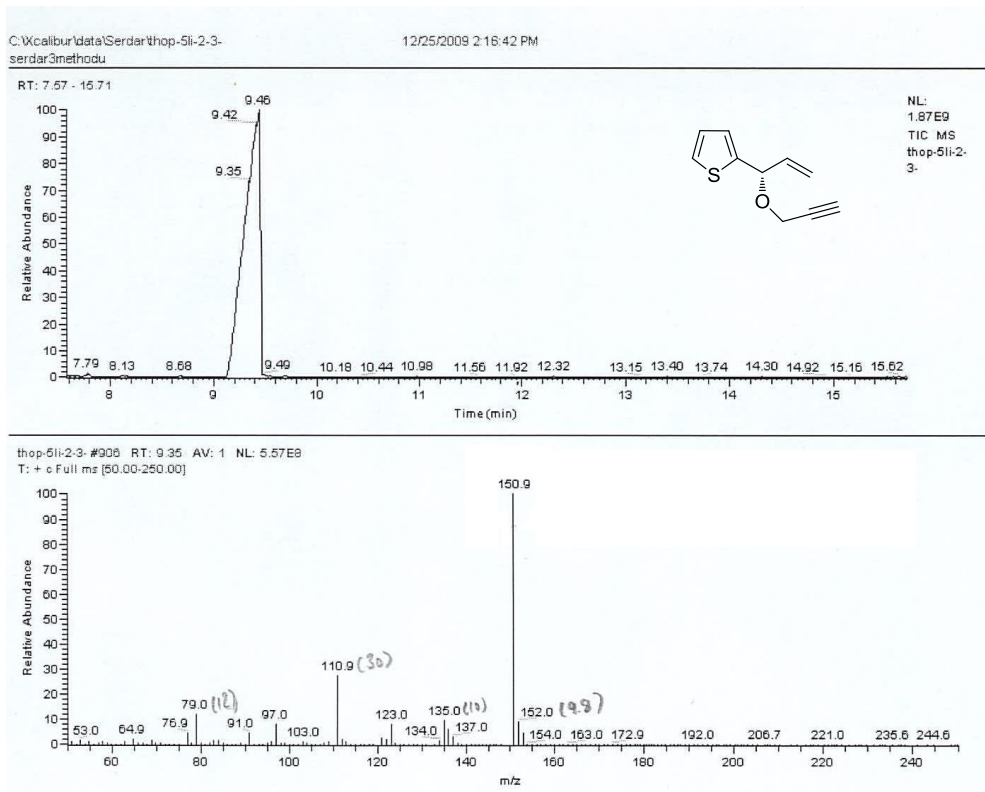


Figure A107. GC-MS spectrum of (S)-(-)-120

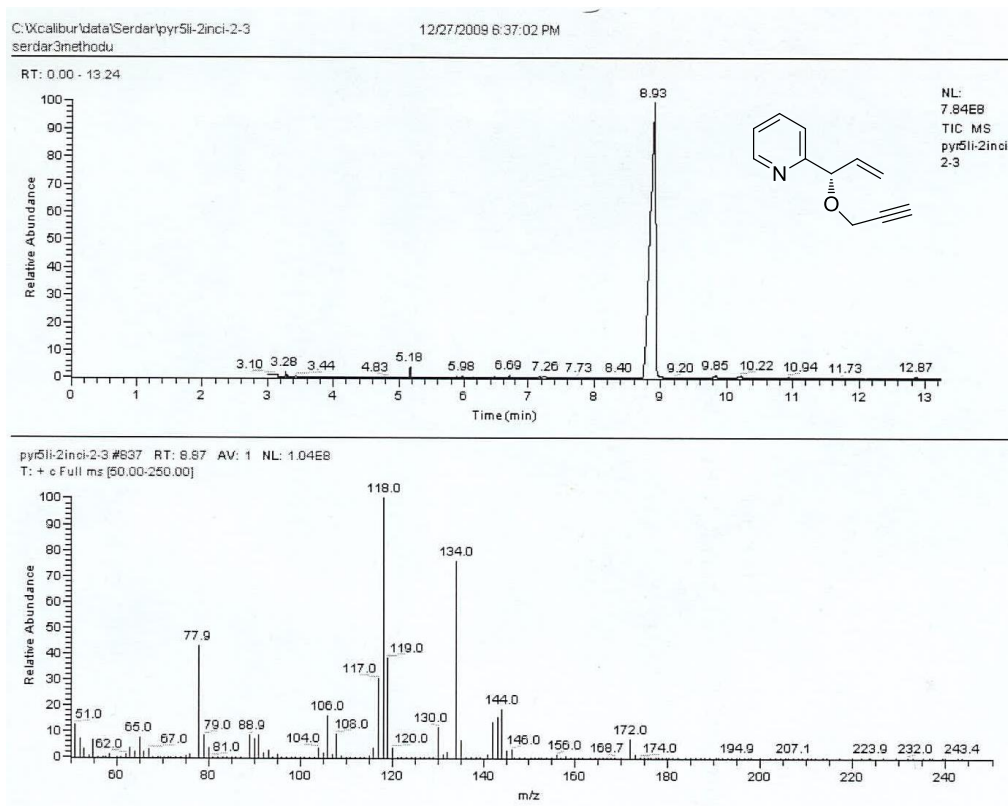


Figure A108. GC-MS spectrum of (S)-(-)-121

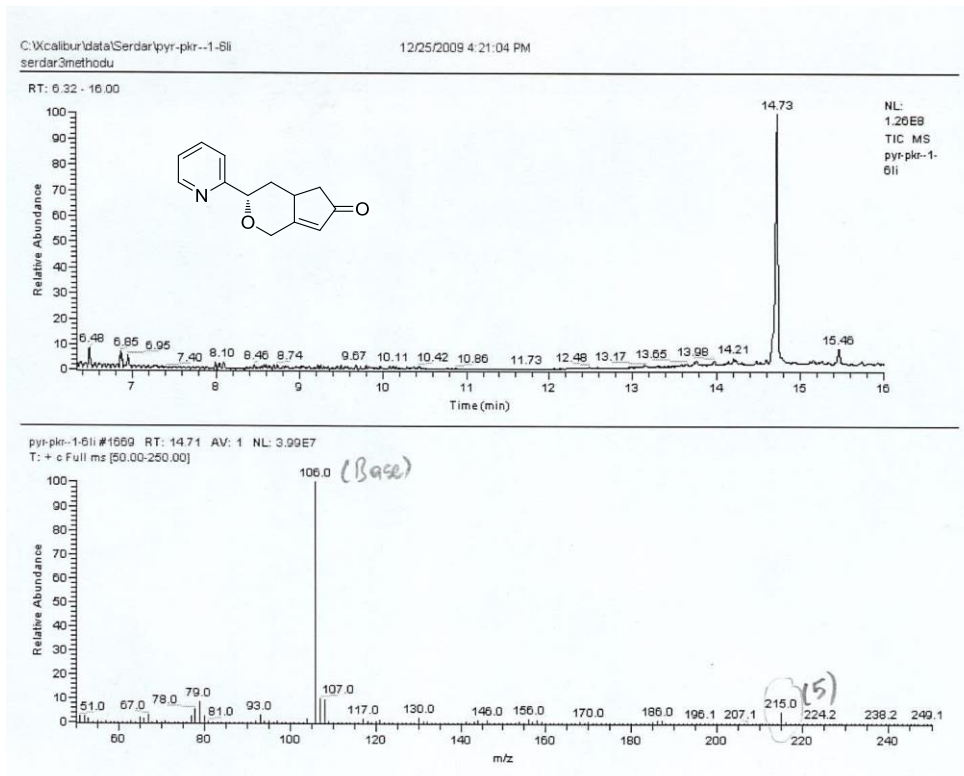


Figure A109. GC-MS spectrum of (S)-(+)-127

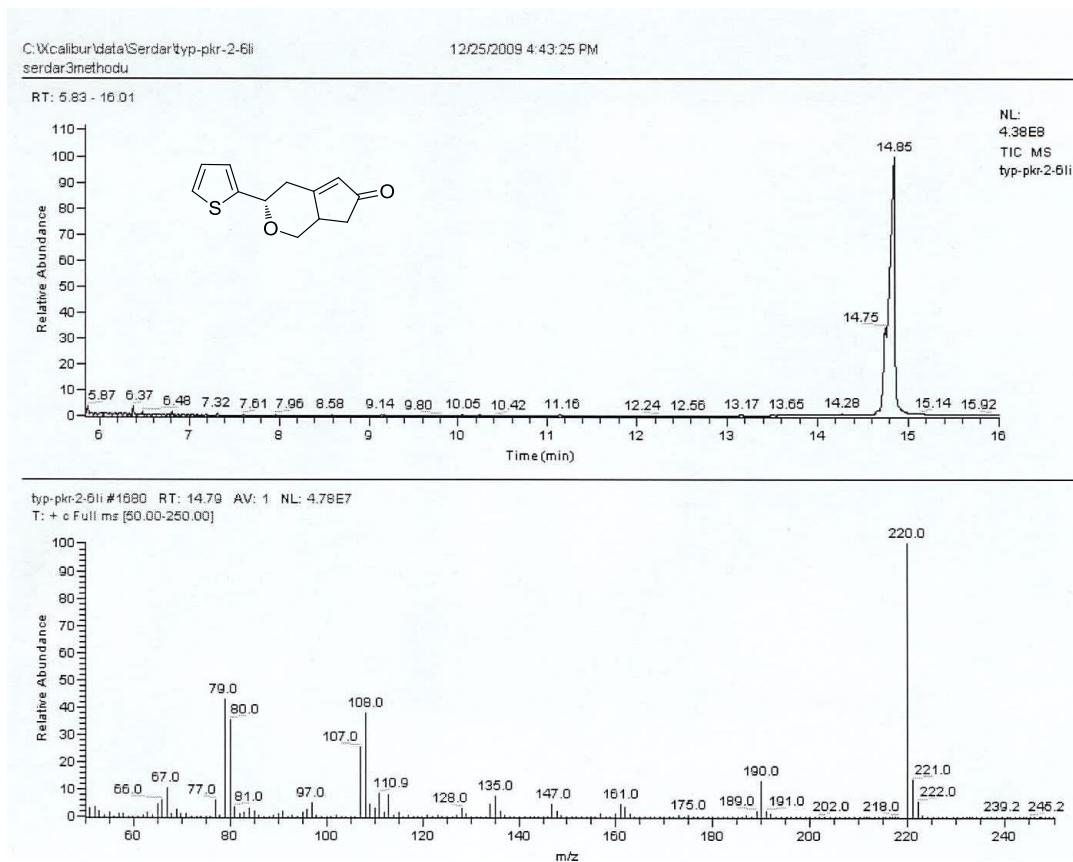


Figure A110. GC-MS spectrum of (S)-(+)-129

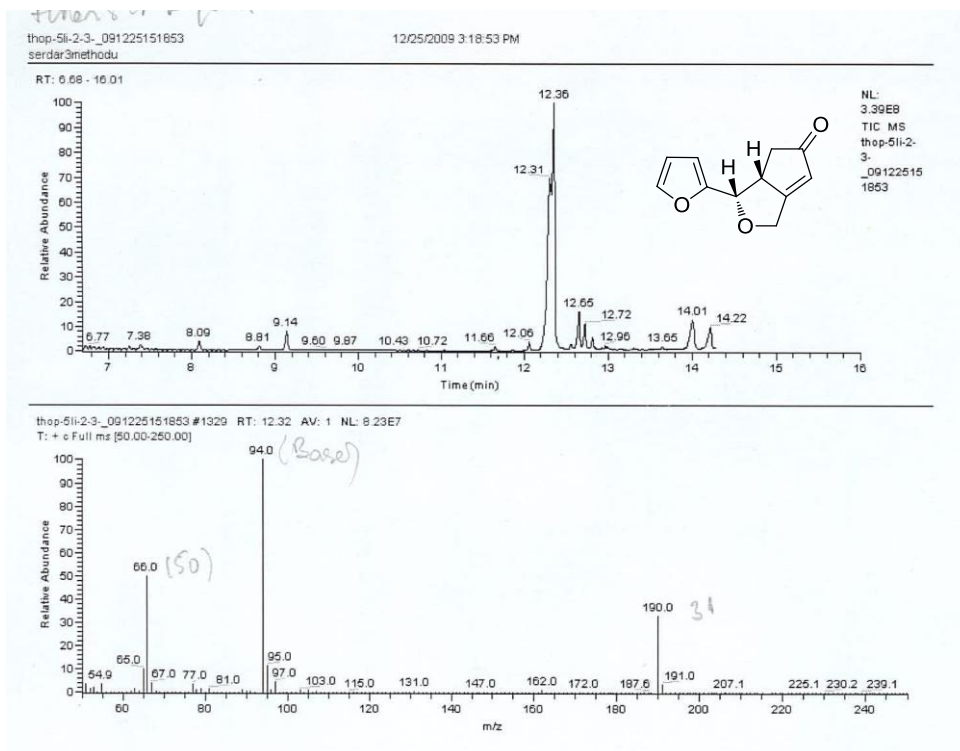


Figure A111. GC-MS spectrum of (-)-131

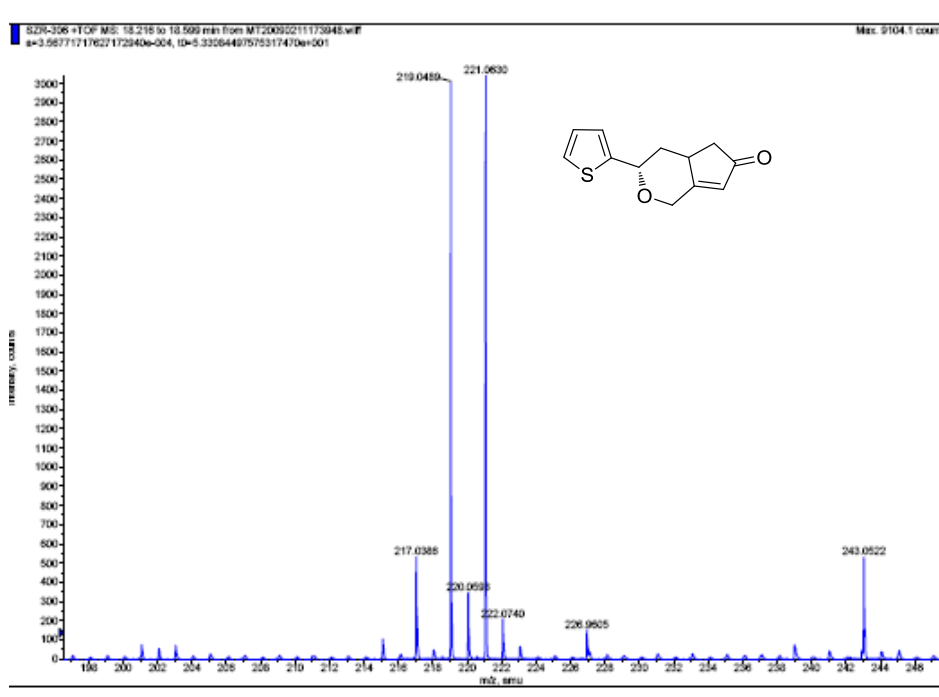


Figure A112. HRMS spectrum of (+)-126

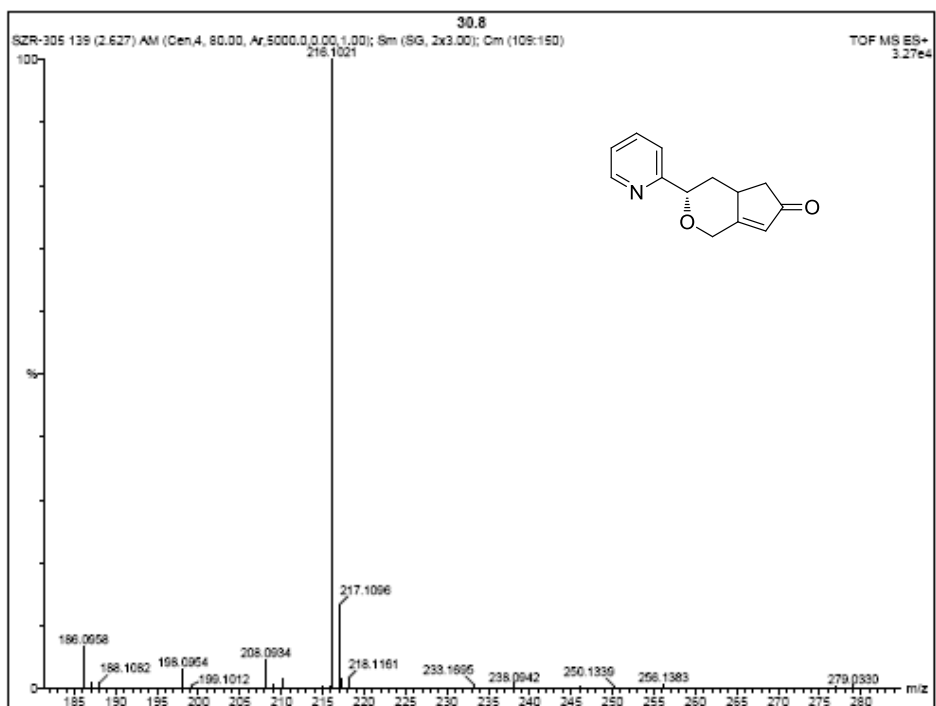


Figure A113. HRMS spectrum of (+)-127

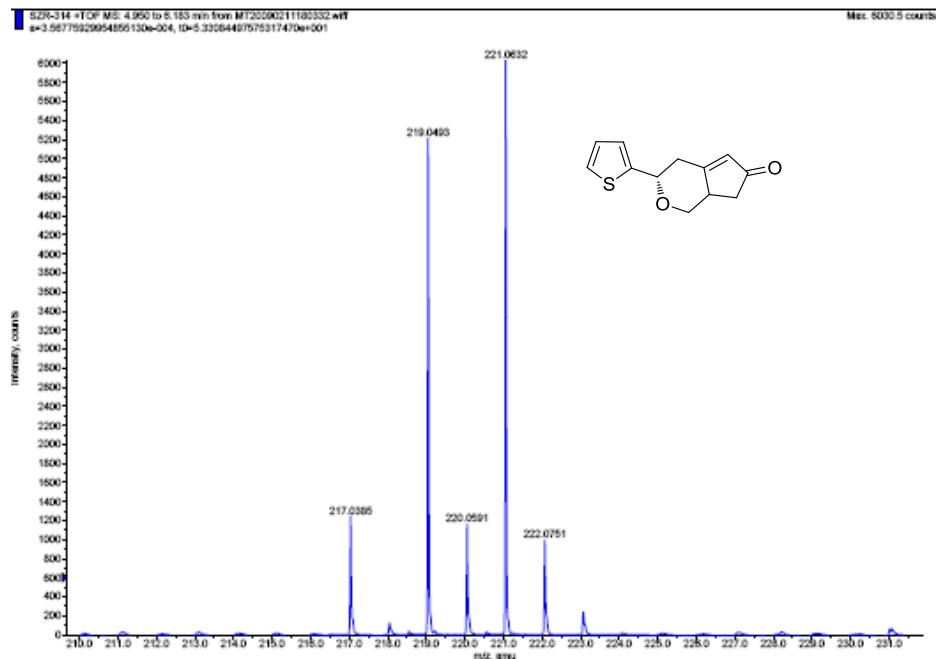


Figure A114. HRMS spectrum of (+)-129

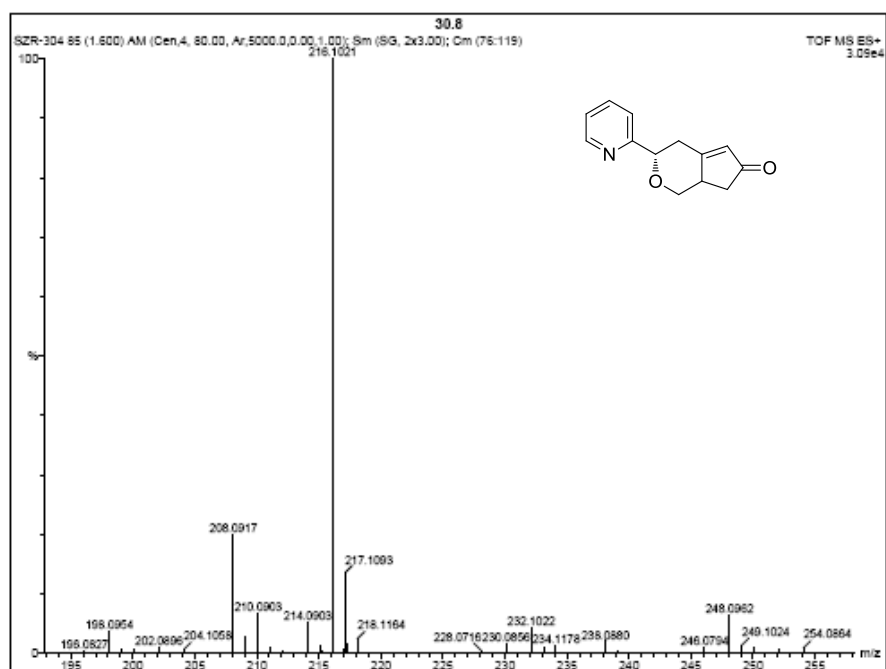


Figure A115. HRMS spectrum of (+)-130

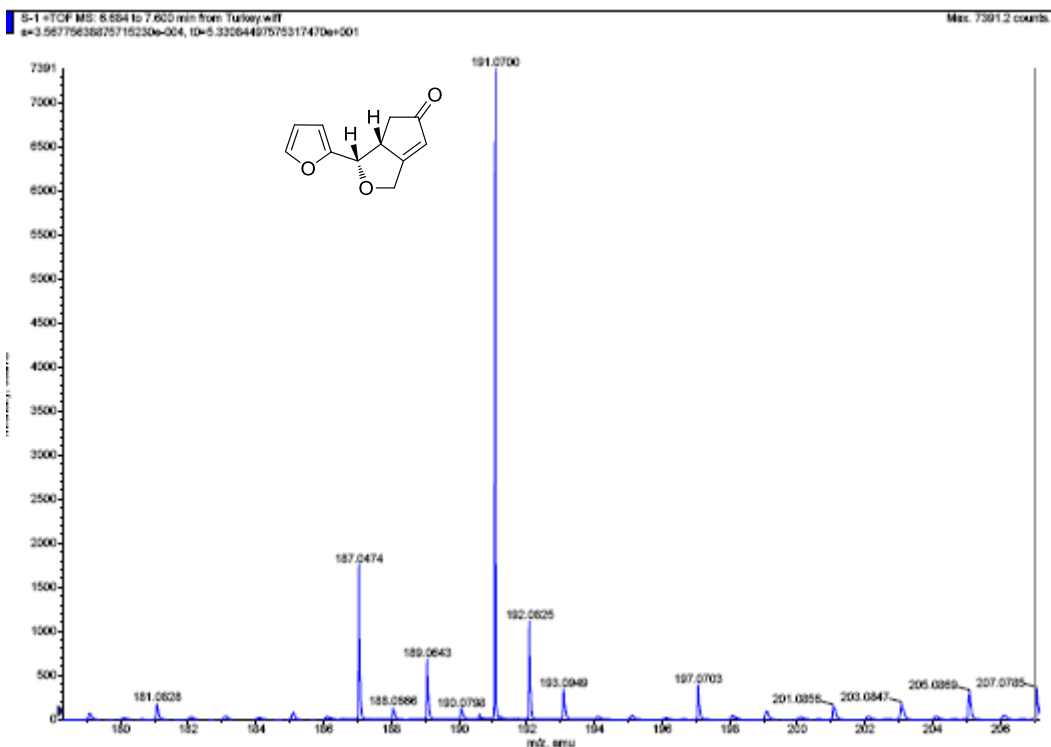


Figure A116. HRMS spectrum of (-)-131

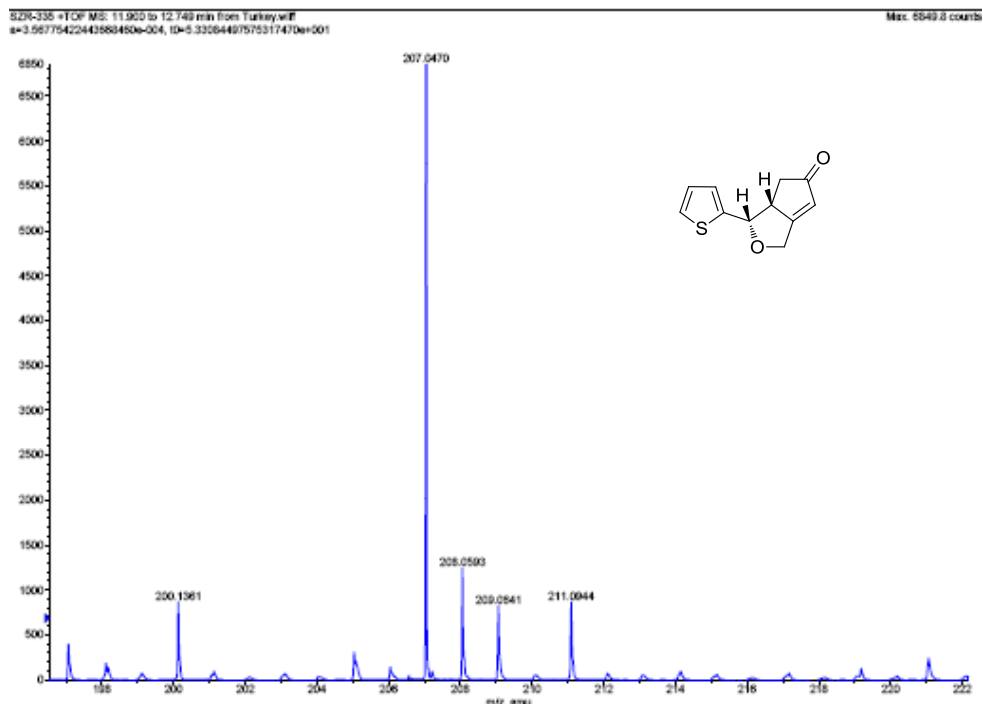


Figure A117. HRMS spectrum of (-)-132

CURRICULUM VITAE

PERSONAL INFORMATION

Surname, Name: Serdar SEZER

Nationality: Turkish

Date of Birth: 04.05.1980

Place of Birth: Sakarya/TURKEY

Gender: Male

Marital status: Married

E-Mail: ssezer@metu.edu.tr

Phone Number: 0312 210 76 09

Fax: 0312 210 32 00

EDUCATION

Degree Institution Year of Graduation

PhD, METU Chemistry 2011

Visiting PhD, Oxford, Chemistry 2010-2011 (1 year)

BS, SAU Chemistry 2002

Sakarya Atatürk High School 1997

WORK EXPERIENCE

2000

Internship TUVASAS

2001

Internship GOODYEAR

2002-2011

Teaching Asisstant, Middle East Technical University, Chemistry Department

2005-2007

Instructor, International Chemistry Olympiads, Student Training Programme, TÜBİTAK

2008-2009

Researcher, Government Project

FOREIGN LANGUAGES

English, Basic Spanish

PUBLICATIONS

- [1]. Sezer, S. Ozdemirhan, D. Sahin, E. Tanyeli, C. *Tetrahedron: Asymmetry* **2006**, *17*, 2981.
- [2]. Sezer, S. Gumrukcu, Y. Sahin, E. Tanyeli, C. *Tetrahedron: Asymmetry* **2008**, *19*, 2705.
- [3]. Ozdemirhan, D. Sezer, S. Sönmez, Y. *Tetrahedron: Asymmetry* **2008**, *19*, 2717-2720
- [4]. Sezer, S. Sahin, E. Tanyeli, C. *Tetrahedron: Asymmetry* **2010**, *21*, 476-485.
- [5]. Karaca, H. Sezer, S. Tanyeli, C. *Dyes and Pigments* **2010**, *90*, 100.
- [6]. Cayir, M. Demirci, S. Sezer, S. Tanyeli, C. *Tetrahedron: Asymmetry* **2011**, *22*, 1161.

HOBBIES

Football, Music, Walking